

# World Journal of *Gastroenterology*

*World J Gastroenterol* 2021 February 21; 27(7): 545-665



### REVIEW

- 545 *Helicobacter pylori*: Commensal, symbiont or pathogen?  
*Reshetnyak VI, Burmistrov AI, Maev IV*
- 561 Digestive system involvement of infections with SARS-CoV-2 and other coronaviruses: Clinical manifestations and potential mechanisms  
*Zhan GF, Wang Y, Yang N, Luo AL, Li SY*

### ORIGINAL ARTICLE

#### Basic Study

- 576 Xiangbinfang granules enhance gastric antrum motility *via* intramuscular interstitial cells of Cajal in mice  
*Chen QC, Jiang Z, Zhang JH, Cao LX, Chen ZQ*
- 592 Sinapic acid ameliorates D-galactosamine/lipopolysaccharide-induced fulminant hepatitis in rats: Role of nuclear factor erythroid-related factor 2/heme oxygenase-1 pathways  
*Ansari MA, Raish M, Bin Jordan YA, Ahmad A, Shahid M, Ahmad SF, Haq N, Khan MR, Bakheet SA*

#### Clinical and Translational Research

- 609 Quantitative multiparametric magnetic resonance imaging can aid non-alcoholic steatohepatitis diagnosis in a Japanese cohort  
*Imajo K, Tetlow L, Dennis A, Shumbayawonda E, Mouchti S, Kendall TJ, Fryer E, Yamanaka S, Honda Y, Kessoku T, Ogawa Y, Yoneda M, Saito S, Kelly C, Kelly MD, Banerjee R, Nakajima A*

#### Retrospective Study

- 624 Clinicopathological features and prognostic factors associated with gastroenteropancreatic mixed neuroendocrine non-neuroendocrine neoplasms in Chinese patients  
*Huang YC, Yang NN, Chen HC, Huang YL, Yan WT, Yang RX, Li N, Zhang S, Yang PP, Feng ZZ*
- 641 Effect of liver inflammation on accuracy of FibroScan device in assessing liver fibrosis stage in patients with chronic hepatitis B virus infection  
*Huang LL, Yu XP, Li JL, Lin HM, Kang NL, Jiang JJ, Zhu YY, Liu YR, Zeng DW*

#### Clinical Trials Study

- 654 Simultaneous partial splenectomy during liver transplantation for advanced cirrhosis patients combined with severe splenomegaly and hypersplenism  
*Jiang WT, Yang J, Xie Y, Guo QJ, Tian DZ, Li JJ, Shen ZY*

**ABOUT COVER**

Emilio De Raffele, MD, PhD, Consultant Surgeon, Division of Pancreatic Surgery, Department of Digestive Diseases, Azienda Ospedaliero-Universitaria di Bologna, IRCCS, Policlinico S.Orsola-Malpighi, Università degli Studi di Bologna, Via Albertoni 15, Bologna 40138, Italy. e.deraffele@aosp.bo.it

**AIMS AND SCOPE**

The primary aim of *World Journal of Gastroenterology* (WJG, *World J Gastroenterol*) is to provide scholars and readers from various fields of gastroenterology and hepatology with a platform to publish high-quality basic and clinical research articles and communicate their research findings online. WJG mainly publishes articles reporting research results and findings obtained in the field of gastroenterology and hepatology and covering a wide range of topics including gastroenterology, hepatology, gastrointestinal endoscopy, gastrointestinal surgery, gastrointestinal oncology, and pediatric gastroenterology.

**INDEXING/ABSTRACTING**

The WJG is now indexed in Current Contents®/Clinical Medicine, Science Citation Index Expanded (also known as SciSearch®), Journal Citation Reports®, Index Medicus, MEDLINE, PubMed, PubMed Central, and Scopus. The 2020 edition of Journal Citation Report® cites the 2019 impact factor (IF) for WJG as 3.665; IF without journal self cites: 3.534; 5-year IF: 4.048; Ranking: 35 among 88 journals in gastroenterology and hepatology; and Quartile category: Q2. The WJG's CiteScore for 2019 is 7.1 and Scopus CiteScore rank 2019: Gastroenterology is 17/137.

**RESPONSIBLE EDITORS FOR THIS ISSUE**

Production Editor: *Yan-Jie Ma*; Production Department Director: *Xiang Li*; Editorial Office Director: *Ze-Mao Gong*.

**NAME OF JOURNAL**

*World Journal of Gastroenterology*

**ISSN**

ISSN 1007-9327 (print) ISSN 2219-2840 (online)

**LAUNCH DATE**

October 1, 1995

**FREQUENCY**

Weekly

**EDITORS-IN-CHIEF**

Andrzej S Tarnawski, Subrata Ghosh

**EDITORIAL BOARD MEMBERS**

<http://www.wjgnet.com/1007-9327/editorialboard.htm>

**PUBLICATION DATE**

February 21, 2021

**COPYRIGHT**

© 2021 Baishideng Publishing Group Inc

**INSTRUCTIONS TO AUTHORS**

<https://www.wjgnet.com/bpg/gerinfo/204>

**GUIDELINES FOR ETHICS DOCUMENTS**

<https://www.wjgnet.com/bpg/GerInfo/287>

**GUIDELINES FOR NON-NATIVE SPEAKERS OF ENGLISH**

<https://www.wjgnet.com/bpg/gerinfo/240>

**PUBLICATION ETHICS**

<https://www.wjgnet.com/bpg/GerInfo/288>

**PUBLICATION MISCONDUCT**

<https://www.wjgnet.com/bpg/gerinfo/208>

**ARTICLE PROCESSING CHARGE**

<https://www.wjgnet.com/bpg/gerinfo/242>

**STEPS FOR SUBMITTING MANUSCRIPTS**

<https://www.wjgnet.com/bpg/GerInfo/239>

**ONLINE SUBMISSION**

<https://www.f6publishing.com>



## *Helicobacter pylori*: Commensal, symbiont or pathogen?

Vasiliy Ivanovich Reshetnyak, Alexandr Igorevich Burmistrov, Igor Veniaminovich Maev

**ORCID number:** Vasiliy Ivanovich Reshetnyak 0000-0003-3614-5052; Alexandr Igorevich Burmistrov 0000-0001-8853-3394; Igor Veniaminovich Maev 0000-0001-6114-564X.

**Author contributions:** All authors have equally contributed to the conception and design of the study, literature review and analysis, drafting critical revision and editing, and final approval of the final version.

**Conflict-of-interest statement:** No potential conflicts of interest.

**Open-Access:** This article is an open-access article that was selected by an in-house editor and fully peer-reviewed by external reviewers. It is distributed in accordance with the Creative Commons Attribution NonCommercial (CC BY-NC 4.0) license, which permits others to distribute, remix, adapt, build upon this work non-commercially, and license their derivative works on different terms, provided the original work is properly cited and the use is non-commercial. See: <http://creativecommons.org/licenses/by-nc/4.0/>

**Manuscript source:** Invited manuscript

**Specialty type:** Gastroenterology and hepatology

**Country/Territory of origin:** Russia

**Vasiliy Ivanovich Reshetnyak, Alexandr Igorevich Burmistrov, Igor Veniaminovich Maev,** Department of Propaedeutic of Internal Diseases and Gastroenterology, A.I. Yevdokimov Moscow State University of Medicine and Dentistry, Moscow 127473, Russia

**Corresponding author:** Vasiliy Ivanovich Reshetnyak, DSc, MD, PhD, Full Professor, Department of Propaedeutic of Internal Diseases and Gastroenterology, A.I. Yevdokimov Moscow State University of Medicine and Dentistry, p. 1, 20 Delegatskaya Street, Moscow 127473, Russia. [vasiliy.reshetnyak@yandex.ru](mailto:vasiliy.reshetnyak@yandex.ru)

### Abstract

This review considers the data on *Helicobacter pylori* (*H. pylori*), which have been accumulated over 40 years since its description as an etiological factor in gastrointestinal diseases. The majority of modern publications are devoted to the study of the pathogenic properties of the microorganism in the development of chronic gastritis, peptic ulcer disease, and gastric cancer, as well as methods for its eradication. However, in recent years, there have been more and more studies which have suggested that *H. pylori* has a beneficial, or potentially positive, effect on the human body. The authors have attempted to objectively analyze the information accumulated in the literature on *H. pylori*. Some studies consider it as one of the recently identified human bacterial pathogens, and special attention is paid to the evidence suggesting that it is probably part of the composition of the human microbiome as a commensal (*commensal* from French to English is a table companion) or even a symbiont. The presented data discussing the presence or absence of the effect of *H. pylori* on human health suggest that there is an apparent ambiguity of the problem. The re-assessment of the data available on *H. pylori* infection is important in order to answer the question of whether it is necessary to create a program of mass *H. pylori* eradication or to apply a more personalized approach to treating patients with *H. pylori*-associated gastrointestinal diseases and to perform eradication therapy.

**Key Words:** *Helicobacter pylori*; Pathogen; Commensal; Microbiome; Peptic ulcer; Gastric cancer; Asthma; Inflammatory bowel diseases

©The Author(s) 2021. Published by Baishideng Publishing Group Inc. All rights reserved.

**Core Tip:** This review provides data on *Helicobacter pylori* (*H. pylori*) as one of the recently identified human bacterial pathogens. On the one hand, its role as a human



**Peer-review report's scientific quality classification**

Grade A (Excellent): 0  
 Grade B (Very good): B, B  
 Grade C (Good): C, C, C, C  
 Grade D (Fair): 0  
 Grade E (Poor): 0

**Received:** December 5, 2020

**Peer-review started:** December 5, 2020

**First decision:** December 27, 2020

**Revised:** December 28, 2020

**Accepted:** January 21, 2021

**Article in press:** January 21, 2021

**Published online:** February 21, 2021

**P-Reviewer:** Chivu-Economescu M, Keikha M, Lombardo L, Romano M

**S-Editor:** Fan JR

**L-Editor:** Webster JR

**P-Editor:** Liu JH



pathogenic bacterium that is commonly found in patients with chronic gastritis, peptic ulcer disease, and gastric cancer is discussed. On the other hand, the high prevalence of *H. pylori* in the population and its asymptomatic coexistence with humans in most of the world's population indicates its persistence in the body as a representative of the microbiome and as a nonpathogenic microorganism. The presented data suggest that there is an apparent ambiguity of the problem and a need for an analytically developed, comprehensive approach to study the effect of *H. pylori* infection on human health and to perform eradication therapy.

**Citation:** Reshetnyak VI, Burmistrov AI, Maev IV. *Helicobacter pylori*: Commensal, symbiont or pathogen? *World J Gastroenterol* 2021; 27(7): 545-560

**URL:** <https://www.wjgnet.com/1007-9327/full/v27/i7/545.htm>

**DOI:** <https://dx.doi.org/10.3748/wjg.v27.i7.545>

## INTRODUCTION

Over four decades, the problem of studying *Helicobacter pylori* (*H. pylori*) has occupied the minds of many scientists around the world. *H. pylori* is a bacterium that is commonly found in patients with chronic gastritis, peptic ulcer disease (PUD) and gastric cancer (GC), as well as among the healthy population. *H. pylori* was first reported in 1875, when Bottcher and Letulle observed it on the margins of peptic ulcers<sup>[1]</sup>. Despite the high prevalence of the microorganism demonstrated later, its discovery occurred only at the beginning of the 1980s<sup>[2]</sup>. It is obvious that since 1983 *H. pylori* has been colonizing more than half of the world population<sup>[3]</sup>. This event has produced a major multidisciplinary interest including gastroenterologists, microbiologists, and infectious disease specialists among others. The role of *H. pylori* as a true pathogen has been the center of major discussions for many years. *H. pylori* infection has been linked to gastric and duodenal ulcers (in 1%-10% of infected patients), gastric carcinoma (0.1%-3%), and gastric mucosa-associated lymphoid tissue (MALT) lymphoma (less than 0.01%)<sup>[4,5]</sup>. However, the vast majority of the infected population will never develop symptoms related to *H. pylori* infection.

*H. pylori* colonization of the human stomach occurs early in life and persists indefinitely unless treated<sup>[3]</sup>. At the same time, transmission of *H. pylori* is mainly in a family setting<sup>[6]</sup>.

The decline in *H. pylori* prevalence with time was first reported in 1997<sup>[7]</sup>, and later confirmed in two large population-based studies in the United States<sup>[8]</sup>. As a result of *H. pylori*'s gradual decline, a series of negative consequences have been described<sup>[2]</sup>. There has been an alarming increase in asthma<sup>[9,10]</sup>, as well as a potential increase in the susceptibility to diarrheal diseases<sup>[11]</sup>. However, a more serious consequence related to the decline of *H. pylori* is the escalation of esophageal diseases, such as gastroesophageal reflux disease (GERD), Barrett's esophagus, and adenocarcinoma of the esophagus<sup>[12,13]</sup>. We do not know if the decline in *H. pylori* infections is the cause of these emerging diseases or if it is just an indicator of the hygiene hypothesis<sup>[2]</sup>. Due to its low virulence and the fact that disease is observed mostly in elderly infected individuals, *H. pylori* could be considered a commensal organism and only an opportunistic pathogen.

## GENERAL CHARACTERISTICS OF *H. PYLORI*

### Basic facts

*H. pylori* is a gram-negative, S-shaped, or helical microaerophilic bacterium belonging to the genus *Helicobacteraceae*<sup>[14,15]</sup>. In 1979, R. Warren identified *Campylobacter pylori* and suggested that this microorganism was an etiological agent of gastritis. In 1982, B.J. Marshall isolated a culture of *H. pylori* and showed the relationship between its persistence and PUD development<sup>[16]</sup>.

According to the modern concepts, the predominant habitat (life, growth, and reproduction) of *H. pylori* is the supraepithelial mucus layer in the region of the gastric pits and in the first parts of the duodenum<sup>[16]</sup>. *H. pylori* is generally not detected neither

in the subepithelial space of the stomach nor in the epithelium of gastric glands<sup>[13]</sup>. The motility of the microorganism through the mucus layer occurs due to the presence of several mobile flagella, which contributes to the migration of the bacterium to areas with suitable conditions for existence<sup>[17]</sup>.

The most favorable conditions for bacterial life have been found to be the optimum temperature of 37°C, pH 4.0-6.0, microaerophilic conditions, the presence of water and nutrients<sup>[15]</sup>. *H. pylori* does not contain enzymes that metabolize carbohydrates. The metabolism of a bacterial cell is provided by the energy released during the utilization of amino acids obtained from the host<sup>[18]</sup>. The microorganism is characterized by its possible persistence in the human body as S-shaped, C(U)-shaped, and coccoid forms<sup>[2,15,16]</sup>. The similar mechanism of transition from one form to another is an adaptation to survival during adverse environmental conditions (temperature or pH shifts, long intervals between meals, and antibiotic therapy)<sup>[15]</sup>.

### **Epidemiology and routes of transmission**

The data currently available suggest that there is a high prevalence of *H. pylori* in the population. The detection rates of *H. pylori* vary from 35% to 90% in representatives of the population in different regions<sup>[15,19-22]</sup>. A large variation of the indicator depends on a number of factors, including the socio-economic state of the country, age, the method of detecting *H. pylori* and other factors<sup>[20]</sup>. Thus, in their article, Mentis *et al.*<sup>[19]</sup> reported the detection of *H. pylori* in 71.6% of the population in Italy and in 84.2% of those surveyed in Poland. Luzzza *et al.*<sup>[20]</sup> reported that in Italy among 518 subjects who were evaluated by both the <sup>13</sup>C-urea breath test (UBT) and serology, 310 (59.8%) were UBT positive, 479 (92.4%) *vacA*-positive, and 369 (71.2%) *cagA*-positive. Similar indicators for Africa and Asia were distributed in the following order: Ethiopia (72.2%) and Rwanda (75.3%), China 83.4%, Japan (39.9%), and Taiwan (72.1%)<sup>[19]</sup>. Burucoa *et al.*<sup>[21]</sup> established the largest proportion of *H. pylori*-positive patients in Africa (70.1%) [95% confidence interval (CI): 62.6%-77.6%], South America (69.4%) (95%CI: 63.9%-74.9%), and West Asia (66.6%) (95%CI: 56.1%-77.0%). The regions with least occurrence were Oceania (24.4%) (95%CI: 18.5%-30.4%), Western Europe (34.3%) (95%CI: 31.3%-37.2%), and North America (37.1%) (95%CI: 32.3%-41.9%). In Russia, the prevalence of *H. pylori* in children aged 5-10 and 11-14 years and in adults was 29%, 50%, and 70%-92%, respectively<sup>[13,23]</sup>.

To date, the main route of transmission of *H. pylori* is not known. Infection most often occurs from person to person; in this case this generalized mechanism can be divided into vertical (that is, transmission of the pathogen within one family), and horizontal (contact with people outside the family or infection with environmental objects-environmental contamination)<sup>[19]</sup>. Possible transmission routes, such as fecal-oral, oral-oral, and gastro-oral, have been comprehensively studied in recent years<sup>[21,24,25]</sup>. *H. pylori* can be isolated from different body fluids. The pathogen was detected in the dental plaque, saliva, tonsil tissue, root canals, and on the oral mucosa (including on the surface of the tongue), using a polymerase chain reaction assay<sup>[21]</sup>. Particular attention is paid to the environmental contamination associated with the consumption of *H. pylori*-containing water and food<sup>[26]</sup>.

The majority of authors consider the intrafamilial transmission of the pathogen to be the predominant and most significant route. This opinion is confirmed by factors, such as close interpersonal contacts in the family, the single socioeconomic status of family members, and genetic predisposition to *H. pylori* persistence<sup>[24,27]</sup>.

---

## **PATHOGENIC PROPERTIES OF *H. PYLORI***

---

### ***H. pylori* virulence factors and its role in systemic diseases**

To survive the unfavorable, hyperacid conditions of the stomach, *H. pylori* synthesizes a number of virulence factors that both improve conditions for vital activity in an acidic environment and have a damaging effect on the gastric mucosa.

In their work, Kao *et al.*<sup>[28]</sup> noted that on entry into the host stomach, *H. pylori* uses urease activity to neutralize hydrochloric acid that is one of the protective factors and has a pronounced antimicrobial effect. Regulation of urease synthesis is encoded by a number of genes called the *urease gene cluster*. This set of genes includes catalytic units (*urea A/B*), an acid-gated urea channel (*ureI*), and accessory assembly proteins (*ure E-H*)<sup>[29]</sup>.

Of interest is the fact that urease synthesis depends on the pH surrounding the bacterium: The *ureI*-channels are tightly closed at pH 7.0 and are completely open at pH 5.0<sup>[28,30]</sup>. That is, when the external conditions change, namely, when stomach

lumen acidity increases, *H. pylori* releases urease that hydrolyzes urea into CO<sub>2</sub> and ammonia (NH<sub>3</sub>) that in turn binds to water and forms unstable ammonium hydroxide. This sequence of biochemical reactions leads to medium alkalization<sup>[28]</sup>. This mechanism of overcoming the acid barrier is extremely important for the survival of the bacterium along with a spiral shape, a smooth cell wall, and helicoidal movements. Schoep *et al.*<sup>[31]</sup> demonstrated that urease-negative bacteria were unable to colonize the gastric mucosa of gnotobiotic piglets.

Another important virulence factor promoting the spread of the bacterium to the gastric epithelium is its motility due to the presence of 4-7 mobile sheathed flagella. The flagellum is a complex organ that is composed of several types of protein subunits and consists of the basal body, hook, and filament<sup>[32,33]</sup>. There are several types of flagella-driven motility: "Swimming motility", "spreading motility", and "swarming motility"<sup>[33]</sup>. Along with urease activity, flagellar motility has been shown to be an essential factor for colonization of the gastric mucosa<sup>[34]</sup>. There are also studies which demonstrate the utmost importance of flagella in the formation of microbial biofilms on the surface of the gastric mucosa<sup>[35,36]</sup>.

Bacterial adhesion is the key stage of colonization, which determines a whole set of processes of gastric *H. pylori* persistence. The literature describes adhesion molecules (outer membrane proteins), such as blood-antigen-binding protein A, sialic acid-binding adhesin, neutrophil-activating protein, heat shock protein (Hsp) 60, adherence-associated proteins (AlpA and AlpB), *H. pylori* outer membrane protein, and LacDiNAc binding adhesin<sup>[28,37-40]</sup>. Among the key factors of colonization, virulence factors that have a direct damaging effect on the gastric mucosal epithelium can be separated out; these are cagA,  $\gamma$ -glutamine transferase, high-temperature requirement A, and vacuolating cytotoxin A (vacA)<sup>[38,39]</sup>.

CagA is a highly antigenic protein with a molecular weight of 120-145 kDa<sup>[41,42]</sup>. The locus of a gene responsible for the synthesis of cagA and a type IV secretion system (T4SS) is named *the cag pathogenicity island*<sup>[38]</sup>. CagA acts intracellularly through the epithelial cells *via* the T4SS: The latter forms a syringe-like pilus structure, through which the cagA molecule enters the host epithelial cell<sup>[40]</sup>. After translocation into the cell, cagA undergoes phosphorylation on the inner side of the cytoplasmic membrane of an epithelial cell and thus acquires biochemical activity<sup>[43]</sup>. It was found experimentally that cagA phosphorylation-competent mice developed cancers, such as gastrointestinal adenocarcinoma, myeloid leukemia, and B-cell lymphoma. Moreover, these pathogenic processes were not observed in phosphorylation-resistant forms<sup>[44]</sup>. The main pathogenetic effect of cagA is to enhance the mitotic activity of gastric epithelial cells, which contributes to malignancy if the microbe persists long-term<sup>[43,45]</sup>.

VacA is a protein with a molecular weight of 88 kDa, which consists of two subunits (p33 and p55) and has multiple pathogenetic effects<sup>[43]</sup>. After protein internalization, large pores are formed in the cytoplasmic membrane of gastric epithelial cells, which makes the cells more susceptible to the effects of bacterial urease<sup>[46]</sup>. Beyond that point, the launch of a cascade of biochemical reactions promotes the accumulation of large vacuoles inside the cells, which leads to the functional inferiority of epithelial cells. Through the intracellular transporter system, vacA is able to enter the mitochondria, where it disrupts the integrity of the inner mitochondrial membrane. This induces a drop in the mitochondrial transmembrane potential ( $\Delta\Psi_m$ ) with the subsequent release of cytochrome C and the activation of the proapoptotic factor Bcl-2 associated X protein<sup>[47]</sup>. There are data showing that vacA is involved in avoiding a pronounced immune response to the entry of an infectious agent. This is achieved by both the reduction in the activation of T lymphocytes in the lamina propria and disruption of the autophagy process<sup>[48]</sup>.

### **Immune response to *H. pylori* invasion**

When entering the human body, *H. pylori* is constantly controlled by the immune system. The inflammatory response is well-known to be a marker for a developing immune response. In *H. pylori* persistence, the focus of inflammation primarily affects gastric epithelial cells; in this case the inflammatory reaction involves neutrophils, lymphocytes, macrophages, and dendritic cells (DCs), which migrate to the site of infection through the systemic circulation<sup>[49,50]</sup>.

The contact of DCs with *H. pylori* antigenic determinants results in autocrine activation of the pool of immature CD4<sup>+</sup> T cells, followed by their differentiation into T-helper (Th) 1 lymphocytes through interleukin (IL)-12 production<sup>[51]</sup>. There are Th1 lymphocytes that are the major inflammatory effector cells for *H. pylori* invasion<sup>[52]</sup>. In addition, proinflammatory cytokines, such as IL-1, IL-6, tumor necrosis factor (TNF)- $\alpha$ , and interferon (IFN)- $\gamma$ , are involved in the immune response<sup>[53]</sup>.

The initial Th1 cell immune response is aimed at completely eradicating the

infectious agent. However, it has been shown experimentally that *vacA* is able to exert an immunosuppressive effect on the cells of the immune system, by inhibiting the production of IL-23 by DCs<sup>[54]</sup>. Furthermore, *H. pylori* HspB is capable of inhibiting the proliferation of mitogen-stimulated T cells, by enhancing the suppressive effects of regulatory T (Treg) cells in both innate and adaptive immune responses<sup>[55,56]</sup>.

The interaction of *H. pylori* with Th2 lymphocytes is not obvious. Due to the activation of the Th1 cellular component of the immune system, the Th2 cellular pathway for differentiation of immature lymphocytes is not believed to play a considerable role in the immune response<sup>[52]</sup>. At the same time, it has been proven that the level of immunoglobulin G (IgG) is a reliable indicator of *H. pylori* persistence. In infected individuals, a Th2 response induces IgG1 production while a Th1 response contributes to a significant increase in the overall levels of IgG2 through IL-2 and IFN- $\gamma$  production. IgG2 titers are higher than IgG1 titers in *H. pylori*-infected patients, particularly in those with ulcer disease<sup>[57]</sup>.

Thus, the persistence of *H. pylori* in the human body is accompanied by the pronounced immune response to bacterial invasion, which is subsequently replaced by immune tolerance. This fact may suggest that the relationship between *H. pylori* and the host is symbiotic.

### ***H. pylori*-associated diseases**

The currently available data may suggest that *H. pylori* persistence in the stomach is associated with the development of gastroduodenal diseases, such as chronic gastritis, PUD, gastric adenocarcinoma, and gastric MALT lymphoma<sup>[3,28,58,59]</sup>. Recent data show a statistically significant relationship between *H. pylori* detection and pancreatic cancer development<sup>[60,61]</sup>.

The risk of developing symptoms of a gastrointestinal disease depends on the degree of pathogenic properties in a persistent strain, the genetic characteristics of the host, environmental factors, and the pattern of diet<sup>[62,63]</sup>. The researchers emphasize the fact that the persistence of *H. pylori* in the gastric mucosa is constantly controlled by the immune system, as a result of which the pathogenic properties of *H. pylori* and, as a consequence, the symptoms of the disease manifest in the presence of favorable factors. Beyond that point, more and more attention is paid to the implication of *H. pylori* in the pathogenesis of extragastric diseases. Thus, the role of the microorganism in developing a number of neurological, cardiovascular, hematological, skin, and metabolic diseases is being actively investigated<sup>[62-66]</sup>. The results of the available studies are undoubtedly quite contradictory and require a more thorough study.

The meta-analysis by Wang *et al*<sup>[67]</sup> demonstrated that chronic *H. pylori* infection is a predictor for the possible development of ischemic brain injury. Reports suggesting a relationship between *H. pylori* detection and Alzheimer's disease development have been published<sup>[68,69]</sup>. Huang *et al*<sup>[70]</sup> were able to establish that the risk of Parkinson's disease was significantly higher in the *H. pylori*-positive group than in the *H. pylori*-negative (HPN) group (adjusted hazard ratio: 2.29, 95%CI: 1.44-3.66;  $P < 0.001$ ).

Little experience has been accumulated in studying the effects of *H. pylori* on the development of cardiovascular diseases. Some studies confirm a significant relationship between the detection of *H. pylori*, the development of atherosclerotic vascular lesions, and, as a consequence, a higher risk of coronary heart disease<sup>[71-74]</sup>. Jukic *et al*<sup>[73]</sup> found that *H. pylori*-positive patients more often suffered from hypertension ( $P = 0.014$ ), had higher systolic ( $P = 0.043$ ) and diastolic ( $P = 0.005$ ) blood pressure, as well as elevated plasma triglyceride levels ( $P = 0.013$ ) and a low antiatherogenic high-density lipoprotein level ( $P = 0.01$ ). At the same time, there was no significant difference in the severity of the disease between the two groups.

Vijayvergiya *et al*<sup>[75]</sup> described the considered hypotheses on the mechanisms of endothelial dysfunction in *H. pylori* infection. Some hypotheses state that pathophysiological changes in the microvascular bed result from a secondary increase in homocysteine levels: *H. pylori* induces vitamin B<sub>12</sub> and folic acid malabsorption, by elevating the homocysteine level that negatively affects the endothelium<sup>[76,77]</sup>. The theory of cytokine-induced vascular wall injury, which in turn is the first stage of atherosclerotic changes, should also be actively studied. The work by Rasmi *et al*<sup>[78]</sup> confirmed that *H. pylori* *cagA*-positive patients with cardiac syndrome X were found to have increased IL-1 and TNF- $\alpha$  levels. The experimental data obtained by de Jesus Souza *et al*<sup>[79]</sup> showed that urease is a potent stimulus for endothelial cell production of reactive oxygen species and NO, which also leads to the enhanced production of nuclear factor kappa B, activation and upregulated expression of cyclooxygenase-2, heme oxygenase-1, IL-1 $\beta$ , and intercellular adhesion molecule-1. Such experimentally established changes in the pro-inflammatory molecule profile can indirectly indicate the possible pathogenetic features of *H. pylori*-induced injury to the vascular bed.



An association between *H. pylori* infection and skin diseases is being actively studied. Yu *et al*<sup>[80]</sup> provided evidence that the detection rate of *H. pylori* was 49.5% among 1038 representatives in a study group (patients diagnosed with psoriasis), while the rate was 38.8% in a control group ( $n = 703$ ) (the pooled OR was 1.70; 95%CI: 1.15-2.52;  $P = 0.008$ ). Onsun *et al*<sup>[81]</sup> concluded that *H. pylori* was detected in 184 (61.3%) individuals among 300 patients with psoriasis and in 89 (59.3%) representatives in a control group (among 150 healthy people). At the same time, it was noted that the disease severity, as assessed by the Psoriasis area and severity index scores, was noted to be significantly higher in *H. pylori*-positive patients. The literature provides a large number of reports on *H. pylori* detection in patients who, in addition to psoriasis, have lichen ruber planus, scabies, rosacea, Sweet's syndrome, Behcet's disease, and Schönlein-Henoch purpura<sup>[82]</sup>.

It should be noted that antibacterial drug manufacturers have an impact on more attention to the pathogenic properties of *H. pylori* and mass (program) eradication therapy<sup>[3]</sup>.

## IS EVERYTHING SO CLEAR?

### **Rare development of symptoms with high prevalence in the population**

Following the discoveries by R. Warren and B.J. Marshall, the concept of pathogenesis and treatment regimens for PUD implied mainly the identification and eradication of *H. pylori*. It is currently known that the occurrence of *H. pylori* is high in the healthy population (about 50% of the population worldwide and more than 70% of that in developing countries)<sup>[2]</sup>. *H. pylori* infection is usually acquired in childhood and generally persists lifelong. Thus *H. pylori* has infected the majority of the world's population for the majority of their lifetime and in most cases causes no symptoms<sup>[3,83]</sup>. The infectious process in *H. pylori* is chronic and only one in ten colonized individuals; most commonly the elderly, develop clinical manifestations years later<sup>[2]</sup>. Tsimmerman<sup>[43]</sup> reported that less than 1% of individuals infected with *H. pylori* develop various diseases and about 70% of people who are found to have the bacterium are healthy bacterial carriers. The available data show that only 5%-10% of those infected develop symptoms of gastritis or PUD<sup>[84-87]</sup>. Moreover, the review data (Araújo *et al*<sup>[88]</sup>) indicate that the detection rate of *H. pylori* infection in patients diagnosed with PUD does not differ from that of *H. pylori* in the general population. The authors also noted that in 20%-50% of cases of PUD, they are unable to identify the overarching etiological factor of an ulcerative lesion, that is to say, an idiopathic ulcer (*H. pylori* negative, non-steroidal anti-inflammatory drug-negative peptic ulcer/NSAIDs). Sidorenko<sup>[89]</sup> stated that the given facts provide a strong argument that refutes the leading role of *H. pylori* in the development of gastroduodenal diseases. The wide spread of *H. pylori* infection among individuals without signs of pathology and the low incidence rate during chronic colonization of the gastric mucosa clearly indicate that *H. pylori* is more likely to be an opportunistic or latent pathogen than a truly pathogenic bacterium.

The presented data suggest that the infectious theory of chronic gastritis, PUD, and GC seems to be rather an exception to the rule. In addition, the severity of chronic gastritis and/or PUD appears to be directly related to other etiological factors, along with the density of *H. pylori* contamination.

### ***H. pylori* and PUD**

PUD is a chronic multifactorial disease characterized by an imbalance between the aggressive components of the gastroduodenal contents and the protective mechanisms of the gastric mucosa. A significant role in the pathophysiological changes characteristic of PUD is played by important components, such as hereditary predisposition, psychoemotional and psychosocial stress effects, autonomic dysfunction, local pathogenetic effects (acidity of the stomach contents), immunodeficiency state, oxidative stress, smoking, excessive alcohol consumption, and the use of steroid drugs and nonsteroidal anti-inflammatory drugs<sup>[87,90]</sup>. In their review, Malfertheiner *et al*<sup>[87]</sup> focused on the fact that the development of PUD depends on the complex influence and/or a combination of both exo- and endogenous factors. In addition to the above described exogenous factors, the most important endogenous components of ulcerogenesis are the level and adequate function of enteric hormones (gastrin, somatostatin), genetic predisposing factors (the number of parietal cells, the basal level of gastric hydrochloric acid secretion, and defects in bicarbonate secretion). Such observations show that the presence of *H. pylori* infection may be only one (but

far short of being single) component in the genesis of ulcerative disorders.

It is essential to also recall the fact that in the case of *Helicobacter* etiology, the risk of developing the disease depends on the genotype of *H. pylori*: The patients with a confirmed diagnosis of PUD were found to have *vacA*-positive and *cagA*-positive genotypes<sup>[91,92]</sup>. At the same time, the genotypes containing the *vacA* gene are known to account for about 60% of all detected forms of *Helicobacter*<sup>[93]</sup>.

In addition to *H. pylori*-associated ulcers, the current classification identifies tumor ulcers, ulcerative lesions in Zollinger-Ellison syndrome, Crohn's disease, eosinophilic gastroenteritis, radiation damage, and viral infections (cytomegalovirus or herpesvirus infection in immunocompromised patients). The idiopathic form occupies a separate place<sup>[87]</sup>.

Interestingly, epidemiological studies in recent years demonstrate a progressive increase in the idiopathic forms of PUD with a decrease in the global prevalence of *H. pylori* infection<sup>[94,95]</sup>. Thus, Indian researchers have shown that 45.9% of cases of peptic ulcers of the stomach and 29.6% of those of the duodenum are idiopathic (they are unassociated with either *H. pylori* detection or a history of steroid/NSAID intake)<sup>[96]</sup>.

Reshetnyak *et al.*<sup>[97]</sup> presented data on the role of *H. pylori* and drugs in the development of gastric mucosal (GM) lesions in patients with systemic lupus erythematosus (SLE) and antiphospholipid syndrome (APS). Endoscopic examinations of patients with SLE and APS revealed the following GM changes: antral gastritis (82.4%), erosion (24.7%), hemorrhages (8.2%), and pangastritis (8.2%). The rate of *H. pylori* infection in patients with SLE and APS corresponded to that in the general population. The authors' data showed that there was no direct correlation between the observed GM changes and *H. pylori* infection. However, therapy with glucocorticoid, low-dose acetylsalicylic acid, NSAIDs, and anticoagulants was in this case responsible for GM damage in patients with SLE and APS.

There is evidence suggesting the most favorable course of *H. pylori*-associated ulcers compared with other diagnosed types. Kanno *et al.*<sup>[98]</sup> established that among 382 examinees diagnosed with PUD, the patients with a confirmed diagnosis of *H. pylori*-positive ulcer had a statistically significant increase in healing rates. In the study, the patients were divided into 4 groups: A simple *H. pylori* group; a *H. pylori* (+)/NSAIDs (+) group; a simple NSAIDs group; and an idiopathic ulcer (IPU) group. Indicators, such as healing rates at 3 mo, treatment course, and recurrence rates, were estimated. According to the data presented, the healing rates in these groups were distributed as follows: 95.0%, 94.9%, 73.3%, and 77.4%, respectively. This indicator for idiopathic forms was statistically significantly different ( $P < 0.01$ ). The recurrence rate in the IPU group was also much higher: 13.9% in the IPU group and 2.1% in the simple *H. pylori* group ( $P < 0.01$ ). The cumulative recurrence rates estimated by the Kaplan-Meier method were also significantly higher in the IPU group than those in the simple *H. pylori* group ( $P = 0.015$ ).

Rasane *et al.*<sup>[99]</sup> demonstrated that patients with HPN PUD had a more pronounced severe course of the disease and a more negative prognosis than those with *H. pylori*-associated forms. Thus, albumin levels in the HPN group were higher than those in the *H. pylori*-positive group: 2.97-0.96 *vs* 3.86-0.91,  $P = 0.0001$ . The same pattern was observed when evaluating the patients' state on admission to hospital: In the HPN group, the scores of scales, such as the American Society of Anesthesiologists scoring system and the Charlson comorbidity index, were much higher: 3.11-0.85 *vs* 2.60-0.73 ( $P = 0.005$ ) and 4.81-2.74 *vs* 2.98-2.71 ( $P = 0.004$ ), respectively. There were also significant differences in indicators, such as hospital length of stay: 20.20-13.82 *vs* 8.48-7.24;  $P = 0.0001$  and 30 d readmission rate (11; 29.73% *vs* 5; 11.91%;  $P = 0.049$ ).

The diversity of causes that lead to the ulcerative process allows PUD to be considered as a polyetiological and polypathogenetic disease. When *H. pylori* was discovered, there were many theories of PUD development: Vascular, stomach inflammatory, allergic, hormonal, motor-primacy, corticovisceral, neurogenic, psychosomatic, and acidopeptic theories. Each of them deserves attention, as it reflects one of the facets of this complex problem. The above data suggest that for people who are predisposed to this pathology, the emergence of an infectious theory has become an important and significant addition to the already existing etiological factors. Also, not in all cases, but only in a certain state of the macroorganism, *H. pylori* becomes a pathogen and is an additional cause of chronic gastritis, PUD, and even GC.

### ***H. pylori* and GC**

GC occupies one of the leading places in the pattern of cancers. Epidemiological studies have demonstrated that GC develops in *H. pylori*-infected people 1.4-4.2 times more often than in the general population<sup>[100-102]</sup>. At the same time it should be noted that GC develops only in 1%-2% of cases with a 50% or more frequency of gastric

colonization with *Helicobacter* worldwide<sup>[13,103]</sup>. Among the population of India and Africa, where the *H. pylori* infection rates reach 90%-95%, GC is diagnosed much less frequently than in Western Europe and the United States, where the prevalence of *H. pylori* does not exceed 35%-50%<sup>[104]</sup>. The carcinogenic potential of *H. pylori* is rather ambiguous: It has been found that *H. pylori* toxins do not exert a direct mutagenic effect on gastric epithelial cells<sup>[105]</sup>. Virulence factors have been described in *H. pylori*, but the presence or absence of these factors is not critical in disease development<sup>[2]</sup>. In addition, there is evidence that *H. pylori* persistence increases the risk of developing only distal (pyloroantral) GC, whereas proximal (cardiac) GC is unassociated with *H. pylori*. Moreover, antral colonization with *H. pylori*, especially with its *cagA*-positive strains, somehow prevents the development of cardiac GC and carcinoma of the lower third of the esophagus, performing a protective function<sup>[106]</sup>. Rokkas *et al*<sup>[107]</sup> called the relationship between *H. pylori* infection and subsequent GC development an unclear epidemiological paradox.

Blaser<sup>[108]</sup> has stated his belief that there is a certain balance between the negative and positive effects of *H. pylori* on humans. Some authors consider that *H. pylori* shows its pathogenicity, by regulating the expression of different genes to the extent that is dictated by the response of a macroorganism<sup>[109,110]</sup>. Thus, the microorganism and the macroorganism create a finely tuned balance system, the resulting impairment of which develops a specific disease with certain clinical signs and prognosis<sup>[111]</sup>. In the vast majority of cases, long-lasting *H. pylori* infection induces chronic gastritis, while only some patients develop PUD and GC. For this reason, the bacterium is considered to be a risk factor for the development and recurrence of PUD and GC<sup>[112,113]</sup>. Therefore, *H. pylori* is assigned to the group of pathogenic bacteria. However, it would be more correct to treat only those individuals at high risk for GC or to establish programs for early detection of GC without implementing massive eradication programs for this bacterium that may be important to colonize the gastric stomach of young humans<sup>[2]</sup>.

## BENEFICIAL “PROTECTIVE ROLE” OF *H. PYLORI*

### *H. pylori* and asthma

The literature in recent years has enough works, the results of which suggest that there is an inverse correlation between the persistence of *H. pylori* and the detection of asthma cases<sup>[8,114-117]</sup>.

Chen *et al*<sup>[8]</sup> reported that the detection of *H. pylori* in young and middle-aged patients (mean age 25 years) is inversely correlated not only with asthma, but also with other atopic diseases (dermatitis, atopic rash, and eczema). These researchers found a strong inverse relationship between the detection of *H. pylori* and the early onset of asthma ( $\leq 5$  years old): OR = 0.58; 95%CI: 0.38-0.88. The difference in the patients' current status was also statistically significant: Asthma was observed less frequently in patients with detected *H. pylori* infection ( $P = 0.03$ ). Elias *et al*<sup>[115]</sup> showed that 25% and 40% of children were seropositive for IgG in the study and control groups, respectively ( $P = 0.03$ ) (the children's age ranged from 4.8 to 17.3 years). Interestingly, *cagA* IgG seropositivity was associated with a low risk of asthma [adjusted OR 0.30 (95%CI: 0.10-0.87)]. However, this pattern was not found for *cagA*-negative serology [adjusted OR = 0.64 (95%CI: 0.30-1.37)]. As in a previous study, *H. pylori* seropositive children had a lower likelihood of asthma than seronegative children [adjusted OR = 0.29 (95%CI: 0.10-0.82)].

Greek colleagues found that the detection rate of *H. pylori* was 11.1% in children aged  $8.6 \pm 4.5$  years with asthma symptoms, while it was 29.6% in the control group of the same age without bronchial obstruction symptoms (OR = 0.1; 95%CI: 0.039-0.305;  $P = 0.026$ )<sup>[109]</sup>. This correlation has been confirmed by a number of other earlier studies<sup>[118,119]</sup>.

Oertli *et al*<sup>[120]</sup> investigated in detail and described the mechanism of anti-atopic action of *Helicobacter*. Their study indicated that immune tolerance could be acquired due to the immune system's constant response to bacterial  $\gamma$ -glutamyl transpeptidase (GGT) and *vacA*. At the same time, there was a gradual maturation of DCs and their more targeted interaction with Treg cells, which contributed to the more targeted autoactivation of the lymphocyte pool to various antigens. Such mechanisms ultimately result in immune tolerance to benign antigens (allergens). Special attention should also be paid to the fact that isogenic *H. pylori* mutants lacking either GGT or *vacA* are incapable of preventing DC maturation and fail to drive DC tolerization as assessed by induction of Treg properties in cocultured naive T cells.

Pachathundikandi *et al*<sup>[121]</sup> associated the phenomenon of tolerance with the ability

of *H. pylori* antigens to activate inflammasomes and to stimulate the production of cytokines, such as IL-1b and IL-18. The authors argue that such cytokine regulation assists in reducing the hyper-reactivation of the immune system and, as a consequence, prevents the development of both asthma and inflammatory bowel diseases.

### ***H. pylori* and inflammatory bowel diseases**

The negative association between *H. pylori* persistence and inflammatory bowel diseases (IBD) development has also been studied for a long time. *H. pylori* persistence may be supposed to be a potentially beneficial factor against the development of IBD. Several large meta-analyses have concluded that the risk of IBD is higher in HPN patients<sup>[122]</sup>. Wu *et al*<sup>[123]</sup> showed that 24.9% of IBD patients had *H. pylori* infection *vs* 48.3% of the controls. The pooled risk ratio for *H. pylori* infection in IBD patients compared with the controls was 0.48 (95%CI: 0.43-0.54;  $P < 0.001$ ). Rokkas *et al*<sup>[124]</sup> obtained similar results: 26.5% (95%CI: 25.2-27.8) of IBD patients were positive for *H. pylori* infection, compared to 44.7% (43.3%-46.1%) of individuals in the control group. In the literature, there are also studies proving that *H. pylori* eradication leads to the development of intestinal lesions<sup>[125]</sup>. However, there is also a contradiction in the accumulated data, since existing studies link *H. pylori* infection with the development of colorectal cancer<sup>[126]</sup>.

### ***H. pylori* and GERD**

In addition to the impact of *H. pylori* infection on the development of atopic reactions, considerable attention has been paid to the detection of *H. pylori* in patients with GERD. There remain a number of controversial points around the question of how eradication therapy affects the development or progression of GERD symptoms. The available data are rather contradictory and do not give a general insight into the problem. In their studies, a number of authors prove that there is no significant difference between *H. pylori*-positive and HPN patients and the development of GERD symptoms in these patients<sup>[127,128]</sup>. Thus, on the basis of their study, Bor *et al*<sup>[127]</sup> have come to the conclusion that the detection of *H. pylori* does not affect either the development of GERD symptoms or the severity of the disease course. The detection rate of *H. pylori* was 77.1% in asymptomatic patients *vs* 71.4% in GERD patients ( $\chi^2 = 2.6$ ;  $P = 0.27$ ). Xue *et al*<sup>[129]</sup> believe that eradication therapy fails to affect esophageal mucosal changes; therefore, there is no association with *H. pylori*. In their study, the investigators divided patients with endoscopically confirmed GERD into 2 groups (*H. pylori*-positive and HPN patients, respectively). The *H. pylori*-positive group received eradication therapy before treatment with proton pump inhibitors (10 d eradication, then esomeprazole 20 mg bid for 46 d). The other group was treated only with proton pump inhibitors (esomeprazole 20 mg bid therapy for 8 wk). As a result, there were 176 *H. pylori*-positive cases (with 92 eradication cases) and 180 negative cases. The healing rates in the *H. pylori*-positive eradicated group and the *H. pylori*-positive non-eradicated group reached 80.4% and 79.8%, respectively ( $P = 0.911$ ), with reflux symptom scores of 0.22 and 0.14 ( $P = 0.588$ ). The healing rates of esophagitis in the *H. pylori*-positive non-eradicated group and the *H. pylori*-negative group were 79.8 and 82.2%, respectively ( $P = 0.848$ ); the reflux symptom scores were 0.14 and 0.21 ( $P = 0.546$ ).

At the same time, contrary cases have been also described. The meta-analysis by Zhao *et al*<sup>[130]</sup> demonstrated that eradication therapy can lead to erosive GERD: The OR for the development of erosive GERD after *H. pylori* eradication was 1.67 (95%CI: 1.12-2.48;  $P = 0.01$ ). Chung *et al*<sup>[131]</sup> revealed a clear inverse relationship between the detection of *H. pylori* and GERD: The prevalence of *H. pylori* infection was lower in cases with reflux esophagitis than in the controls (38.4% *vs* 58.2%,  $P < 0.001$ ). The severity of esophagitis was also found to be inversely correlated with the detection of *H. pylori*. It is anticipated that *H. pylori* urease activity contributes to the neutralization of gastric acidity and, therefore, reduces the risk of acid reflux disease<sup>[132]</sup>.

There are studies indicating the possible positive effect of *H. pylori* on the human body. In this connection, *H. pylori* in the majority of bacteria carriers can probably be attributed to bacteria that colonize the human body and constitute a population of commensal bacteria that use the host for their vital activity, but do not exhibit their pathogenic properties (as their persistence is under strict control by the host immune system). Such relationships between commensal bacteria and humans are typified by co-evolution, co-adaptation, and interactions<sup>[133]</sup>. Taking into account immune tolerance to *H. pylori* in the presence of long-term persistence in the host, the microorganism can also be considered as a symbiont<sup>[13]</sup>.



## CONCLUSION

The presented data suggest that there is clear ambiguity related to the problem of studying the mechanisms of ulcerogenesis, and the role of *H. pylori* in the processes of ulceration and carcinogenesis. On this basis, the management strategies for these inpatients are extremely difficult for clinicians. It is evident that a complete understanding of the mechanisms of inflammatory gastroduodenal mucosal injuries requires a more thorough approach, by considering the infectious and noninfectious, exogenous and endogenous factors, and an evaluation of the pathogenic and positive effects of *H. pylori* on human vital processes. Given the discussions surrounding the active eradication of *H. pylori* from the human population<sup>[134]</sup>, it is more important than ever to critically assess its role within the microbiome. There is no coordinated attempt to eradicate these organisms from the human population; Malnick *et al*<sup>[9]</sup> suggested that there should not be a similar effort to eradicate *H. pylori*. Considering the growing number of publications on the potentially positive effects of the microorganism on the human body, it is not improbable that *H. pylori* is one of the bacteria in the healthy microbiome for the majority of the human population. There is a complex biological relationship between humans and commensal bacteria that is only now beginning to be understood. To better understand the mutualistic (*mutual* from Latin) role of *H. pylori* in cohorts at low risk for *H. pylori*-associated diseases, more investigations are needed to qualitatively and quantitatively estimate its benefits in healthy humans<sup>[132]</sup>.

The manifestation of the pathogenic properties of *H. pylori*, which is characteristic of a smaller proportion of the human population having a genetic predisposition to develop gastrointestinal diseases, requires a reassessment of the available data on *H. pylori* infection. The “test and treat” approach to *H. pylori* does not address this issue at all<sup>[9]</sup>. It may be that the more correct way is an individualized approach to the patient according to the *H. pylori* endemic region, the presence of gastrointestinal diseases among relatives, or the impossibility of excluding nonmodifiable risk factors. Therefore, the most correct approach will be used to consider *H. pylori* persistence in terms of the possible positive role of the bacterium in the body and, therefore, to perform more individualized eradication therapy in the context of assessment of additional risk factors. Answers to such considerations should be obtained during further research.

## ACKNOWLEDGEMENTS

The authors would like to express their gratitude to Aglaya Svyatoslavovna Yakovleva for technical assistance in preparing this article.

## REFERENCES

- 1 **Fernandes YC**, Bonatto Gda R, Bonatto MW. Recurrence rate of *Helicobacter pylori* in patients with peptic ulcer five years or more after successful eradication. *Arq Gastroenterol* 2016; **53**: 152-155 [PMID: 27438419 DOI: 10.1590/S0004-28032016000300006]
- 2 **Li J**, Perez-Perez GI. *Helicobacter pylori* the Latent Human Pathogen or an Ancestral Commensal Organism. *Front Microbiol* 2018; **9**: 609 [DOI: 10.3389/fmicb.2018.00609]
- 3 **Malnick SD**, Melzer E, Attali M, Duek G, Yahav J. *Helicobacter pylori*: friend or foe? *World J Gastroenterol* 2014; **20**: 8979-8985 [PMID: 25083071 DOI: 10.3748/wjg.v20.i27.8979]
- 4 **McColl KE**. Clinical practice. *Helicobacter pylori* infection. *N Engl J Med* 2010; **362**: 1597-1604 [PMID: 20427808 DOI: 10.1056/NEJMcp1001110]
- 5 **Crowe SE**. *Helicobacter pylori* Infection. *N Engl J Med* 2019; **380**: 1158-1165 [PMID: 30893536 DOI: 10.1056/NEJMcp1710945]
- 6 **Everhart JE**. Recent developments in the epidemiology of *Helicobacter pylori*. *Gastroenterol Clin North Am* 2000; **29**: 559-578 [PMID: 11030073 DOI: 10.1016/s0889-8553(05)70130-8]
- 7 **Haruma K**, Okamoto S, Kawaguchi H, Gotoh T, Kamada T, Yoshihara M, Sumii K, Kajiyama G. Reduced incidence of *Helicobacter pylori* infection in young Japanese persons between the 1970s and the 1990s. *J Clin Gastroenterol* 1997; **25**: 583-586 [PMID: 9451667 DOI: 10.1097/00004836-199712000-00006]
- 8 **Chen Y**, Blaser MJ. *Helicobacter pylori* colonization is inversely associated with childhood asthma. *J Infect Dis* 2008; **198**: 553-560 [PMID: 18598192 DOI: 10.1086/590158]
- 9 **Eder W**, Ege MJ, von Mutius E. The asthma epidemic. *N Engl J Med* 2006; **355**: 2226-2235 [PMID: 17124020 DOI: 10.1056/NEJMra054308]
- 10 **Holster IL**, Vila AM, Caudri D, den Hoed CM, Perez-Perez GI, Blaser MJ, de Jongste JC, Kuipers

- EJ. The impact of *Helicobacter pylori* on atopic disorders in childhood. *Helicobacter* 2012; **17**: 232-237 [PMID: 22515362 DOI: 10.1111/j.1523-5378.2012.00934.x]
- 11 **Rothenbacher D**, Blaser MJ, Bode G, Brenner H. Inverse relationship between gastric colonization of *Helicobacter pylori* and diarrheal illnesses in children: results of a population-based cross-sectional study. *J Infect Dis* 2000; **182**: 1446-1449 [PMID: 11015236 DOI: 10.1086/315887]
  - 12 **Hunt RH**, Yaghoobi M. The Esophageal and Gastric Microbiome in Health and Disease. *Gastroenterol Clin North Am* 2017; **46**: 121-141 [PMID: 28164846 DOI: 10.1016/j.gtc.2016.09.009]
  - 13 **Tsimmerman YS**. [Critical analysis of the *Helicobacter pylori*-infection leading role in the development of gastroduodenal diseases]. *Clin Pharmacol Ther* 2019; **28**: 19-27
  - 14 **Kanizaj TF**, Kunac N. *Helicobacter pylori*: future perspectives in therapy reflecting three decades of experience. *World J Gastroenterol* 2014; **20**: 699-705 [PMID: 24574743 DOI: 10.3748/wjg.v20.i3.699]
  - 15 **Reshetnyak VI**, Reshetnyak TM. Significance of dormant forms of *Helicobacter pylori* in ulcerogenesis. *World J Gastroenterol* 2017; **23**: 4867-4878 [PMID: 28785141 DOI: 10.3748/wjg.v23.i27.4867]
  - 16 **Christopher JA**, Abiodun OJ. *Helicobacter pylori* infection: past, present and future. *Pan Afr Med J* 2016; **23**: 216 [DOI: 10.11604/pamj.2016.23.216.8852]
  - 17 **de Bernard M**, Josenhans C. Pathogenesis of *Helicobacter pylori* infection. *Helicobacter* 2014; **19** Suppl 1: 11-18 [PMID: 25167940 DOI: 10.1111/hel.12160]
  - 18 **Stark RM**, Suleiman MS, Hassan IJ, Greenman J, Millar MR. Amino acid utilisation and deamination of glutamine and asparagine by *Helicobacter pylori*. *J Med Microbiol* 1997; **46**: 793-800 [PMID: 9291892 DOI: 10.1099/00222615-46-9-793]
  - 19 **Mentis A**, Lehours P, Mégraud F. Epidemiology and Diagnosis of *Helicobacter pylori* infection. *Helicobacter* 2015; **20** Suppl 1: 1-7 [PMID: 26372818 DOI: 10.1111/hel.12250]
  - 20 **Luzza F**, Suraci E, Larussa T, Leone I, Imeneo M. High exposure, spontaneous clearance, and low incidence of active *Helicobacter pylori* infection: the Sorbo San Basile study. *Helicobacter* 2014; **19**: 296-305 [PMID: 24758553 DOI: 10.1111/hel.12133]
  - 21 **Burucoa C**, Axon A. Epidemiology of *Helicobacter pylori* infection. *Helicobacter* 2017; **22** Suppl 1 [PMID: 28891138 DOI: 10.1111/hel.12403]
  - 22 **Hooi JKY**, Lai WY, Ng WK, Suen MMY, Underwood FE, Tanyingoh D, Malfertheiner P, Graham DY, Wong VWS, Wu JCY, Chan FKL, Sung JY, Kaplan GG, Ng SC. Global Prevalence of *Helicobacter pylori* Infection: Systematic Review and Meta-Analysis. *Gastroenterology* 2017; **153**: 420-429 [PMID: 28456631 DOI: 10.1053/j.gastro.2017.04.022]
  - 23 **Tsimmerman IaS**. [The problem of growing resistance of microorganisms to antibiotic therapy and prospects for *Helicobacter pylori* eradication]. *Klin Med (Mosk)* 2013; **91**: 14-20 [PMID: 24417061]
  - 24 **Kayali S**, Manfredi M, Gaiani F, Bianchi L, Bizzarri B, Leandro G, Di Mario F, De' Angelis GL. *Helicobacter pylori*, transmission routes and recurrence of infection: state of the art. *Acta Biomed* 2018; **89**: 72-76 [PMID: 30561421 DOI: 10.23750/abm.v89i8-S.7947]
  - 25 **Mladenova I**, Durazzo M. Transmission of *Helicobacter pylori*. *Minerva Gastroenterol Dietol* 2018; **64**: 251-254 [PMID: 29458239 DOI: 10.23736/S1121-421X.18.02480-7]
  - 26 **Zamani M**, Vahedi A, Maghdouri Z, Shokri-Shirvani J. Role of food in environmental transmission of *Helicobacter pylori*. *Caspian J Intern Med* 2017; **8**: 146-152 [PMID: 28932364 DOI: 10.22088/cjim.8.3.146]
  - 27 **Sgambato D**, Visciola G, Ferrante E, Miranda A, Romano L, Tuccillo C, Manguso F, Romano M. Prevalence of *Helicobacter pylori* infection in sexual partners of *H. pylori*-infected subjects: Role of gastroesophageal reflux. *United European Gastroenterol J* 2018; **6**: 1470-1476 [PMID: 30574317 DOI: 10.1177/2050640618800628]
  - 28 **Kao CY**, Sheu BS, Wu JJ. *Helicobacter pylori* infection: An overview of bacterial virulence factors and pathogenesis. *Biomed J* 2016; **39**: 14-23 [DOI: 10.1016/j.bj.2015.06.002]
  - 29 **Marcus EA**, Sachs G, Scott DR. Acid-regulated gene expression of *Helicobacter pylori*: Insight into acid protection and gastric colonization. *Helicobacter* 2018; **23**: e12490 [PMID: 29696729 DOI: 10.1111/hel.12490]
  - 30 **Weeks DL**, Eskandari S, Scott DR, Sachs G. A H<sup>+</sup>-gated urea channel: the link between *Helicobacter pylori* urease and gastric colonization. *Science* 2000; **287**: 482-485 [PMID: 10642549 DOI: 10.1126/science.287.5452.482]
  - 31 **Schoep TD**, Fulurija A, Good F, Lu W, Himbeck RP, Schwan C, Choi SS, Berg DE, Mittl PR, Benghezal M, Marshall BJ. Surface properties of *Helicobacter pylori* urease complex are essential for persistence. *PLoS One* 2010; **5**: e15042 [PMID: 21124783 DOI: 10.1371/journal.pone.0015042]
  - 32 **Lowenthal AC**, Hill M, Sycuro LK, Mehmood K, Salama NR, Ottemann KM. Functional analysis of the *Helicobacter pylori* flagellar switch proteins. *J Bacteriol* 2009; **191**: 7147-7156 [PMID: 19767432 DOI: 10.1128/JB.00749-09]
  - 33 **Gu H**. Role of Flagella in the Pathogenesis of *Helicobacter pylori*. *Curr Microbiol* 2017; **74**: 863-869 [PMID: 28444418 DOI: 10.1007/s00284-017-1256-4]
  - 34 **Gupta N**, Maurya S, Verma H, Verma VK. Unraveling the factors and mechanism involved in persistence: Host-pathogen interactions in *Helicobacter pylori*. *J Cell Biochem* 2019; **120**: 18572-18587 [PMID: 31237031 DOI: 10.1002/jcb.29201]
  - 35 **Hathroubi S**, Zerebinski J, Ottemann KM. *Helicobacter pylori* Biofilm Involves a Multigene Stress-Biased Response, Including a Structural Role for Flagella. *mBio* 2018; **9**: e01973-18 [PMID: 30377283 DOI: 10.1128/mBio.01973-18]

- 36 **García A**, Salas-Jara MJ, Herrera C, González C. Biofilm and *Helicobacter pylori*: from environment to human host. *World J Gastroenterol* 2014; **20**: 5632-5638 [PMID: [24914322](#) DOI: [10.3748/wjg.v20.i19.5632](#)]
- 37 **Matsuo Y**, Kido Y, Yamaoka Y. *Helicobacter pylori* Outer Membrane Protein-Related Pathogenesis. *Toxins (Basel)* 2017; **9**: 101 [PMID: [28287480](#) DOI: [10.3390/toxins9030101](#)]
- 38 **Chang WL**, Yeh YC, Sheu BS. The impacts of *H. pylori* virulence factors on the development of gastroduodenal diseases. *J Biomed Sci* 2018; **25**: 68 [PMID: [30205817](#) DOI: [10.1186/s12929-018-0466-9](#)]
- 39 **Ricci V**, Giannouli M, Romano M, Zarrilli R. *Helicobacter pylori* gamma-glutamyl transpeptidase and its pathogenic role. *World J Gastroenterol* 2014; **20**: 630-638 [PMID: [24574736](#) DOI: [10.3748/wjg.v20.i3.630](#)]
- 40 **Javed S**, Skoog EC, Solnick JV. Impact of *Helicobacter pylori* Virulence Factors on the Host Immune Response and Gastric Pathology. *Curr Top Microbiol Immunol* 2019; **421**: 21-52 [PMID: [31123884](#) DOI: [10.1007/978-3-030-15138-6\\_2](#)]
- 41 **Tohidpour A**. CagA-mediated pathogenesis of *Helicobacter pylori*. *Microb Pathog* 2016; **93**: 44-55 [PMID: [26796299](#) DOI: [10.1016/j.micpath.2016.01.005](#)]
- 42 **Ansari S**, Yamaoka Y. Survival of *Helicobacter pylori* in gastric acidic territory. *Helicobacter* 2017; **22**: 10.1111/hel.12386 [PMID: [28402047](#) DOI: [10.1111/hel.12386](#)]
- 43 **Maleki Kakelar H**, Barzegari A, Dehghani J, Hanifian S, Saeedi N, Barar J, Omid Y. Pathogenicity of *Helicobacter pylori* in cancer development and impacts of vaccination. *Gastric Cancer* 2019; **22**: 23-36 [PMID: [30145749](#) DOI: [10.1007/s10120-018-0867-1](#)]
- 44 **Ohnishi N**, Yuasa H, Tanaka S, Sawa H, Miura M, Matsui A, Higashi H, Musashi M, Iwabuchi K, Suzuki M, Yamada G, Azuma T, Hatakeyama M. Transgenic expression of *Helicobacter pylori* CagA induces gastrointestinal and hematopoietic neoplasms in mouse. *Proc Natl Acad Sci USA* 2008; **105**: 1003-1008 [PMID: [18192401](#) DOI: [10.1073/pnas.0711183105](#)]
- 45 **Romano M**, Ricci V, Zarrilli R. Mechanisms of disease: *Helicobacter pylori*-related gastric carcinogenesis--implications for chemoprevention. *Nat Clin Pract Gastroenterol Hepatol* 2006; **3**: 622-632 [PMID: [17068500](#) DOI: [10.1038/ncpgasthep0634](#)]
- 46 **De Falco M**, Lucariello A, Iaquinto S, Esposito V, Guerra G, De Luca A. Molecular Mechanisms of *Helicobacter pylori* Pathogenesis. *J Cell Physiol* 2015; **230**: 1702-1707 [PMID: [25639461](#) DOI: [10.1002/jcp.24933](#)]
- 47 **Rassow J**, Meinecke M. *Helicobacter pylori* VacA: a new perspective on an invasive chloride channel. *Microbes Infect* 2012; **14**: 1026-1033 [DOI: [10.1016/j.micinf.2012.07.002](#)]
- 48 **Raju D**, Hussey S, Ang M, Terebiznik MR, Sibony M, Galindo-Mata E, Gupta V, Blanke SR, Delgado A, Romero-Gallo J, Ramjeet MS, Mascarenhas H, Peek RM, Correa P, Streutker C, Hold G, Kunstmann E, Yoshimori T, Silverberg MS, Girardin SE, Philpott DJ, El Omar E, Jones NL. Vacuolating cytotoxin and variants in Atg16L1 that disrupt autophagy promote *Helicobacter pylori* infection in humans. *Gastroenterology* 2012; **142**: 1160-1171 [PMID: [22333951](#) DOI: [10.1053/j.gastro.2012.01.043](#)]
- 49 **McGee DJ**, Mobley HL. Pathogenesis of *Helicobacter pylori* infection. *Curr Opin Gastroenterol* 2000; **16**: 24-31 [PMID: [17024012](#)]
- 50 **Suzuki T**, Kato K, Ohara S, Noguchi K, Sekine H, Nagura H, Shimosegawa T. Localization of antigen-presenting cells in *Helicobacter pylori*-infected gastric mucosa. *Pathol Int* 2002; **52**: 265-271 [PMID: [12031081](#)]
- 51 **Figueiredo CA**, Marques CR, Costa Rdos S, da Silva HB, Alcantara-Neves NM. Cytokines, cytokine gene polymorphisms and *Helicobacter pylori* infection: friend or foe? *World J Gastroenterol* 2014; **20**: 5235-5243 [PMID: [24833853](#) DOI: [10.3748/wjg.v20.i18.5235](#)]
- 52 **D'Elis MM**, Codolo G, Amedei A, Mazzi P, Berton G, Zanotti G, Del Prete G, de Bernard M. *Helicobacter pylori*, asthma and allergy. *FEMS Immunol Med Microbiol* 2009; **56**: 1-8 [PMID: [19220467](#) DOI: [10.1111/j.1574-695X.2009.00537.x](#)]
- 53 **Bimczok D**, Clements RH, Waites KB, Novak L, Eckhoff DE, Mannon PJ, Smith PD, Smythies LE. Human primary gastric dendritic cells induce a Th1 response to *H. pylori*. *Mucosal Immunol* 2010; **3**: 260-269 [PMID: [20237463](#) DOI: [10.1038/mi.2010.10](#)]
- 54 **Altobelli A**, Bauer M, Velez K, Cover TL, Müller A. *Helicobacter pylori* VacA Targets Myeloid Cells in the Gastric Lamina Propria To Promote Peripherally Induced Regulatory T-Cell Differentiation and Persistent Infection. *mBio* 2019; **10** [PMID: [30890606](#) DOI: [10.1128/mBio.00261-19](#)]
- 55 **Hsu WT**, Ho SY, Jian TY, Huang HN, Lin YL, Chen CH, Lin TH, Wu MS, Wu CJ, Chan YL, Liao KW. *Helicobacter pylori*-derived heat shock protein 60 increases the induction of regulatory T-cells associated with persistent infection. *Microb Pathog* 2018; **119**: 152-161 [PMID: [29660522](#) DOI: [10.1016/j.micpath.2018.04.016](#)]
- 56 **Lehours P**, Ferrero RL. Review: *Helicobacter*: Inflammation, immunology, and vaccines. *Helicobacter* 2019; **24** Suppl 1: e12644 [PMID: [31486236](#) DOI: [10.1111/hel.12644](#)]
- 57 **Watanabe M**, Kato J, Inoue I, Yoshimura N, Yoshida T, Mukoubayashi C, Deguchi H, Enomoto S, Ueda K, Maekita T, Iguchi M, Tamai H, Utsunomiya H, Yamamichi N, Fujishiro M, Iwane M, Tekeshita T, Mohara O, Ushijima T, Ichinose M. Development of gastric cancer in nonatrophic stomach with highly active inflammation identified by serum levels of pepsinogen and *Helicobacter pylori* antibody together with endoscopic rugal hyperplastic gastritis. *Int J Cancer* 2012; **131**: 2632-2642 [PMID: [22383377](#) DOI: [10.1002/ijc.27514](#)]

- 58 **Sokic-Milutinovic A**, Alempijevic T, Milosavljevic T. Role of *Helicobacter pylori* infection in gastric carcinogenesis: Current knowledge and future directions. *World J Gastroenterol* 2015; **21**: 11654-11672 [PMID: 26556993 DOI: 10.3748/wjg.v21.i41.11654]
- 59 **Huang JQ**, Sridhar S, Hunt RH. Role of *Helicobacter pylori* infection and non-steroidal anti-inflammatory drugs in peptic-ulcer disease: a meta-analysis. *Lancet* 2002; **359**: 14-22 [PMID: 11809181 DOI: 10.1016/S0140-6736(02)07273-2]
- 60 **Ertz-Archambault N**, Keim P, Von Hoff D. Microbiome and pancreatic cancer: A comprehensive topic review of literature. *World J Gastroenterol* 2017; **23**: 1899-1908 [PMID: 28348497 DOI: 10.3748/wjg.v23.i10.1899]
- 61 **Xiao M**, Wang Y, Gao Y. Association between *Helicobacter pylori* infection and pancreatic cancer development: a meta-analysis. *PLoS One* 2013; **8**: e75559 [PMID: 24086571 DOI: 10.1371/journal.pone.0075559]
- 62 **Otero LL**, Ruiz VE, Perez GIP. *Helicobacter pylori*: The balance between a role as colonizer and pathogen. *Best Pract Res Clin Gastroenterol* 2014; **28**: 1017-1029 [DOI: 10.1016/j.bpg.2014.09.003]
- 63 **Mentis AFA**, Boziki M, Grigoriadis N, Papavassiliou AG. *Helicobacter pylori* infection and gastric cancer biology: tempering a double-edged sword. *Cell Mol Life Sci* 2019; **76**: 2477-2486 [DOI: 10.1007/s00018-019-03044-1]
- 64 **Gravina AG**, Zagari RM, De Musis C, Romano L, Loguercio C, Romano M. *Helicobacter pylori* and extragastric diseases: A review. *World J Gastroenterol* 2018; **24**: 3204-3221 [PMID: 30090002 DOI: 10.3748/wjg.v24.i29.3204]
- 65 **German SV**, Bobrovitsky IP. [New aspects of *Helicobacter pylori* infection: Association with metabolic disturbances]. *Ter Arkh* 2017; **89**: 102-107 [PMID: 29171479 DOI: 10.17116/terarkh20178910102-107]
- 66 **Maev IV**, Samsonov AA, Andreev DN, Grechushnikov VB, Korovina TI. [Clinical significance of *Helicobacter pylori* infection]. *Clin Med* 2013; **91**: 4-12 [PMID: 24437177]
- 67 **Wang ZW**, Li Y, Huang LY, Guan QK, Xu DW, Zhou WK, Zhang XZ. *Helicobacter pylori* infection contributes to high risk of ischemic stroke: evidence from a meta-analysis. *J Neurol* 2012; **259**: 2527-2537 [PMID: 22688569 DOI: 10.1007/s00415-012-6558-7]
- 68 **Kountouras J**, Boziki M, Zavos C, Gavalas E, Giartza-Taxidou E, Venizelos I, Deretzi G, Grigoriadis N, Tsiaousi E, Vardaka E. A potential impact of chronic *Helicobacter pylori* infection on Alzheimer's disease pathobiology and course. *Neurobiol Aging* 2012; **33**: e3-e4 [PMID: 22325590 DOI: 10.1016/j.neurobiolaging.2012.01.003]
- 69 **Franceschi F**, Covino M, Roubaud Baudron C. Review: *Helicobacter pylori* and extragastric diseases. *Helicobacter* 2019; **24** Suppl 1: e12636 [PMID: 31486239 DOI: 10.1111/hel.12636]
- 70 **Huang HK**, Wang JH, Lei WY, Chen CL, Chang CY, Liou LS. *Helicobacter pylori* infection is associated with an increased risk of Parkinson's disease: A population-based retrospective cohort study. *Parkinsonism Relat Disord* 2018; **47**: 26-31 [PMID: 29174171 DOI: 10.1016/j.parkreldis.2017.11.331]
- 71 **Izadi M**, Fazel M, Sharubandi SH, Saadat SH, Farahani MM, Nasser MH, Dabiri H, SafiAryan R, Esfahani AA, Ahmadi A, Jonaidi Jafari N, Ranjbar R, Jamali-Moghaddam SR, Kazemi-Saleh D, Kalantar-Motamed MH, Taheri S. *Helicobacter* species in the atherosclerotic plaques of patients with coronary artery disease. *Cardiovasc Pathol* 2012; **21**: 307-311 [PMID: 22104005 DOI: 10.1016/j.carpath.2011.09.011]
- 72 **Park MJ**, Choi SH, Kim D, Kang SJ, Chung SJ, Choi SY, Yoon DH, Lim SH, Kim YS, Yim JY, Kim JS, Jung HC. Association between *Helicobacter pylori* Seropositivity and the Coronary Artery Calcium Score in a Screening Population. *Gut Liver* 2011; **5**: 321-327 [PMID: 21927661 DOI: 10.5009/gnl.2011.5.3.321]
- 73 **Jukic A**, Bozic D, Kardum D, Becic T, Luksic B, Vrsalovic M, Ljubkovic M, Fabijanic D. *Helicobacter pylori* infection and severity of coronary atherosclerosis in patients with chronic coronary artery disease. *Ther Clin Risk Manag* 2017; **13**: 933-938 [PMID: 28794636 DOI: 10.2147/TCRM.S142193]
- 74 **Sharma V**, Aggarwal A. *Helicobacter pylori*: Does it add to risk of coronary artery disease. *World J Cardiol* 2015; **7**: 19-25 [PMID: 25632315 DOI: 10.4330/wjc.v7.i1.19]
- 75 **Vijayvergiya R**, Vadivelu R. Role of *Helicobacter pylori* infection in pathogenesis of atherosclerosis. *World J Cardiol* 2015; **7**: 134-143 [PMID: 25810813 DOI: 10.4330/wjc.v7.i3.134]
- 76 **Cárdenas VM**, Boller F, Román GC. *Helicobacter pylori*, Vascular Risk Factors and Cognition in U.S. Older Adults. *Brain Sci* 2019; **9**: 370 [PMID: 31842501 DOI: 10.3390/brainsci9120370]
- 77 **Santarelli L**, Gabrielli M, Cremonini F, Santoliquido A, Candelli M, Nista EC, Pola P, Gasbarrini G, Gasbarrini A. Atrophic gastritis as a cause of hyperhomocysteinaemia. *Aliment Pharmacol Ther* 2004; **19**: 107-111 [PMID: 14687172 DOI: 10.1046/j.1365-2036.2003.01820.x]
- 78 **Rasmi Y**, Raeisi S, Seyyed Mohammadzad MH. Association of inflammation and cytotoxin-associated gene a positive strains of *Helicobacter pylori* in cardiac syndrome x. *Helicobacter* 2012; **17**: 116-120 [PMID: 22404441 DOI: 10.1111/j.1523-5378.2011.00923.x]
- 79 **de Jesus Souza M**, de Moraes JA, Da Silva VN, Helal-Neto E, Uberty AF, Scopel-Guerra A, Olivera-Severo D, Carlini CR, Barja-Fidalgo C. *Helicobacter pylori* urease induces pro-inflammatory effects and differentiation of human endothelial cells: Cellular and molecular mechanism. *Helicobacter* 2019; **24**: e12573 [PMID: 30907046 DOI: 10.1111/hel.12573]
- 80 **Yu M**, Zhang R, Ni P, Chen S, Duan G. *Helicobacter pylori* Infection and Psoriasis: A Systematic



- Review and Meta-Analysis. *Medicina (Kaunas)* 2019; **55** [PMID: [31561576](#) DOI: [10.3390/medicina55100645](#)]
- 81 **Onsun N**, Arda Ulusal H, Su O, Beycan I, Biyik Ozkaya D, Senocak M. Impact of Helicobacter pylori infection on severity of psoriasis and response to treatment. *Eur J Dermatol* 2012; **22**: 117-120 [PMID: [22063790](#) DOI: [10.1684/ejd.2011.1579](#)]
  - 82 **Yorulmaz A**, Kulcu SC. Helicobacter pylori and inflammatory skin diseases. *World J Dermatol* 2015; **4**: 120-128 [DOI: [10.5314/wjd.v4.i3.120](#)]
  - 83 **Atherton JC**, Blaser MJ. Coadaptation of Helicobacter pylori and humans: ancient history, modern implications. *J Clin Invest* 2009; **119**: 2475-2487 [PMID: [19729845](#) DOI: [10.1172/JCI38605](#)]
  - 84 **Stein M**, Ruggiero P, Rappuoli R, Bagnoli F. Helicobacter pylori CagA: From Pathogenic Mechanisms to Its Use as an Anti-Cancer Vaccine. *Front Immunol* 2013; **4**: 328 [PMID: [24133496](#) DOI: [10.3389/fimmu.2013.00328](#)]
  - 85 **Walker MM**, Talley NJ. Review article: bacteria and pathogenesis of disease in the upper gastrointestinal tract--beyond the era of Helicobacter pylori. *Aliment Pharmacol Ther* 2014; **39**: 767-779 [PMID: [24612362](#) DOI: [10.1111/apt.12666](#)]
  - 86 **Calvet X**, Ramirez Lázaro MJ, Lehours P, Mégraud F. Diagnosis and epidemiology of Helicobacter pylori infection. *Helicobacter* 2013; **18** Suppl 1: 5-11 [PMID: [24011238](#) DOI: [10.1111/hel.12071](#)]
  - 87 **Malfertheiner P**, Chan FK, McColl KE. Peptic ulcer disease. *Lancet* 2009; **374**: 1449-1461 [PMID: [19683340](#) DOI: [10.1016/S0140-6736\(09\)60938-7](#)]
  - 88 **Araújo MB**, Borini P, Guimarães RC. Etiopathogenesis of peptic ulcer: back to the past? *Arq Gastroenterol* 2014; **51**: 155-161 [PMID: [25003270](#) DOI: [10.1590/s0004-28032014000200016](#)]
  - 89 **Sidorenko SV**. [Diagnosis and treatment of infections caused by Helicobacter pylori]. *Antibiot Khimioter* 2001; **46**: 23-31 [PMID: [11871316](#)]
  - 90 **Rosenstock S**, Jørgensen T, Bonnevie O, Andersen L. Risk factors for peptic ulcer disease: a population based prospective cohort study comprising 2416 Danish adults. *Gut* 2003; **52**: 186-193 [PMID: [12524398](#) DOI: [10.1136/gut.52.2.186](#)]
  - 91 **Figura N**, Guglielmetti P, Rossolini A, Barberi A, Cusi G, Musmanno RA, Russi M, Quaranta S. Cytotoxin production by Campylobacter pylori strains isolated from patients with peptic ulcers and from patients with chronic gastritis only. *J Clin Microbiol* 1989; **27**: 225-226 [PMID: [2913034](#) DOI: [10.1128/JCM.27.1.225-226.1989](#)]
  - 92 **Atherton JC**, Cao P, Peek RM Jr, Tummuru MK, Blaser MJ, Cover TL. Mosaicism in vacuolating cytotoxin alleles of Helicobacter pylori. Association of specific vacA types with cytotoxin production and peptic ulceration. *J Biol Chem* 1995; **270**: 17771-17777 [PMID: [7629077](#) DOI: [10.1074/jbc.270.30.17771](#)]
  - 93 **Atherton JC**. The clinical relevance of strain types of Helicobacter pylori. *Gut* 1997; **40**: 701-703 [PMID: [9245920](#) DOI: [10.1136/gut.40.6.701](#)]
  - 94 **Iijima K**, Kanno T, Koike T, Shimosegawa T. Helicobacter pylori-negative, non-steroidal anti-inflammatory drug: negative idiopathic ulcers in Asia. *World J Gastroenterol* 2014; **20**: 706-713 [PMID: [24574744](#) DOI: [10.3748/wjg.v20.i3.706](#)]
  - 95 **Charpignon C**, Lesgourgues B, Pariente A, Nahon S, Pelaquier A, Gatineau-Sailliant G, Roucayrol AM, Courillon-Mallet A; Group de l'Observatoire National des Ulcères de l'Association Nationale des Hépatogastroentérologues des Hôpitaux Généraux (ANGH). Peptic ulcer disease: one in five is related to neither Helicobacter pylori nor aspirin/NSAID intake. *Aliment Pharmacol Ther* 2013; **38**: 946-954 [PMID: [23981105](#) DOI: [10.1111/apt.12465](#)]
  - 96 **Goenka MK**, Majumder S, Sethy PK, Chakraborty M. Helicobacter pylori negative, non-steroidal anti-inflammatory drug-negative peptic ulcers in India. *Indian J Gastroenterol* 2011; **30**: 33-37 [PMID: [21424697](#) DOI: [10.1007/s12664-011-0085-9](#)]
  - 97 **Reshetnyak TM**, Doroshkevich IA, Seredavkina NV, Nasonov EL, Maev IV, Reshetnyak VI. The Contribution of Drugs and Helicobacter pylori to Gastric Mucosa Changes in Patients with Systemic Lupus Erythematosus and Antiphospholipid Syndrome. *Int J Rheumatol* 2019; **2019**: 9698086 [PMID: [31191660](#) DOI: [10.1155/2019/9698086](#)]
  - 98 **Kanno T**, Iijima K, Abe Y, Yagi M, Asonuma S, Ohyauchi M, Ito H, Koike T, Shimosegawa T. Helicobacter pylori-negative and non-steroidal anti-inflammatory drugs-negative idiopathic peptic ulcers show refractoriness and high recurrence incidence: Multicenter follow-up study of peptic ulcers in Japan. *Dig Endosc* 2016; **28**: 556-563 [PMID: [26866510](#) DOI: [10.1111/den.12635](#)]
  - 99 **Rasane RK**, Horn CB, Coleoglou Centeno AA, Fiore NB, Torres Barboza M, Zhang Q, Bochicchio KM, Punch LJ, Bochicchio GV, Ilahi ON. Are Patients with Perforated Peptic Ulcers Who are Negative for Helicobacter pylori at a Greater Risk? *Surg Infect (Larchmt)* 2019; **20**: 444-448 [PMID: [30939075](#) DOI: [10.1089/sur.2018.249](#)]
  - 100 **Tsimmerman YS**. [Gastric cancers: a modern approach to the problem]. *Vestnik chirurgicheskoy gastroenterologii* 2011; **2**: 77-88
  - 101 **Laine L**, Hopkins RJ, Girardi LS. Has the impact of Helicobacter pylori therapy on ulcer recurrence in the United States been overstated? *Am J Gastroenterol* 1998; **93**: 1409-1415 [PMID: [9732917](#) DOI: [10.1111/j.1572-0241.1998.452\\_a.x](#)]
  - 102 **Leodolter A**, Kulig M, Brasch H, Meyer-Sabellek W, Willich SN, Malfertheiner P. A meta-analysis comparing eradication, healing and relapse rates in patients with Helicobacter pylori-associated gastric or duodenal ulcer. *Aliment Pharmacol Ther* 2001; **15**: 1949-1958 [PMID: [11736726](#) DOI: [10.1046/j.1365-2036.2001.01109.x](#)]
  - 103 **Lamb A**, Chen LF. Role of the Helicobacter pylori-induced inflammatory response in the

- development of gastric cancer. *J Cell Biochem* 2013; **114**: 491-497 [PMID: [22961880](#) DOI: [10.1002/jcb.24389](#)]
- 104 **Correa P.** Human gastric carcinogenesis: a multistep and multifactorial process--First American Cancer Society Award Lecture on Cancer Epidemiology and Prevention. *Cancer Res* 1992; **52**: 6735-6740 [PMID: [1458460](#)]
  - 105 **Danesh J.** Helicobacter pylori infection and gastric cancer: systematic review of the epidemiological studies. *Aliment Pharmacol Ther* 1999; **13**: 851-856 [PMID: [10383517](#) DOI: [10.1046/j.1365-2036.1999.00546.x](#)]
  - 106 **Hansen S, Melby KK, Aase S, Jellum E, Vollset SE.** Helicobacter pylori infection and risk of cardia cancer and non-cardia gastric cancer. A nested case-control study. *Scand J Gastroenterol* 1999; **34**: 353-360 [PMID: [10365894](#) DOI: [10.1080/003655299750026353](#)]
  - 107 **Rokkas F.** [Helicobacter pylori infection as risk factor of a carcinoma of the stomach: current evidence]. *Russ J Gastroenterol Hepatol Coloproctol* 2002; **3**: 66-70
  - 108 **Blaser MJ.** Helicobacter pylori: Balance and imbalance. *Europ J Gastroenterol Hepatol* 1998; **10** Suppl 1: 15-18 [DOI: [10.1097/00042737-199806001-00004](#)]
  - 109 **Cover TL, Blaser MJ.** Helicobacter pylori in health and disease. *Gastroenterology* 2009; **136**: 1863-1873 [PMID: [19457415](#) DOI: [10.1053/j.gastro.2009.01.073](#)]
  - 110 **Blaser MJ.** Helicobacter pylori and the pathogenesis of gastroduodenal inflammation. *J Infect Dis* 1990; **161**: 626-633 [PMID: [2181029](#) DOI: [10.1093/infdis/161.4.626](#)]
  - 111 **Bardakhch'ian EA, Kharlanova NG, Kamneva NV, Lomov SIu, Saiaimov SR, Golubev BP.** [Cocoid forms of Helicobacter pylori and their role in human pathology]. *Eksp Klin Gastroenterol* 2003; **(6)**: 11-15, 153 [PMID: [15065521](#)]
  - 112 **Yamaoka Y.** Pathogenesis of Helicobacter pylori-Related Gastroduodenal Diseases from Molecular Epidemiological Studies. *Gastroenterol Res Pract* 2012; **2012**: 371503 [PMID: [22829807](#) DOI: [10.1155/2012/371503](#)]
  - 113 **Liu J, He C, Chen M, Wang Z, Xing C, Yuan Y.** Association of presence/absence and on/off patterns of Helicobacter pylori oipA gene with peptic ulcer disease and gastric cancer risks: a meta-analysis. *BMC Infect Dis* 2013; **13**: 555 [PMID: [24256489](#) DOI: [10.1186/1471-2334-13-555](#)]
  - 114 **Miftahussurur M, Nusi IA, Graham DY, Yamaoka Y.** Helicobacter, Hygiene, Atopy, and Asthma. *Front Microbiol* 2017; **8**: 1034 [PMID: [28642748](#) DOI: [10.3389/fmicb.2017.01034](#)]
  - 115 **Elias N, Nasrallah E, Khoury C, Mansour B, Abu Zuher L, Asato V, Muhsen K.** Associations of Helicobacter pylori seropositivity and gastric inflammation with pediatric asthma. *Pediatr Pulmonol* 2020; **55**: 2236-2245 [PMID: [32543787](#) DOI: [10.1002/ppul.24905](#)]
  - 116 **Tsigalou C, Konstantinidis TG, Cassimos D, Karvelas A, Grapsa A, Tsalkidis A, Panopoulou M, Tsakris A.** Inverse association between *Helicobacter pylori* infection and childhood asthma in Greece: a case-control study. *Germs* 2019; **9**: 182-187 [PMID: [32042724](#) DOI: [10.18683/germs.2019.1174](#)]
  - 117 **Ierardi E, Losurdo G, Giorgio F, Di Leo A.** Might helicobacter pylori play a role in allergic or cross-reaction related disorders? *Expert Rev Gastroenterol Hepatol* 2020; **14**: 643-646 [PMID: [32510247](#) DOI: [10.1080/17474124.2020.1780119](#)]
  - 118 **Amberbir A, Medhin G, Erku W, Alem A, Simms R, Robinson K, Fogarty A, Britton J, Venn A, Davey G.** Effects of Helicobacter pylori, geohelminth infection and selected commensal bacteria on the risk of allergic disease and sensitization in 3-year-old Ethiopian children. *Clin Exp Allergy* 2011; **41**: 1422-1430 [PMID: [21831135](#) DOI: [10.1111/j.1365-2222.2011.03831.x](#)]
  - 119 **Zevit N, Balicer RD, Cohen HA, Karsh D, Niv Y, Shamir R.** Inverse association between Helicobacter pylori and pediatric asthma in a high-prevalence population. *Helicobacter* 2012; **17**: 30-35 [PMID: [22221613](#) DOI: [10.1111/j.1523-5378.2011.00895.x](#)]
  - 120 **Oertli M, Noben M, Engler DB, Semper RP, Reuter S, Maxeiner J, Gerhard M, Taube C, Müller A.** Helicobacter pylori  $\gamma$ -glutamyl transpeptidase and vacuolating cytotoxin promote gastric persistence and immune tolerance. *Proc Natl Acad Sci USA* 2013; **110**: 3047-3052 [PMID: [23382221](#) DOI: [10.1073/pnas.1211248110](#)]
  - 121 **Pachathundikandi SK, Müller A, Backert S.** Inflammasome Activation by Helicobacter pylori and Its Implications for Persistence and Immunity. *Curr Top Microbiol Immunol* 2016; **397**: 117-131 [PMID: [27460807](#) DOI: [10.1007/978-3-319-41171-2\\_6](#)]
  - 122 **Kyburz A, Müller A.** Helicobacter pylori and Extragastric Diseases. *Curr Top Microbiol Immunol* 2017; **400**: 325-347 [PMID: [28124160](#) DOI: [10.1007/978-3-319-50520-6\\_14](#)]
  - 123 **Wu XW, Ji HZ, Yang MF, Wu L, Wang FY.** Helicobacter pylori infection and inflammatory bowel disease in Asians: a meta-analysis. *World J Gastroenterol* 2015; **21**: 4750-4756 [PMID: [25914487](#) DOI: [10.3748/wjg.v21.i15.4750](#)]
  - 124 **Rokkas T, Gisbert JP, Niv Y, O'Morain C.** The association between Helicobacter pylori infection and inflammatory bowel disease based on meta-analysis. *United European Gastroenterol J* 2015; **3**: 539-550 [PMID: [26668747](#) DOI: [10.1177/2050640615580889](#)]
  - 125 **Jovanovic IR, Milosavjevic TN, Jankovic GP, Micev MM, Dugalic PD, Saranovic D, Ugljesic MM, Popovic DV, Bulajic MM.** Clinical onset of the Crohn's disease after eradication therapy of Helicobacter pylori infection. Does Helicobacter pylori infection interact with natural history of inflammatory bowel diseases? *Med Sci Monit* 2001; **7**: 137-141 [PMID: [11208510](#)]
  - 126 **Papamichael K, Konstantopoulos P, Mantzaris GJ.** Helicobacter pylori infection and inflammatory bowel disease: is there a link? *World J Gastroenterol* 2014; **20**: 6374-6385 [PMID: [24914359](#) DOI: [10.3748/wjg.v20.i21.6374](#)]

- 127 **Bor S**, Kitapcioglu G, Kasap E. Prevalence of gastroesophageal reflux disease in a country with a high occurrence of *Helicobacter pylori*. *World J Gastroenterol* 2017; **23**: 525-532 [PMID: 28210089 DOI: 10.3748/wjg.v23.i3.525]
- 128 **Mungan Z**, Pınarbaşı Şimşek B. Gastroesophageal reflux disease and the relationship with *Helicobacter pylori*. *Turk J Gastroenterol* 2017; **28**: S61-S67 [PMID: 29199171 DOI: 10.5152/tjg.2017.16]
- 129 **Xue Y**, Zhou LY, Lin SR, Hou XH, Li ZS, Chen MH, Yan XE, Meng LM, Zhang J, Lu JJ. Effect of *Helicobacter pylori* eradication on reflux esophagitis therapy: a multi-center randomized control study. *Chin Med J (Engl)* 2015; **128**: 995-999 [PMID: 25881589 DOI: 10.4103/0366-6999.155049]
- 130 **Zhao Y**, Li Y, Hu J, Wang X, Ren M, Lu G, Lu X, Zhang D, He S. The Effect of *Helicobacter pylori* Eradication in Patients with Gastroesophageal Reflux Disease: A Meta-Analysis of Randomized Controlled Studies. *Dig Dis* 2020; **38**: 261-268 [PMID: 32396919 DOI: 10.1159/000504086]
- 131 **Chung SJ**, Lim SH, Choi J, Kim D, Kim YS, Park MJ, Yim JY, Kim JS, Cho SH, Jung HC, Song IS. *Helicobacter pylori* Serology Inversely Correlated With the Risk and Severity of Reflux Esophagitis in *Helicobacter pylori* Endemic Area: A Matched Case-Control Study of 5,616 Health Check-Up Koreans. *J Neurogastroenterol Motil* 2011; **17**: 267-273 [PMID: 21860818 DOI: 10.5056/jnm.2011.17.3.267]
- 132 **Lin D**, Koskella B. Friend and foe: factors influencing the movement of the bacterium *Helicobacter pylori* along the parasitism-mutualism continuum. *Evol Appl* 2015; **8**: 9-22 [PMID: 25667600 DOI: 10.1111/eva.12231]
- 133 **Blaser MJ**, Falkow S. What are the consequences of the disappearing human microbiota? *Nat Rev Microbiol* 2009; **7**: 887-894 [PMID: 19898491 DOI: 10.1038/nrmicro2245]
- 134 **Lee YC**, Chen TH, Chiu HM, Shun CT, Chiang H, Liu TY, Wu MS, Lin JT. The benefit of mass eradication of *Helicobacter pylori* infection: a community-based study of gastric cancer prevention. *Gut* 2013; **62**: 676-682 [PMID: 22698649 DOI: 10.1136/gutjnl-2012-302240]



## Digestive system involvement of infections with SARS-CoV-2 and other coronaviruses: Clinical manifestations and potential mechanisms

Gao-Feng Zhan, Yue Wang, Ning Yang, Ai-Lin Luo, Shi-Yong Li

**ORCID number:** Gao-Feng Zhan 0000-0003-3002-9333; Yue Wang 0000-0002-0456-1273; Ning Yang 0000-0002-7977-1128; Ai-Lin Luo 0000-0003-0152-1628; Shi-Yong Li 0000-0001-7442-1826.

**Author contributions:** Zhan GF, Wang Y, and Yang N reviewed the literature and drafted the manuscript; Luo AL and Li SY checked and revised the manuscript; all authors contributed to the conception and design of the review and approved the final manuscript for submission.

**Conflict-of-interest statement:** All the authors declare no conflict of interest related to this manuscript.

**Open-Access:** This article is an open-access article that was selected by an in-house editor and fully peer-reviewed by external reviewers. It is distributed in accordance with the Creative Commons Attribution NonCommercial (CC BY-NC 4.0) license, which permits others to distribute, remix, adapt, build upon this work non-commercially, and license their derivative works on different terms, provided the original work is properly cited and the use is non-commercial. See: <http://creativecommons.org/License>

**Gao-Feng Zhan, Yue Wang, Ai-Lin Luo, Shi-Yong Li,** Department of Anesthesiology, Tongji Hospital, Tongji Medical College, Huazhong University of Science and Technology, Wuhan 430030, Hubei Province, China

**Ning Yang,** Department of Anesthesiology, Union Hospital, Tongji Medical College, Huazhong University of Science and Technology, Wuhan 430030, Hubei Province, China

**Corresponding author:** Shi-Yong Li, MD, PhD, Doctor, Department of Anesthesiology, Tongji Hospital, Tongji Medical College, Huazhong University of Science and Technology, No. 1095 Jiefang Avenue, Wuhan 430030, Hubei Province, China. [shiyongli@hust.edu.cn](mailto:shiyongli@hust.edu.cn)

### Abstract

Although coronavirus (CoV) infection is often characterized by respiratory symptoms, the virus can also result in extrapulmonary symptoms, especially the symptoms related to the digestive system. The outbreak of coronavirus disease 2019 (COVID-19) is currently the world's most pressing public health threat and has a significant impact on civil societies and the global economy. The occurrence of digestive symptoms in patients with COVID-19 is closely related to the development and prognosis of the disease. Moreover, thus far, there are no specific antiviral drug or vaccine approved for the treatment or prevention of COVID-19. Therefore, we elaborate on the effects of CoVs on the digestive system and the potential underlying mechanisms.

**Key Words:** SARS-CoV-2; Gastrointestinal diseases; Liver dysfunction; COVID-19; Coronavirus; Mechanisms

©The Author(s) 2021. Published by Baishideng Publishing Group Inc. All rights reserved.

**Core Tip:** In this review, it is reported that coronavirus infections can cause a series of digestive diseases, and may also be accompanied by digestive manifestations and abnormal digestive function. Furthermore, the potential mechanisms of coronavirus disease 2019 on the digestive system, such as angiotensin-converting enzyme 2, immune injury, gut microbiota, hypoxemia, and psychological stress, are also



s/by-nc/4.0/

**Manuscript source:** Unsolicited manuscript**Specialty type:** Gastroenterology and hepatology**Country/Territory of origin:** China**Peer-review report's scientific quality classification**

Grade A (Excellent): 0

Grade B (Very good): B, B

Grade C (Good): 0

Grade D (Fair): 0

Grade E (Poor): 0

**Received:** December 11, 2020**Peer-review started:** December 11, 2020**First decision:** December 27, 2020**Revised:** December 28, 2020**Accepted:** January 13, 2021**Article in press:** January 13, 2021**Published online:** February 21, 2021**P-Reviewer:** Dogrul AB, Galloro G**S-Editor:** Fan JR**L-Editor:** Wang TQ**P-Editor:** Liu JH

discussed. This review provides a new perspective for the prevention and treatment of infections with severe acute respiratory syndrome coronavirus 2 and other coronaviruses.

**Citation:** Zhan GF, Wang Y, Yang N, Luo AL, Li SY. Digestive system involvement of infections with SARS-CoV-2 and other coronaviruses: Clinical manifestations and potential mechanisms. *World J Gastroenterol* 2021; 27(7): 561-575

**URL:** <https://www.wjgnet.com/1007-9327/full/v27/i7/561.htm>

**DOI:** <https://dx.doi.org/10.3748/wjg.v27.i7.561>

## INTRODUCTION

In December 2019, an outbreak of coronavirus disease 2019 (COVID-19) caused by severe acute respiratory syndrome coronavirus 2 (SARS-CoV-2; previously called 2019-nCoV), initially emerged in Wuhan, China. It has posed a serious threat to human health worldwide. The World Health Organization has declared that COVID-19 is a public health emergency of pandemic proportions<sup>[1]</sup>. As of December 9, 2020, a total of 67780361 laboratory-confirmed cases including 1551214 deaths have been reported in 220 countries, areas, and territories<sup>[1]</sup>. The COVID-19 pandemic is currently the world's most pressing public health threat and has a significant impact on civil societies and the global economy.

It is well established that most individuals with COVID-19 present with fever and typical respiratory symptoms, such as cough and dyspnea, similar to those of SARS and Middle East respiratory syndrome (MERS)<sup>[2-5]</sup>. Therefore, nasopharyngeal and oropharyngeal swabs are the suitable samples for reverse transcriptase-polymerase chain reaction detection of SARS-CoV-2. However, concurrent extra-pulmonary symptoms, such as gastrointestinal manifestations, mainly including diarrhea, nausea, vomiting, abdominal pain, and anorexia, have also been reported in recent studies<sup>[6,7]</sup>. In addition, rectal swabs and stool specimens of patients with COVID-19 have shown to be positive for SARS-CoV-2, and the virus remained detectable even after the clearance of the virus in the respiratory tract<sup>[7-10]</sup>. Furthermore, Pan *et al*<sup>[11]</sup> demonstrated that patients with digestive symptoms have a longer time from onset to admission and a worse prognosis than that of patients without digestive symptoms<sup>[11]</sup>. Together, these indicate that SARS-CoV-2 can infect and replicate in the gastrointestinal tract, and it may also have potential to cause digestive system damage. With the ongoing COVID-19 pandemic, those studies are of great guiding significance for disease prevention, control, and management. The present review aims to summarize data regarding epidemiology, gastrointestinal characteristics, possible mechanisms, and potential therapeutic strategy in patients infected with coronaviruses (CoVs) from the perspective of the digestive system (Figure 1).

## EFFECTS OF COVS ON THE DIGESTIVE SYSTEM

CoVs are a group of enveloped, positive-sense, single-stranded RNA viruses (+ssRNA) with a crown-like appearance, which belongs to the family Coronaviridae of order Nidovirales<sup>[12,13]</sup>. CoVs harbor the largest genome among those known RNA viruses, with a genome length ranging from 26-32 kilobases (kb) and a diameter in the range of 120-160 nm<sup>[14-16]</sup>. CoVs are genetically classified into four genera: *Alpha-coronavirus*, *Beta-coronavirus*, *Gamma-coronavirus*, and *Delta-coronavirus*<sup>[12,17]</sup>. *Alpha-coronavirus* and *Beta-coronavirus* primarily infect mammals, whereas *Gamma-coronavirus* and *Delta-coronavirus* usually infect birds<sup>[16]</sup>. To date, seven coronavirus species under two genera have been identified to cause diseases in human: *Alpha-coronavirus* (HCoV-NL63 and HCoV-229E) and *Beta-coronavirus* (HCoV-OC43, HCoV-HKU1, SARS-CoV, MERS-CoV, and SARS-CoV-2)<sup>[18]</sup>.

HCoV-NL63, HCoV-229E, HCoV-OC43, and HCoV-HKU1 cause mild common cold symptoms, whereas the other three highly pathogenic CoVs have caused large-scale pandemic since the beginning of the 21<sup>st</sup> century: SARS-CoV in 2002 and 2003, MERS-CoV in 2012, and the newly emerged SARS-CoV-2<sup>[9]</sup>. The three highly contagious pathogens are zoonotic in origin and have crossed the species barrier to human.

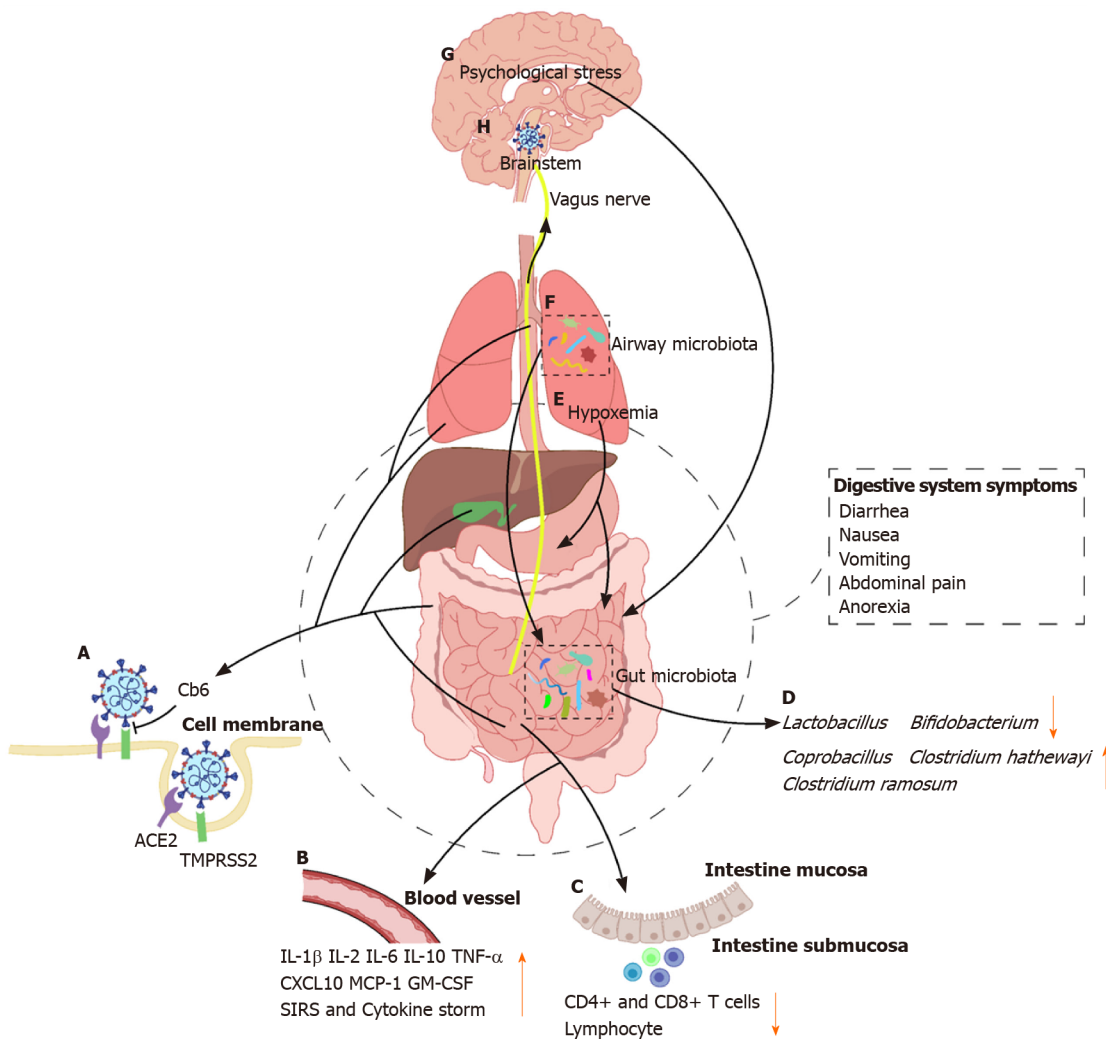


**Figure 1** Possible mechanisms of coronavirus disease 2019 on the digestive system. ACE2: Angiotensin-converting enzyme 2; CXCL10: Interferon-gamma-inducible protein-10; GM-CSF: Granulocyte-macrophage colony stimulating factor; IL: Interleukin; MCP: Monocyte chemoattractant protein; SIRS: Systemic inflammatory response syndrome; TMPRSS2: Transmembrane serine protease 2; TNF: Tumour necrosis factor.

Furthermore, these three viruses are known to cause digestive symptoms.

### CoVs and digestive manifestations

**SARS-CoV:** SARS-CoV has a large RNA genome length of 27.9 kb, emerged in the Guangdong Province of China, and had spread to 29 countries and areas worldwide. By July 2003, there were a total of 8098 laboratory-confirmed cases including 774 deaths (case-fatality rate: 9.6%) of SARS<sup>[20]</sup>. SARS-CoV has been considered to originate from bats, and market palm civets and racoon dogs have been unequivocally considered the intermediate hosts<sup>[21]</sup>.

SARS is characterized by fever and respiratory complications, and it may also lead to acute respiratory distress syndrome and multiple organ failure in severe cases. Moreover, gastrointestinal manifestations are frequently observed in patients with SARS-CoV infection<sup>[22]</sup>. The tropism of SARS-CoV in the digestive system is commonly known to occur, and a retrospective study demonstrated that 38.4% of patients with SARS had diarrhea, usually within the first week of the disease course<sup>[23]</sup>. It was also demonstrated that up to 60% of patients with SARS suffered from liver impairment, and SARS-CoV was detected in liver tissue although viral inclusions were not observed<sup>[24]</sup>. In addition, the rate of SARS-CoV RNA positivity in collected stool specimens increased progressively and peaked at day 11 of the illness, with viral RNA remaining detectable in a stool sample in a patient even 73 d after symptom onset<sup>[23,25]</sup>. Furthermore, the presence of SARS-CoV RNA in the gastrointestinal tract may indicate a poor prognosis, and the viral load in the stool is correlated with death<sup>[26]</sup>.

**MERS-CoV:** MERS-CoV has a large RNA genome length of 30.1 kb, emerged in the Saudi Arabia, and then spread to 27 countries and areas with a total of 2468 confirmed

cases and including 851 associated deaths (case-fatality rate: 34.4%) by the end of September 2019<sup>[27]</sup>. MERS-CoV has originated from bats, but dromedary camels has been considered the intermediate host<sup>[28]</sup>.

Human-to-human transmission of MERS-CoV occurred mainly through nosocomial transmission<sup>[29]</sup>. Although most patients with MERS present with nonspecific respiratory symptoms, such as fever, cough, and shortness of breath, approximately one third of patients have gastrointestinal symptoms, such as diarrhea, vomiting, and abdominal pain, which were the most commonly demonstrated extrapulmonary clinical features<sup>[30]</sup>. In addition, MERS-CoV RNA was detected in 14.6% of stool specimens from patients with MERS, but the positive rate of virus detection was lower than that of SARS<sup>[31,32]</sup>. Moreover, an *in vitro* study has shown that MERS-CoV can successfully replicate in human primary intestinal epithelial cells<sup>[33]</sup>.

**SARS-CoV-2:** SARS-CoV-2 has a genome length of 29.9 kb, shares an approximately 79% sequence identity to the SARS-CoV and the similarity of the whole-genome to BatCoV RaTG13 (a bat coronavirus detected in *Rhinolophus affinis*) is up to 96.2%<sup>[34]</sup>. Recent studies have suggested that bats may be the natural reservoir of SARS-CoV-2, and that there may be multiple potential intermediate hosts, such as pangolins, minks, and snakes<sup>[35-37]</sup>. In terms of the current pandemic situation, the case fatality of COVID-19 may not reach as high as that of SARS and MERS.

The majority of patients with COVID-19 exhibit mild to moderate pulmonary symptoms, and SARS-CoV-2 can extend to multiple extra-pulmonary organs including the heart, brain, kidneys, liver, and gut. Based on the data presented in Table 1, 6.7% of the total patients with SARS-CoV-2 infection have diarrhea and there are a great number of patients who had abnormal liver function with a paucity of concurrent or isolated pre-existing digestive system comorbidities. It was reported that COVID-19 patients with diarrhea presented severe symptoms of pneumonia compared to those without diarrhea, and COVID-19 patients with gastrointestinal manifestations or liver injury are more likely to require mechanical ventilation and hospitalization in the intensive care unit than those without gastrointestinal manifestations or liver injury<sup>[7,38-40]</sup>. Followed by the detection of SARS-CoV-2 RNA in the stool of the first case of COVID-19 in the United States, it was recently reported that viral RNA was detected in 59% of patients with COVID-19 in stool samples and the SARS-CoV-2 lasts significantly longer in stool samples than in respiratory and serum specimens<sup>[41,42]</sup>. In addition, To and colleagues demonstrated that SARS-CoV-2 was detected in the self-collected saliva specimens in 91.7% patients with COVID-19<sup>[43]</sup>. Furthermore, autopsy studies have demonstrated varying degrees of degeneration, necrosis, and shedding in the gastrointestinal mucosa and segmental dilatation and stenosis in the small intestine of patients with COVID-19<sup>[44,45]</sup>. Taken together, it is therefore likely that SARS-CoV-2 poses a serious threat to the digestive system.

### **Digestive diseases related to CoV infections**

Digestive diseases include a series of disorders that affect the oropharynx and digestive tract, liver and biliary system, and pancreas, affecting human lives commonly. At the beginning of the COVID-19 outbreak, more medical resources were freed up to control the spread of the virus so that more individuals can be protected. Meanwhile, it is safe for most patients with pre-existing diseases. However, it may also increase the relative risk of complications caused by delayed screening, diagnosis, and treatment, and being afraid of seeking medical attention<sup>[46]</sup>. Challenges encountered regarding the most common pre-existing digestive diseases during the ongoing COVID-19 pandemic are described below.

### **Liver diseases**

Hepatitis refers to inflammation of the liver caused by multiple pathogens (viruses, bacteria, drugs, autoimmune factors, and so on), which can progress to fibrosis, cirrhosis, and even liver cancer, posing a great threat to human health. The most common causes of hepatitis are the five main hepatitis virus types (A, B, C, D, and E)<sup>[47]</sup>. In a number of studies, hepatitis was noted in patients with SARS and COVID-19<sup>[7,11,48,49]</sup>. SARS patients with hepatitis B are more likely to develop severe hepatitis than in those without. Similarly, severe cases of COVID-19 were more prone to infect HBV than non-severe cases<sup>[48,50]</sup>. Collectively, these findings show that CoVs might play a significant role in hepatitis, although detailed studies are needed to confirm this.

Fatty liver disease is a spectrum of disorders characterized predominantly by macrovesicular hepatic steatosis, and it presents a condition of excess fat stored in the

**Table 1 Presentation of gastrointestinal symptoms, abnormal liver function, and pre-existing digestive diseases in patients with severe acute respiratory syndrome coronavirus 2 infection**

Ref.	Patients with COVID-19	Gastrointestinal symptoms			Patients with abnormal biochemical indicators of liver function	Patients with pre-existing digestive diseases	Patients testing positive for SARS-CoV-2 in stool or rectal swab specimens
		Diarrhoea	Nausea and vomiting	Abdominal pain			
Guan <i>et al</i> <sup>[7]</sup>	1099	42 (3.8%)	55 (5.0%)	NA	Abnormal AST: 168/757 (22.2%). Abnormal ALT: 158/741 (21.3%). Abnormal TBIL: 76/722 (10.5%)	CHB: 23 (2.1%)	Stool specimens: 4/NA. Rectal swab: 4/NA
Wang <i>et al</i> <sup>[6]</sup>	138	14 (10.1%)	19 (13.7%)	3 (2.2%)	Mild elevation of AST and ALT	4 (2.9%)	NA
Huang <i>et al</i> <sup>[40]</sup>	41	1/38 (2.6%)	NA	NA	Abnormal AST: 15 (31.0%)	Chronic liver disease: 1 (2%)	NA
Fan <i>et al</i> <sup>[116]</sup>	148	6 (4.1%)	3 (2.0%)	NA	Abnormal AST: 32 (21.6%). Abnormal ALT: 27 (18.2%). Abnormal TBIL: 9 (6.1%)	9 (6.1%)	NA
Cai <i>et al</i> <sup>[49]</sup>	298	9 (3.0%)	NA	NA	Abnormal AST: 25 (8.4%). Abnormal ALT: 39 (13.1%). Abnormal TBIL: 24 (8.1%)	CHB: 5 (1.7%). NAFLD: 14 (4.7%). ALD: 9 (3.0%)	NA
Chen <i>et al</i> <sup>[3]</sup>	99	2 (2.0%)	1 (1.0%)	NA	Abnormal AST: 35 (35.0%). Abnormal ALT: 28 (28.0%). Abnormal TBIL: 18 (18.0%). Abnormal albumin: 97 (98.0%)	NA	NA
Holshue <i>et al</i> <sup>[41]</sup>	1	1	1	NA	Abnormal AST: 1. Abnormal ALT: 1. Abnormal TBIL: 1. Abnormal albumin: 1	NA	Stool specimens: 1/1
Zhang <i>et al</i> <sup>[117]</sup>	140	18/139 (12.9%)	31/139 (22.3%)	8/139 (5.8%)	NA	FLD and abnormal liver function: 8 (5.7%). Chronic gastritis and gastric ulcer: 7 (5.0%). Cholelithiasis: 6 (4.3%)	NA
Xiao <i>et al</i> <sup>[10]</sup>	73	26 (35.6%)	NA	NA	NA	NA	Stool specimens: 39/73 (53.4%)
Zhou <i>et al</i> <sup>[118]</sup>	191	9 (4.7%)	7 (3.7%)	NA	Abnormal ALT: 59/189 (31.2%)	NA	NA
Zhang <i>et al</i> <sup>[119]</sup>	82 (Deaths)	10 (12.2%)	2 (2.3%)	NA	Abnormal AST: 44/72 (61.1%). Abnormal ALT: 22/72 (30.6%). Abnormal TBIL: 22/72 (30.6%). Abnormal albumin: 56/72 (77.8%)	Liver disease: 2/82 (2.4%)	NA
Xu <i>et al</i> <sup>[120]</sup>	62	3 (4.8%)	NA	NA	Abnormal AST: 10 (16.1%)	Liver disease: 7 (11.3%)	NA
Chen <i>et al</i> <sup>[121]</sup>	21	4/20 (20.0%)	NA	NA	Abnormal AST: 6 (28.6%). Abnormal albumin: 8 (38.1%)	NA	NA
Pan <i>et al</i> <sup>[11]</sup>	204	29 (14.2%)	8 (3.9%)	4 (2.0%)	Abnormal AST: NA. Abnormal albumin: NA	CHB: 1 (0.5%). FLD: 1 (0.5%). Gastritis: 1 (0.5%)	NA
Luo <i>et al</i> <sup>[122]</sup>	1141	68 (5.9%)	Nausea: 134 (11.7%). Vomiting: 119 (10.4%)	45 (3.9%)	Mild elevation of AST and ALT	NA	NA
Total	3738	174/2592					



(6.7%)

ALD: Alcoholic fatty liver disease; ALT: Alanine transaminase; AST: Aspartate aminotransferase; CHB: Chronic hepatitis B; COVID-19: Coronavirus disease 2019; FLD: Fatty liver disease; NAFLD: Non-alcoholic fatty liver disease; SARS-CoV-2: Severe acute respiratory syndrome coronavirus 2; TBIL: Total bilirubin.

liver, including non-alcoholic fatty liver disease (NAFLD) and alcoholic fatty liver disease (ALD). Patients with hypertension, diabetes, obesity, and old age have a high risk of developing severe COVID-19<sup>[51]</sup>. These comorbidities also increase the risk of NAFLD, thus leading to liver injury. The ongoing COVID-19 pandemic has several negative effects on individuals, especially those encountering job loss, financial strain, death of a loved one, and so on. Under these stressors, an individual's alcohol consumption is likely to increase<sup>[52]</sup>. Therefore, COVID-19 is likely to have a long-lasting impact on the development of ALD.

Given that patients with liver cirrhosis and cancer have a high risk of infection due to the immunocompromised status<sup>[53]</sup>, measures to prevent SARS-CoV-2 infection are needed. Xiao and colleagues designed a study showing that none of the participants who undertook precautionary and protective measures had clinical symptoms suggestive of SARS-CoV-2 infection, whereas 17 of 101 patients with decompensated cirrhosis who did not undertake these measures were diagnosed with COVID-19<sup>[54]</sup>. This research suggests that more strategies should be implemented to prevent SARS-CoV-2 infection in patients with liver cirrhosis and cancer, such as online health education and medication guidance.

The outbreaks of SARS and MERS might potentially increase the risk of transmission of viral infection from donors to recipients and thus even lead to death<sup>[40,55]</sup>. Tzedakis *et al.*<sup>[56]</sup> reported that a local liver transplant center decreased transplant activity by 60% since the COVID-19 pandemic and that it is crucial and necessary to balance costs and benefits while performing liver transplant<sup>[56]</sup>. During the COVID-19 pandemic, all donors and recipients of liver transplant must be screened for the presence of SARS-CoV-2 to ensure the safety and success of the liver transplantation.

### Gastrointestinal diseases

Ulcerative colitis and Crohn's disease are two major idiopathic inflammatory bowel disorders (IBDs) that could cause prolonged inflammation of the gastrointestinal tract<sup>[57]</sup>. Patients with IBD who use immunosuppressive and biological agents are more susceptible to opportunistic and severe infections than those who do not<sup>[58,59]</sup>. Therefore, it is reasonable to assume that patients with IBD have more severe COVID-19, although there has been no direct clinical evidence to prove it. An and colleagues showed that none of the 318 patients with IBD (204 with ulcerative colitis and 114 with Crohn's disease) developed SARS-CoV-2 infection with early effective warning and protective measures<sup>[60]</sup>. In addition, patients with cancer also have an increased risk of infection<sup>[61]</sup>. Furthermore, it was demonstrated that individuals with cancer may have a

high risk of severe COVID-19 and a poorer prognosis<sup>[62]</sup>. Although the risk of SARS-CoV-2 infection in patients with gastrointestinal cancer remains unknown, effective precautionary approaches are necessary to better protect patients.

## POSSIBLE MECHANISMS OF COVID-19 ON THE DIGESTIVE SYSTEM

It has been commonly known that respiratory droplets and direct contact are the two major transmission pathways of SARS-CoV-2. However, a recent study performed by Liu and colleagues has shown a possibility of aerosol transmission<sup>[63]</sup>. A large number of studies have reported gastrointestinal symptoms and liver dysfunction in patients with SARS-CoV-2 infection. At the same time, SARS-CoV-2 could be detected in rectal swabs and stool specimens in patients with COVID-19<sup>[7,10]</sup>. Moreover, biopsy and autopsy reports have revealed that COVID-19 caused pathological changes in the digestive system. In addition, high airborne concentration of SARS-CoV-2 was detected in toilet room of Fangcang Hospital where patients with COVID-19 were treated<sup>[63]</sup>. Taken together, these research findings provide a theoretical basis for the spread of COVID-19 through the faecal-oral route, although there is no direct evidence for the transmission pathway thus far.

The digestive tract communicates with the outside world directly, similar to the respiratory tract. Therefore, SARS-CoV-2 has the opportunity to enter the gastrointestinal tract and cause a direct cytopathic effect by local replication. In addition, systemic responses to excessive immune inflammation induced by SARS-CoV-2 infection may also cause damage to the digestive system indirectly. However, the mechanisms of how COVID-19 affects the digestive system remain poorly known. Furthermore, there is also no specific antiviral drug or vaccine approved to treat or prevent COVID-19 to date. Hence, it is particularly urgent to identify the potential therapeutic strategies for COVID-19.

### Angiotensin-converting enzyme 2 and transmembrane serine protease 2

Angiotensin-converting enzyme 2 (ACE2) is a well-known receptor located on cells of various organs for regulating cardiovascular function through the renin-angiotensin system, playing a major role in regulating hypertension and anti-atherosclerosis mechanisms<sup>[64,65]</sup>. In recent two decades, the role of ACE2 in SARS-CoV and influenza virus infection as a target functional receptor has attracted widespread attention<sup>[66-68]</sup>. It has been reported that the entry of SARS-CoV-2 into the host cell depends on the binding of viral spike (S) proteins to the SARS-CoV receptor ACE2 followed by the transmembrane serine protease 2 (TMPRSS2) for the S protein priming<sup>[69]</sup>. Therefore, human cells co-expressing ACE2 and TMPRSS2 are susceptible to SARS-CoV-2 infection<sup>[70]</sup>. A recent study performed by Zhang and colleagues has demonstrated that type II alveolar cells have higher expression of ACE2 and TMPRSS2 than type I alveolar cells in the lung. Besides, co-expression of ACE2 and TMPRSS2 has also been found in the glandular cells of upper esophageal and absorptive enterocytes of the ileum and colon<sup>[70,71]</sup>. Intestinal epithelial cells can act as a barrier and help to coordinate immune responses in microbial infections<sup>[72]</sup>. A number of studies have reported that absorptive enterocytes can be damaged or developed malabsorption and intestinal secretion abnormalities due to coronavirus or rotavirus infection, thus resulting in diarrhea and vomiting<sup>[73,74]</sup>. Therefore, gastrointestinal manifestations in patients with COVID-19 might be associated with infected enterocytes co-expressing ACE2 and TMPRSS2. Moreover, co-expression of ACE2 and TMPRSS2 has been observed in cholangiocytes, but not in hepatocytes<sup>[75]</sup>. Cholangiocytes play a pivotal role in liver regeneration and immune responses, and injury of cholangiocytes may cause a variety of diseases and even lead to liver failure<sup>[76]</sup>. Therefore, we can preliminarily conclude that the abnormal liver function in patients with COVID-19 may not be directly caused by the damage to hepatocytes, but it may be caused by damage to cholangiocytes. Liver damages may also be caused by other factors, such as drugs used in the treatment or systemic inflammatory response.

Compared with control mice, ACE2 knockout mice are more susceptible to induced colitis upon treatment with chemical irritants<sup>[77]</sup>. The expression of ACE2 protein is downregulated after virus entry, which may worsen the digestive symptoms. Recently, studies have demonstrated that the fusion protein of human recombinant ACE2 (hrACE2) with the Fc fragment of the human immunoglobulin IgG1 showed high affinity to the receptor-binding domain (RBD) of SARS-CoV-2 and potently neutralized SARS-CoV-2 *in vitro*<sup>[78,79]</sup>. A newly online published report in *Nature* demonstrated that CB6, a neutralizing monoclonal antibody (mAb) isolated from a

patient with convalescent COVID-19, can block the binding of soluble SARS-CoV-2 RBD with ACE2 receptor and showed inhibitory effect to SARS-CoV-2 infection *in vitro* and in rhesus monkeys<sup>[80]</sup>. Additionally, a recent *in vivo* study has reported that hrACE2 can block the early stages of SARS-CoV-2 infection at the organoid level in engineered human blood vessels, kidneys, and small intestinal enterocytes<sup>[78,81]</sup>. Moreover, a serine protease TMPRSS2 inhibitor has been approved for clinical use to block the entry of CoVs<sup>[69]</sup>. Taken together, it is therefore likely that ACE2 and TMPRSS2 may be the potential targets for prevention and treatment of the COVID-19 patients with digestive symptoms.

### Immune injury

Immune injury plays an important role in the occurrence, development, and prognosis of digestive diseases<sup>[82-84]</sup>. A growing body of evidence suggests that severe SARS-CoV-2 infection can activate innate and adaptive immune responses, increase serum levels of pro-inflammatory cytokines and chemokines including interleukin (IL)-6, IL-1 $\beta$ , IL-2, IL-10, tumor necrosis factor  $\alpha$  (TNF- $\alpha$ ), interferon-gamma-inducible protein-10 (CXCL10), monocyte chemoattractant protein-1, and granulocyte-macrophage colony stimulating factor, and even induce systemic inflammatory response syndrome (SIRS) and cytokine storm, thus leading to local and systemic tissue damage<sup>[40,85,86]</sup>. Concentrations of IL-6 were significantly different between patients with mild and severe COVID-19, and elevated IL-6 was found to be a stable indicator of adverse outcomes for severe COVID-19 patients. A clinical trial (ChiCTR2000029765) that explored the potential therapeutic effect of IL-6 receptor-targeted mAb in patients with severe COVID-19, has shown the effectiveness of controlling fever and improving respiratory function quickly<sup>[87]</sup>. It has been reported that vagus nerve stimulation (VNS) can exert anti-inflammatory effects *via* activation of the cholinergic anti-inflammatory pathway<sup>[88,89]</sup>. Based on preliminary observations and available scientific and clinical data, it is speculated that VNS may play a vital role in improving the prognosis of patients with COVID-19<sup>[90]</sup>. Additionally, patients with severe COVID-19 more frequently have lymphopenia, and drastically decreased numbers of CD4<sup>+</sup> and CD8<sup>+</sup>T cells than moderate cases. Furthermore, inflammation-mediated gastrointestinal tissue damage in patients with COVID-19 is supported by the histopathological evidence of diffuse endothelial inflammation in the small intestine submucosa<sup>[91]</sup>. It has also been confirmed by the presence of numerous infiltrating plasma cells and lymphocytes with interstitial edema in the lamina propria of the stomach, duodenum, and rectum of patients with COVID-19<sup>[10]</sup>.

### Gut microbiota

The human intestine harbors nearly 100 trillion microorganisms, which are composed of more than 1000 different bacterial species, including but not limited to bacteria, fungi, and viruses<sup>[92,93]</sup>. It is known that gut microbiota plays a vital role in a variety of diseases, including digestive, metabolic, respiratory, and even neuropsychiatric diseases<sup>[94-96]</sup>. Additionally, many studies have reported that chronic respiratory diseases and pneumonia can not only change the airway microbiota, but also alter the gut microbiota indirectly through the circulatory and lymphatic systems<sup>[97-100]</sup>. SARS-CoV-2 can down-regulate the expression of ACE2 in the intestine, which affects the absorption of tryptophan, resulting in damage to the gut microbiota and possibly influencing intestinal inflammation<sup>[101,102]</sup>. Xu *et al*<sup>[103]</sup> indicated that some patients with COVID-19 showed gut microbial dysbiosis with decreased abundance of *Lactobacillus* and *Bifidobacterium*<sup>[103]</sup>. Zuo *et al*<sup>[104]</sup> showed that the increased levels of *Coprobacillus*, *Clostridium hathewayi*, and *Clostridium ramosum* were positively correlated with the susceptibility and severity of COVID-19<sup>[104]</sup>. Furthermore, studies have shown that short-chain fatty acids, the most critical metabolites of the gut microbiota, play an important role in reducing the intestinal pH, maintaining the integrity of the intestinal epithelium, and enhancing the host systemic immunity<sup>[105-107]</sup>. Antibiotics are commonly prescribed in patients with COVID-19, however, it can also profoundly perturb the composition of the human gut microbiota<sup>[108]</sup>. Guidance from China's National Health Commission and National Administration of Traditional Chinese Medicine suggested that the use of probiotics has a good curative effect in patients with severe SARS-CoV-2 infection. Taken together, improvement of the composition of the gut microbiota and its metabolites may be a potential strategy for the treatment of COVID-19.

### Hypoxemia

After SARS-CoV-2 infects the lungs, it causes inflammation and edema of the

pulmonary parenchyma and interstitium, which in turn affect alveolar gas exchange and thereby lead to hypoxemia<sup>[109]</sup>. Hypoxemia can cause metabolism and normal physiological dysfunctions in various tissues and organs including the digestive system. Long-term hypoxemia can cause cell necrosis, which in turn leads to damage of the gastrointestinal mucosal cells, thus leading to gastrointestinal ulceration and bleeding.

### Psychological stress

Psychological stress has a profound influence on the digestive system, it can alter the intestinal motility, increase the gastrointestinal permeability, and change the composition of intestinal microbiota<sup>[110]</sup>. A study on active Weibo users showed that individuals were more concerned about their health and showed more negative emotions, such as anxiety and depression, after the outbreak of the COVID-19<sup>[111]</sup>. Quarantine is an effective measure to protect individuals from contagious patients and those who are at risk of infection, however, it may also increase negative psychological stress<sup>[112]</sup>. Taken together, digestive diseases and symptoms in patients with COVID-19 may be partially caused by psychological stress.

### Others

Multiple lines of evidence has shown that some patients with COVID-19 have digestive system symptoms, such as nausea, vomiting, and anorexia, which indirectly reflect the impairment of the dorsal vagal complex<sup>[6,113,114]</sup>. One of the possible mechanisms is that the neurotropic virus retrogrades along the vagus nerve once the virus enters the vagal nerve endings, thus damaging the brainstem<sup>[115]</sup>. Moreover, the virus may reach the brainstem through the circulatory system with or without crossing the blood-brain barrier<sup>[113]</sup>.

## CONCLUSION

CoV infections can cause a series of digestive diseases, and may also be accompanied by digestive manifestations and abnormal digestive function. Although it is still unknown whether the SARS-CoV-2, which causes abnormalities in the digestive system, enters the digestive system directly or indirectly affects the digestive system, it is necessary to undertake early measures to prevent the spread of the virus through the fecal-oral transmission. In addition to ACE2 and immune injury, gut microbiota, hypoxemia, and psychological stress may also be targets for future intervention and treatment of digestive system damage caused by SARS-CoV-2 infection. Further research is warranted to elucidate the relationship between the COVID-19 and the digestive system.

## REFERENCES

- 1 World Health Organization. WHO Coronavirus Disease (COVID-19) situation Dashboard. 2020 [cited 9 December 2020]. Available from: <https://www.who.int/>
- 2 Young BE, Ong SWX, Kalimuddin S, Low JG, Tan SY, Loh J, Ng OT, Marimuthu K, Ang LW, Mak TM, Lau SK, Anderson DE, Chan KS, Tan TY, Ng TY, Cui L, Said Z, Kurupatham L, Chen MI, Chan M, Vasoo S, Wang LF, Tan BH, Lin RTP, Lee VJM, Leo YS, Lye DC; Singapore 2019 Novel Coronavirus Outbreak Research Team. Epidemiologic Features and Clinical Course of Patients Infected With SARS-CoV-2 in Singapore. *JAMA* 2020; **323**: 1488-1494 [PMID: 32125362 DOI: 10.1001/jama.2020.3204]
- 3 Chen N, Zhou M, Dong X, Qu J, Gong F, Han Y, Qiu Y, Wang J, Liu Y, Wei Y, Xia J, Yu T, Zhang X, Zhang L. Epidemiological and clinical characteristics of 99 cases of 2019 novel coronavirus pneumonia in Wuhan, China: a descriptive study. *Lancet* 2020; **395**: 507-513 [PMID: 32007143 DOI: 10.1016/S0140-6736(20)30211-7]
- 4 Zumla A, Hui DS, Perlman S. Middle East respiratory syndrome. *Lancet* 2015; **386**: 995-1007 [PMID: 26049252 DOI: 10.1016/S0140-6736(15)60454-8]
- 5 Cheng VC, Lau SK, Woo PC, Yuen KY. Severe acute respiratory syndrome coronavirus as an agent of emerging and reemerging infection. *Clin Microbiol Rev* 2007; **20**: 660-694 [PMID: 17934078 DOI: 10.1128/CMR.00023-07]
- 6 Wang D, Hu B, Hu C, Zhu F, Liu X, Zhang J, Wang B, Xiang H, Cheng Z, Xiong Y, Zhao Y, Li Y, Wang X, Peng Z. Clinical Characteristics of 138 Hospitalized Patients With 2019 Novel Coronavirus-Infected Pneumonia in Wuhan, China. *JAMA* 2020; **323**: 1061-1069 [PMID: 32031570 DOI: 10.1001/jama.2020.1585]



- 7 **Guan WJ**, Ni ZY, Hu Y, Liang WH, Ou CQ, He JX, Liu L, Shan H, Lei CL, Hui DSC, Du B, Li LJ, Zeng G, Yuen KY, Chen RC, Tang CL, Wang T, Chen PY, Xiang J, Li SY, Wang JL, Liang ZJ, Peng YX, Wei L, Liu Y, Hu YH, Peng P, Wang JM, Liu JY, Chen Z, Li G, Zheng ZJ, Qiu SQ, Luo J, Ye CJ, Zhu SY, Zhong NS; China Medical Treatment Expert Group for Covid-19. Clinical Characteristics of Coronavirus Disease 2019 in China. *N Engl J Med* 2020; **382**: 1708-1720 [PMID: [32109013](#) DOI: [10.1056/NEJMoa2002032](#)]
- 8 **Xu Y**, Li X, Zhu B, Liang H, Fang C, Gong Y, Guo Q, Sun X, Zhao D, Shen J, Zhang H, Liu H, Xia H, Tang J, Zhang K, Gong S. Characteristics of pediatric SARS-CoV-2 infection and potential evidence for persistent fecal viral shedding. *Nat Med* 2020; **26**: 502-505 [PMID: [32284613](#) DOI: [10.1038/s41591-020-0817-4](#)]
- 9 **Tang A**, Tong ZD, Wang HL, Dai YX, Li KF, Liu JN, Wu WJ, Yuan C, Yu ML, Li P, Yan JB. Detection of Novel Coronavirus by RT-PCR in Stool Specimen from Asymptomatic Child, China. *Emerg Infect Dis* 2020; **26**: 1337-1339 [PMID: [32150527](#) DOI: [10.3201/eid2606.200301](#)]
- 10 **Xiao F**, Tang M, Zheng X, Liu Y, Li X, Shan H. Evidence for Gastrointestinal Infection of SARS-CoV-2. *Gastroenterology* 2020; **158**: 1831-1833. e3 [PMID: [32142773](#) DOI: [10.1053/j.gastro.2020.02.055](#)]
- 11 **Pan L**, Mu M, Yang P, Sun Y, Wang R, Yan J, Li P, Hu B, Wang J, Hu C, Jin Y, Niu X, Ping R, Du Y, Li T, Xu G, Hu Q, Tu L. Clinical Characteristics of COVID-19 Patients With Digestive Symptoms in Hubei, China: A Descriptive, Cross-Sectional, Multicenter Study. *Am J Gastroenterol* 2020; **115**: 766-773 [PMID: [32287140](#) DOI: [10.14309/ajg.0000000000000620](#)]
- 12 **Zumla A**, Chan JF, Azhar EI, Hui DS, Yuen KY. Coronaviruses - drug discovery and therapeutic options. *Nat Rev Drug Discov* 2016; **15**: 327-347 [PMID: [26868298](#) DOI: [10.1038/nrd.2015.37](#)]
- 13 **Woo PC**, Huang Y, Lau SK, Yuen KY. Coronavirus genomics and bioinformatics analysis. *Viruses* 2010; **2**: 1804-1820 [PMID: [21994708](#) DOI: [10.3390/v2081803](#)]
- 14 **Schoeman D**, Fielding BC. Coronavirus envelope protein: current knowledge. *Virol J* 2019; **16**: 69 [PMID: [31133031](#) DOI: [10.1186/s12985-019-1182-0](#)]
- 15 **Wu Y**, Xu X, Chen Z, Duan J, Hashimoto K, Yang L, Liu C, Yang C. Nervous system involvement after infection with COVID-19 and other coronaviruses. *Brain Behav Immun* 2020; **87**: 18-22 [PMID: [32240762](#) DOI: [10.1016/j.bbi.2020.03.031](#)]
- 16 **Tang Q**, Song Y, Shi M, Cheng Y, Zhang W, Xia XQ. Inferring the hosts of coronavirus using dual statistical models based on nucleotide composition. *Sci Rep* 2015; **5**: 17155 [PMID: [26607834](#) DOI: [10.1038/srep17155](#)]
- 17 **Li F**. Structure, Function, and Evolution of Coronavirus Spike Proteins. *Annu Rev Virol* 2016; **3**: 237-261 [PMID: [27578435](#) DOI: [10.1146/annurev-virology-110615-042301](#)]
- 18 **Wu A**, Peng Y, Huang B, Ding X, Wang X, Niu P, Meng J, Zhu Z, Zhang Z, Wang J, Sheng J, Quan L, Xia Z, Tan W, Cheng G, Jiang T. Genome Composition and Divergence of the Novel Coronavirus (2019-nCoV) Originating in China. *Cell Host Microbe* 2020; **27**: 325-328 [PMID: [32035028](#) DOI: [10.1016/j.chom.2020.02.001](#)]
- 19 **Singh A**, Shaikh A, Singh R, Singh AK. COVID-19: From bench to bed side. *Diabetes Metab Syndr* 2020; **14**: 277-281 [PMID: [32283498](#) DOI: [10.1016/j.dsx.2020.04.011](#)]
- 20 **World Health Organization**. Summary of probable SARS cases with onset of illness from 1 November 2002 to 31 July 2003. Available from: <https://www.who.int/csr/sars/>
- 21 **Kan B**, Wang M, Jing H, Xu H, Jiang X, Yan M, Liang W, Zheng H, Wan K, Liu Q, Cui B, Xu Y, Zhang E, Wang H, Ye J, Li G, Li M, Cui Z, Qi X, Chen K, Du L, Gao K, Zhao YT, Zou XZ, Feng YJ, Gao YF, Hai R, Yu D, Guan Y, Xu J. Molecular evolution analysis and geographic investigation of severe acute respiratory syndrome coronavirus-like virus in palm civets at an animal market and on farms. *J Virol* 2005; **79**: 11892-11900 [PMID: [16140765](#) DOI: [10.1128/JVI.79.18.11892-11900.2005](#)]
- 22 **Peiris JS**, Lai ST, Poon LL, Guan Y, Yam LY, Lim W, Nicholls J, Yee WK, Yan WW, Cheung MT, Cheng VC, Chan KH, Tsang DN, Yung RW, Ng TK, Yuen KY; SARS study group. Coronavirus as a possible cause of severe acute respiratory syndrome. *Lancet* 2003; **361**: 1319-1325 [PMID: [12711465](#) DOI: [10.1016/s0140-6736\(03\)13077-2](#)]
- 23 **Leung WK**, To KF, Chan PK, Chan HL, Wu AK, Lee N, Yuen KY, Sung JJ. Enteric involvement of severe acute respiratory syndrome-associated coronavirus infection. *Gastroenterology* 2003; **125**: 1011-1017 [PMID: [14517783](#) DOI: [10.1016/s0016-5085\(03\)01215-0](#)]
- 24 **Chau TN**, Lee KC, Yao H, Tsang TY, Chow TC, Yeung YC, Choi KW, Tso YK, Lau T, Lai ST, Lai CL. SARS-associated viral hepatitis caused by a novel coronavirus: report of three cases. *Hepatology* 2004; **39**: 302-310 [PMID: [14767982](#) DOI: [10.1002/hep.20111](#)]
- 25 **Chan KH**, Poon LL, Cheng VC, Guan Y, Hung IF, Kong J, Yam LY, Seto WH, Yuen KY, Peiris JS. Detection of SARS coronavirus in patients with suspected SARS. *Emerg Infect Dis* 2004; **10**: 294-299 [PMID: [15030700](#) DOI: [10.3201/eid1002.030610](#)]
- 26 **Hung IF**, Cheng VC, Wu AK, Tang BS, Chan KH, Chu CM, Wong MM, Hui WT, Poon LL, Tse DM, Chan KS, Woo PC, Lau SK, Peiris JS, Yuen KY. Viral loads in clinical specimens and SARS manifestations. *Emerg Infect Dis* 2004; **10**: 1550-1557 [PMID: [15498155](#) DOI: [10.3201/eid1009.040058](#)]
- 27 **World Health Organization**. Middle East respiratory syndrome coronavirus (MERS-CoV). Available from: <https://www.who.int/emergencies/mers-cov/>
- 28 **Haagmans BL**, Al Dhahiry SH, Reusken CB, Raj VS, Galiano M, Myers R, Godeke GJ, Jonges M, Farag E, Diab A, Ghobashy H, Alhajri F, Al-Thani M, Al-Marri SA, Al Romaihi HE, Al Khal A,

- Bermingham A, Osterhaus AD, AlHajri MM, Koopmans MP. Middle East respiratory syndrome coronavirus in dromedary camels: an outbreak investigation. *Lancet Infect Dis* 2014; **14**: 140-145 [PMID: 24355866 DOI: 10.1016/S1473-3099(13)70690-X]
- 29 **Chowell G**, Abdirizak F, Lee S, Lee J, Jung E, Nishiura H, Viboud C. Transmission characteristics of MERS and SARS in the healthcare setting: a comparative study. *BMC Med* 2015; **13**: 210 [PMID: 26336062 DOI: 10.1186/s12916-015-0450-0]
  - 30 **Assiri A**, McGeer A, Perl TM, Price CS, Al Rabeeah AA, Cummings DA, Alabdullatif ZN, Assad M, Almulhim A, Makhdoom H, Madani H, Alhakeem R, Al-Tawfiq JA, Cotten M, Watson SJ, Kellam P, Zumla AI, Memish ZA; KSA MERS-CoV Investigation Team. Hospital outbreak of Middle East respiratory syndrome coronavirus. *N Engl J Med* 2013; **369**: 407-416 [PMID: 23782161 DOI: 10.1056/NEJMoa1306742]
  - 31 **Poon LL**, Guan Y, Nicholls JM, Yuen KY, Peiris JS. The aetiology, origins, and diagnosis of severe acute respiratory syndrome. *Lancet Infect Dis* 2004; **4**: 663-671 [PMID: 15522678 DOI: 10.1016/S1473-3099(04)01172-7]
  - 32 **Corman VM**, Albarrak AM, Omrani AS, Albarrak MM, Farah ME, Almasri M, Muth D, Sieberg A, Meyer B, Assiri AM, Binger T, Steinhagen K, Lattwein E, Al-Tawfiq J, Müller MA, Drosten C, Memish ZA. Viral Shedding and Antibody Response in 37 Patients With Middle East Respiratory Syndrome Coronavirus Infection. *Clin Infect Dis* 2016; **62**: 477-483 [PMID: 26565003 DOI: 10.1093/cid/civ951]
  - 33 **Zhou J**, Li C, Zhao G, Chu H, Wang D, Yan HH, Poon VK, Wen L, Wong BH, Zhao X, Chiu MC, Yang D, Wang Y, Au-Yeung RKH, Chan IH, Sun S, Chan JF, To KK, Memish ZA, Corman VM, Drosten C, Hung IF, Zhou Y, Leung SY, Yuen KY. Human intestinal tract serves as an alternative infection route for Middle East respiratory syndrome coronavirus. *Sci Adv* 2017; **3**: eaao4966 [PMID: 29152574 DOI: 10.1126/sciadv.aao4966]
  - 34 **Zhou P**, Yang XL, Wang XG, Hu B, Zhang L, Zhang W, Si HR, Zhu Y, Li B, Huang CL, Chen HD, Chen J, Luo Y, Guo H, Jiang RD, Liu MQ, Chen Y, Shen XR, Wang X, Zheng XS, Zhao K, Chen QJ, Deng F, Liu LL, Yan B, Zhan FX, Wang YY, Xiao GF, Shi ZL. A pneumonia outbreak associated with a new coronavirus of probable bat origin. *Nature* 2020; **579**: 270-273 [PMID: 32015507 DOI: 10.1038/s41586-020-2012-7]
  - 35 **Ji W**, Wang W, Zhao X, Zai J, Li X. Cross-species transmission of the newly identified coronavirus 2019-nCoV. *J Med Virol* 2020; **92**: 433-440 [PMID: 31967321 DOI: 10.1002/jmv.25682]
  - 36 **Cheng ZJ**, Shan J. 2019 Novel coronavirus: where we are and what we know. *Infection* 2020; **48**: 155-163 [PMID: 32072569 DOI: 10.1007/s15010-020-01401-y]
  - 37 **Wu D**, Wu T, Liu Q, Yang Z. The SARS-CoV-2 outbreak: What we know. *Int J Infect Dis* 2020; **94**: 44-48 [PMID: 32171952 DOI: 10.1016/j.ijid.2020.03.004]
  - 38 **Wan Y**, Li J, Shen L, Zou Y, Hou L, Zhu L, Faden HS, Tang Z, Shi M, Jiao N, Li Y, Cheng S, Huang Y, Wu D, Xu Z, Pan L, Zhu J, Yan G, Zhu R, Lan P. Enteric involvement in hospitalised patients with COVID-19 outside Wuhan. *Lancet Gastroenterol Hepatol* 2020; **5**: 534-535 [PMID: 32304638 DOI: 10.1016/S2468-1253(20)30118-7]
  - 39 **Jin X**, Lian JS, Hu JH, Gao J, Zheng L, Zhang YM, Hao SR, Jia HY, Cai H, Zhang XL, Yu GD, Xu KJ, Wang XY, Gu JQ, Zhang SY, Ye CY, Jin CL, Lu YF, Yu X, Yu XP, Huang JR, Xu KL, Ni Q, Yu CB, Zhu B, Li YT, Liu J, Zhao H, Zhang X, Yu L, Guo YZ, Su JW, Tao JJ, Lang GJ, Wu XX, Wu WR, Qv TT, Xiang DR, Yi P, Shi D, Chen Y, Ren Y, Qiu YQ, Li LJ, Sheng J, Yang Y. Epidemiological, clinical and virological characteristics of 74 cases of coronavirus-infected disease 2019 (COVID-19) with gastrointestinal symptoms. *Gut* 2020; **69**: 1002-1009 [PMID: 32213556 DOI: 10.1136/gutjnl-2020-320926]
  - 40 **Huang C**, Wang Y, Li X, Ren L, Zhao J, Hu Y, Zhang L, Fan G, Xu J, Gu X, Cheng Z, Yu T, Xia J, Wei Y, Wu W, Xie X, Yin W, Li H, Liu M, Xiao Y, Gao H, Guo L, Xie J, Wang G, Jiang R, Gao Z, Jin Q, Wang J, Cao B. Clinical features of patients infected with 2019 novel coronavirus in Wuhan, China. *Lancet* 2020; **395**: 497-506 [PMID: 31986264 DOI: 10.1016/S0140-6736(20)30183-5]
  - 41 **Holshue ML**, DeBolt C, Lindquist S, Lofy KH, Wiesman J, Bruce H, Spitters C, Ericson K, Wilkerson S, Tural A, Diaz G, Cohn A, Fox L, Patel A, Gerber SI, Kim L, Tong S, Lu X, Lindstrom S, Pallansch MA, Weldon WC, Biggs HM, Uyeki TM, Pillai SK; Washington State 2019-nCoV Case Investigation Team. First Case of 2019 Novel Coronavirus in the United States. *N Engl J Med* 2020; **382**: 929-936 [PMID: 32004427 DOI: 10.1056/NEJMoa2001191]
  - 42 **Zheng S**, Fan J, Yu F, Feng B, Lou B, Zou Q, Xie G, Lin S, Wang R, Yang X, Chen W, Wang Q, Zhang D, Liu Y, Gong R, Ma Z, Lu S, Xiao Y, Gu Y, Zhang J, Yao H, Xu K, Lu X, Wei G, Zhou J, Fang Q, Cai H, Qiu Y, Sheng J, Chen Y, Liang T. Viral load dynamics and disease severity in patients infected with SARS-CoV-2 in Zhejiang province, China, January-March 2020: retrospective cohort study. *BMJ* 2020; **369**: m1443 [PMID: 32317267 DOI: 10.1136/bmj.m1443]
  - 43 **To KK**, Tsang OT, Yip CC, Chan KH, Wu TC, Chan JM, Leung WS, Chik TS, Choi CY, Kandamby DH, Lung DC, Tam AR, Poon RW, Fung AY, Hung IF, Cheng VC, Chan JF, Yuen KY. Consistent Detection of 2019 Novel Coronavirus in Saliva. *Clin Infect Dis* 2020; **71**: 841-843 [PMID: 32047895 DOI: 10.1093/cid/ciaa149]
  - 44 **Hanley B**, Lucas SB, Youd E, Swift B, Osborn M. Autopsy in suspected COVID-19 cases. *J Clin Pathol* 2020; **73**: 239-242 [PMID: 32198191 DOI: 10.1136/jclinpath-2020-206522]
  - 45 **Tian Y**, Rong L, Nian W, He Y. Review article: gastrointestinal features in COVID-19 and the possibility of faecal transmission. *Aliment Pharmacol Ther* 2020; **51**: 843-851 [PMID: 32222988 DOI: 10.1111/apt.15731]

- 46 **Tapper EB**, Asrani SK. The COVID-19 pandemic will have a long-lasting impact on the quality of cirrhosis care. *J Hepatol* 2020; **73**: 441-445 [PMID: [32298769](#) DOI: [10.1016/j.jhep.2020.04.005](#)]
- 47 **World Health Organization**. Hepatitis. Available from: <https://www.who.int/health-topics/hepatitis>
- 48 **Fiore C**, Eisenhut M, Krausse R, Ragazzi E, Pellati D, Armanini D, Bielenberg J. Antiviral effects of Glycyrrhiza species. *Phytother Res* 2008; **22**: 141-148 [PMID: [17886224](#) DOI: [10.1002/ptr.2295](#)]
- 49 **Cai Q**, Huang D, Ou P, Yu H, Zhu Z, Xia Z, Su Y, Ma Z, Zhang Y, Li Z, He Q, Liu L, Fu Y, Chen J. COVID-19 in a designated infectious diseases hospital outside Hubei Province, China. *Allergy* 2020; **75**: 1742-1752 [PMID: [32239761](#) DOI: [10.1111/all.14309](#)]
- 50 **Musa S**. Hepatic and gastrointestinal involvement in coronavirus disease 2019 (COVID-19): What do we know till now? *Arab J Gastroenterol* 2020; **21**: 3-8 [PMID: [32253172](#) DOI: [10.1016/j.ajg.2020.03.002](#)]
- 51 **Stefan N**, Birkenfeld AL, Schulze MB, Ludwig DS. Obesity and impaired metabolic health in patients with COVID-19. *Nat Rev Endocrinol* 2020; **16**: 341-342 [PMID: [32327737](#) DOI: [10.1038/s41574-020-0364-6](#)]
- 52 **Keyes KM**, Hatzenbuehler ML, Hasin DS. Stressful life experiences, alcohol consumption, and alcohol use disorders: the epidemiologic evidence for four main types of stressors. *Psychopharmacology (Berl)* 2011; **218**: 1-17 [PMID: [21373787](#) DOI: [10.1007/s00213-011-2236-1](#)]
- 53 **Strnad P**, Tacke F, Koch A, Trautwein C. Liver - guardian, modifier and target of sepsis. *Nat Rev Gastroenterol Hepatol* 2017; **14**: 55-66 [PMID: [27924081](#) DOI: [10.1038/nrgastro.2016.168](#)]
- 54 **Xiao Y**, Pan H, She Q, Wang F, Chen M. Prevention of SARS-CoV-2 infection in patients with decompensated cirrhosis. *Lancet Gastroenterol Hepatol* 2020; **5**: 528-529 [PMID: [32197093](#) DOI: [10.1016/S2468-1253\(20\)30080-7](#)]
- 55 **Kumar D**, Tellier R, Draker R, Levy G, Humar A. Severe Acute Respiratory Syndrome (SARS) in a liver transplant recipient and guidelines for donor SARS screening. *Am J Transplant* 2003; **3**: 977-981 [PMID: [12859532](#) DOI: [10.1034/j.1600-6143.2003.00197.x](#)]
- 56 **Tzedakis S**, Jeddou H, Houssel-Debry P, Sulpice L, Boudjema K. COVID-19: Thoughts and comments from a tertiary liver transplant center in France. *Am J Transplant* 2020; **20**: 1952-1953 [PMID: [32282972](#) DOI: [10.1111/ajt.15918](#)]
- 57 **Baumgart DC**, Sandborn WJ. Inflammatory bowel disease: clinical aspects and established and evolving therapies. *Lancet* 2007; **369**: 1641-1657 [PMID: [17499606](#) DOI: [10.1016/S0140-6736\(07\)60751-X](#)]
- 58 **Toruner M**, Loftus EV Jr, Harmsen WS, Zinsmeister AR, Orenstein R, Sandborn WJ, Colombel JF, Egan LJ. Risk factors for opportunistic infections in patients with inflammatory bowel disease. *Gastroenterology* 2008; **134**: 929-936 [PMID: [18294633](#) DOI: [10.1053/j.gastro.2008.01.012](#)]
- 59 **Kucharzik T**, Maaser C. Infections and Chronic Inflammatory Bowel Disease. *Viszeralmedizin* 2014; **30**: 326-332 [PMID: [26288602](#) DOI: [10.1159/000366463](#)]
- 60 **An P**, Ji M, Ren H, Su J, Kang J, Yin A, Zhou Q, Shen L, Zhao L, Jiang X, Xiao Y, Tan W, Lv X, Li J, Liu S, Zhou J, Chen H, Xu Y, Liu J, Chen M, Cao J, Zhou Z, Shen L, Tan S, Yu H, Dong W, Ding Y. Protection of 318 inflammatory bowel disease patients from the outbreak and rapid spread of COVID-19 infection in Wuhan, China. *Soc Sci Elec Publishing* 2020 [DOI: [10.2139/ssrn.3543590](#)]
- 61 **Mao R**, Liang J, Shen J, Ghosh S, Zhu LR, Yang H, Wu KC, Chen MH; Chinese Society of IBD; Chinese Elite IBD Union; Chinese IBD Quality Care Evaluation Center Committee. Implications of COVID-19 for patients with pre-existing digestive diseases. *Lancet Gastroenterol Hepatol* 2020; **5**: 425-427 [PMID: [32171057](#) DOI: [10.1016/S2468-1253\(20\)30076-5](#)]
- 62 **Liang W**, Guan W, Chen R, Wang W, Li J, Xu K, Li C, Ai Q, Lu W, Liang H, Li S, He J. Cancer patients in SARS-CoV-2 infection: a nationwide analysis in China. *Lancet Oncol* 2020; **21**: 335-337 [PMID: [32066541](#) DOI: [10.1016/S1470-2045\(20\)30096-6](#)]
- 63 **Liu Y**, Ning Z, Chen Y, Guo M, Liu Y, Gali NK, Sun L, Duan Y, Cai J, Westerdahl D, Liu X, Xu K, Ho KF, Kan H, Fu Q, Lan K. Aerodynamic analysis of SARS-CoV-2 in two Wuhan hospitals. *Nature* 2020; **582**: 557-560 [PMID: [32340022](#) DOI: [10.1038/s41586-020-2271-3](#)]
- 64 **Patel VB**, Zhong JC, Grant MB, Oudit GY. Role of the ACE2/Angiotensin 1-7 Axis of the Renin-Angiotensin System in Heart Failure. *Circ Res* 2016; **118**: 1313-1326 [PMID: [27081112](#) DOI: [10.1161/CIRCRESAHA.116.307708](#)]
- 65 **Miller AJ**, Arnold AC. The renin-angiotensin system in cardiovascular autonomic control: recent developments and clinical implications. *Clin Auton Res* 2019; **29**: 231-243 [PMID: [30413906](#) DOI: [10.1007/s10286-018-0572-5](#)]
- 66 **Kuba K**, Imai Y, Rao S, Gao H, Guo F, Guan B, Huan Y, Yang P, Zhang Y, Deng W, Bao L, Zhang B, Liu G, Wang Z, Chappell M, Liu Y, Zheng D, Leibbrandt A, Wada T, Slutsky AS, Liu D, Qin C, Jiang C, Penninger JM. A crucial role of angiotensin converting enzyme 2 (ACE2) in SARS coronavirus-induced lung injury. *Nat Med* 2005; **11**: 875-879 [PMID: [16007097](#) DOI: [10.1038/nm1267](#)]
- 67 **Wrapp D**, Wang N, Corbett KS, Goldsmith JA, Hsieh CL, Abiona O, Graham BS, McLellan JS. Cryo-EM structure of the 2019-nCoV spike in the prefusion conformation. *Science* 2020; **367**: 1260-1263 [PMID: [32075877](#) DOI: [10.1126/science.abb2507](#)]
- 68 **Yang P**, Gu H, Zhao Z, Wang W, Cao B, Lai C, Yang X, Zhang L, Duan Y, Zhang S, Chen W, Zhen W, Cai M, Penninger JM, Jiang C, Wang X. Angiotensin-converting enzyme 2 (ACE2) mediates influenza H7N9 virus-induced acute lung injury. *Sci Rep* 2014; **4**: 7027 [PMID: [25391767](#) DOI: [10.1038/s41598-014-07027-7](#)]

- 10.1038/srep07027]
- 69 **Hoffmann M**, Kleine-Weber H, Schroeder S, Krüger N, Herrler T, Erichsen S, Schiergens TS, Herrler G, Wu NH, Nitsche A, Müller MA, Drosten C, Pöhlmann S. SARS-CoV-2 Cell Entry Depends on ACE2 and TMPRSS2 and Is Blocked by a Clinically Proven Protease Inhibitor. *Cell* 2020; **181**: 271-280. e8 [PMID: [32142651](#) DOI: [10.1016/j.cell.2020.02.052](#)]
  - 70 **Zhang H**, Kang Z, Gong H, Xu D, Wang J, Li Z, Li Z, Cui X, Xiao J, Zhan J, Meng T, Zhou W, Liu J, Xu H. Digestive system is a potential route of COVID-19: an analysis of single-cell coexpression pattern of key proteins in viral entry process. *Gut* 2020; gutjnl-2020 [DOI: [10.1136/gutjnl-2020-320953](#)]
  - 71 **Van Pelt J**, Van Kuik JA, Kamerling JP, Vliegenthart JF, Van Diggelen OP, Galjaard H. Storage of sialic acid-containing carbohydrates in the placenta of a human galactosialidosis fetus. Isolation and structural characterization of 16 sialyloligosaccharides. *Eur J Biochem* 1988; **177**: 327-338 [PMID: [3142773](#) DOI: [10.1111/j.1432-1033.1988.tb14380.x](#)]
  - 72 **Haber AL**, Biton M, Rogel N, Herbst RH, Shekhar K, Smillie C, Burgin G, Delorey TM, Howitt MR, Katz Y, Tirosh I, Beyaz S, Dionne D, Zhang M, Raychowdhury R, Garrett WS, Rozenblatt-Rosen O, Shi HN, Yilmaz O, Xavier RJ, Regev A. A single-cell survey of the small intestinal epithelium. *Nature* 2017; **551**: 333-339 [PMID: [29144463](#) DOI: [10.1038/nature24489](#)]
  - 73 **Desmarests LMB**, Theuns S, Roukaerts IDM, Acar DD, Nauwynck HJ. Role of sialic acids in feline enteric coronavirus infections. *J Gen Virol* 2014; **95**: 1911-1918 [PMID: [24876305](#) DOI: [10.1099/vir.0.064717-0](#)]
  - 74 **Crawford SE**, Ramani S, Tate JE, Parashar UD, Svensson L, Hagbom M, Franco MA, Greenberg HB, O'Ryan M, Kang G, Desselberger U, Estes MK. Rotavirus infection. *Nat Rev Dis Primers* 2017; **3**: 17083 [PMID: [29119972](#) DOI: [10.1038/nrdp.2017.83](#)]
  - 75 **Seow J**, Pai R, Mishra A, Shepherdson E, Lim T, Goh B, Chan J, Chow P, Ginhoux F, DasGupta R, Sharma A. scRNA-seq reveals ACE2 and TMPRSS2 expression in TROP2+ Liver Progenitor Cells: Implications in COVID-19 associated Liver Dysfunction. *bioRxiv* 2020 [DOI: [10.1101/2020.03.23.002832](#)]
  - 76 **Banales JM**, Huebert RC, Karlsen T, Strazzabosco M, LaRusso NF, Gores GJ. Cholangiocyte pathobiology. *Nat Rev Gastroenterol Hepatol* 2019; **16**: 269-281 [PMID: [30850822](#) DOI: [10.1038/s41575-019-0125-y](#)]
  - 77 **Hashimoto T**, Perlot T, Rehman A, Trichereau J, Ishiguro H, Paolino M, Sigl V, Hanada T, Hanada R, Lipinski S, Wild B, Camargo SM, Singer D, Richter A, Kuba K, Fukamizu A, Schreiber S, Clevers H, Verrey F, Rosenstiel P, Penninger JM. ACE2 links amino acid malnutrition to microbial ecology and intestinal inflammation. *Nature* 2012; **487**: 477-481 [PMID: [22837003](#) DOI: [10.1038/nature11228](#)]
  - 78 **Monteil V**, Kwon H, Prado P, Hagelkrüys A, Wimmer RA, Stahl M, Leopoldi A, Garreta E, Hurtado Del Pozo C, Prosper F, Romero JP, Wirnsberger G, Zhang H, Slutsky AS, Conder R, Montserrat N, Mirazimi A, Penninger JM. Inhibition of SARS-CoV-2 Infections in Engineered Human Tissues Using Clinical-Grade Soluble Human ACE2. *Cell* 2020; **181**: 905-913. e7 [PMID: [32333836](#) DOI: [10.1016/j.cell.2020.04.004](#)]
  - 79 **Lei C**, Qian K, Li T, Zhang S, Fu W, Ding M, Hu S. Neutralization of SARS-CoV-2 spike pseudotyped virus by recombinant ACE2-Ig. *Nat Commun* 2020; **11**: 2070 [PMID: [32332765](#) DOI: [10.1038/s41467-020-16048-4](#)]
  - 80 **Shi R**, Shan C, Duan X, Chen Z, Liu P, Song J, Song T, Bi X, Han C, Wu L, Gao G, Hu X, Zhang Y, Tong Z, Huang W, Liu WJ, Wu G, Zhang B, Wang L, Qi J, Feng H, Wang FS, Wang Q, Gao GF, Yuan Z, Yan J. A human neutralizing antibody targets the receptor-binding site of SARS-CoV-2. *Nature* 2020; **584**: 120-124 [PMID: [32454512](#) DOI: [10.1038/s41586-020-2381-y](#)]
  - 81 **Lamers MM**, Beumer J, van der Vaart J, Knoops K, Puschhof J, Breugem TI, Ravelli RBG, Paul van Schayck J, Mykytyn AZ, Duimel HQ, van Donselaar E, Riesebosch S, Kuijpers HJH, Schipper D, van de Wetering WJ, de Graaf M, Koopmans M, Cuppen E, Peters PJ, Haagmans BL, Clevers H. SARS-CoV-2 productively infects human gut enterocytes. *Science* 2020; **369**: 50-54 [PMID: [32358202](#) DOI: [10.1126/science.abc1669](#)]
  - 82 **Adams DH**, Ju C, Ramaiah SK, Uetrecht J, Jaeschke H. Mechanisms of immune-mediated liver injury. *Toxicol Sci* 2010; **115**: 307-321 [PMID: [20071422](#) DOI: [10.1093/toxsci/kfq009](#)]
  - 83 **Zhou JA**, Jiang M, Yang X, Liu Y, Guo J, Zheng J, Qu Y, Song Y, Li R, Qin X, Wang X. Unconjugated bilirubin ameliorates the inflammation and digestive protease increase in TNBS-induced colitis. *Mol Med Rep* 2017; **16**: 1779-1784 [PMID: [28656252](#) DOI: [10.3892/mmr.2017.6825](#)]
  - 84 **Lohse AW**, Weiler-Normann C, Tiegs G. Immune-mediated liver injury. *J Hepatol* 2010; **52**: 136-144 [PMID: [19913936](#) DOI: [10.1016/j.jhep.2009.10.016](#)]
  - 85 **Qin C**, Zhou L, Hu Z, Zhang S, Yang S, Tao Y, Xie C, Ma K, Shang K, Wang W, Tian DS. Dysregulation of Immune Response in Patients With Coronavirus 2019 (COVID-19) in Wuhan, China. *Clin Infect Dis* 2020; **71**: 762-768 [PMID: [32161940](#) DOI: [10.1093/cid/ciaa248](#)]
  - 86 **Tan M**, Liu Y, Zhou R, Deng X, Li F, Liang K, Shi Y. Immunopathological characteristics of coronavirus disease 2019 cases in Guangzhou, China. *Immunology* 2020; **160**: 261-268 [PMID: [32460357](#) DOI: [10.1111/imm.13223](#)]
  - 87 **Cao X**. COVID-19: immunopathology and its implications for therapy. *Nat Rev Immunol* 2020; **20**: 269-270 [PMID: [32273594](#) DOI: [10.1038/s41577-020-0308-3](#)]
  - 88 **Tracey KJ**. Physiology and immunology of the cholinergic antiinflammatory pathway. *J Clin Invest*



- 2007; **117**: 289-296 [PMID: [17273548](#) DOI: [10.1172/JCI30555](#)]
- 89 **Tracey KJ**. The inflammatory reflex. *Nature* 2002; **420**: 853-859 [PMID: [12490958](#) DOI: [10.1038/nature01321](#)]
- 90 **Staats P**, Giannakopoulos G, Blake J, Liebler E, Levy RM. The Use of Non-invasive Vagus Nerve Stimulation to Treat Respiratory Symptoms Associated With COVID-19: A Theoretical Hypothesis and Early Clinical Experience. *Neuromodulation* 2020; **23**: 784-788 [PMID: [32342609](#) DOI: [10.1111/ner.13172](#)]
- 91 **Varga Z**, Flammer AJ, Steiger P, Haberecker M, Andermatt R, Zinkernagel AS, Mehra MR, Schuepbach RA, Ruschitzka F, Moch H. Endothelial cell infection and endotheliitis in COVID-19. *Lancet* 2020; **395**: 1417-1418 [PMID: [32325026](#) DOI: [10.1016/S0140-6736\(20\)30937-5](#)]
- 92 **Feng T**, Elson CO. Adaptive immunity in the host-microbiota dialog. *Mucosal Immunol* 2011; **4**: 15-21 [PMID: [20944557](#) DOI: [10.1038/mi.2010.60](#)]
- 93 **Sender R**, Fuchs S, Milo R. Revised Estimates for the Number of Human and Bacteria Cells in the Body. *PLoS Biol* 2016; **14**: e1002533 [PMID: [27541692](#) DOI: [10.1371/journal.pbio.1002533](#)]
- 94 **Selber-Hnatiw S**, Rukundo B, Ahmadi M, Akoubi H, Al-Bizri H, Aliu AF, Ambeaghen TU, Avetisyan L, Bahar I, Baird A, Begum F, Ben Soussan H, Blondeau-Éthier V, Bordaries R, Bramwell H, Briggs A, Bui R, Carnevale M, Chancharoen M, Chevassus T, Choi JH, Coulombe K, Couvrette F, D'Abreu S, Davies M, Desbiens MP, Di Maulo T, Di Paolo SA, Do Ponte S, Dos Santos Ribeiro P, Dubuc-Kanary LA, Duncan PK, Dupuis F, El-Nounou S, Eyangos CN, Ferguson NK, Flores-Chinchilla NR, Fotakis T, Gado Oumarou H D M, Georgiev M, Ghiassy S, Glibetic N, Grégoire Bouchard J, Hassan T, Huseen I, Ibuna Quilatan MF, Iozzo T, Islam S, Jaunky DB, Jeyasegaram A, Johnston MA, Kahler MR, Kaler K, Kamani C, Karimian Rad H, Konidis E, Konieczny F, Kurianowicz S, Lamothe P, Legros K, Leroux S, Li J, Lozano Rodriguez ME, Luponio-Yoffe S, Maalouf Y, Mantha J, McCormick M, Mondragon P, Narayana T, Neretin E, Nguyen TTT, Niu I, Nkemazem RB, O'Donovan M, Oueis M, Paquette S, Patel N, Pecs E, Peters J, Pettoirelli A, Poirier C, Pompa VR, Rajen H, Ralph RO, Rosales-Vasquez J, Rubinshtein D, Sakr S, Sebai MS, Serravalle L, Sidibe F, Sinnathurai A, Soho D, Sundarakrishnan A, Svistkova V, Ugbeye TE, Vasconcelos MS, Vincelli M, Voitovich O, Vrabel P, Wang L, Wasfi M, Zha CY, Gamberi C. Human Gut Microbiota: Toward an Ecology of Disease. *Front Microbiol* 2017; **8**: 1265 [PMID: [28769880](#) DOI: [10.3389/fmicb.2017.01265](#)]
- 95 **Schirmer M**, Franzosa EA, Lloyd-Price J, McIver LJ, Schwager R, Poon TW, Ananthakrishnan AN, Andrews E, Barron G, Lake K, Prasad M, Sauk J, Stevens B, Wilson RG, Braun J, Denson LA, Kugathasan S, McGovern DPB, Vlamakis H, Xavier RJ, Huttenhower C. Dynamics of metatranscription in the inflammatory bowel disease gut microbiome. *Nat Microbiol* 2018; **3**: 337-346 [PMID: [29311644](#) DOI: [10.1038/s41564-017-0089-z](#)]
- 96 **Jiang C**, Li G, Huang P, Liu Z, Zhao B. The Gut Microbiota and Alzheimer's Disease. *J Alzheimers Dis* 2017; **58**: 1-15 [PMID: [28372330](#) DOI: [10.3233/JAD-161141](#)]
- 97 **Rutten EPA**, Lenaerts K, Buurman WA, Wouters EFM. Disturbed intestinal integrity in patients with COPD: effects of activities of daily living. *Chest* 2014; **145**: 245-252 [PMID: [23928850](#) DOI: [10.1378/chest.13-0584](#)]
- 98 **Wang J**, Li F, Wei H, Lian ZX, Sun R, Tian Z. Respiratory influenza virus infection induces intestinal immune injury via microbiota-mediated Th17 cell-dependent inflammation. *J Exp Med* 2014; **211**: 2397-2410 [PMID: [25366965](#) DOI: [10.1084/jem.20140625](#)]
- 99 **Yildiz S**, Mazel-Sanchez B, Kandasamy M, Manicassamy B, Schmolke M. Influenza A virus infection impacts systemic microbiota dynamics and causes quantitative enteric dysbiosis. *Microbiome* 2018; **6**: 9 [PMID: [29321057](#) DOI: [10.1186/s40168-017-0386-z](#)]
- 100 **Budden KF**, Gellatly SL, Wood DL, Cooper MA, Morrison M, Hugenholtz P, Hansbro PM. Emerging pathogenic links between microbiota and the gut-lung axis. *Nat Rev Microbiol* 2017; **15**: 55-63 [PMID: [27694885](#) DOI: [10.1038/nrmicro.2016.142](#)]
- 101 **Ma C**, Cong Y, Zhang H. COVID-19 and the Digestive System. *Am J Gastroenterol* 2020; **115**: 1003-1006 [PMID: [32618648](#) DOI: [10.14309/ajg.0000000000000691](#)]
- 102 **Perlot T**, Penninger JM. ACE2 - from the renin-angiotensin system to gut microbiota and malnutrition. *Microbes Infect* 2013; **15**: 866-873 [PMID: [23962453](#) DOI: [10.1016/j.micinf.2013.08.003](#)]
- 103 **Xu K**, Cai H, Shen Y, Ni Q, Chen Y, Hu S, Li J, Wang H, Yu L, Huang H, Qiu Y, Wei G, Fang Q, Zhou J, Sheng J, Liang T, Li L. [Management of corona virus disease-19 (COVID-19): the Zhejiang experience]. *Zhejiang Da Xue Xue Bao Yi Xue Ban* 2020; **49**: 147-157 [PMID: [32096367](#) DOI: [10.3785/j.issn.1008-9292.2020.02.02](#)]
- 104 **Zuo T**, Zhang F, Lui GCY, Yeoh YK, Li AYL, Zhan H, Wan Y, Chung ACK, Cheung CP, Chen N, Lai CKC, Chen Z, Tso EYK, Fung KSC, Chan V, Ling L, Joynt G, Hui DSC, Chan FKL, Chan PKS, Ng SC. Alterations in Gut Microbiota of Patients With COVID-19 During Time of Hospitalization. *Gastroenterology* 2020; **159**: 944-955. e8 [PMID: [32442562](#) DOI: [10.1053/j.gastro.2020.05.048](#)]
- 105 **Jung TH**, Park JH, Jeon WM, Han KS. Butyrate modulates bacterial adherence on LS174T human colorectal cells by stimulating mucin secretion and MAPK signaling pathway. *Nutr Res Pract* 2015; **9**: 343-349 [PMID: [26244071](#) DOI: [10.4162/nrp.2015.9.4.343](#)]
- 106 **Fukuda S**, Toh H, Hase K, Oshima K, Nakanishi Y, Yoshimura K, Tobe T, Clarke JM, Topping DL, Suzuki T, Taylor TD, Itoh K, Kikuchi J, Morita H, Hattori M, Ohno H. Bifidobacteria can protect from enteropathogenic infection through production of acetate. *Nature* 2011; **469**: 543-547 [PMID: [21270894](#) DOI: [10.1038/nature09646](#)]

- 107 **Li M**, van Esch BCAM, Wagenaar GTM, Garssen J, Folkerts G, Henricks PAJ. Pro- and anti-inflammatory effects of short chain fatty acids on immune and endothelial cells. *Eur J Pharmacol* 2018; **831**: 52-59 [PMID: [29750914](#) DOI: [10.1016/j.ejphar.2018.05.003](#)]
- 108 **Dethlefsen L**, Huse S, Sogin ML, Relman DA. The pervasive effects of an antibiotic on the human gut microbiota, as revealed by deep 16S rRNA sequencing. *PLoS Biol* 2008; **6**: e280 [PMID: [19018661](#) DOI: [10.1371/journal.pbio.0060280](#)]
- 109 **Duan J**, Wu Y, Liu C, Yang C, Yang L. Deleterious effects of viral pneumonia on cardiovascular system. *Eur Heart J* 2020; **41**: 1833-1838 [PMID: [32383765](#) DOI: [10.1093/eurheartj/ehaa325](#)]
- 110 **Konturek PC**, Brzozowski T, Konturek SJ. Stress and the gut: pathophysiology, clinical consequences, diagnostic approach and treatment options. *J Physiol Pharmacol* 2011; **62**: 591-599 [PMID: [22314561](#)]
- 111 **Li S**, Wang Y, Xue J, Zhao N, Zhu T. The Impact of COVID-19 Epidemic Declaration on Psychological Consequences: A Study on Active Weibo Users. *Int J Environ Res Public Health* 2020; **17** [PMID: [32204411](#) DOI: [10.3390/ijerph17062032](#)]
- 112 **Brooks SK**, Webster RK, Smith LE, Woodland L, Wessely S, Greenberg N, Rubin GJ. The psychological impact of quarantine and how to reduce it: rapid review of the evidence. *Lancet* 2020; **395**: 912-920 [PMID: [32112714](#) DOI: [10.1016/S0140-6736\(20\)30460-8](#)]
- 113 **Chigr F**, Merzouki M, Najimi M. Autonomic Brain Centers and Pathophysiology of COVID-19. *ACS Chem Neurosci* 2020; **11**: 1520-1522 [PMID: [32427468](#) DOI: [10.1021/acscchemneuro.0c00265](#)]
- 114 **Cholankeril G**, Podboy A, Aivaliotis VI, Tarlow B, Pham EA, Spencer SP, Kim D, Hsing A, Ahmed A. High Prevalence of Concurrent Gastrointestinal Manifestations in Patients With Severe Acute Respiratory Syndrome Coronavirus 2: Early Experience From California. *Gastroenterology* 2020; **159**: 775-777 [PMID: [32283101](#) DOI: [10.1053/j.gastro.2020.04.008](#)]
- 115 **Tassorelli C**, Mojoli F, Baldanti F, Bruno R, Benazzo M. COVID-19: what if the brain had a role in causing the deaths? *Eur J Neurol* 2020; **27**: e41-e42 [PMID: [32333819](#) DOI: [10.1111/ene.14275](#)]
- 116 **Fan Z**, Chen L, Li J, Cheng X, Yang J, Tian C, Zhang Y, Huang S, Liu Z, Cheng J. Clinical Features of COVID-19-Related Liver Functional Abnormality. *Clin Gastroenterol Hepatol* 2020; **18**: 1561-1566 [PMID: [32283325](#) DOI: [10.1016/j.cgh.2020.04.002](#)]
- 117 **Zhang JJ**, Dong X, Cao YY, Yuan YD, Yang YB, Yan YQ, Akdis CA, Gao YD. Clinical characteristics of 140 patients infected with SARS-CoV-2 in Wuhan, China. *Allergy* 2020; **75**: 1730-1741 [PMID: [32077115](#) DOI: [10.1111/all.14238](#)]
- 118 **Zhou F**, Yu T, Du R, Fan G, Liu Y, Liu Z, Xiang J, Wang Y, Song B, Gu X, Guan L, Wei Y, Li H, Wu X, Xu J, Tu S, Zhang Y, Chen H, Cao B. Clinical course and risk factors for mortality of adult inpatients with COVID-19 in Wuhan, China: a retrospective cohort study. *Lancet* 2020; **395**: 1054-1062 [PMID: [32171076](#) DOI: [10.1016/S0140-6736\(20\)30566-3](#)]
- 119 **Zhang B**, Zhou X, Qiu Y, Song Y, Feng F, Feng J, Song Q, Jia Q, Wang J. Clinical characteristics of 82 cases of death from COVID-19. *PLoS One* 2020; **15**: e0235458 [PMID: [32645044](#) DOI: [10.1371/journal.pone.0235458](#)]
- 120 **Xu XW**, Wu XX, Jiang XG, Xu KJ, Ying LJ, Ma CL, Li SB, Wang HY, Zhang S, Gao HN, Sheng JF, Cai HL, Qiu YQ, Li LJ. Clinical findings in a group of patients infected with the 2019 novel coronavirus (SARS-Cov-2) outside of Wuhan, China: retrospective case series. *BMJ* 2020; **368**: m606 [PMID: [32075786](#) DOI: [10.1136/bmj.m606](#)]
- 121 **Chen G**, Wu D, Guo W, Cao Y, Huang D, Wang H, Wang T, Zhang X, Chen H, Yu H, Zhang X, Zhang M, Wu S, Song J, Chen T, Han M, Li S, Luo X, Zhao J, Ning Q. Clinical and immunological features of severe and moderate coronavirus disease 2019. *J Clin Invest* 2020; **130**: 2620-2629 [PMID: [32217835](#) DOI: [10.1172/JCI137244](#)]
- 122 **Luo S**, Zhang X, Xu H. Don't Overlook Digestive Symptoms in Patients With 2019 Novel Coronavirus Disease (COVID-19). *Clin Gastroenterol Hepatol* 2020; **18**: 1636-1637 [PMID: [32205220](#) DOI: [10.1016/j.cgh.2020.03.043](#)]



## Basic Study

# Xiangbinfang granules enhance gastric antrum motility via intramuscular interstitial cells of Cajal in mice

Qi-Cheng Chen, Zhi Jiang, Jun-Hong Zhang, Li-Xing Cao, Zhi-Qiang Chen

**ORCID number:** Qi-Cheng Chen 0000-0001-5852-3056; Zhi Jiang 0000-0001-5261-1493; Jun-Hong Zhang 0000-0003-0611-9478; Li-Xing Cao 0000-0001-6602-7730; Zhi-Qiang Chen 0000-0001-7658-2746.

**Author contributions:** Chen QC, Cao LX and Chen ZQ designed the research study; Chen QC, Jiang Z and Zhang JH performed the research; Chen QC analyzed the data and wrote the manuscript; all authors have read and approved the final manuscript.

**Supported by** The Specific Research Fund for TCM Science and Technology of Guangdong Provincial Hospital of Chinese Medicine, No. YN10101902; and the National Regional Traditional Chinese Medicine (Specialist) Clinic Construction, No. (2018)205.

**Institutional review board statement:** The study was reviewed and approved by the Institutional Animal Care and Ethics Committee of Guangdong Provincial Hospital of Traditional Chinese Medicine (approval No. 2018003).

**Institutional animal care and use committee statement:** All animal procedures were conducted according to the Regulations for the Care and Use of Laboratory

**Qi-Cheng Chen, Zhi Jiang, Li-Xing Cao, Zhi-Qiang Chen**, The Research Team of TCM Applications of Perioperative, The Second Affiliated Hospital of Guangzhou University of Chinese Medicine, Guangdong Provincial Hospital of Traditional Chinese Medicine, Guangzhou 510120, Guangdong Province, China

**Jun-Hong Zhang**, Department of Research Public Service Center, The Second Affiliated Hospital of Guangzhou University of Chinese Medicine, Guangdong Provincial Hospital of Traditional Chinese Medicine, Guangzhou 510120, Guangdong Province, China

**Corresponding author:** Zhi-Qiang Chen, MD, Professor, The Research Team of TCM Applications of Perioperative, The Second Affiliated Hospital of Guangzhou University of Chinese Medicine, Guangdong Provincial Hospital of Traditional Chinese Medicine, No. 111 Dade Road, Guangzhou 510120, Guangdong Province, China. [wssq@gzucm.edu.cn](mailto:wssq@gzucm.edu.cn)

## Abstract

### BACKGROUND

Interdigestive migrating motor complexes (MMC) produce periodic contractions in the gastrointestinal tract, but the exact mechanism of action still remains unclear. Intramuscular interstitial cells of Cajal (ICC-IM) participate in gastrointestinal hormone and neuromodulation, but the correlation between ICC-IM and MMC is also unclear. We found that xiangbinfang granules (XBF) mediated the phase III contraction of MMC. Here, the effects of XBF on gastric antrum motility in *W/W<sup>s</sup>* mice and the effects of ICC-IM on gastric antrum MMC are reported.

### AIM

To observe the effects of ICC-IM on gastric antrum motility and to establish the mechanism of XBF in promoting gastric antrum motility.

### METHODS

The density of c-kit-positive ICC myenteric plexus (ICC-MP) and ICC-IM in the antral muscularis of *W/W<sup>s</sup>* and wild-type (WT) mice was examined by confocal microscopy. The effects of XBF on gastric antrum slow waves in *W/W<sup>s</sup>* and WT mice were recorded by intracellular amplification recording. Micro-strain-gauge force transducers were implanted into the gastric antrum to monitor the MMC and the effect of XBF on gastric antrum motility in conscious *W/W<sup>s</sup>* and WT mice.

### RESULTS

Animals in Guangzhou University of Chinese Medicine.

**Conflict-of-interest statement:** The authors declare that there is no conflict of interest in this study.

**Data sharing statement:** Technical appendix, statistical code, and dataset are available from the corresponding author at [wssq@gzucm.edu.cn](mailto:wssq@gzucm.edu.cn).

**ARRIVE guidelines statement:** The authors have read the ARRIVE guidelines, and the manuscript was prepared and revised according to the ARRIVE guidelines.

**Open-Access:** This article is an open-access article that was selected by an in-house editor and fully peer-reviewed by external reviewers. It is distributed in accordance with the Creative Commons Attribution NonCommercial (CC BY-NC 4.0) license, which permits others to distribute, remix, adapt, build upon this work non-commercially, and license their derivative works on different terms, provided the original work is properly cited and the use is non-commercial. See: <http://creativecommons.org/licenses/by-nc/4.0/>

**Manuscript source:** Unsolicited manuscript

**Specialty type:** Gastroenterology and hepatology

**Country/Territory of origin:** China

**Peer-review report's scientific quality classification**

Grade A (Excellent): 0  
Grade B (Very good): B  
Grade C (Good): C  
Grade D (Fair): 0  
Grade E (Poor): 0

**Received:** October 27, 2020

**Peer-review started:** October 27, 2020

**First decision:** December 13, 2020

**Revised:** December 24, 2020

**Accepted:** January 13, 2021

**Article in press:** January 13, 2021

**Published online:** February 21, 2021

In the gastric antrum of  $W/W^v$  mice, c-kit immunoreactivity was significantly reduced, and no ICC-IM network was observed. Spontaneous rhythmic slow waves also appeared in the antrum of  $W/W^v$  mice, but the amplitude of the antrum slow wave decreased significantly in  $W/W^v$  mice ( $22.62 \pm 2.23$  mV *vs*  $2.92 \pm 0.52$  mV,  $P < 0.0001$ ). MMCs were found in 7 of the 8 WT mice but no complete MMC cycle was found in  $W/W^v$  mice. The contractile frequency and amplitude index of the gastric antrum were significantly increased in conscious WT compared to  $W/W^v$  mice (frequency,  $3.53 \pm 0.18$  cpm *vs*  $1.28 \pm 0.12$  cpm; amplitude index,  $23014.26 \pm 1798.65$  mV  $\cdot$  20 min *vs*  $3782.16 \pm 407.13$  mV  $\cdot$  20 min;  $P < 0.0001$ ). XBF depolarized smooth muscle cells of the gastric antrum in WT and  $W/W^v$  mice in a dose-dependent manner. Similarly, the gastric antrum motility in WT mice was significantly increased after treatment with XBF 5 mg ( $P < 0.05$ ). Atropine (0.1 mg/kg) blocked the enhancement of XBF in WT and  $W/W^v$  mice completely, while tetrodotoxin (0.05 mg/kg) partially inhibited the enhancement by XBF.

## CONCLUSION

ICC-IM participates in the regulation of gastric antrum MMC in mice. XBF induces MMC III-like contractions that enhance gastric antrum motility *via* ICC-IM in mice.

**Key Words:** Interstitial cells of Cajal; Migrating motor complex;  $W/W^v$ ; Gastric antrum motility; Xiangbinfang granules; Chinese medicine

©The Author(s) 2021. Published by Baishideng Publishing Group Inc. All rights reserved.

**Core Tip:** This study shows that intramuscular interstitial cells of Cajal (ICC-IM) play crucial roles in regulating the activity of gastric antral migrating motor complexes (MMC). This may be an important bridge between the vagus, enteric nervous system and motilin to regulate smooth muscle contraction. Through the muscarinic receptor pathway on ICC-IM, the Chinese medicine Xiangbinfang granules depolarize smooth muscle cells and initiates an action potential, changing the periodic motion of MMC into a phase III-like contraction pattern in the gastric antrum of mice.

**Citation:** Chen QC, Jiang Z, Zhang JH, Cao LX, Chen ZQ. Xiangbinfang granules enhance gastric antrum motility *via* intramuscular interstitial cells of Cajal in mice. *World J Gastroenterol* 2021; 27(7): 576-591

**URL:** <https://www.wjgnet.com/1007-9327/full/v27/i7/576.htm>

**DOI:** <https://dx.doi.org/10.3748/wjg.v27.i7.576>

## INTRODUCTION

Interdigestive migrating motor complexes (MMC) induce periodic contractions of the gastric, small intestine, or colon smooth muscle, propagating along the gastrointestinal (GI) tract. Although the exact mechanism of MMC action still remains unclear, MMC have been classified into four stages. The MMC phase III consists of a high-frequency, high-amplitude rhythmic contraction, which has important physiological significance in normal GI motility and digestion<sup>[1]</sup>. Interstitial cells of Cajal (ICC), which are electrically coupled to smooth muscle cells (SMCs), produce slow waves that function as pacemaker activity<sup>[2]</sup>. There are several ICC subtypes based on their anatomical locations, morphology, and function in the GI tract. ICC associated with the myenteric plexus (ICC-MP) are responsible for producing slow waves. Intramuscular ICC (ICC-IM), which are located in muscle bundles between muscle cells, mediate information transmission from autonomic nerves to SMCs<sup>[3]</sup>. In the small intestine of  $W/W^v$  mice lacking ICC-MP, there are no rhythmic slow waves and there are irregular contractions of longitudinal and circular muscles<sup>[4]</sup>. However, the MMC cycle still exists in the isolated intestine of  $W/W^v$  mice, suggesting that MMC do not require ICC-MP<sup>[5]</sup>. Other studies have shown that with the depletion of gastric ICC, disorders of the MMC cycle are common in diabetic gastroparesis<sup>[6,7]</sup>. This seems to indicate that ICC, especially ICC-IM, may also be involved in regulating the movement of MMC.



**P-Reviewer:** Baker SA, Huizinga JD**S-Editor:** Chen XF**L-Editor:** Webster JR**P-Editor:** Ma YJ

The Chinese herbal medicine xiangbinfang granules (XBF) is an effective treatment for promoting the post-surgical recovery of GI function<sup>[8,9]</sup>. Previous studies have shown that XBF significantly enhanced MMC activity in the antrum, pylorus, duodenum, jejunum, and the colon in beagles<sup>[10]</sup>. XBF was also found to promote contraction of the stomach, duodenum, and jejunum in healthy volunteers<sup>[11]</sup>. However, the mechanism of XBF in enhancing MMC activity in the GI tract is still unclear.

In this study, we observed the MMC activity of the gastric antrum in *W/W<sup>v</sup>* mice that lacked ICC-IM and analyzed the effects of the traditional Chinese medicine XBF in promoting gastric antrum motility.

## MATERIALS AND METHODS

### Animals

This study included 36 *W/W<sup>v</sup>* and 36 wild-type (WT) mice. *W/W<sup>v</sup>* mice were obtained from Jackson Laboratory (Bar Harbor, ME, United States) and bred in Guangdong Provincial Experimental Animal Center. The *W/W<sup>v</sup>* and WT mice (weighing 18–25 g) were allowed free access to a standard laboratory chow diet and water and housed at a temperature of 22–24°C under a 12:12 h light/dark cycle. The study protocol was approved by the Institutional Animal Care and Ethics Committee of Guangdong Provincial Hospital of Traditional Chinese Medicine (No. 2018003). All animal procedures were conducted according to the Regulations for the Care and Use of Laboratory Animals in Guangzhou University of Chinese Medicine.

### Tissue preparation

The mice were initially anesthetized with isoflurane before being killed by cervical dislocation. The whole stomach was placed in Krebs-Ringer buffer that was constantly perfused with oxygen. A cut was made along the lesser curvature of the stomach, the stomach was washed with ice-cold Krebs with the mucosa facing upward, and then the mucosa and submucosa were carefully removed.

### Immunofluorescence staining of the gastric antrum

Ten *W/W<sup>v</sup>* and 10 WT mice were used for immunofluorescence staining of the gastric antrum. The immunolabeling of mouse tissues was carried out on whole tissue mounts devoid of mucosa and submucosa. The whole mounts were stained with the primary antibodies for 1:100 c-kit (SC-168; Santa Cruz, CA, United States) and incubated for 1 h with 1:400 donkey anti-Rb IgG and Alexa Fluor 594. All immunostaining was imaged with a confocal microscope (Zeiss LSM 710; Göttingen, Germany) at an excitation wavelength of 594 nm. The c-kit-positive cells were observed under a 20 × objective lens. The confocal micrographs shown are digital composites of the Z-series with a depth of 6–10 μm for ICC-MP and 15–30 μm for ICC-IM. The density of ICC-MP and ICC-IM was estimated by scanning through a 6-μm thickness of tissue area, counting the number of positive cells. The area of each micrograph was 424.3 μm × 424.3 μm = 0.18 mm<sup>2</sup>. The unit volume was 424.3 μm × 424.3 μm × 6 μm = 0.0011 mm<sup>3</sup>. The immunofluorescence staining of the gastric antrum was performed as previously described<sup>[12]</sup>.

### Intracellular microelectrode recording

Eighteen *W/W<sup>v</sup>* and 18 WT mice were used for intracellular microelectrode recording. Full-thickness muscle strips (8 mm × 4 mm) were cut from the gastric antrum and pinned onto the base of a silica layer and continuously perfused with oxygenated Krebs-Ringer buffer at 37°C. Before recording, the strips were incubated for 2 h. The glass microelectrodes with resistance ranging between 50 and 80 MΩ were filled with 1 mol/L KCl for penetrating cells. The electrical response was recorded and amplified using a high input impedance amplifier (AXON 210B; Molecular Devices, San Jose, CA, United States). The data were recorded on a computer using Clampfit 10.4 software.

### Recording of MMC in the gastric antrum

When the 8 *W/W<sup>v</sup>* and 8 WT mice were anesthetized by isoflurane inhalation, the limbs were fixed on the Baoding frame, and the abdominal hair was shaved with a razor and disinfected with iodophor. The abdominal cavity was carefully opened and the gastric antrum fully exposed. Then the micro-strain-gauge force transducers (J2A-

06-S108N-10C; Micro-Measurements, Raleigh, NC, United States) were sutured to the gastric serosa with a needle and nylon thread. The electrode leads were drawn from the back of the neck through the subcutaneous layer before closing the abdomen. After monitoring the animal's wakefulness for more than 15 min, the micro-strain-gauge force transducers were connected to the Porti physiological recorder (TMSI, Netherlands) to measure the gastric contractile motion. The first 30 min were recorded for baseline control and the next 30 min for treatment. The gastric contractile frequency and amplitude index (sum of amplitudes within 20 min) were analyzed.

### Solutions and drugs

XBF was produced by Hunan Academy of Chinese Medicine and contains *Areca catechu* L. (Binlang), *Ginseng* (Renshen), *Fructus amomi* (Sharen), *Radix linderae* (Wuyao) and *Prunus persica* Batsch (Taoren). Atropine (Lot A0132), tetrodotoxin (TTX, Lot T8024) and other chemicals were all acquired from Sigma (Sigma-Aldrich, St. Louis, MO, United States) unless indicated otherwise. The XBF, atropine, and TTX were dissolved in dH<sub>2</sub>O and further diluted in Krebs-Ringer buffer to the final concentration. Krebs buffer consisted of 121.9 mmol/L NaCl, 15.5 mmol/L NaHCO<sub>3</sub>, 5.9 mmol/L KCl, 1.2 mmol/L MgSO<sub>4</sub>, 1.2 mmol/L KH<sub>2</sub>PO<sub>4</sub>, 11.5 mmol/L glucose, and 2.5 mmol/L CaCl<sub>2</sub>. The pH of the Krebs buffer was 7.3-7.4 when bubbled with 95% O<sub>2</sub>-5% CO<sub>2</sub> at 37 ± 0.5 °C.

### Statistical analysis

The data are shown as mean ± SD. Welch's *t*-test was used to compare the difference between WT and *W/W<sup>h</sup>* mice. The paired *t*-test was used to analyze the data before and after administration. The number of MMC was compared by Fisher's exact test. A *P* value < 0.05 was considered significant. Data statistics were calculated with GraphPad Prism 5 (GraphPad Software, La Jolla, CA, United States).

## RESULTS

### Immunogenicity of c-kit-positive cells in the gastric antrum of WT and *W/W<sup>h</sup>* mice

Immunofluorescence showed that there were many c-kit-positive ICC in the myenteric plexus of the gastric antrum in WT mice. The c-kit-positive cells were connected to form a rich and dense ICC-MP network (Figure 1Aa). In *W/W<sup>h</sup>* mice, the c-kit immunogenicity of ICC-MP decreased (Figure 1Ab). Compared with WT mice, the density of ICC-MP in the gastric antrum of *W/W<sup>h</sup>* mice was significantly decreased (Figure 1B; *P* < 0.001). A large number of bipolar ICC were found in the longitudinal and circular muscles of the gastric antrum in WT mice (Figure 1Ac). Although sparse c-kit immunoreactivity was visible occasionally, no ICC-IM network was found in the antrum of *W/W<sup>h</sup>* mice (Figure 1Ad). There was a significant difference in ICC-IM density between WT and *W/W<sup>h</sup>* mice (Figure 1C; *P* < 0.001).

### Characteristics of the gastric antrum slow waves in WT and *W/W<sup>h</sup>* mice

The spontaneous periodic depolarization slow wave of the gastric antrum was observed in WT mice (Figure 2A). In WT mice, the resting membrane potential (RMP) was  $-56.49 \pm 3.58$  mV, the amplitude was  $22.62 \pm 2.23$  mV, and the frequency was  $6.16 \pm 1.12$  cpm. Spontaneous periodic depolarization slow waves with low amplitude were also observed in the antrum of *W/W<sup>h</sup>* mice (Figure 2B). In *W/W<sup>h</sup>* mice, the RMP was  $-52.95 \pm 2.34$  mV, the amplitude was  $2.92 \pm 0.52$  mV, and the frequency was  $7.48 \pm 0.66$  cpm. The difference determined was statistically significant between WT and *W/W<sup>h</sup>* mice (Figure 2C-E; <sup>a</sup>*P* < 0.05, <sup>c</sup>*P* < 0.0001).

### Effect of XBF on the gastric antrum slow wave in WT and *W/W<sup>h</sup>* mice

With perfused XBF at the concentration of 10<sup>-2</sup> g/L, the slow waves of the gastric antrum began to depolarize in WT and *W/W<sup>h</sup>* mice (Figure 3A and B). After treatment with concentrations of 10<sup>-2</sup> g/L, 5 × 10<sup>-2</sup> g/L, and 10<sup>-1</sup> g/L XBF, RMP decreased from  $-56.49 \pm 0.53$  mV to  $-52.31 \pm 0.82$  mV,  $-51.08 \pm 0.61$  mV, and  $-49.87 \pm 1.58$  mV, respectively. The frequency changed from  $5.99 \pm 0.18$  cpm to  $5.95 \pm 0.44$  cpm,  $6.47 \pm 0.37$  cpm, and  $6.79 \pm 0.14$  cpm, respectively, and the amplitude decreased from  $21.78 \pm 0.65$  mV to  $20.85 \pm 0.90$  mV,  $19.56 \pm 1.60$  mV, and  $18.15 \pm 0.65$  mV, respectively in WT mice. The differences in RMP and amplitude were significantly different at all XBF concentrations between the control and treatment groups (*P* < 0.05 or 0.01), and the frequency increased significantly except at the concentration of 10<sup>-2</sup> g/L (Figure 3C-E).

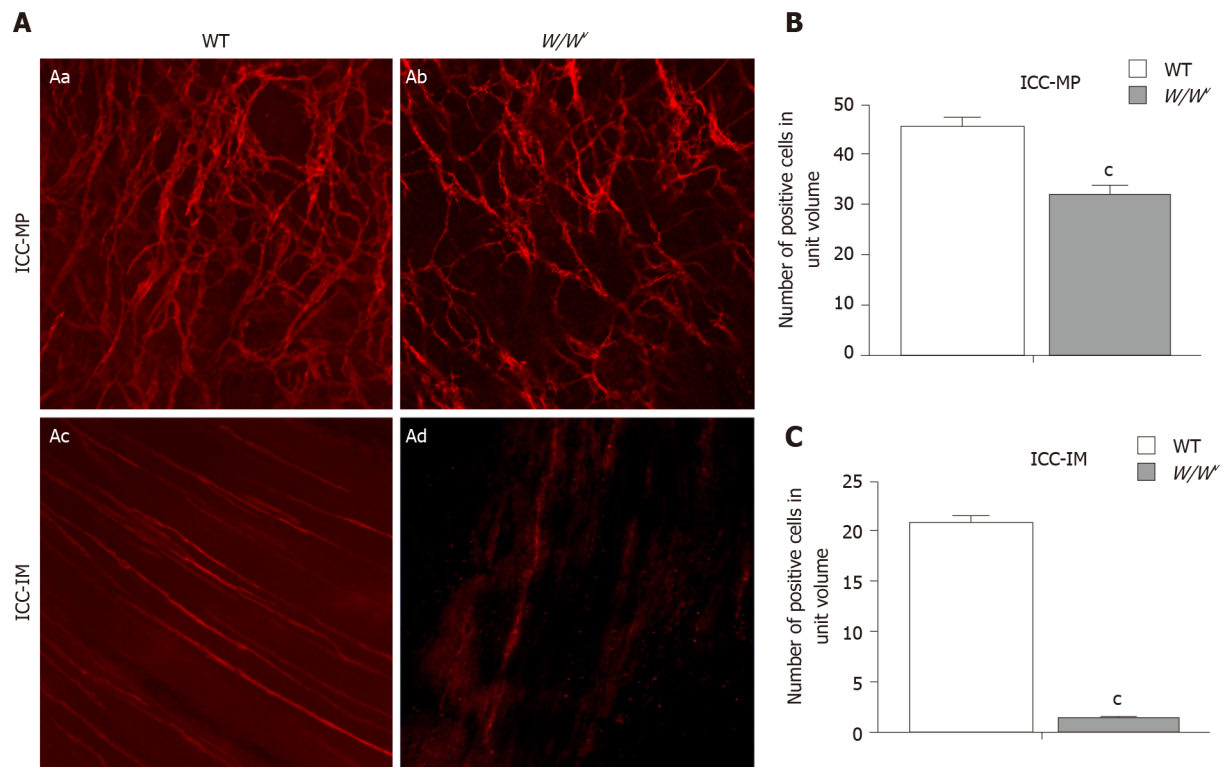


**Figure 1 Immunogenicity of c-kit positive cells in the gastric antrum of wild-type and  $W/W^v$  mice.** The c-kit positive cells were observed under a confocal microscope. The unit volume was  $424.3 \mu\text{m} \times 424.3 \mu\text{m} \times 6 \mu\text{m} \approx 0.0011 \text{ mm}^3$ . A: Immunostaining images showing the networks of interstitial cells of Cajal myenteric plexus (ICC-MP) and intramuscular interstitial cells of Cajal (ICC-IM), respectively: The abundant c-kit positive ICC-MP network of gastric antrum in wild-type (WT) mice (Aa); the sparse c-kit positive ICC-MP network of the gastric antrum in  $W/W^v$  mice (Ab); c-kit positive ICC-IM network of the gastric antrum in WT mice (Ac); no ICC-IM network distribution in the antrum of  $W/W^v$  mice (Ad); B and C: The number of c-kit positive cells in ICC-MP and ICC-IM was compared in the gastric antrum of WT and  $W/W^v$  mice under unit volume ( $424.3 \mu\text{m} \times 424.3 \mu\text{m}$ ) ( $n = 10$ ,  $^{\circ}P < 0.001$ ). ICC-MP: Interstitial cells of Cajal myenteric plexus; ICC-IM: Intramuscular interstitial cells of Cajal; WT: Wild-type.

In  $W/W^v$  mice, the RMP decreased from  $-(53.13 \pm 0.53) \text{ mV}$  to  $-(49.47 \pm 0.79) \text{ mV}$ ,  $-(48.41 \pm 1.24) \text{ mV}$ , and  $-(46.98 \pm 1.40) \text{ mV}$ , respectively. The frequency changed from  $7.55 \pm 0.12 \text{ cpm}$  to  $8.02 \pm 0.19 \text{ cpm}$ ,  $8.25 \pm 0.18 \text{ cpm}$ , and  $7.65 \pm 0.15 \text{ cpm}$ , respectively, and the amplitude decreased from  $2.84 \pm 0.08 \text{ mV}$  to  $2.71 \pm 0.11 \text{ mV}$ ,  $2.87 \pm 0.10 \text{ mV}$ , and  $2.66 \pm 0.21 \text{ mV}$ , respectively, at concentrations of  $10^{-2} \text{ g/L}$ ,  $5 \times 10^{-2} \text{ g/L}$ , and  $10^{-1} \text{ g/L}$ . Compared to the WT controls, the differences in RMP were statistically significant at all concentrations ( $P < 0.01$ ). At concentrations of  $10^{-2} \text{ g/L}$  and  $5 \times 10^{-2} \text{ g/L}$ , the slow-wave frequency increased significantly ( $P < 0.05$ ). However, the amplitude was not significantly altered at any XBF concentration in  $W/W^v$  mice.

#### Effects of atropine and TTX on gastric antral slow waves induced by XBF

The results of intracellular recording showed that atropine could completely abolish the effect of XBF on gastric antrum slow waves in WT and  $W/W^v$  mice (Figure 4A and B). After pretreatment with  $0.5 \text{ mmol/L}$  atropine, perfusion of XBF at a concentration of  $10^{-1} \text{ g/L}$  did not alter the RMP, frequency, or amplitude of the gastric antrum slow waves in WT and  $W/W^v$  mice (Figure 4C-E). In the presence of TTX  $10^{-7} \text{ M}$ , perfusion of XBF at a concentration of  $10^{-1} \text{ g/L}$  was able to decrease the RMP of gastric antrum slow waves in WT and  $W/W^v$  mice (Figure 4F and G). TTX did not block the enhancement of gastric antrum slow waves in WT and  $W/W^v$  mice (Figure 4H-J).

#### Characteristics of gastric antrum motility in WT and $W/W^v$ mice

The MMCs in the gastric antrum were recorded by a micro-strain-gauge force transducer for 30 min. As shown in Figure 5, it was very difficult to distinguish between MMC phase I and phase II in WT. With the increase of irregular contraction frequency, regular contractions with the frequency  $3.53 \pm 0.18 \text{ cpm}$  and amplitude index  $23014.26 \pm 1798.65 \text{ mV} \cdot 20 \text{ min}$  occurred in the antrum of WT mice. In the 30 min recording, there were only sporadic contractions in the gastric antrum of  $W/W^v$ . Occasionally, there was a strong paroxysmal contraction with a frequency of  $1.28 \pm 0.12 \text{ cpm}$  and an amplitude index of  $3782.16 \pm 407.13 \text{ mV} \cdot 20 \text{ min}$ . The differences in the frequency and amplitude index were all statistically significant ( $P < 0.0001$ ). We

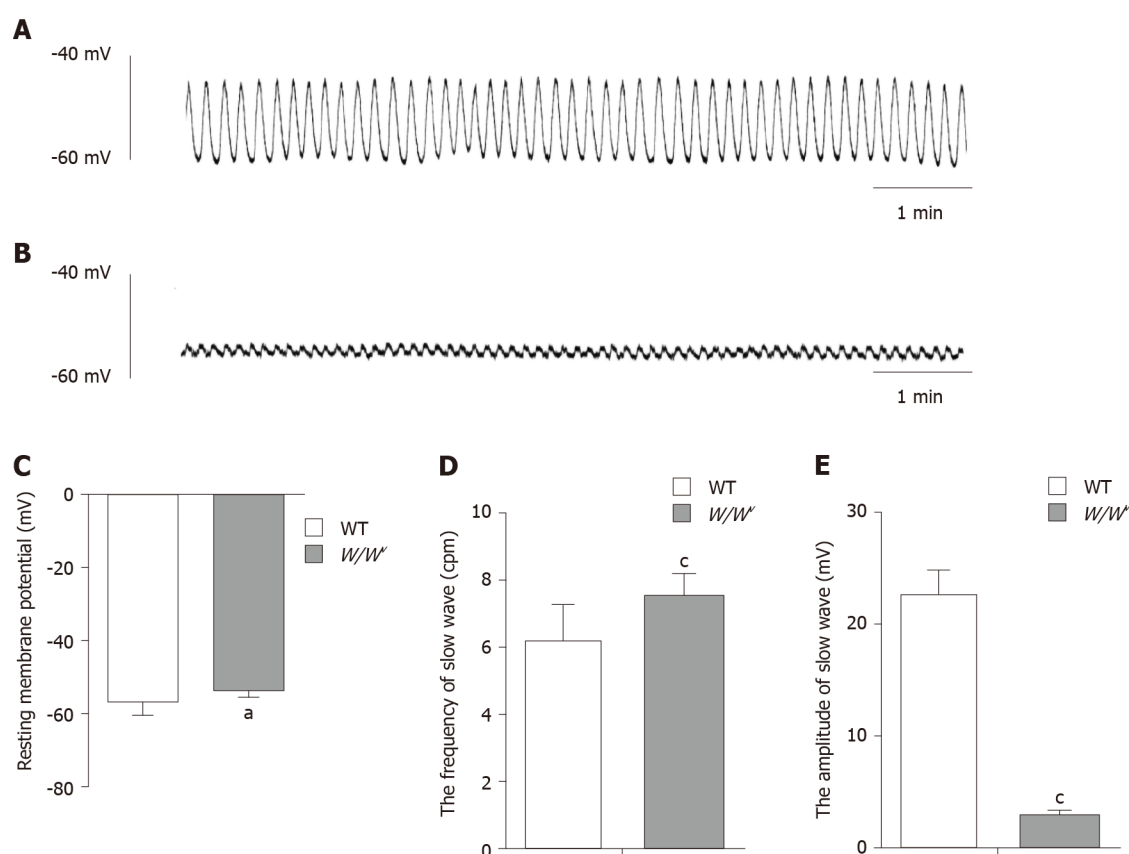


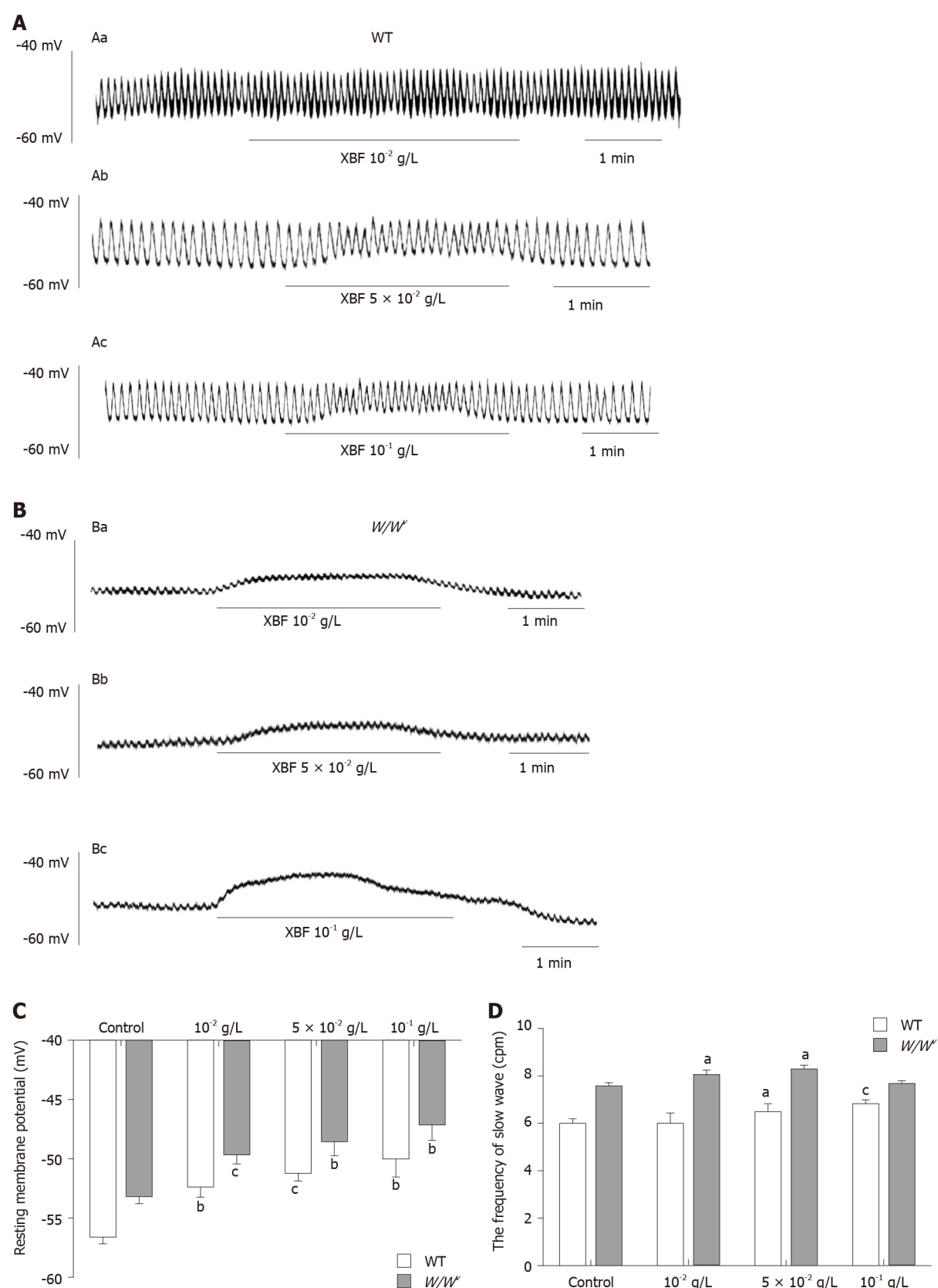
**Figure 2** Characteristics of the gastric antrum slow waves in wild-type and *W/W<sup>v</sup>* mice. A: Spontaneous rhythmic slow waves in the antrum of wild-type (WT) mice; B: Spontaneous rhythmic slow waves with the lower amplitude in the antrum of *W/W<sup>v</sup>* mice; C-E: Comparison of resting membrane potential, frequency and amplitude of the gastric antrum slow waves between WT and *W/W<sup>v</sup>* mice ( $n = 18$ , Welch's *t*-test, <sup>a</sup> $P < 0.05$ , <sup>c</sup> $P < 0.0001$ ). WT: Wild-type.

observed that 7 out of 8 WT mice developed a total of 13 MMC III phase contractions, while in the 8 *W/W<sup>v</sup>* mice, only 2 developed 3 MMC phase III-like contractions of shorter duration, lower amplitude, and lower frequency. There was a significant difference in the number of MMCs between both groups (Fisher's exact test,  $P = 0.0406$ ). For the gastric antrum of WT mice, the duration of the MMC phase III was  $151.08 \pm 8.87$  s, the amplitude was  $315.45 \pm 5.55$  mV, and the interval between MMCs was  $10.75 \pm 0.61$  min. In the gastric antrum of *W/W<sup>v</sup>* mice, the duration of the MMC phase III-like contractions was  $123.67 \pm 2.96$  s, the amplitude was  $194.12 \pm 4.76$  mV, and during the 30 min observation, no phase III-like contractions were found twice in the same *W/W<sup>v</sup>* mice. Compared to WT mice, the duration and amplitude of the MMC III phase in the gastric antrum was significantly reduced in *W/W<sup>v</sup>* mice ( $P = 0.0117$  and  $0.0020$ , respectively), suggesting there was no typical MMC cycle in the gastric antrum of *W/W<sup>v</sup>* mice.

#### Effect of XBF on gastric antrum motility in WT and *W/W<sup>v</sup>* mice

After the administration of XBF (5 mg), strong contractions in the antrum of WT mice were observed instantaneously (Figure 6). The periodic MMC movement turned into a high frequency and high amplitude MMC III phase contraction. However, XBF did not significantly enhance the contraction of the gastric antrum in *W/W<sup>v</sup>* mice (Figure 6). After treatment in turn with 0.6 mg, 1.25 mg, and 5 mg of XBF, the frequency index of the gastric antrum in WT mice was  $3.16 \pm 0.39$  cpm,  $3.30 \pm 0.26$  cpm, and  $5.58 \pm 0.62$  cpm and the amplitude index was  $13415.25 \pm 1694.38$  mV · 20 min,  $24537.89 \pm 2406.33$  mV · 20 min, and  $51807.48 \pm 9255.04$  mV · 20 min, respectively, while the frequency index of the gastric antrum in *W/W<sup>v</sup>* mice was  $1.85 \pm 0.48$  cpm,  $1.93 \pm 0.37$  cpm, and  $1.99 \pm 0.37$  cpm and the amplitude index was  $6488.43 \pm 1490.04$  mV · 20 min,  $7733.07 \pm 1469.27$  mV · 20 min, and  $6901.26 \pm 807.34$  mV · 20 min, respectively. These results demonstrated that with high-dose XBF treatment, there was a significant difference in the frequency and amplitude indices of the gastric antrum between WT and *W/W<sup>v</sup>* mice (all  $P < 0.05$  or  $0.01$ ).





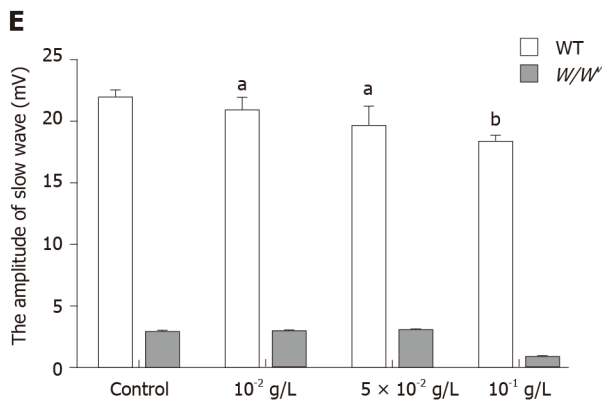


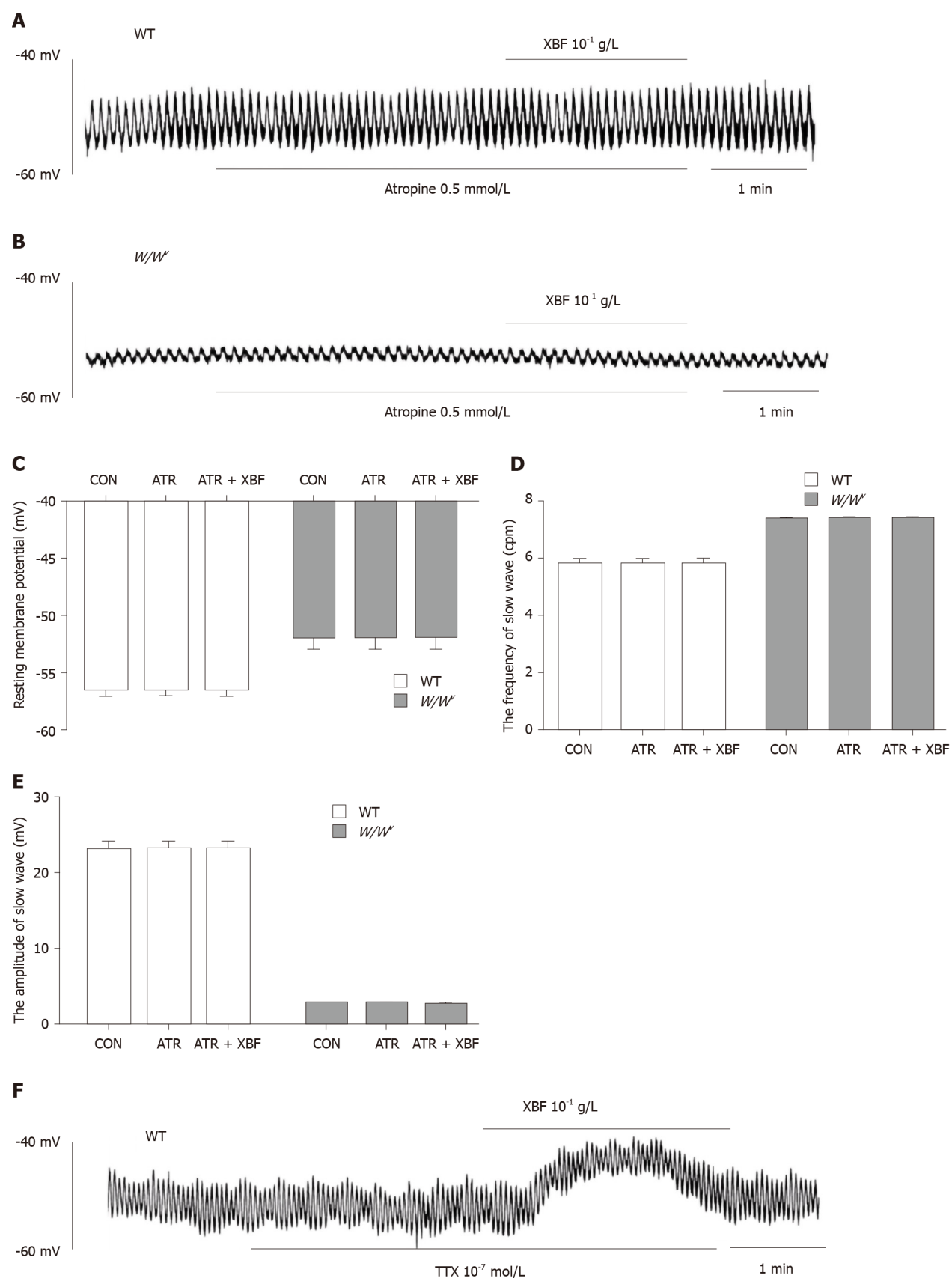
**Figure 3 Effect of Xiangbinfang granule on gastric antrum slow wave in wild-type and *W/W<sup>v</sup>* mice.** A: Representative trace of the effect of different concentrations of Champaign formula on gastric antrum slow waves in wild-type (WT) mice. After infusion of Xiangbinfang granule (XBF) at the concentration of 10<sup>-2</sup> g/L (Aa), 5 × 10<sup>-2</sup> g/L (Ab) and 10<sup>-1</sup> g/L (Ac), the slow waves resting membrane potential (RMP) decreased, frequency increased and amplitude decreased; B: Representative trace of the effect of different concentrations of Champaign formula on gastric antrum slow waves in *W/W<sup>v</sup>* mice. Infused XBF at the concentrations of 10<sup>-2</sup> g/L (Ba), 5 × 10<sup>-2</sup> g/L (Bb) and 10<sup>-1</sup> g/L (Bc) decreased the RMP in *W/W<sup>v</sup>* gastric antrum slow waves; C-E: Histogram of XBF for gastric slow wave RMP (C), frequency (D) and amplitude (E) in WT and *W/W<sup>v</sup>* mice. (Control, *n* = 18; treatment, *n* = 6. Paired *t*-test was used to compare the difference before and after administration, <sup>a</sup>*P* < 0.05, <sup>b</sup>*P* < 0.001, <sup>c</sup>*P* < 0.0001). WT: Wild type; XBF: Xiangbinfang granule.

### Effects of atropine and TTX on the gastric antrum motility induced by XBF

To clarify the mechanism of XBF in promoting antral motility, atropine and TTX were injected intraperitoneally, and then XBF was administered by gavage. The results indicated that contractions were inhibited in the antrum of WT and *W/W<sup>v</sup>* mice after intraperitoneal injection of 0.1 mg/kg of atropine, and subsequent treatment with 5 mg of XBF did not increase the contractile activity of the gastric antrum (Figure 7A and C). These results suggest that atropine could completely eliminate the motility-promoting effect of XBF in both WT and *W/W<sup>v</sup>* mice (Figure 7E). The frequency and amplitude of gastric antral contractions were abolished by 0.05 mg/kg of TTX. Subsequent treatment with 5 mg of XBF induced a contraction enhancement in WT and *W/W<sup>v</sup>* mice (Figure 7B and D). In comparison with XBF without TTX, TTX pretreatment could partially reduce the gastric antrum motility-promoting effect mediated by XBF (Figure 7F).

## DISCUSSION

C-kit is a necessary condition for the development of a GI pacemaker system<sup>[13]</sup>. Previous studies have shown that the *W*-mutation causes loss of the ICC network in the GI tract of *W/W<sup>v</sup>* mice, such as the disappearance of ICC-MP and decreased ICC-MP in the jejunum and ileum<sup>[4]</sup>. In the *W/W<sup>v</sup>* colon, the density of c-kit positive ICC-MP was reduced by 50%-60% compared to that of WT mice<sup>[12]</sup>. While a normal ICC-MP network was observed, the ICC-IM disappeared completely in the gastric antrum of *W/W<sup>v</sup>* mice<sup>[14]</sup>. We scanned whole muscle specimens to obtain a more accurate number of ICC and compared them to WT mice; about 60% of ICC-MP was retained in the antrum of *W/W<sup>v</sup>* mice, and no ICC-IM network was observed. GI slow waves are mainly produced by ICC-MP<sup>[2]</sup>, and ICC-IM is responsible for the regenerative component of the slow wave<sup>[15]</sup>. Our immunofluorescent staining showed that the ICC-MP network density decreased but did not disappear, and the slow-wave activity in *W/W<sup>v</sup>* mice was preserved. However, due to the lack of an ICC-IM network in the antrum of *W/W<sup>v</sup>* mice, there is no regenerative component in the *W/W<sup>v</sup>* antrum slow wave. Therefore, *W/W<sup>v</sup>* mice showed a low-amplitude slow wave and disturbed movement in the antrum. ICC-IM were also innervated and provided mechanisms for neural signal transduction to the gastric musculature<sup>[16]</sup>. ICC-IM were densely innervated by excitatory and inhibitory enteric motor neurons and in close contact with nerve terminals. ICC-IM played a role in both nitrergic inhibitor and cholinergic excitatory motor neurotransmission in the gastric antrum<sup>[17,18]</sup>. Excitatory junctional potential and inhibitory junctional potential after intrinsic nerve stimulation were greatly attenuated in the antrum of *W/W<sup>v</sup>* mice, and the reduced density of ICC-IM leads to reduced neural regulation in the *W/W<sup>v</sup>* antrum<sup>[19]</sup>. Hirst *et al.*<sup>[19]</sup> have shown that excitatory vagal stimulation response resembles the regenerative response which



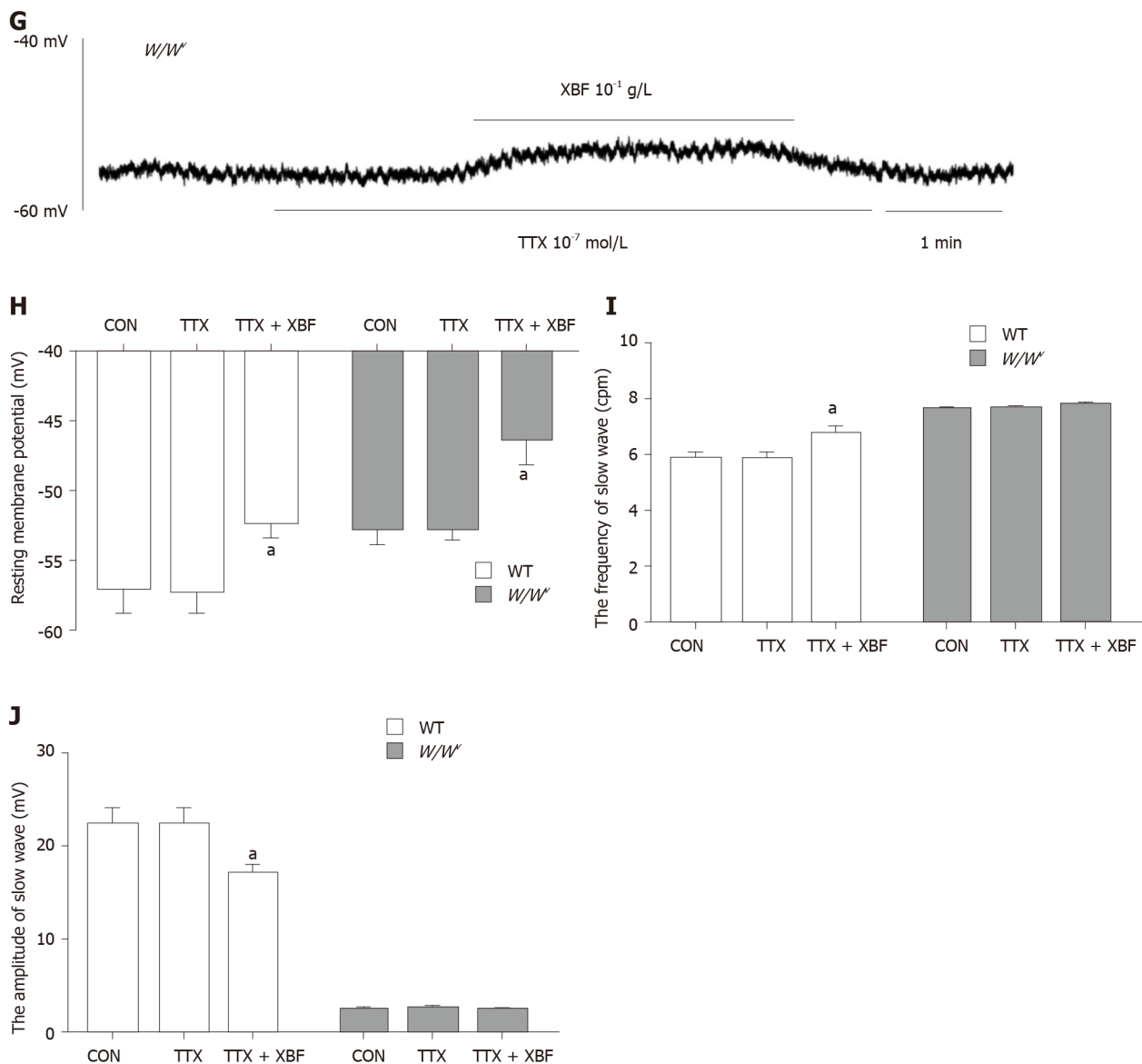


**Figure 4** Effects of atropine and tetrodotoxin on the enhancement of gastric antrum slow wave by Xiangbinfang granule. A and B: Representative trace of the effect of Xiangbinfang granule (XBF)  $10^{-1}$  g/L on slow waves of the gastric antrum pretreated with atropine 5 mmol/L in wild-type (WT) (A) and  $W/W^m$  mice (B); C-G: Histogram of atropine blocking the effect of XBF on the enhancement of resting membrane potential (C), frequency (D) and amplitude (E) of antral slow waves. Representative trace of the effect of  $10^{-1}$  g/L of XBF on slow waves of the gastric antrum pretreated with  $10^{-7}$  M of tetrodotoxin (TTX) in WT (F) and  $W/W^m$  (G) mice; H-J: Histogram of TTX blocking the effect of XBF on the enhancement of the resting membrane potential (H), frequency (I) and amplitude (J) of antral slow waves. (Compared with pretreatment,  $n = 3$ ,  $^aP < 0.05$ ). WT: Wild-type; XBF: Xiangbinfang granule; TTX: Tetrodotoxin; CON: Basic control; ATR: Atropine.

was initiated in this tissue by ICC-IM. Regenerative responses were the dominant responses produced by neural stimulation. This suggested that ICC-IM is regulated by vagus nerve.

The MMC has been found to be a complex system that may be regulated by motilin<sup>[20]</sup>, the enteric nervous system, and the vagus nerve. Mondal *et al*<sup>[21]</sup> found that treatment with motilin induced phase III contractions *in vivo* and *in vitro*, while motilin antagonists can abolish the occurrence of spontaneous gastric phase III contractions. Their other experiment showed that motilin-induced gastric contractions were mediated through the myenteric plexus in a vagus-independent manner<sup>[22]</sup>. ICC-IM may play an important role in this process.

The MMC have a temporally coordinated cyclic motor pattern during the interdigestive state of the stomach and small intestine in many animals. In the human and dog gastrointestinal tracts, the occurrence of MMC is regulated at 90-120-min intervals<sup>[23,24]</sup>. Because of motilin and motilin receptor pseudogenes<sup>[25]</sup>, mice and rats have shown different MMC patterns. Strain-gauge force transducer implantation is a crucial technique for recording GI MMC movement in conscious animals<sup>[23,24,26,27]</sup>. Takayama *et al*<sup>[26]</sup> examined the gastrointestinal motility of W-mutant rats by an



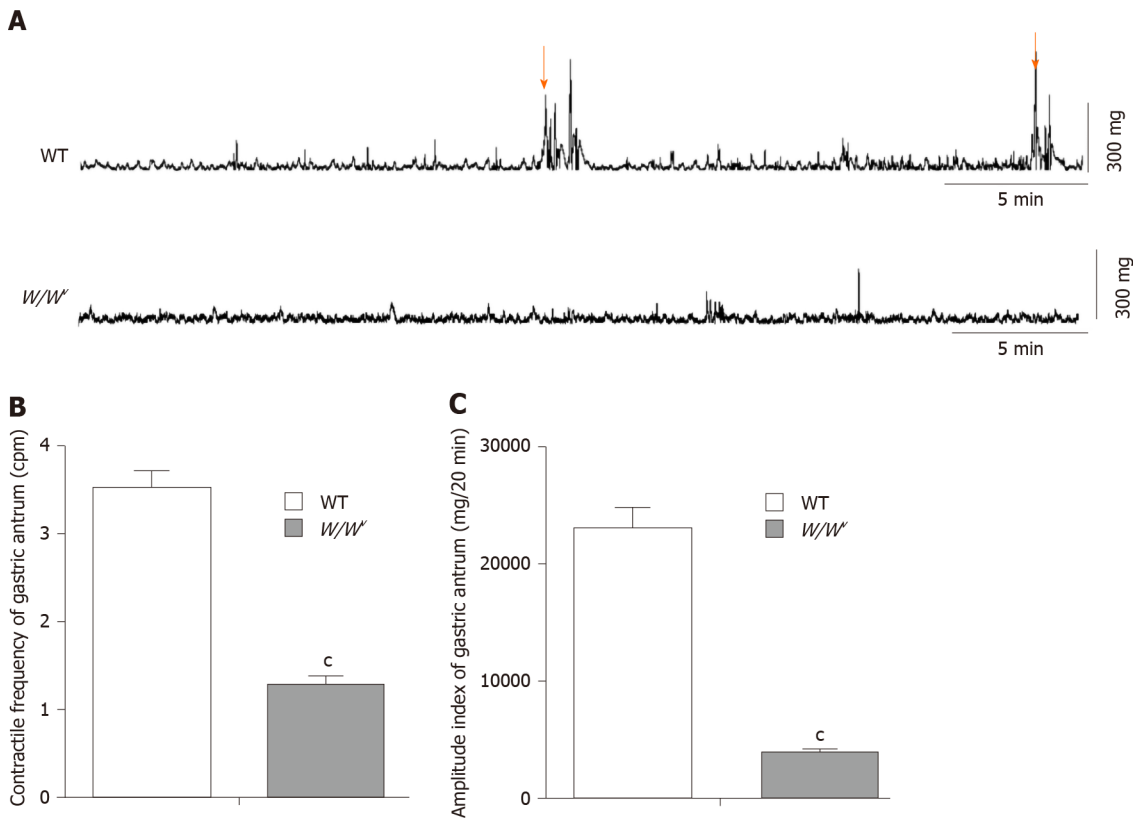


**Figure 5 Characteristics of gastric antrum motility in conscious wild-type and *W/W<sup>v</sup>* mice.** Micro strain-gauge force transducers were implanted into the gastric antrum to observe the migrating motor complex (MMC). A: Representative trace of the gastric antrum contractions in conscious wild-type (WT) and *W/W<sup>v</sup>* mice. The black arrow shows the MMC III phase contraction; B and C: The histograms of the comparison of the contractile frequency (B) and amplitude index (C) of the gastric antrum in WT and *W/W<sup>v</sup>* mice. ( $n = 8$ , Welch's  $t$ -test,  $^cP < 0.0001$ ). WT: Wild-type.

extraluminal strain-gauge force transducer method. They found the duration of MMC was  $2.5 \pm 2.3$  min and the interval of MMC was  $5.4 \pm 2.9$  min. Similar results were observed by Taniguchi *et al*<sup>[27]</sup> in their study, spontaneous phase III contractions were observed every 13-16 min. It was difficult to record the gastrointestinal motor pattern of the mice *in situ*. Spencer *et al*<sup>[5]</sup> tried to record MMC in the isolated small intestine of mice. They found the interval between MMCs in the mouse small intestine was  $5 \pm 1$  min, and the durations of MMC contractions were about 30 s. The MMC was regulated by motilin, the enteric nervous system, and the vagus nerve. Motilin-induced contractions are much less potent than those of MMC *in vivo*<sup>[28]</sup>. The complex regulatory system of MMC was not complete *in vitro*. Therefore, we miniaturized the strain-gauge force transducer to facilitate MMC recording in the gastric antrum of conscious mice. In this study, we found that the duration of the MMC phase III was  $151.08 \pm 8.87$  s, the amplitude was  $315.45 \pm 5.55$  mV, and the interval between MMCs was  $10.75 \pm 0.61$  min in WT mice. There was no complete MMC cycle in the gastric antrum of *W/W<sup>v</sup>* mice. The gastric antrum of *W/W<sup>v</sup>* mice lacked ICC-IM and the corresponding motor nerve conduction was inhibited<sup>[29]</sup>. The typical MMC disappeared in *W/W<sup>v</sup>* mice, suggesting that ICC-IM is an important factor in regulating the MMC activity.

In this study, we found that XBF enhanced the contractions of the gastric antrum in WT mice through slow-wave depolarization of SMCs. The effect of XBF on enhancing the antral motility was greatly reduced in *W/W<sup>v</sup>* mice. ICC specifically express calcium-activated chloride channels (CACC), which are regulated by anoctamine 1 (Ano1). Exogenous nerve stimulation or GI hormones could act on ICC to produce slow waves by CACC<sup>[30]</sup>. SMCs respond to slow waves to generate action potentials by activating voltage-dependent L-type calcium channels<sup>[31]</sup>. Under physiological conditions, cell-membrane potential depolarization increased the probability of the L-type calcium channels opening, allowing calcium influx to induce SMCs to generate action potentials and contractions<sup>[32-34]</sup>. In Ano1-knockout mice, the excitability of smooth muscle contraction induced by carbachol was decreased. This is caused by cholinergic nerve stimulation that first activates muscarinic receptors on ICC-IM and then stimulates the CACC channel, thereby causing the SMCs to depolarize and

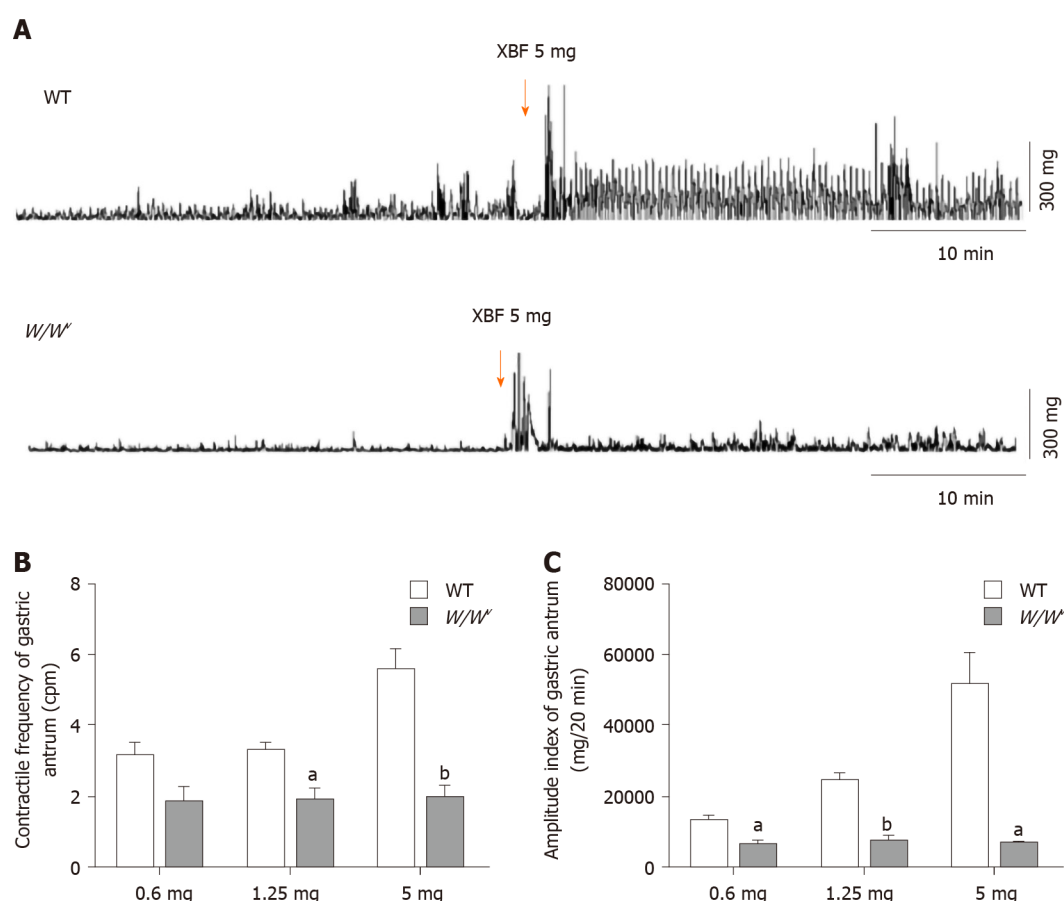


**Figure 6** Effect of Xiangbinfang granule on gastric antrum motility in wild-type and *W/W<sup>v</sup>* mice. A: Representative trace of the enhancement of the gastric antrum motility in wild-type (WT) and *W/W<sup>v</sup>* by Xiangbinfang granule (XBF); B: Comparison of the antral contractile frequency of WT and *W/W<sup>v</sup>* mice after intragastric administration of 0.6 mg, 1.25 mg and 5 mg XBF; C: Comparison of antral contractile amplitude index of WT and *W/W<sup>v</sup>* mice after intragastric administration of 0.6 mg, 1.25 mg and 5 mg XBF ( $n = 8$ , Welch's  $t$ -test, <sup>a</sup> $P < 0.05$ , <sup>b</sup> $P < 0.01$ ). WT: Wild-type; XBF: Xiangbinfang granule.

generate action potentials through gap junctions<sup>[35]</sup>. Thus, the response of the distal stomach to cholinergic stimulation was weakened and blocked the neural activation of regenerative potentials in *W/W<sup>v</sup>* mice deficient in ICC-IM, and the low level of potential depolarization during the slow-wave plateau period reduced the probability of L-type calcium channels opening. Therefore, XBF depolarized the SMCs slow waves (Figure 3) but did not significantly enhance the mechanical contraction (Figure 6) of the gastric antrum in *W/W<sup>v</sup>* mice. Our study showed that atropine completely blocked the gastric antral motility induced by XBF, but TTX just partially reduced the effect of XBF in both WT and *W/W<sup>v</sup>* mice (Figure 7). This suggested that XBF enhances the smooth muscle contraction of the gastric antrum through the cholinergic pathway of ICC-IM and the enteric nervous system.

The Chinese medicine XBF, composed of *Areca catechu* L., *Ginseng*, *Fructus amomi*, *Radix linderae*, and *Prunus persica* Batsch, promotes entire GI motility in the treatment of postoperative ileus<sup>[8-11]</sup>. Previous studies have shown that *Areca catechu* L. enhances gastric motility in healthy people<sup>[36]</sup>. Arecoline, the main active component of *Areca*, with an XBF content of 0.112 mg/g<sup>[37]</sup>, promoted GI motility through the M3 receptor<sup>[38,39]</sup>. Ginsenoside RF, an extract of *Ginseng*, induced membrane depolarization of ICC<sup>[40]</sup> and *Fructus amomi* promoted the contraction of the antrum and duodenum in beagle dogs<sup>[41]</sup>. The promotion of GI motility by XBF is the result of the interaction of these Chinese herbs, and the most important active components still need to be further characterized.

## CONCLUSION

Our study shows that ICC-IM play a crucial role in regulating gastric antral MMC activity. They may be an important bridge between the vagus nerve, the enteric nervous system, and motilin in regulating smooth muscle contraction. Through the

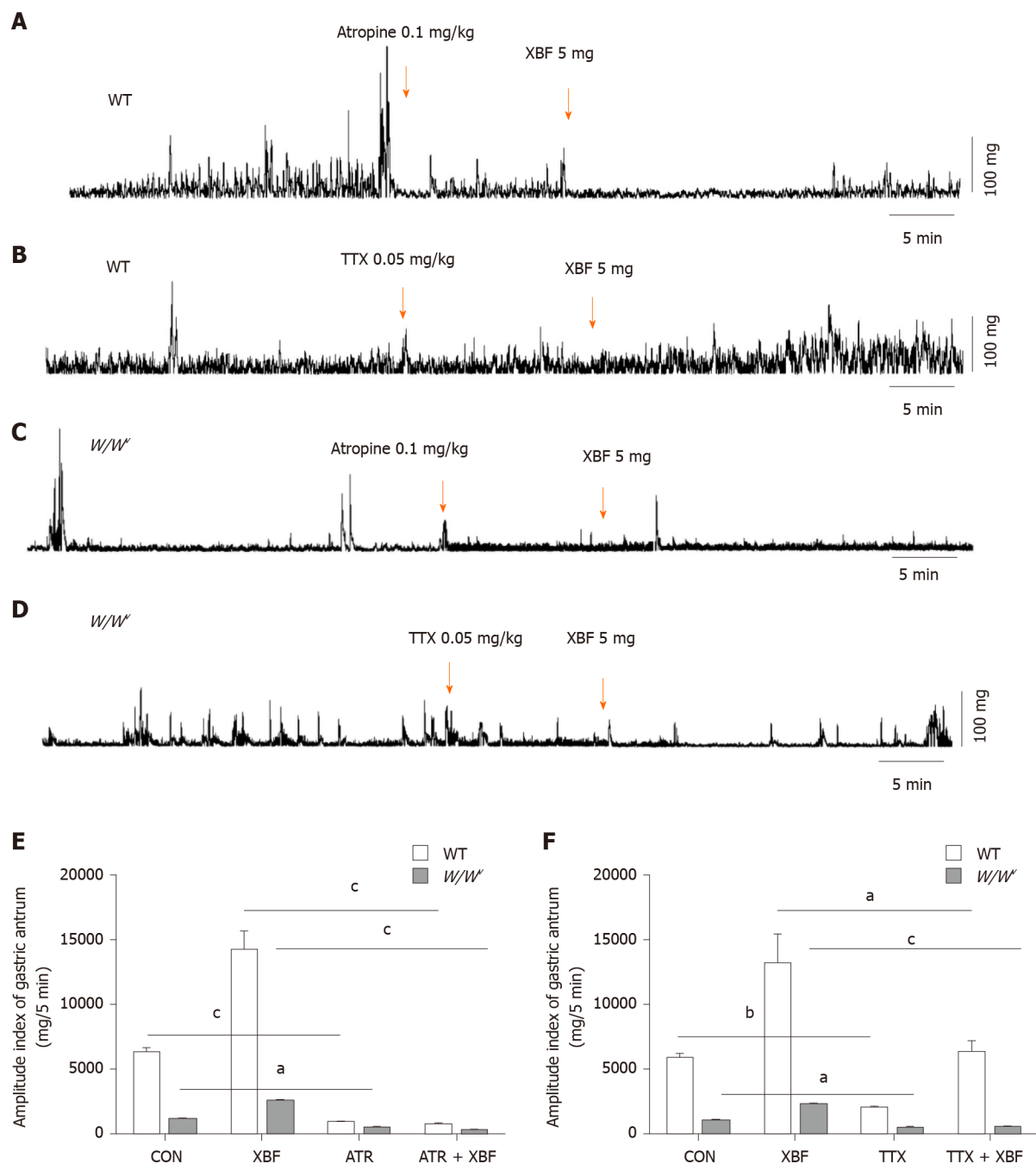


**Figure 7 Atropine and tetrodotoxin block the enhancement of antrum motility induced by Xiangbinfang granule.** A-D: Intraperitoneal injection of 0.1 mg/kg atropine (ATR) completely blocked the enhancement effect of Xiangbinfang granule (XBF, 5 mg) on gastric antrum in wild-type (WT) (A) and *W/W'* (C) mice. Tetrodotoxin (TTX) partially reduced the gastric antrum motility enhancement mediated by XBF in WT (B) and *W/W'* (D) mice; E-F: Comparison of the effect of XBF 5 mg of antral contractile amplitude index in WT and *W/W'* mice after pretreatment with ATR 0.1 mg/kg (E) and TTX 0.05 mg/kg (F). ( $n = 4$ , Welch's *t*-test, <sup>a</sup> $P < 0.05$ , <sup>b</sup> $P < 0.01$ , <sup>c</sup> $P < 0.001$ ). WT: Wild-type; XBF: Xiangbinfang granule; TTX: Tetrodotoxin; CON: Basic control; ATR: Atropine.

muscarinic receptor pathway on ICC-IM, XBF depolarizes SMCs and initiates an action potential, changing the periodic motion of MMC into a phase III-like contraction pattern in the gastric antrum of mice.

## ARTICLE HIGHLIGHTS

### Research background

The Chinese medicine Xiangbinfang granule (XBF) is an effective prescribed treatment for promoting the recovery of gastrointestinal (GI) function post-surgery. In previous studies, we found that XBF mediated the phase III contraction of migrating motor

complexes (MMC). However, the mechanism of XBF in enhancing MMC activity in the GI tract is still unclear.

### Research motivation

In this study, we observed the MMC activity of gastric antrum in  $W/W^v$  mice that lack intramuscular interstitial cells of Cajal (ICC-IM) and analyzed the effect of the traditional Chinese medicine XBF in promoting gastric antrum movement. From this study, we will further understand the role of ICC-IM in MMC activities. Meanwhile, the mechanism of XBF promoting gastrointestinal motility through ICC-IM was discussed, so as to provide the basis for the development and application of XBF.

### Research objectives

$W/W^v$  mice were used to observe the effects of ICC-IM on gastric antrum motility and to establish the mechanism of XBF in promoting gastric antrum motility. We further investigated the correlation between ICC-IM and MMC in mouse gastric antrum.

### Research methods

The density of c-kit positive ICC myenteric plexus and ICC-IM in the antral muscularis of  $W/W^v$  and wild-type (WT) mice was examined by confocal microscopy. The effects of XBF on the gastric antrum slow waves in  $W/W^v$  and WT mice were recorded by intracellular amplification recording. The micro-strain-gauge force transducers were implanted into the gastric antrum to monitor the MMC and the effect of XBF on gastric antrum motility in conscious  $W/W^v$  and WT mice.

### Research results

In the gastric antrum of  $W/W^v$  mice, no ICC-IM network was observed. Spontaneous rhythmic slow waves with the low amplitude also appeared in the antrum of  $W/W^v$  mice. In this study, we found that the duration of MMC phase III was  $151.08 \pm 8.87$  s, the amplitude was  $315.45 \pm 5.55$  mg, and the interval between MMCs was  $10.75 \pm 0.61$  min in the gastric antrum of WT mice. There was no complete MMC cycle in  $W/W^v$  gastric antrum lacking ICC-IM. The gastric antrum motility in WT and  $W/W^v$  antrum was significantly increased after treatment with XBF. Atropine blocked the enhancement of XBF completely, while tetrodotoxin partially inhibited the enhancement of XBF.

### Research conclusions

In this study, we first examined the gastrointestinal motility of W-mutant mice by an extraluminal strain-gauge force transducer method. It showed that ICC-IM plays an important role in the regulation of gastric antrum MMC.

### Research perspectives

In this study, MMC were recorded only at a single site in the gastric antrum. It was impossible to describe the propulsion of gastrointestinal movement. Therefore, recording at multiple gastrointestinal sites is important to further clarify the motility of gastrointestinal MMC in mice.

## REFERENCES

- 1 Singaram K, Gold-Smith FD, Petrov MS. Motilin: a panoply of communications between the gut, brain, and pancreas. *Expert Rev Gastroenterol Hepatol* 2020; **14**: 103-111 [PMID: 31996050 DOI: 10.1080/17474124.2020.1718492]
- 2 Parsons SP, Huizinga JD. Slow wave contraction frequency plateaus in the small intestine are composed of discrete waves of interval increase associated with dislocations. *Exp Physiol* 2018; **103**: 1087-1100 [PMID: 29860720 DOI: 10.1113/EP086871]
- 3 Yadak R, Breur M, Bugiani M. Gastrointestinal Dysmotility in MNGIE: from thymidine phosphorylase enzyme deficiency to altered interstitial cells of Cajal. *Orphanet J Rare Dis* 2019; **14**: 33 [PMID: 30736844 DOI: 10.1186/s13023-019-1016-6]
- 4 Der-Silaphet T, Malysz J, Hagel S, Larry Arseneault A, Huizinga JD. Interstitial cells of cajal direct normal propulsive contractile activity in the mouse small intestine. *Gastroenterology* 1998; **114**: 724-736 [PMID: 9516393 DOI: 10.1016/s0016-5085(98)70586-4]
- 5 Spencer NJ, Sanders KM, Smith TK. Migrating motor complexes do not require electrical slow waves in the mouse small intestine. *J Physiol* 2003; **553**: 881-893 [PMID: 14514874 DOI: 10.1113/jphysiol.2003.049700]
- 6 Hayashi Y, Toyomasu Y, Saravanaperumal SA, Bardsley MR, Smestad JA, Lorincz A, Eisenman ST,



- Cipriani G, Nelson Holte MH, Al Khazal FJ, Syed SA, Gajdos GB, Choi KM, Stoltz GJ, Miller KE, Kendrick ML, Rubin BP, Gibbons SJ, Bharucha AE, Linden DR, Maher LJ 3rd, Farrugia G, Ordog T. Hyperglycemia Increases Interstitial Cells of Cajal *via* MAPK1 and MAPK3 Signaling to ETV1 and KIT, Leading to Rapid Gastric Emptying. *Gastroenterology* 2017; **153**: 521-535. e20 [PMID: 28438610 DOI: 10.1053/j.gastro.2017.04.020]
- 7 **Park KS**, Cho KB, Hwang IS, Park JH, Jang BI, Kim KO, Jeon SW, Kim ES, Park CS, Kwon JG. Characterization of smooth muscle, enteric nerve, interstitial cells of Cajal, and fibroblast-like cells in the gastric musculature of patients with diabetes mellitus. *World J Gastroenterol* 2016; **22**: 10131-10139 [PMID: 28028361 DOI: 10.3748/wjg.v22.i46.10131]
- 8 **Gan H**, Lin J, Jiang Z, Chen Q, Cao L, Chen Z. Xiangbin prescription for the recovery of gastrointestinal function after abdominal surgery (the XBPRS trial): study protocol for a randomized controlled trial. *Trials* 2018; **19**: 146 [PMID: 29486765 DOI: 10.1186/s13063-018-2484-z]
- 9 **Wen SL**, Feng X, Chen ZQ, Xiao J, Zhang WX. Effect of XiangBin granules on post-operative gastrointestinal function and brain-gut peptides after transabdominal gynecological surgery. *Eur J Obstet Gynecol Reprod Biol* 2016; **205**: 1-6 [PMID: 27552171 DOI: 10.1016/j.ejogrb.2016.07.496]
- 10 **Chen ZQ**, Cao LX, Shang WF, Yang RX, Ye F, Chen QC, Pang FS, Jiang Z, Liu WP, Zhou L. The effect of xiangbin fang on gastrointestinal motility of dogs after abdominal operation. *Zhongyi Zazhi* 2015; **56**: 1953-1957 [DOI: 10.13288/j.11-2166/r.2015.22.018]
- 11 **Jiang Z**, Cao LX, Liu B, Chen QC, Shang WF, Zhou L, Li DY, Guo DA, Chen ZQ. Effects of Chinese herbal medicine Xiangbin prescription on gastrointestinal motility. *World J Gastroenterol* 2017; **23**: 2987-2994 [PMID: 28522917 DOI: 10.3748/wjg.v23.i16.2987]
- 12 **Wang XY**, Chen JH, Li K, Zhu YF, Wright GW, Huizinga JD. Discrepancies between c-Kit positive and Ano1 positive ICC-SMP in the W/W<sup>v</sup> and wild-type mouse colon; relationships with motor patterns and calcium transients. *Neurogastroenterol Motil* 2014; **26**: 1298-1310 [PMID: 25039457 DOI: 10.1111/nmo.12395]
- 13 **Kluppel M**, Huizinga JD, Malysz J, Bernstein A. Developmental origin and Kit-dependent development of the interstitial cells of cajal in the mammalian small intestine. *Dev Dyn* 1998; **211**: 60-71 [PMID: 9438424 DOI: 10.1002/(SICI)1097-0177(199801)211:1<60::AID-AJA6>3.0.CO;2-5]
- 14 **Dickens EJ**, Edwards FR, Hirst GD. Selective knockout of intramuscular interstitial cells reveals their role in the generation of slow waves in mouse stomach. *J Physiol* 2001; **531**: 827-833 [PMID: 11251061 DOI: 10.1111/j.1469-7793.2001.0827h.x]
- 15 **Edwards FR**, Hirst GD. An electrical description of the generation of slow waves in the antrum of the guinea-pig. *J Physiol* 2005; **564**: 213-232 [PMID: 15613372 DOI: 10.1113/jphysiol.2004.077123]
- 16 **Wright GW**, Parsons SP, Loera-Valencia R, Wang XY, Barajas-López C, Huizinga JD. Cholinergic signalling-regulated KV7.5 currents are expressed in colonic ICC-IM but not ICC-MP. *Pflugers Arch* 2014; **466**: 1805-1818 [PMID: 24375291 DOI: 10.1007/s00424-013-1425-7]
- 17 **Lies B**, Gil V, Groneberg D, Seidler B, Saur D, Wischmeyer E, Jiménez M, Friebe A. Interstitial cells of Cajal mediate nitroergic inhibitory neurotransmission in the murine gastrointestinal tract. *Am J Physiol Gastrointest Liver Physiol* 2014; **307**: G98-106 [PMID: 24833707 DOI: 10.1152/ajpgi.00082.2014]
- 18 **Blair PJ**, Bayguinov Y, Sanders KM, Ward SM. Relationship between enteric neurons and interstitial cells in the primate gastrointestinal tract. *Neurogastroenterol Motil* 2012; **24**: e437-e449 [PMID: 22805588 DOI: 10.1111/j.1365-2982.2012.01975.x]
- 19 **Hirst GD**, Dickens EJ, Edwards FR. Pacemaker shift in the gastric antrum of guinea-pigs produced by excitatory vagal stimulation involves intramuscular interstitial cells. *J Physiol* 2002; **541**: 917-928 [PMID: 12068050 DOI: 10.1113/jphysiol.2002.018614]
- 20 **Deloose E**, Vos R, Corsetti M, Depoortere I, Tack J. Endogenous motilin, but not ghrelin plasma levels fluctuate in accordance with gastric phase III activity of the migrating motor complex in man. *Neurogastroenterol Motil* 2015; **27**: 63-71 [PMID: 25393165 DOI: 10.1111/nmo.12470]
- 21 **Mondal A**, Xie Z, Miyano Y, Tsutsui C, Sakata I, Kawamoto Y, Aizawa S, Tanaka T, Oda S, Sakai T. Coordination of motilin and ghrelin regulates the migrating motor complex of gastrointestinal motility in *Suncus murinus*. *Am J Physiol Gastrointest Liver Physiol* 2012; **302**: G1207-G1215 [PMID: 22383491 DOI: 10.1152/ajpgi.00379.2011]
- 22 **Mondal A**, Kawamoto Y, Yanaka T, Tsutsui C, Sakata I, Oda SI, Tanaka T, Sakai T. Myenteric neural network activated by motilin in the stomach of *Suncus murinus* (house musk shrew). *Neurogastroenterol Motil* 2011; **23**: 1123-1131 [PMID: 22029733 DOI: 10.1111/j.1365-2982.2011.01801.x]
- 23 **Itoh Z**, Honda R, Hiwatashi K, Takeuchi S, Aizawa I, Takayanagi R, Couch EF. Motilin-induced mechanical activity in the canine alimentary tract. *Scand J Gastroenterol Suppl* 1976; **39**: 93-110 [PMID: 1069368]
- 24 **Vantrappen G**, Janssens J, Peeters TL, Bloom SR, Christofides ND, Hellemans J. Motilin and the interdigestive migrating motor complex in man. *Dig Dis Sci* 1979; **24**: 497-500 [PMID: 456236 DOI: 10.1007/BF01489315]
- 25 **He J**, Irwin DM, Chen R, Zhang YP. Stepwise loss of motilin and its specific receptor genes in rodents. *J Mol Endocrinol* 2010; **44**: 37-44 [PMID: 19696113 DOI: 10.1677/JME-09-0095]
- 26 **Takayama I**, Seto E, Zai H, Ohno S, Tezuka H, Daigo Y, Fujino MA. Changes of *in vivo* gastrointestinal motor pattern in pacemaker-deficient (WsRC-Ws/Ws) rats. *Dig Dis Sci* 2000; **45**: 1901-1906 [PMID: 11117558 DOI: 10.1023/a:1005612109863]

- 27 **Taniguchi H**, Ariga H, Zheng J, Ludwig K, Takahashi T. Effects of ghrelin on interdigestive contractions of the rat gastrointestinal tract. *World J Gastroenterol* 2008; **14**: 6299-6302 [PMID: 19009642 DOI: 10.3748/wjg.14.6299]
- 28 **Mizumoto A**, Sano I, Matsunaga Y, Yamamoto O, Itoh Z, Ohshima K. Mechanism of motilin-induced contractions in isolated perfused canine stomach. *Gastroenterology* 1993; **105**: 425-432 [PMID: 8335198 DOI: 10.1016/0016-5085(93)90716-p]
- 29 **Kito Y**. The functional role of intramuscular interstitial cells of Cajal in the stomach. *J Smooth Muscle Res* 2011; **47**: 47-53 [PMID: 21757854 DOI: 10.1540/jsmr.47.47]
- 30 **Gomez-Pinilla PJ**, Gibbons SJ, Bardsley MR, Lorincz A, Pozo MJ, Pasricha PJ, Van de Rijn M, West RB, Sarr MG, Kendrick ML, Cima RR, Dozois EJ, Larson DW, Ordog T, Farrugia G. Ano1 is a selective marker of interstitial cells of Cajal in the human and mouse gastrointestinal tract. *Am J Physiol Gastrointest Liver Physiol* 2009; **296**: G1370-G1381 [PMID: 19372102 DOI: 10.1152/ajpgi.00074.2009]
- 31 **Kim YC**, Suzuki H, Xu WX, Hashitani H, Choi W, Yun HY, Park SM, Youn SJ, Lee SJ, Lee SJ. Voltage-dependent Ca Current Identified in Freshly Isolated Interstitial Cells of Cajal (ICC) of Guinea-pig Stomach. *Korean J Physiol Pharmacol* 2008; **12**: 323-330 [PMID: 19967074 DOI: 10.4196/kjpp.2008.12.6.323]
- 32 **Thornbury KD**, Hollywood MA, McHale NG, Sergeant GP. Cajal beyond the gut: interstitial cells in the urinary system--towards general regulatory mechanisms of smooth muscle contractility? *Acta Gastroenterol Belg* 2011; **74**: 536-542 [PMID: 22319963]
- 33 **McClain JL**, Fried DE, Gulbransen BD. Agonist-evoked Ca<sup>2+</sup> signaling in enteric glia drives neural programs that regulate intestinal motility in mice. *Cell Mol Gastroenterol Hepatol* 2015; **1**: 631-645 [PMID: 26693173 DOI: 10.1016/j.jcmgh.2015.08.004]
- 34 **Sanders KM**, Koh SD, Ro S, Ward SM. Regulation of gastrointestinal motility--insights from smooth muscle biology. *Nat Rev Gastroenterol Hepatol* 2012; **9**: 633-645 [PMID: 22965426 DOI: 10.1038/nrgastro.2012.168]
- 35 **Sung TS**, Hwang SJ, Koh SD, Bayguinov Y, Peri LE, Blair PJ, Webb TI, Pardo DM, Rock JR, Sanders KM, Ward SM. The cells and conductance mediating cholinergic neurotransmission in the murine proximal stomach. *J Physiol* 2018; **596**: 1549-1574 [PMID: 29430647 DOI: 10.1113/JP275478]
- 36 **Sun J**, Cao LX, Chen QC, Jiang Z, Chen ZQ, Zhou L. Effect of semen arecae on multichannel electrogastrogram and motilin and corticotropin-releasing hormone levels of healthy people. *Zhongyao Xinyao Yu Linchuang Yaoli* 2016; **27**: 281-285 [DOI: 10.3969/j.issn.1003-9783.2016.02.028]
- 37 **Xu FF**, Qi R, Jiang SW, Wang W, Chen ZQ, Guo DA, Liu B. Simultaneous determination of ten compounds in xiangbin fang by LC-MRM-MS. *Zhonghua Zhongyiyao Zazhi* 2017; **32**: 2226-2229
- 38 **Xie DP**, Chen LB, Liu CY, Zhang CL, Liu KJ, Wang PS. Arecoline excites the colonic smooth muscle motility via M3 receptor in rabbits. *Chin J Physiol* 2004; **47**: 89-94 [PMID: 15481791]
- 39 **Zhang JH**, Cao LX, Deng SG, Chen QC, Jiang Z, Chen ZQ, Zhou L. Effects of arecoline hydrobromide on the motility of isolated gastric smooth muscle strips in rats. *Guangdong Yixue* 2016; **37**: 2881-2885 [DOI: 10.3969/j.issn.1001-9448.2016.19.011]
- 40 **Han S**, Kim JS, Jung BK, Han SE, Nam JH, Kwon YK, Nah SY, Kim BJ. Effects of ginsenoside on pacemaker potentials of cultured interstitial cells of Cajal clusters from the small intestine of mice. *Mol Cells* 2012; **33**: 243-249 [PMID: 22350744 DOI: 10.1007/s10059-012-2204-6]
- 41 **Chen QC**, Pang FS, Cao LX, Jiang Z, Zhou L, Chen ZQ. Effect of Chinese herbs on gastrointestinal motility of chronic experimental beagle model. *Guangzhou Zhongyiyao Daxue Xuebao* 2016; **33**: 674-678 [DOI: 10.13359/j.cnki.gzxhtcm.2016.05.014]

## Basic Study

# Sinapic acid ameliorates D-galactosamine/lipopolysaccharide-induced fulminant hepatitis in rats: Role of nuclear factor erythroid-related factor 2/heme oxygenase-1 pathways

Mushtaq Ahmad Ansari, Mohammad Raish, Yousef A Bin Jardan, Ajaz Ahmad, Mudassar Shahid, Sheikh Fayaz Ahmad, Nazrul Haq, Mohammad Rashid Khan, Saleh A Bakheet

**ORCID number:** Mushtaq Ahmad Ansari 0000-0002-9106-0978; Mohammad Raish 0000-0002-6015-6125; Yousef A Bin Jardan 0000-0002-9106-0970; Ajaz Ahmad 0000-0001-6295-8685; Mudassar Shahid 0000-0003-3714-4772; Sheikh Fayaz Ahmad 0000-0002-8282-3726; Nazrul Haq 0000-0003-0666-808X; Mohammad Rashid Khan 0000-0002-9106-09784; Saleh A Bakheet 0000-0003-2322-9732.

**Author contributions:** Ansari MA and Raish M conceptualized the study; Ahmad A, Bin Jardan YA and Shahid M helped in the methodology; Shahid M did the formal analysis; Ahmad SF, Khan MR and Haq N helped in managing resources; Ansari MA, Raish M and Bakheet SA wrote the original first draft and supervised the study and the project was administered by Ansari MA; Shahid M and Raish M did the review, editing, and finalized the manuscript draft; Ansari MA acquired funding for this research.

**Supported by** Deanship of Scientific Research at King Saud University, No. RG-1439-083.

**Institutional review board statement:** The experiment

**Mushtaq Ahmad Ansari, Sheikh Fayaz Ahmad, Mohammad Rashid Khan, Saleh A Bakheet,** Department of Pharmacology and Toxicology, College of Pharmacy, King Saud University, Riyadh 11451, Saudi Arabia

**Mohammad Raish, Yousef A Bin Jardan, Mudassar Shahid, Nazrul Haq,** Department of Pharmaceutics, College of Pharmacy, King Saud University, Riyadh 11451, Saudi Arabia

**Ajaz Ahmad,** Department of Clinical Pharmacy, College of Pharmacy, King Saud University, Riyadh 11451, Saudi Arabia

**Corresponding author:** Mushtaq Ahmad Ansari, PhD, Associate Professor, Department of Pharmacology and Toxicology, College of Pharmacy, King Saud University, King Khalid Road, Riyadh 11451, Saudi Arabia. [muansari@ksu.edu.sa](mailto:muansari@ksu.edu.sa)

## Abstract

### BACKGROUND

Sinapic acid (SA) has been shown to have various pharmacological properties such as antioxidant, antifibrotic, anti-inflammatory, and anticancer activities. Its mechanism of action is dependent upon its ability to curb free radical production and protect against oxidative stress-induced tissue injuries.

### AIM

To study the hepatoprotective effects of SA against lipopolysaccharide (LPS)/D-galactosamine (D-GalN)-induced acute liver failure (ALF) in rats.

### METHODS

Experimental ALF was induced with an intraperitoneal (i.p.) administration of 8 µg LPS and 800 mg/kg D-GalN in normal saline. SA was administered orally once daily starting 7 d before LPS/D-GalN treatment.

### RESULTS

Data showed that SA ameliorates acute liver dysfunction, decreases serum levels of alanine transaminase (ALT), and aspartate aminotransferase (AST), as well as malondialdehyde (MDA) and NO levels in ALF model rats. However, pretreatment with SA (20 mg/kg and 40 mg/kg) reduced nuclear factor kappa-

proposal was authorized by the Ethics Committee of the Experimental Animal Care Society, King Saud University, Saudi Arabia (No. KSU-SE-20-13).

**Institutional animal care and use committee statement:** The experiment proposal was authorized by the Ethics Committee of the Experimental Animal Care Society, King Saud University, Saudi Arabia (No. KSU-SE-20-13).

**Conflict-of-interest statement:** The author declares that there are no conflicts of interest.

**Data sharing statement:** No additional data are available.

**ARRIVE guidelines statement:** The authors have read the ARRIVE Guidelines, and the manuscript was prepared and revised according to the ARRIVE Guidelines.

**Open-Access:** This article is an open-access article that was selected by an in-house editor and fully peer-reviewed by external reviewers. It is distributed in accordance with the Creative Commons Attribution NonCommercial (CC BY-NC 4.0) license, which permits others to distribute, remix, adapt, build upon this work non-commercially, and license their derivative works on different terms, provided the original work is properly cited and the use is non-commercial. See: <http://creativecommons.org/licenses/by-nc/4.0/>

**Manuscript source:** Unsolicited manuscript

**Specialty type:** Gastroenterology and hepatology

**Country/Territory of origin:** Saudi Arabia

**Peer-review report's scientific quality classification**

Grade A (Excellent): 0  
Grade B (Very good): B  
Grade C (Good): C, C  
Grade D (Fair): 0  
Grade E (Poor): 0

light-chain-enhancer of activated B cells (NF- $\kappa$ B) activation and levels of inflammatory cytokines (tumor necrosis factor- $\alpha$  and interleukin 6). Also, SA increased the activity of the nuclear factor erythroid-related factor 2/heme oxygenase-1 (Nrf2/HO-1) signaling pathway.

## CONCLUSION

In conclusion, SA offers significant protection against LPS/D-GalN-induced ALF in rats by upregulating Nrf2/HO-1 and downregulating NF- $\kappa$ B.

**Key Words:** Sinapic acid; D-galactosamine/lipopolysaccharide; Oxidative stress; Fulminant hepatitis; Antioxidant; Nuclear factor erythroid-related factor 2/heme oxygenase-1 pathways

©The Author(s) 2021. Published by Baishideng Publishing Group Inc. All rights reserved.

**Core Tip:** This work demonstrated for the first time that the sinapic acid (SA) has hepatoprotective effects in the D-galactosamine/lipopolysaccharide (D-GalN/LPS)-induced rat model through its ability to suppress oxidative stress, inflammation, and apoptosis. The protective mechanism of SA depends on the downregulation of nuclear factor kappa-light-chain-enhancer of activated B cells and the restoration of antioxidant enzyme levels through the activation of the Nrf2/HO-1 pathway. Thus, SA could be applied to treat or prevent D-GalN/LPS-induced acute liver failure in the future.

**Citation:** Ansari MA, Raish M, Bin Jordan YA, Ahmad A, Shahid M, Ahmad SF, Haq N, Khan MR, Bakheet SA. Sinapic acid ameliorates D-galactosamine/lipopolysaccharide-induced fulminant hepatitis in rats: Role of nuclear factor erythroid-related factor 2/heme oxygenase-1 pathways. *World J Gastroenterol* 2021; 27(7): 592-608

**URL:** <https://www.wjgnet.com/1007-9327/full/v27/i7/592.htm>

**DOI:** <https://dx.doi.org/10.3748/wjg.v27.i7.592>

## INTRODUCTION

Naturally occurring phenolic compounds play a significant role in disease prevention and treatment<sup>[1]</sup>. Natural phenols from plants include phenolic acids, tannins, flavonoids, stilbenes, coumarins, curcuminoids, quinones, lignans, and others. Sinapic acid (SA) Hydroxycinnamic acids (HCAs) are a group of naturally occurring phenolic acid and highly abundant in the human diet, such as fruits, vegetables, and grains<sup>[2]</sup>. Previous studies demonstrate that SA is a bioactive phenolic acid and has the potential to attenuate various chemically induced toxicities<sup>[3]</sup>. Fulminant hepatitis is a life-threatening clinical syndrome that is associated with overwhelming inflammation, hepatic encephalopathy, liver injury, and eventually liver failure<sup>[4]</sup>. Several studies have identified various etiologies for acute liver failure such as viral infections, bacterial infections, alcohol, and drugs<sup>[5-7]</sup>. Lipopolysaccharide (LPS) contains endotoxin prompted inflammation, and D-galactosamine (D-GalN) consequences in lipid peroxidation *via* promoting the release of reactive oxygen species (ROS) in liver cells<sup>[8]</sup>. There is an urgent need for the development of novel hepatoprotective therapies. The pathogenesis of fulminant hepatitis is currently under extensive investigation using LPS/D-GalN-prompted acute liver failure (ALF) model. This is a well-known model to probe the mechanism, pathogenesis, and agents for human liver injury<sup>[9,10]</sup>. D-GalN, a well-established hepatotoxic agent, produces hepatic necrosis by inhibiting mRNA translation<sup>[11]</sup>. LPS is known to stimulate Kupffer cells and promote the release of inflammatory cytokines such as tumor necrosis factor- $\alpha$  and interleukin 6 (TNF- $\alpha$  and IL-6), that successively produce hepatonecrosis and ALF. Furthermore, ROS-induced mitochondrial dysfunction was identified as a probable mechanism in LPS/D-GalN-induced ALF<sup>[12,13]</sup>.

Several reports indicated that decreasing inflammation and oxidative stress could mitigate liver damage<sup>[14]</sup>. The homeostasis of metabolism, redox equilibrium and production of ROS are easily apparent at the mitochondrial level in which superoxide is generated as a result of the electron transport chain and Kerb's cycle reaction. The



**Received:** October 26, 2020**Peer-review started:** October 26, 2020**First decision:** November 25, 2020**Revised:** November 30, 2020**Accepted:** January 21, 2021**Article in press:** January 21, 2021**Published online:** February 21, 2021**P-Reviewer:** Marickar F, Valenzuela R**S-Editor:** Gao CC**L-Editor:** A**P-Editor:** Ma YJ

recent data demonstrate that nutritional intake, energy metabolism is also associated at nuclear level *via* the nuclear factor erythroid-related factor-2 (Nrf2)/antioxidant response element (ARE) pathway<sup>[15]</sup>. Several genes that contribute to oxidative stress are controlled by the key Nrf2. Before elevation in ROS, the Nrf2 transcription factor present in cytoplasm causes it to translocate to the nucleus. Activated, Nrf2 binds to the promoter region cis-acting enhancer ARE sequence (core sequence: TGAG/CNNNGC) of antioxidant genes to increase their expression of 500 genes including *Gsts*, *Nqo1*, *Ugts*, *Gclc*, *Gclm*, and *Ho-1* *etc.* referred to as the “Nrf2 regulon”<sup>[16]</sup>, which enhanced the capacity of the cellular radical-scavenging systems which decrease oxidative stress and activate pro-inflammatory pathways<sup>[17,18]</sup>. Nrf2/ARE pathway predominantly involves in phase-II detoxification organs including liver, kidney, heart, intestine *etc.* A link between liver diseases and oxidative stress is indispensable. Nrf2 is a key regulator of cytodefence *via* mediation of antioxidant response, anti-inflammatory and chemoprotective activity<sup>[19]</sup>. The capacities of Nrf2 to enhance the expressions of antioxidant proteins and suppress oxidative stress-related injury have been broadly studied<sup>[14,20]</sup>. Therefore, implication of Nrf2/ARE activating regimens may be used for liver diseases. The generation of ROS devastates the antioxidant capacity, which contributes to the pathogenesis of several diseases, including fulminant hepatitis<sup>[10,21]</sup>. SA, also known as 3,5-dimethoxy-4-hydroxycinnamic acid, is a key phytoconstituent of citrus fruits, spices, berries, cereals, vegetables and oilseed crops commonly used in food and beverages<sup>[22]</sup>. SA is known to possess activities, such as antimicrobial, antioxidant, anti-inflammatory, anticancer, antidiabetic, antihypertensive, anti-anxiety, neuroprotective and hepatoprotective activities<sup>[3,22-26]</sup>. SA is a prominent member of the Brassicaceae family<sup>[24]</sup>. Literature reveals that SA is a bioactive phenolic acid and has the potential to attenuate various chemically induced toxicities<sup>[3]</sup>. SA is a potent scavenger of ROS; this property allows it to protect against tissue injuries<sup>[3,25,26]</sup>. SA induced NRF2/HO-1 has been reported in various disease models<sup>[25-29]</sup>. The amelioration of LPS/D-GalN-induced fulminant hepatitis through NRF2/HO-1 activation have been previously documented<sup>[30-32]</sup>. However, the hepatoprotective effects of SA in LPS/D-GalN-induced fulminant hepatitis has not been previously investigated. To identify the detailed mechanisms of action for SA, we tested its antioxidant and anti-inflammatory activities in a rat model of LPS/D-GalN-induced fulminant hepatitis. Thus, the purpose of the current study was to explore the underlying hepatoprotective mechanism of SA against LPS/D-GalN-induced ALF in rats. We also aimed to identify its effects on ROS production, inflammation and apoptosis and the roles of Nrf2/heme oxygenase 1 (HO-1) and NF-κB pathways.

## MATERIALS AND METHODS

### Drugs and chemicals

SA, LPS, and D-GalN were acquired from Sigma-Aldrich (Switzerland). The following primary antibodies were purchased from Santa Cruz Biotechnology (Dallas, TX, United States): transforming growth factor (TGF-β), Nrf2, HO-1, B-cell lymphoma 2 (Bcl-2), Caspase 3, Bcl2-Associated X, Apoptosis Regulator (Bax), nuclear factor of kappa light polypeptide gene enhancer in B cells inhibitor alpha (IκBα), NF-κB, and beta-actin (β-actin). HRP-conjugated secondary antibodies were also purchased from Santa Cruz Biotechnology (Dallas, TX, United States). A nuclear and cytoplasmic protein NE-PER kit was purchased from Pierce Biotechnology (Rockford, IL, United States). Enzyme-linked immunosorbent assay (ELISA) kits for rat TNF-α, IL-6, and myeloperoxidase (MPO) were purchased from R&D Systems, Inc. (MN, United States).

### Animals

Wistar adult male rats (weight, 212-226 g) were taken from the animal facility of King Saud University, Riyadh, Saudi Arabia. The experiment proposal was authorized by the Ethics Committee of the Experimental Animal Care Society, King Saud University, Saudi Arabia (KSU-SE-20-13). They were kept under standard conditions 24 ± 2 °C, 12 h light/dark cycle, and received water and food *ad libitum*. The studies were performed according to the protocols that were approved by the Animal Ethics Committee of King Saud University, College of Pharmacy, Riyadh, Saudi Arabia.

### Experimental design

The total forty-two rats were arbitrarily categorized into four groups: The control group (*n* = 6), the D-GalN/LPS treated (ALF) group (*n* = 12), the ALF + SA (20 mg/kg)

group ( $n = 12$ ), and the ALF + SA (40 mg/kg) group ( $n = 12$ ). To induce ALF, rats were injected intraperitoneally (i.p.) with 8 µg/kg LPS and 800 mg/kg D-GalN in 800 µL sterile normal saline. SA (20 and 40 mg/kg) solution in normal saline were administered *via* gavage once per day starting seven days before LPS/D-GalN treatment. The normal control group was injected i.p. with an equal volume of normal saline. Rats were anesthetized with ketamine (55 mg/kg) and xylazine (7 mg/kg) and euthanized 72 h after the D-GalN/LPS injection. Both serum and liver samples were collected and stored at -80 °C for further analysis. The dose of SA was selected based on preliminary and published data<sup>[3,23,33]</sup>.

### **Survival rate and liver function activity**

The rate of survival was observed for 48 h after the injection with D-GalN/LPS. Rats were witnessed for morbidity every hour after the injection of D-GalN/LPS. Assay kits to measure levels of aspartate aminotransferase (AST), alanine transaminase (ALT) and the ratio of bilirubin to alkaline phosphatase were purchased from Human Diagnostic Worldwide (Wiesbaden, Germany), using a spectrophotometer (Shimadzu – Model UV 2401, Kyoto, Japan)."

### **Histological evaluation**

Hepatic tissue from each rat was fixed in 12% formalin for histopathological evaluation. The hepatic tissues were gradually dehydrated, embedded in paraffin, cut into 5-µm sections, and stained with hematoxylin and eosin for histological inspection. Briefly, the severity of liver damage was evaluated by a blinded pathologist using four-point scale from 0 to 3 as follows: 0, 1, 2, and 3 represent no damage, mild damage, moderate damage, and very severe damage, scoring system in 20 random fields at 400 × magnification per animal ( $n = 6$ ) for each group. A light microscope (Olympus, Japan) examined the histological anomalies.

### **Preparation of nuclear and total protein extracts**

Total hepatic protein was extracted by homogenizing (T 25 Digital ULTRA-TURRAX®) tissue in cold RIPA buffer (Pierce Biotechnology, United States) and the supernatant was collected after centrifuging at 2500 × *g* for 20 min at 4 °C. Similarly, cytosolic and nuclear proteins were prepared using the NE-PER Kit (Pierce Biotechnology, United States) following the kit instructions. The protein concentration was examined using (Pierce Biotechnology, United States) the method bicinchoninic acid (Pierce™ BCA) assay<sup>[34]</sup>.

### **Oxidative stress indices**

The levels of malondialdehyde (MDA) and NO were examined in hepatic tissues using commercially available colorimetric assay kit (Sigma-Aldrich, St. Louis, MO, United States).

### **Antioxidant enzyme indices**

Hepatic superoxide dismutase (SOD), catalase (CAT), and glutathione peroxidase (GP<sub>x</sub>) activities in homogenized hepatic tissues were examined using commercial kits (Cayman Chemical, Ann Arbor, MI, United States).

### **Cytokine and inflammatory marker**

TNF-α, IL-6, and MPO levels in the hepatic tissue were measured using ELISA kits according to the kit instructions. Absorbance was read at 450 nm.

### **Western blot analysis**

Protein expression was performed using western blot analysis using a previously described protocol<sup>[35]</sup>. Precisely, 30-40 µg of protein was separated *via* sodium dodecyl sulfate-polyacrylamide gel electrophoresis (SDS-PAGE), electrophoretically transferred to nitrocellulose membranes, blocked with 4% casein and BSA in TBS containing 1% Tween-20 (TBST), and incubated at 4 °C overnight with the primary antibodies. The next day, membranes were washed five times with TBST and incubated with secondary antibodies for 2 h at room temperature. Bands were observed using Luminata™ Western Chemiluminescent HRP Substrates (Millipore, Billerica, MA, United States). Densitometric analysis of the immunoblots was also performed using a LI-COR C-Di-Git Blot Scanner (Lincoln, NE, United States).

### Statistical analysis

All results are presented as arithmetic means  $\pm$  SE. Data were analyzed using a one-way analysis of variance followed by Dennett's test by using Graph Pad V6.

## RESULTS

### Effects of SA on the survival rate of animals with D-GalN/LPS-induced ALF

The effect of SA pretreatment (20 and 40 mg/kg) on the 96 h survival rate is shown in [Figure 1](#). After the administration of D-GalN/LPS, five rats died before 12 h with a survival rate of 58.33% after 96 h. Pretreatment with 20 and 40 mg/kg SA increased the survival rate by 66.66% and 75%, respectively, compared to the ALF group.

### Effect of SA pretreatment on liver failure serum markers in D-GalN/LPS-induced ALF

The administration of D-GalN/LPS to rats caused ALF, as demonstrated by the significant increase in ALT, AST, and bilirubin levels (1485.73%, 774.10%, and 374.28%, respectively) compared with the normal controls ( $P < 0.05$ ,  $P < 0.05$ ,  $P < 0.05$ ). Nevertheless, pretreatment with 20 and 40 mg/kg SA prevented ALF, as demonstrated by the 51.93% and 69.65% decreases in ALT levels ( $P < 0.05$ ,  $P < 0.05$ ), 44.29% and 73.66% decreases in AST levels ( $P < 0.05$ ,  $P < 0.05$ ) and 48.67% and 56.22% decreases in bilirubin levels ( $P < 0.01$ ,  $P < 0.01$ ) compared to the ALF rats ([Table 1](#)). Moreover, the histological examination of liver tissues showed that D-GalN/LPS caused focal central vein congestion, massive changes in lipid accumulation, ballooning formation, loss of cellular boundaries, and necrosis with inflammation. SA pretreatment, especially the 40 mg/kg dose, improved liver architecture in comparison to the ALF rats.

### Effect of SA pretreatment on oxidative stress markers in the hepatic tissue of ALF rats

Liver tissue from the D-GalN/LPS-induced ALF animals showed significantly higher levels of MDA (122.90%) ( $P < 0.05$ ) ([Figure 2A](#)) and  $\text{NO}_2^-$  content (230.01%) ( $P < 0.05$ ) ([Figure 2B](#)) compared with the liver tissue from the control animals. However, the oral administration of 20 and 40 mg/kg SA significantly and dose-dependently reduced the MDA levels by 35.24% and 41.22%, respectively ( $P < 0.05$ ; [Figure 2A](#)) and  $\text{NO}_2^-$  levels by 39.05% and 51.82%, respectively ( $P < 0.05$ ; [Figure 2B](#)).

### Effect of SA pretreatment on the activity of antioxidant enzyme markers in hepatic tissue of D-GalN/LPS-induced ALF rats

Hepatic tissue from D-GalN/LPS-induced ALF rats show 55.14% ( $P < 0.05$ ), 70.01% ( $P < 0.05$ ), and 73.37% ( $P < 0.05$ ) reduction in the activities of GPx, SOD, and CAT, respectively ([Figure 3](#)). The oral administration of 20 and 40 mg/kg SA significantly restored the activity of GPx by 29.23% and 78.81%, respectively ( $P < 0.05$ ); the activity of SOD by 117.64% and 185.87%, respectively ( $P < 0.05$ ); and CAT activity by 123.41% and 198.41%, respectively ( $P < 0.05$ ).

### Effect of SA pretreatment on cytokines and inflammatory markers in hepatic tissue of D-GalN/LPS-induced ALF

The data suggested that TNF- $\alpha$ , IL-6 and MPO levels were significantly augmented in the D-GalN/LPS-induced ALF that is 524.61 %, 154.57 % and 118.56 % respectively ( $P < 0.05$ ) as compared to control rats. SA at 20 and 40 mg/kg pretreatment significantly and dose-dependently downregulate these effects of TNF- $\alpha$ , IL-6 and MPO ( $P < 0.05$ ; [Figure 4](#)) that is 29.69% and 50.39% for TNF- $\alpha$ , 37.03%, 46.53% for IL-6 and 23.52% and 32.72% for MPO as compared to D-GalN/LPS -induced ALF rats.

### SA downregulates NF- $\kappa$ B (p65) in ALF

To examine the probable mechanism by which SA blocks TGF $\beta$  and IL-6 generation, we analyzed the activity of 20 and 40 mg/kg SA on NF- $\kappa$ B activation. As illustrated in [Figure 5](#), the protein expression of I $\kappa$ B- $\alpha$  in the ALF group declined compared to the control group; however, this decrease was reversed by 20 and 40 mg/kg SA in a dose-dependent fashion. Moreover, In the ALF group, we detected increased nuclear NF- $\kappa$ B (p65) relative to the control group. However, 20 and 40 mg/kg treatment with SA reduced NF- $\kappa$ B (p65) during ALF in dose-dependent manner. The data proposed that SA may inhibit D-GalN/LPS -induced TGF $\beta$  generation by blocking NF- $\kappa$ B activation. Induction with D-GalN/LPS encouraged the translocation of p65 into the nucleus, and

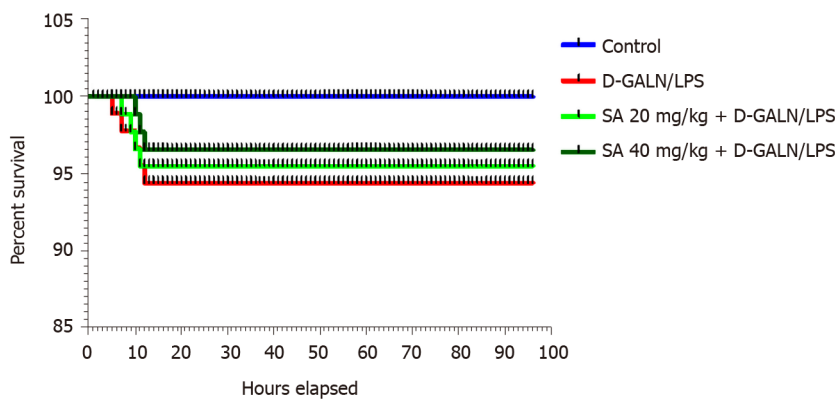
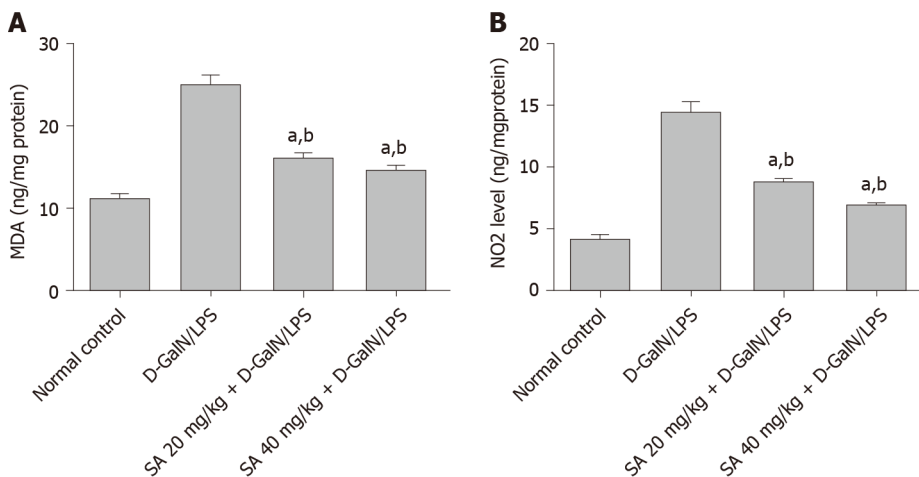
**Table 1** Effect of sinapic acid pretreatment on liver function serum markers in D-galactosamine/lipopolysaccharide-induced acute liver failure

Serum	Control	D-GalN/LPS	SA 20 mg/kg + D-GalN/LPS	SA 40 mg/kg + D-GalN/LPS
Total protein (mg/dL)	121.98 ± 1.45	82.48 ± 1.84	92.70 ± 1.17 <sup>a,b</sup>	104.96 ± 2.24 <sup>a,b</sup>
AST (U/L)	85.78 ± 3.26	749.83 ± 36.99	417.67 ± 23.46 <sup>a,b</sup>	197.50 ± 18.25 <sup>a,b</sup>
ALT (U/L)	60.75 ± 4.18	963.33 ± 45.73	463.00 ± 22.41 <sup>a,b</sup>	292.33 ± 23.76 <sup>a,b</sup>
Bilirubin (mg/dL)	0.35 ± 0.04	1.66 ± 0.15	0.85 ± 0.03 <sup>a,b</sup>	0.73 ± 0.02 <sup>a,b</sup>

The results are presented as the mean ± SE of six animals per group.

<sup>a</sup>Denotes significant differences to the in D-galactosamine/lipopolysaccharide-induced acute liver failure group ( $P < 0.05$ ).

<sup>b</sup>Denotes significant differences to the normal control. SA: Sinapic acid; D-GalN/LPS: D-galactosamine/lipopolysaccharide; ALT: Alanine transaminase; AST: Aspartate aminotransferase.

**Figure 1** Effect of sinapic acid (20 and 40 mg/kg bodyweight) pretreatment on the survival rate of D-galactosamine/lipopolysaccharide-induced acute liver failure. SA: Sinapic acid; D-GalN/LPS: D-galactosamine/lipopolysaccharide.**Figure 2** Effect of sinapic acid pretreatment on oxidative stress markers in hepatic tissue of D-galactosamine/lipopolysaccharide-induced acute liver failure. The results are presented as mean ± SE with six animals per group. <sup>a</sup>Denotes significant differences compared to the control group ( $P < 0.05$ ); <sup>b</sup>Denotes significant differences compared to the D-galactosamine/lipopolysaccharide group ( $P < 0.05$ ). MDA: Malondialdehyde; SA: Sinapic acid; D-GalN/LPS: D-galactosamine/lipopolysaccharide.

induced the inflammatory response through the NF- $\kappa$ B signaling pathway. As illustrated in Figure 5, D-GalN/LPS apparently upregulated the expression of Bax, caspase 3, and downregulated the expression of Bcl-2, which indicated apoptosis. On the contrary, dose-dependent downregulation of Bax, caspase 3 and upregulation of Bcl-2 was observed after pretreatment with 20 and 40 mg/kg SA in the D-GalN/LPS



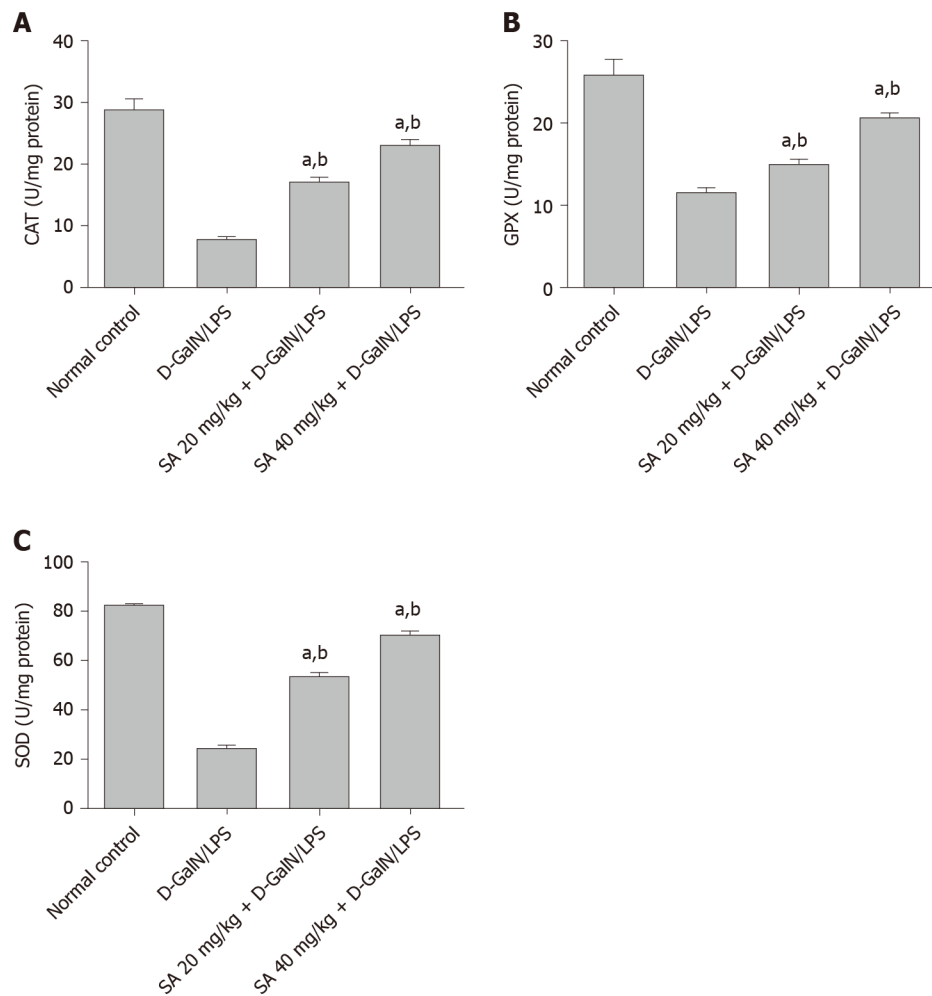
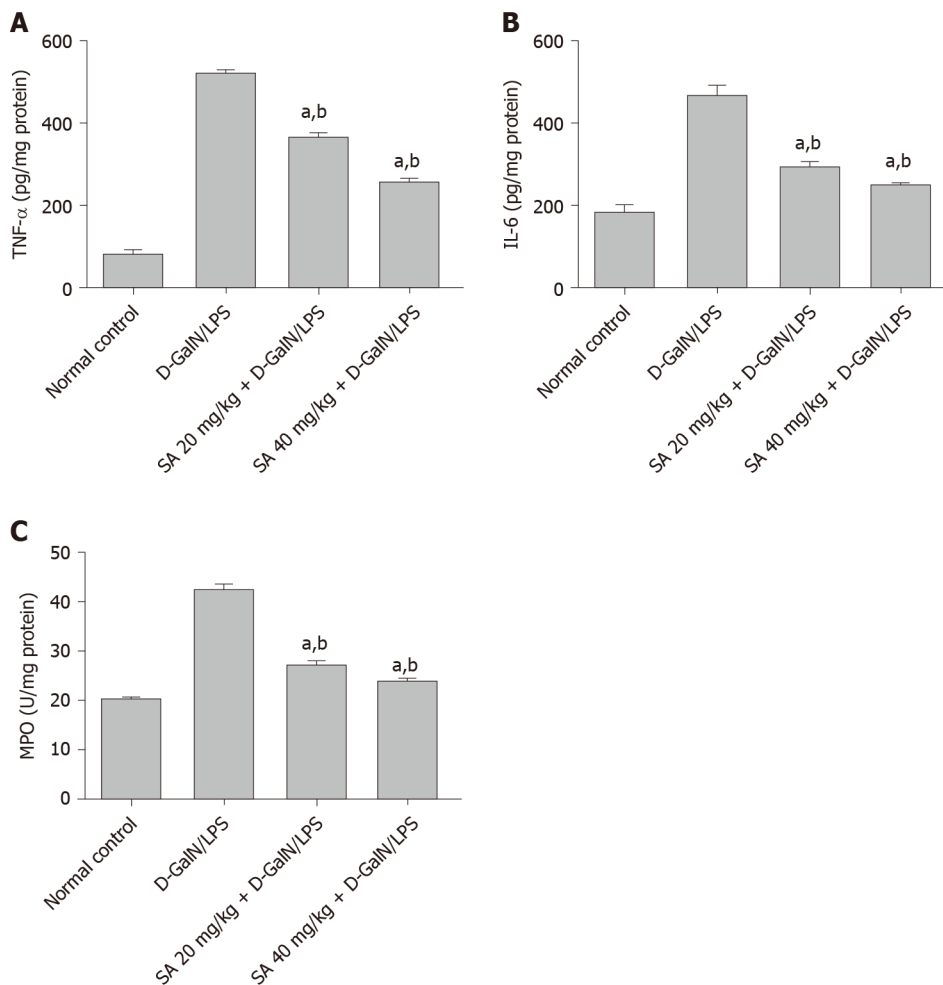


**Figure 3** Effect of sinapic acid pretreatment on antioxidant enzyme activity in hepatic tissue from D-galactosamine/lipopolysaccharide-induced acute liver failure rats. The results are presented as mean  $\pm$  SE with six animals per group. <sup>a</sup>Denotes significant differences compared to the control group ( $P < 0.05$ ); <sup>b</sup>denotes significant differences compared to the D-galactosamine/lipopolysaccharide group ( $P < 0.05$ ). CAT: Catalase; SA: Sinapic acid; D-GalN/LPS: D-galactosamine/lipopolysaccharide.

group. These results indicate that SA inhibited LPS/D-GalN-induced hepatocyte apoptosis by affecting the expression of apoptosis-related factors. D-GalN/LPS administration induced iNOS expression compared to the normal control. Pretreatment with 20 and 40 mg/kg SA significantly and dose-dependently inhibits iNOS expression, thus suggestive its potent anti-inflammatory effects. The antioxidant activity of SA is controlled *via* the modulation of the Nrf2/HO-1 pathway. Hepatic tissue from D-GalN/LPS-induced ALF show lower levels of Nrf2 and HO-1 expression as compared to the normal control rats. However, treatment with 20 mg/kg and 40 mg/kg SA significantly and dose-dependently upregulated the expression of Nrf2 and HO-1 compared with tissues from D-GalN/LP-induced animals ( $P < 0.05$ ).

#### **Effects of SA on histoarchitecture of liver tissues in ALF**

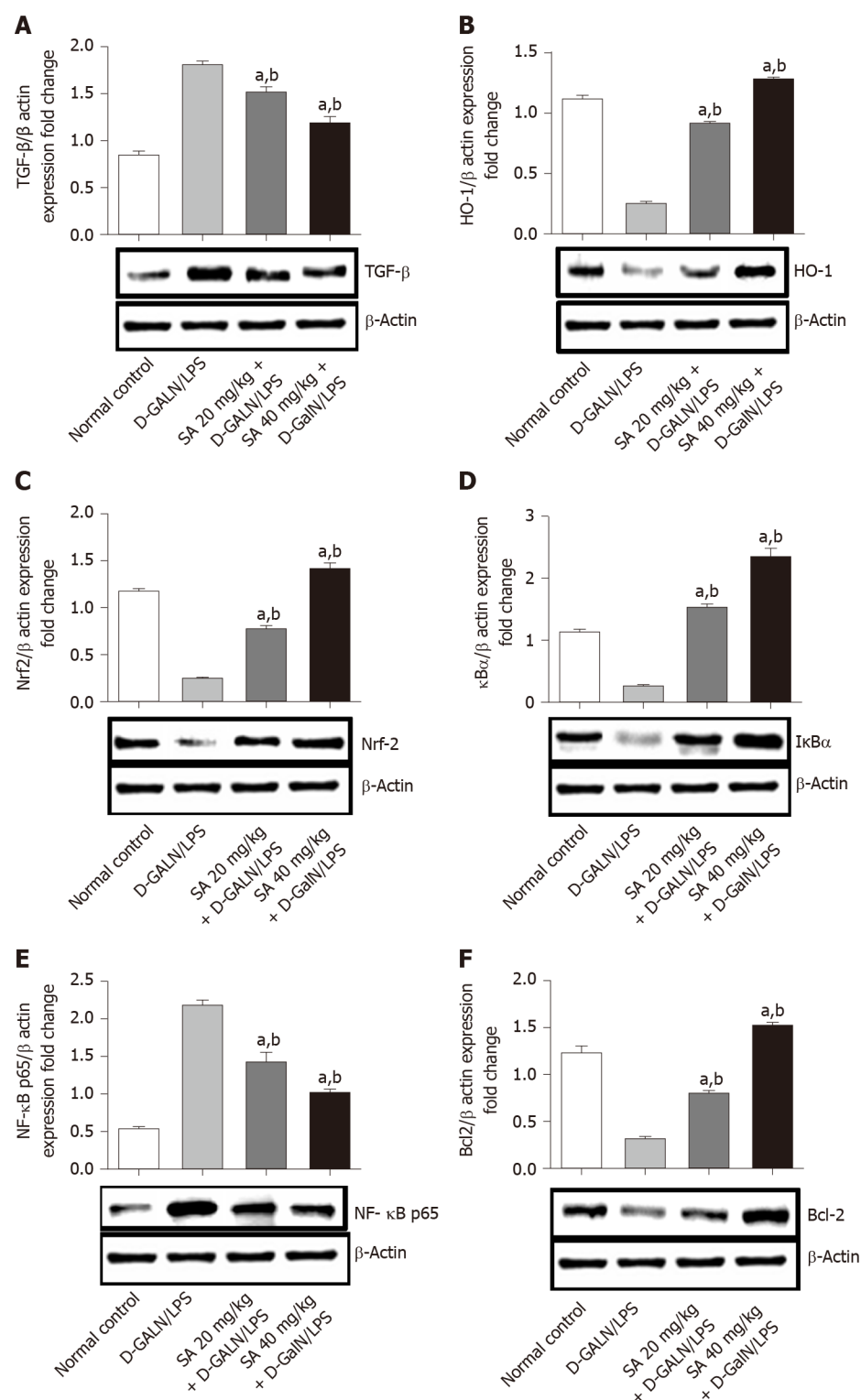
As illustrated in **Figure 6A**, the hepatic tissues from the normal control group exhibited normal cellular and lobular architecture. Hepatic tissue from the ALF group exhibited prominent pathological alterations comprising widespread portal inflammation, hepatic cell necrosis, and infiltration of inflammatory cells (**Figure 6B**). However, pretreatment with 20 mg/kg and 40 mg/kg SA significantly ameliorated the D-GalN/LPS-induced pathological alterations in a dose-dependent manner as demonstrated by the reduced cell infiltration and restored lobular architecture. The severity of liver damage score has been illustrated in **Figure 7**.



**Figure 4** Effect of sinapic acid pretreatment on cytokines and inflammatory markers in hepatic tissue of D-galactosamine/lipopolysaccharide-induced acute liver failure. The results are presented as mean  $\pm$  SE with six animals per group. <sup>a</sup>Denotes significant differences compared to the control group ( $P < 0.05$ ); <sup>b</sup>denotes significant differences compared to the D-galactosamine/lipopolysaccharide group ( $P < 0.05$ ). TNF- $\alpha$ : Tumor necrosis factor- $\alpha$ ; IL-6: Interleukin 6; MPO: Myeloperoxidase; SA: Sinapic acid; D-GalN/LPS: D-galactosamine/lipopolysaccharide.

## DISCUSSION

There is an overwhelming amount of evidence showing that SA protects against liver damage in animal models *via* various mechanisms, such as its antioxidant activity, anti-inflammatory activity, and ability to downregulate NF- $\kappa$ B p65. Therefore, SA has potential as a hepatoprotective agent for decreasing inflammation in CCL<sub>4</sub> and dimethyl nitrosamine-induced acute liver fibrosis<sup>[23]</sup>. The fulminant hepatitis rodent model was not investigated, and more detailed mechanisms remain unclear. Since SA has potent anti-inflammatory and antioxidant functions, we hypothesized that SA could also have hepatoprotective effects against D-GalN/LPS-induced fulminant hepatitis. The D-GalN/LPS-induced animal model of ALF is widely used to check the efficacy of hepatoprotective agents<sup>[36,37]</sup>. To examine the hepatoprotective effect of SA, serum levels of AST and ALT were analyzed to study the extent of liver damage. Several reports have shown that SA decreased AST and ALT<sup>[23]</sup>. AST and ALT are two known serum biomarkers of liver dysfunction<sup>[38,39]</sup>. Elevated levels of AST are indicative of tissue necrosis<sup>[40]</sup>. D-GalN/LPS-induced ALF rats exhibit enhanced serum levels of AST and ALT that were accompanied by enhanced inflammatory infiltration, hemorrhage, hepatocyte necrosis, and the loss of hepatic architecture. Pretreatment with SA (20 and 40 mg/kg) dose-dependently downregulated the AST and ALT levels and helped restore liver functions and structures. These results are consistent with previous reports<sup>[3,23,24,41,42]</sup>. Mitochondrial dysfunction and oxidative stress are two linked cellular events<sup>[43]</sup>. The dysfunction of mitochondrial dynamics leads to accumulation ROS and encourages induction of DNA damage, up or down regulation of apoptotic/anti-apoptotic factors, phosphatases and apoptotic/antiapoptotic factors leading to redox imbalance leading to wide range of disease including fulminant



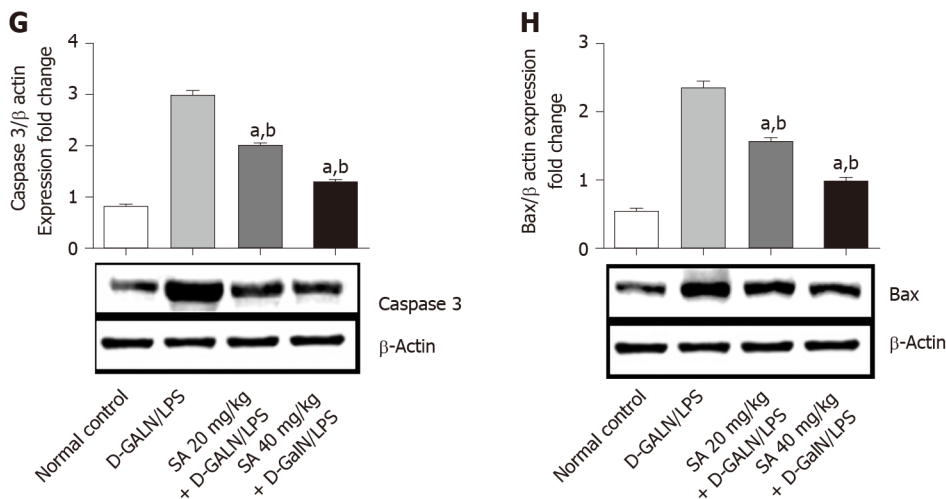


**Figure 5 Sinapic acid downregulates nuclear factor kappa B in acute liver failure.** A-H: Effect of sinapic acid on the protein expression of transforming growth factor- $\beta$ 1 (A), heme oxygenase-1 (B), nuclear factor erythroid 2-related factor 2 (C), nuclear factor of kappa light polypeptide gene enhancer in B cells inhibitor alpha protein (D), nuclear factor kappa B (E), anti-apoptotic protein Bcl2 (F), caspase 3 (G), and Bax in D-galactosamine/lipopolysaccharide (D-GalN/LPS)-induced acute liver failure (ALF) (H). The results are presented as the mean  $\pm$  SE of six animals per group. <sup>a</sup>Denotes significant differences to the D-GalN/LPS-induced ALF group ( $P < 0.05$ ); <sup>b</sup>denotes significant differences compared to the normal control. TGF- $\beta$ 1: Transforming growth factor- $\beta$ 1; HO-1: Heme oxygenase-1; Nrf2: Nuclear factor erythroid 2-related factor 2; I $\kappa$ B $\alpha$ : Nuclear factor of kappa light polypeptide gene enhancer in B cells inhibitor alpha; NF- $\kappa$ B: Nuclear factor kappa B; SA: Sinapic acid; D-GalN/LPS: D-galactosamine/lipopolysaccharide.

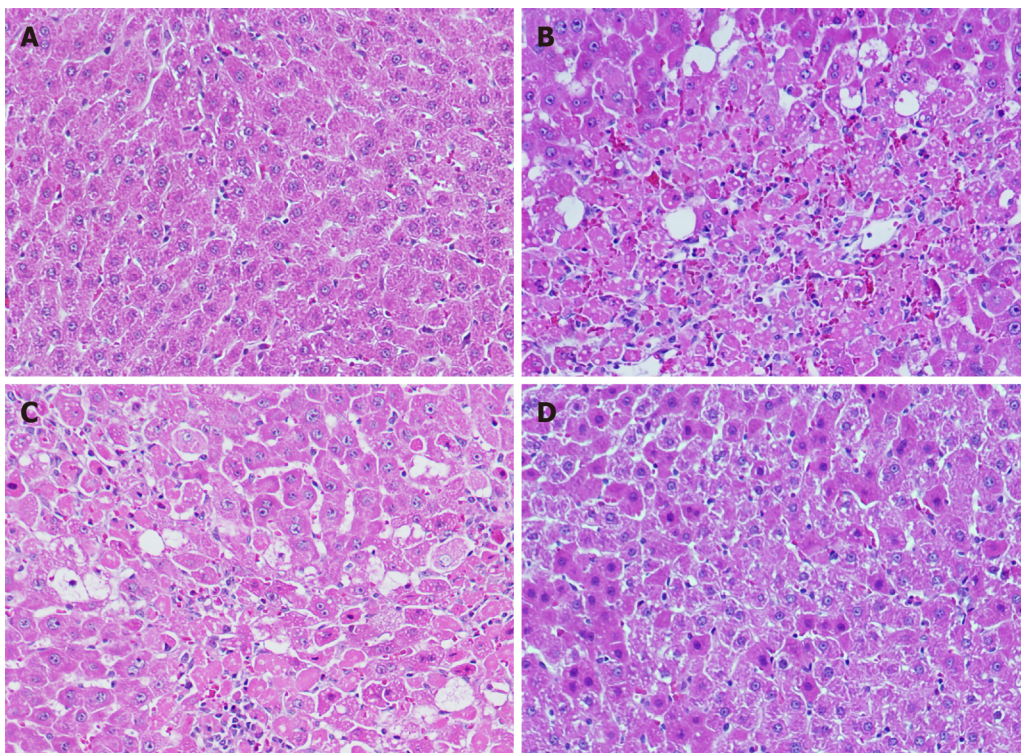


**Figure 6 Light photomicrographs of hepatic tissues.** Hematoxylin and eosin stains, magnification 100  $\times$ . A: Hepatic section of normal control rat exhibits normal architecture of hepatic cord of cells; B: Hepatic section of D-galactosamine/lipopolysaccharide (D-GalN/LPS) treated rats exhibiting massive fatty changes, focal central vein congestion, ballooning formation, necrosis with inflammation, and loss of cellular boundaries, massive cellular infiltration; C: Hepatic section of rats treated D-GalN/LPS and 20 mg/kg of sinapic acid (SA) showing mild central vein congestion, mild fatty changes, ballooning, necrosis with sinusoidal dilatation, mild cellular infiltration; D: Hepatic section of rats treated D-GalN/LPS and 40 mg/kg of SA exhibiting the absence of ballooning, inflammatory cells, and regeneration of hepatocytes around central vein toward near-normal liver architecture but slight congestion in the central vein.

hepatic disease<sup>[42,44,45]</sup>. Previous evidence indicate that mitochondrial defects contribute to liver damage *via* a number of pathways<sup>[46,47]</sup>, involving inhibition of mitochondrial  $\beta$ -oxidation and respiratory chain activity, failure of mitochondrial membrane potential and damage to the antioxidant protection mechanism.



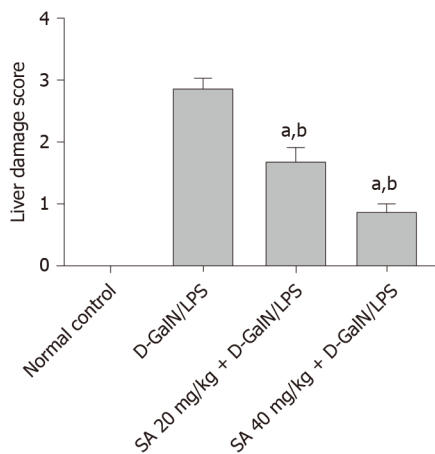


**Figure 7** The liver damage score was examined using four-point scale from 0 to 3. 0, 1, 2, and 3 represent no damage, mild damage, moderate damage, and very severe damage, scoring system in 20 random fields at 400 × magnification per animal ( $n = 6$  per group). <sup>a</sup>Denotes significant differences compared to the control group ( $P < 0.05$ ); <sup>b</sup>Denotes significant differences compared to the D-galactosamine/lipopolysaccharide group ( $P < 0.05$ ). SA: Sinapic acid; D-GalN/LPS: D-galactosamine/lipopolysaccharide.

ROS play a significant role in the pathogenesis of ALF<sup>[21,48]</sup>. Reactive nitrogen species (RNS) and ROS can react with polyunsaturated fatty acids (PUFAs) to cause lipid peroxidation; this process may further damage the cellular membrane and trigger apoptosis<sup>[49,50]</sup>. Kupffer cells and neutrophils undergo apoptosis during vascular oxidative stress, which leads to ALF<sup>[51]</sup>. Several reports have implicated oxidative stress in D-GalN/LPS-induced ALF<sup>[52]</sup>. MDA is the end product of lipid peroxidation and the accumulation of ROS/RNS. It is also an excellent marker for oxidative stress<sup>[53]</sup>. The level of MDA and NO increased significantly in D-GalN/LPS-induced ALF rats as compared to normal control rats. The pretreatment with 20 and 40 mg/kg SA pretreatment substantially and dose-dependently curbed the oxidative stress as indicated by reduced MDA and NO levels. Therefore, SA might have potent antioxidant activity through its ability to inhibit ROS/RNS production induced by D-GalN/LPS. There are several reports that SA has potent antioxidant activity<sup>[3]</sup>. D-GalN/LPS-induced oxidative stress leads to the accumulation of hepatic lipid peroxides and the depletion of antioxidant enzymes such as GPx, SOD, and CAT.

D-GalN/LPS-induced ALF rats exhibit lower levels of GPx, SOD, and CAT as compared to normal control animals. SA (20 and 40 mg/kg) pretreatment significantly restored levels of GPx, SOD, and CAT in hepatic tissues, which is possibly an adaptive response to oxidative stress. SA has been previously shown to restore levels of GPx, SOD and CAT in a CCL4 and dimethyl nitrosamine-induced model of acute liver injury<sup>[23]</sup>. D-GalN/LPS-induced liver failure caused the production of TNF- $\alpha$  and IL-6, which triggered an inflammatory cascade in hepatocytes causing ALF<sup>[54,55]</sup>. Several natural polyphenols have been reported to prevent liver injuries<sup>[52,56]</sup>. Thus, levels of TNF- $\alpha$  and IL-6 in the liver were analyzed in the study. Pretreatment with SA reduced levels of these cytokines in a dose-dependent fashion. This finding may partially explain the hepatoprotective activity of SA. NF- $\kappa$ B is activated by D-GalN/LPS through the phosphorylation and degradation of I $\kappa$ B- $\alpha$ ; this allows NF- $\kappa$ B to translocate to the nucleus and increase the gene expression of cytokines such as TNF- $\alpha$  and IL-6<sup>[57]</sup>. Our data indicate that SA downregulated NF- $\kappa$ B activation by decreasing I $\kappa$ B- $\alpha$  degradation in a dose-dependent fashion.

Nrf2, a crucial transcription factor, controls these enzymes such as SOD, CAT, GPx, and HO-1 by binding to the elements of antioxidant response, inducing adaptive cytoprotective responses, and having a strong influence on the response to oxidative stress<sup>[58]</sup>. Several antioxidant genes are controlled by Nrf2. Upon activation by oxidative stress, Nrf2 translocates to the nucleus and binds to antioxidant transcription elements of Phase II to increase the expression of antioxidant genes<sup>[13,52,59]</sup>. The restoration of antioxidant enzymes SOD, CAT, GPx, and HO-1 and down regulation of TNF- $\alpha$  and IL-6 due to upregulation of NRF2 and down regulation of NF- $\kappa$ B indicates towards cytoprotective effect due to its antioxidant and antiinflammatory nature<sup>[58]</sup>. The data indicates SA mediates Nrf2 nucleus translocation as evident upregulation of NRF2 expression in nucleus that cause upregulation in antioxidant enzyme SOD, CAT, GPx, and HO-1 that performing a defending role against D-Gal/LPS induced inflammation and oxidative stress<sup>[58,60]</sup>. Down regulation of NRF2 is linked with



enhanced inflammation, while its upregulation reduces transcriptionally mediated NF- $\kappa$ B, pro-inflammatory and immune responses<sup>[44,61]</sup>. HO-1 is a rate-limiting enzyme that translates heme into equimolar amounts of iron, carbon monoxide, and biliverdin. HO-1 has cytoprotective and antioxidant activities and is activated in D-GalN/LPS-induced hepatitis<sup>[6,52]</sup>. The pretreatment of D-GalN/LPS-induced ALF rats with SA induced the expression of HO-1 through increased Nrf2 expression. Several studies have shown that there is a reduction in the expression of HO-1 and Nrf2 in D-GalN/LPS-induced ALF, which is similar to our results (Figure 2)<sup>[23,48,52]</sup>. Our data show that HO-1 and Nrf2 were downregulated in liver tissue after D-GalN/LPS administration, but SA pretreatment enhanced their expression in a dose-dependent manner. These outcomes showed that the Nrf2/HO-1 signaling pathways are implicated in the protective mechanism of SA. Apoptosis plays a key role in the pathogenesis of D-GalN/LPS-induced ALF<sup>[62]</sup>. Our data showed that D-GalN/LPS treatment may increase apoptotic and necrotic hepatocellular death through the upregulation of Bax and caspase-3 and the downregulation of Bcl-2. SA pretreatment significantly downregulates the expression of Bax and caspase-3 while upregulating Bcl2 in a dose-dependent manner, thus reducing apoptotic cell damage in hepatocytes. The aforesaid data is consistent with previously published studies<sup>[63,64]</sup>.

## CONCLUSION

This work demonstrated for the first time that the SA has hepatoprotective effects in the D-GalN/LPS-induced rat model through its ability to suppress oxidative stress, inflammation, and apoptosis. The protective mechanism of SA depends on the downregulation of NF- $\kappa$ B and the restoration of antioxidant enzyme levels through the activation of the Nrf2/HO-1 pathway. Thus, SA could be applied to treat or prevent D-GalN/LPS-induced ALF in the future (Figure 8).

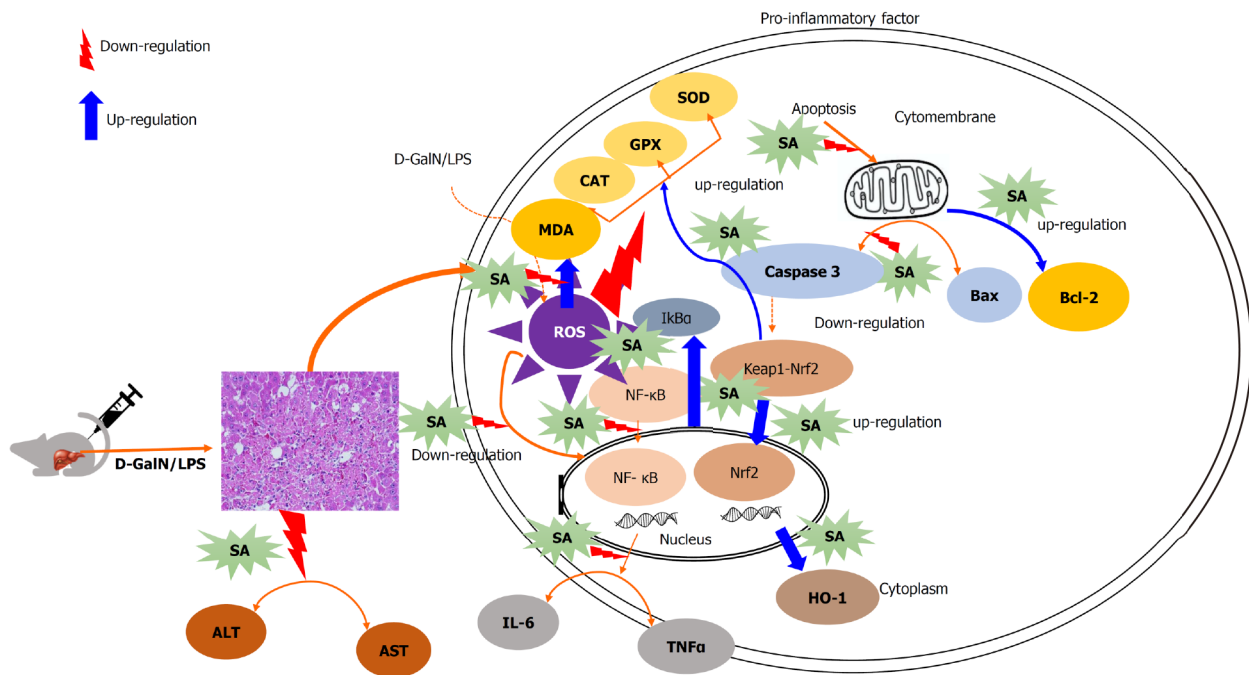


**Figure 8 Graphical abstract.** SA: Sinapic acid; D-GalN/LPS: D-galactosamine/lipopolysaccharide; ALT: Alanine transaminase; AST: Aspartate aminotransferase; TNF- $\alpha$ : Tumor necrosis factor- $\alpha$ ; IL-6: Interleukin 6; TGF- $\beta$ 1: Transforming growth factor- $\beta$ 1; HO-1: Heme oxygenase-1; Nrf2: Nuclear factor erythroid 2-related factor 2; I $\kappa$ B $\alpha$ : Nuclear factor of kappa light polypeptide gene enhancer in B cells inhibitor alpha; NF- $\kappa$ B: Nuclear factor kappa B; ROS: Reactive oxygen species; CAT: Catalase; MDA: Malondialdehyde; GPX: Glutathione peroxidase; SOD: Superoxide dismutase.

## ARTICLE HIGHLIGHTS

### Research background

Sinapic acid (SA) has been shown to have various pharmacological properties such as antioxidant, antifibrotic, anti-inflammatory, and anticancer activities. Its mechanism of action is dependent upon its ability to curb free radical production and protect against oxidative stress-induced tissue injuries.

### Research motivation

In the current study, the hepatoprotective effects of SA against lipopolysaccharide (LPS)/D-galactosamine (D-GalN)-induced acute liver failure (ALF) in rats were studied.

### Research objectives

In the current study, the hepatoprotective effects of SA against LPS/D-GalN-induced acute liver failure (ALF) in rats were studied.

### Research methods

Experimental ALF was induced with an intraperitoneal (i.p.) administration of 8  $\mu$ g LPS and 800 mg/kg D-GalN in normal saline. SA was administered orally once daily starting 7 d before LPS/D-GalN treatment.

### Research results

Data showed that SA ameliorates acute liver dysfunction, decreases serum levels of alanine transaminase (ALT), and aspartate aminotransferase (AST), as well as malondialdehyde (MDA) and NO levels in ALF model rats. However, pretreatment with SA (20 mg/kg and 40 mg/kg) reduced nuclear factor kappa-light-chain-enhancer of activated B cells (NF- $\kappa$ B) activation and levels of inflammatory cytokines (tumor necrosis factor- $\alpha$  and interleukin 6). Also, SA increased the activity of the nuclear factor erythroid-related factor 2/heme oxygenase-1 (Nrf2/HO-1) signaling pathway.

### Research conclusions

In conclusion, SA offers significant protection against LPS/D-GalN-induced ALF in rats by upregulating Nrf2/HO-1 and downregulating NF- $\kappa$ B.

### Research perspectives

The amolearation of LPS/D-GalN-induced fulminant hepatitis through NRF2/HO-1 activation have been previously documented. However, the hepatoprotective effects of SA in LPS/D-GalN-induced fulminant hepatitis has not been previously investigated. To identify the detailed mechanisms of action for SA, we tested its antioxidant and anti-inflammatory activities in a rat model of LPS/D-GalN-induced fulminant hepatitis. Thus, the purpose of the current study was to explore the underlying hepatoprotective mechanism of SA against LPS/D-GalN-induced ALF in rats. We also aimed to identify its effects on ROS production, inflammation and apoptosis and the roles of Nrf2/HO-1 and NF- $\kappa$ B pathways.

### ACKNOWLEDGEMENTS

The authors thank the Deanship of Scientific Research for the funding of this work through the Research Group Number, RG-1439-083 and RSSU for their technical support at King Saud University.

### REFERENCES

- 1 **Huang WY**, Cai YZ, Zhang Y. Natural phenolic compounds from medicinal herbs and dietary plants: potential use for cancer prevention. *Nutr Cancer* 2010; **62**: 1-20 [PMID: [20043255](#) DOI: [10.1080/01635580903191585](#)]
- 2 **Herrmann K**. Occurrence and content of hydroxycinnamic and hydroxybenzoic acid compounds in foods. *Crit Rev Food Sci Nutr* 1989; **28**: 315-347 [PMID: [2690858](#) DOI: [10.1080/10408398909527504](#)]
- 3 **Chen C**. Sinapic Acid and Its Derivatives as Medicine in Oxidative Stress-Induced Diseases and Aging. *Oxid Med Cell Longev* 2016; **2016**: 3571614 [PMID: [27069529](#) DOI: [10.1155/2016/3571614](#)]
- 4 **Ndekwe P**, Ghabril MS, Zang Y, Mann SA, Cummings OW, Lin J. Substantial hepatic necrosis is prognostic in fulminant liver failure. *World J Gastroenterol* 2017; **23**: 4303-4310 [PMID: [28694671](#) DOI: [10.3748/wjg.v23.i23.4303](#)]
- 5 **Rolando N**, Harvey F, Brahm J, Philpott-Howard J, Alexander G, Gimson A, Casewell M, Fagan E, Williams R. Prospective study of bacterial infection in acute liver failure: an analysis of fifty patients. *Hepatology* 1990; **11**: 49-53 [PMID: [2295471](#) DOI: [10.1002/hep.1840110110](#)]
- 6 **Wang YY**, Diao BZ, Zhong LH, Lu BL, Cheng Y, Yu L, Zhu LY. Maslinic acid protects against lipopolysaccharide/d-galactosamine-induced acute liver injury in mice. *Microb Pathog* 2018; **119**: 49-53 [PMID: [29627448](#) DOI: [10.1016/j.micpath.2018.04.002](#)]
- 7 **Yang X**, Fujisawa M, Yoshimura T, Ohara T, Sato M, Mino M, San TH, Gao T, Kunkel SL, Matsukawa A. Spred2 Deficiency Exacerbates D-Galactosamine/Lipopolysaccharide -induced Acute Liver Injury in Mice via Increased Production of TNF $\alpha$ . *Sci Rep* 2018; **8**: 188 [PMID: [29317674](#) DOI: [10.1038/s41598-017-18380-0](#)]
- 8 **Morikawa A**, Kato Y, Sugiyama T, Koide N, Chakravorty D, Yoshida T, Yokochi T. Role of nitric oxide in lipopolysaccharide-induced hepatic injury in D-galactosamine-sensitized mice as an experimental endotoxin shock model. *Infect Immun* 1999; **67**: 1018-1024 [PMID: [10024538](#) DOI: [10.1128/IAI.67.3.1018-1024.1999](#)]
- 9 **Tuñón MJ**, Alvarez M, Culebras JM, González-Gallego J. An overview of animal models for investigating the pathogenesis and therapeutic strategies in acute hepatic failure. *World J Gastroenterol* 2009; **15**: 3086-3098 [PMID: [19575487](#) DOI: [10.3748/wjg.15.3086](#)]
- 10 **Zhang L**, Li HZ, Gong X, Luo FL, Wang B, Hu N, Wang CD, Zhang Z, Wan JY. Protective effects of Asiaticoside on acute liver injury induced by lipopolysaccharide/D-galactosamine in mice. *Phytomedicine* 2010; **17**: 811-819 [PMID: [20171071](#) DOI: [10.1016/j.phymed.2010.01.008](#)]
- 11 **Sathivel A**, Balavinayagamani, Hanumantha Rao BR, Devaki T. Sulfated polysaccharide isolated from *Ulva lactuca* attenuates d-galactosamine induced DNA fragmentation and necrosis during liver damage in rats. *Pharm Biol* 2013; : [PMID: [24329421](#) DOI: [10.3109/13880209.2013.846915](#)]
- 12 **Hoek JB**, Pastorino JG. Ethanol, oxidative stress, and cytokine-induced liver cell injury. *Alcohol* 2002; **27**: 63-68 [PMID: [12062639](#) DOI: [10.1016/s0741-8329\(02\)00215-x](#)]
- 13 **Ma Q**. Role of nrf2 in oxidative stress and toxicity. *Annu Rev Pharmacol Toxicol* 2013; **53**: 401-426 [PMID: [23294312](#) DOI: [10.1146/annurev-pharmtox-011112-140320](#)]
- 14 **Li S**, Tan HY, Wang N, Zhang ZJ, Lao L, Wong CW, Feng Y. The Role of Oxidative Stress and Antioxidants in Liver Diseases. *Int J Mol Sci* 2015; **16**: 26087-26124 [PMID: [26540040](#) DOI: [10.3390/ijms161125942](#)]
- 15 **Vomhof-Dekrey EE**, Picklo MJ Sr. The Nrf2-antioxidant response element pathway: a target for regulating energy metabolism. *J Nutr Biochem* 2012; **23**: 1201-1206 [PMID: [22819548](#) DOI: [10.1016/j.jnutbio.2012.03.005](#)]
- 16 **Kobayashi M**, Yamamoto M. Nrf2-Keap1 regulation of cellular defense mechanisms against electrophiles and reactive oxygen species. *Adv Enzyme Regul* 2006; **46**: 113-140 [PMID: [16887173](#)]

- DOI: [10.1016/j.advenzreg.2006.01.007](https://doi.org/10.1016/j.advenzreg.2006.01.007)]
- 17 **Dreger H**, Westphal K, Wilck N, Baumann G, Stangl V, Stangl K, Meiners S. Protection of vascular cells from oxidative stress by proteasome inhibition depends on Nrf2. *Cardiovasc Res* 2010; **85**: 395-403 [PMID: [19679681](https://pubmed.ncbi.nlm.nih.gov/19679681/) DOI: [10.1093/cvr/cvp279](https://doi.org/10.1093/cvr/cvp279)]
  - 18 **Nioi P**, McMahon M, Itoh K, Yamamoto M, Hayes JD. Identification of a novel Nrf2-regulated antioxidant response element (ARE) in the mouse NAD(P)H:quinone oxidoreductase 1 gene: reassessment of the ARE consensus sequence. *Biochem J* 2003; **374**: 337-348 [PMID: [12816537](https://pubmed.ncbi.nlm.nih.gov/12816537/) DOI: [10.1042/BJ20030754](https://doi.org/10.1042/BJ20030754)]
  - 19 **Alam J**, Stewart D, Touchard C, Boinapally S, Choi AM, Cook JL. Nrf2, a Cap'n/Collar transcription factor, regulates induction of the heme oxygenase-1 gene. *J Biol Chem* 1999; **274**: 26071-26078 [PMID: [10473555](https://pubmed.ncbi.nlm.nih.gov/10473555/) DOI: [10.1074/jbc.274.37.26071](https://doi.org/10.1074/jbc.274.37.26071)]
  - 20 **Cichoż-Lach H**, Michalak A. Oxidative stress as a crucial factor in liver diseases. *World J Gastroenterol* 2014; **20**: 8082-8091 [PMID: [25009380](https://pubmed.ncbi.nlm.nih.gov/25009380/) DOI: [10.3748/wjg.v20.i25.8082](https://doi.org/10.3748/wjg.v20.i25.8082)]
  - 21 **Lingappan K**. NF-κB in Oxidative Stress. *Curr Opin Toxicol* 2018; **7**: 81-86 [PMID: [29862377](https://pubmed.ncbi.nlm.nih.gov/29862377/) DOI: [10.1016/j.cotox.2017.11.002](https://doi.org/10.1016/j.cotox.2017.11.002)]
  - 22 **Andreasen MF**, Landbo AK, Christensen LP, Hansen A, Meyer AS. Antioxidant effects of phenolic rye (*Secale cereale* L.) extracts, monomeric hydroxycinnamates, and ferulic acid dehydromers on human low-density lipoproteins. *J Agric Food Chem* 2001; **49**: 4090-4096 [PMID: [11513715](https://pubmed.ncbi.nlm.nih.gov/11513715/) DOI: [10.1021/jf0101758](https://doi.org/10.1021/jf0101758)]
  - 23 **Shin DS**, Kim KW, Chung HY, Yoon S, Moon JO. Effect of sinapic acid against dimethylnitrosamine-induced hepatic fibrosis in rats. *Arch Pharm Res* 2013; **36**: 608-618 [PMID: [23435910](https://pubmed.ncbi.nlm.nih.gov/23435910/) DOI: [10.1007/s12272-013-0033-6](https://doi.org/10.1007/s12272-013-0033-6)]
  - 24 **Niciforovic N**, Abramovic H. Sinapic Acid and Its Derivatives: Natural Sources and Bioactivity. *Compr Rev Food Sci Food Saf* 2014; **13**: 34-51 [DOI: [10.1111/1541-4337.12041](https://doi.org/10.1111/1541-4337.12041)]
  - 25 **Ansari MA**. Sinapic acid modulates Nrf2/HO-1 signaling pathway in cisplatin-induced nephrotoxicity in rats. *Biomed Pharmacother* 2017; **93**: 646-653 [PMID: [28686978](https://pubmed.ncbi.nlm.nih.gov/28686978/) DOI: [10.1016/j.biopha.2017.06.085](https://doi.org/10.1016/j.biopha.2017.06.085)]
  - 26 **Raish M**, Ahmad A, Ahmad Ansari M, Ahad A, Al-Jenoobi FI, Al-Mohizea AM, Khan A, Ali N. Sinapic acid ameliorates bleomycin-induced lung fibrosis in rats. *Biomed Pharmacother* 2018; **108**: 224-231 [PMID: [30219680](https://pubmed.ncbi.nlm.nih.gov/30219680/) DOI: [10.1016/j.biopha.2018.09.032](https://doi.org/10.1016/j.biopha.2018.09.032)]
  - 27 **Li X**, Lin J, Ding X, Xuan J, Hu Z, Wu D, Zhu X, Feng Z, Ni W, Wu A. The protective effect of sinapic acid in osteoarthritis: In vitro and in vivo studies. *J Cell Mol Med* 2019; **23**: 1940-1950 [PMID: [30604480](https://pubmed.ncbi.nlm.nih.gov/30604480/) DOI: [10.1111/jcmm.14096](https://doi.org/10.1111/jcmm.14096)]
  - 28 **Scapagnini G**, Vasto S, Abraham NG, Caruso C, Zella D, Fabio G. Modulation of Nrf2/ARE pathway by food polyphenols: a nutritional neuroprotective strategy for cognitive and neurodegenerative disorders. *Mol Neurobiol* 2011; **44**: 192-201 [PMID: [21499987](https://pubmed.ncbi.nlm.nih.gov/21499987/) DOI: [10.1007/s12035-011-8181-5](https://doi.org/10.1007/s12035-011-8181-5)]
  - 29 **Ansari MA**, Raish M, Ahmad A, Alkharfy KM, Ahmad SF, Attia SM, Alsaad AMS, Bakheet SA. Sinapic acid ameliorate cadmium-induced nephrotoxicity: In vivo possible involvement of oxidative stress, apoptosis, and inflammation via NF-κB downregulation. *Environ Toxicol Pharmacol* 2017; **51**: 100-107 [PMID: [28233699](https://pubmed.ncbi.nlm.nih.gov/28233699/) DOI: [10.1016/j.etap.2017.02.014](https://doi.org/10.1016/j.etap.2017.02.014)]
  - 30 **Luo JF**, Shen XY, Lio CK, Dai Y, Cheng CS, Liu JX, Yao YD, Yu Y, Xie Y, Luo P, Yao XS, Liu ZQ, Zhou H. Activation of Nrf2/HO-1 Pathway by Nardochinoid C Inhibits Inflammation and Oxidative Stress in Lipopolysaccharide-Stimulated Macrophages. *Front Pharmacol* 2018; **9**: 911 [PMID: [30233360](https://pubmed.ncbi.nlm.nih.gov/30233360/) DOI: [10.3389/fphar.2018.00911](https://doi.org/10.3389/fphar.2018.00911)]
  - 31 **Lim DW**, Choi HJ, Park SD, Kim H, Yu GR, Kim JE, Park WH. Activation of the Nrf2/HO-1 Pathway by *Amomum villosum* Extract Suppresses LPS-Induced Oxidative Stress *In Vitro* and *Ex Vivo*. *Evid Based Complement Alternat Med* 2020; **2020**: 2837853 [PMID: [32454852](https://pubmed.ncbi.nlm.nih.gov/32454852/) DOI: [10.1155/2020/2837853](https://doi.org/10.1155/2020/2837853)]
  - 32 **Lv H**, Yang H, Wang Z, Feng H, Deng X, Cheng G, Ci X. Nrf2 signaling and autophagy are complementary in protecting lipopolysaccharide/d-galactosamine-induced acute liver injury by licochalcone A. *Cell Death Dis* 2019; **10**: 313 [PMID: [30952839](https://pubmed.ncbi.nlm.nih.gov/30952839/) DOI: [10.1038/s41419-019-1543-z](https://doi.org/10.1038/s41419-019-1543-z)]
  - 33 **Cherng YG**, Tsai CC, Chung HH, Lai YW, Kuo SC, Cheng JT. Antihyperglycemic action of sinapic acid in diabetic rats. *J Agric Food Chem* 2013; **61**: 12053-12059 [PMID: [24261449](https://pubmed.ncbi.nlm.nih.gov/24261449/) DOI: [10.1021/jf403092b](https://doi.org/10.1021/jf403092b)]
  - 34 **Smith PK**, Krohn RI, Hermanson GT, Mallia AK, Gartner FH, Provenzano MD, Fujimoto EK, Goeke NM, Olson BJ, Klenk DC. Measurement of protein using bicinchoninic acid. *Anal Biochem* 1985; **150**: 76-85 [PMID: [3843705](https://pubmed.ncbi.nlm.nih.gov/3843705/) DOI: [10.1016/0003-2697\(85\)90442-7](https://doi.org/10.1016/0003-2697(85)90442-7)]
  - 35 **Towbin H**, Staehelin T, Gordon J. Electrophoretic transfer of proteins from polyacrylamide gels to nitrocellulose sheets: procedure and some applications. *Proc Natl Acad Sci USA* 1979; **76**: 4350-4354 [PMID: [388439](https://pubmed.ncbi.nlm.nih.gov/388439/) DOI: [10.1073/pnas.76.9.4350](https://doi.org/10.1073/pnas.76.9.4350)]
  - 36 **Galanos C**, Freudenberg MA, Reutter W. Galactosamine-induced sensitization to the lethal effects of endotoxin. *Proc Natl Acad Sci USA* 1979; **76**: 5939-5943 [PMID: [293694](https://pubmed.ncbi.nlm.nih.gov/293694/) DOI: [10.1073/pnas.76.11.5939](https://doi.org/10.1073/pnas.76.11.5939)]
  - 37 **Silverstein R**. D-galactosamine lethality model: scope and limitations. *J Endotoxin Res* 2004; **10**: 147-162 [PMID: [15198850](https://pubmed.ncbi.nlm.nih.gov/15198850/) DOI: [10.1179/096805104225004879](https://doi.org/10.1179/096805104225004879)]
  - 38 **Johnston DE**. Special considerations in interpreting liver function tests. *Am Fam Physician* 1999; **59**: 2223-2230 [PMID: [10221307](https://pubmed.ncbi.nlm.nih.gov/10221307/)]
  - 39 **McGill MR**. The past and present of serum aminotransferases and the future of liver injury

- biomarkers. *EXCLI J* 2016; **15**: 817-828 [PMID: [28337112](#) DOI: [10.17179/excli2016-800](#)]
- 40 **Gowda S**, Desai PB, Hull VV, Math AA, Vernekar SN, Kulkarni SS. A review on laboratory liver function tests. *Pan Afr Med J* 2009; **3**: 17 [PMID: [21532726](#)]
  - 41 **George J**, Rao KR, Stern R, Chandrakasan G. Dimethylnitrosamine-induced liver injury in rats: the early deposition of collagen. *Toxicology* 2001; **156**: 129-138 [PMID: [11164615](#) DOI: [10.1016/s0300-483x\(00\)00352-8](#)]
  - 42 **Valenzuela R**, Videla LA. Impact of the Co-Administration of N-3 Fatty Acids and Olive Oil Components in Preclinical Nonalcoholic Fatty Liver Disease Models: A Mechanistic View. *Nutrients* 2020; **12** [PMID: [32075238](#) DOI: [10.3390/nu12020499](#)]
  - 43 **Brinkkoetter PT**, Song H, Lösel R, Schnetzke U, Gottmann U, Feng Y, Hanusch C, Beck GC, Schnuelle P, Wehling M, van der Woude FJ, Yard BA. Hypothermic injury: the mitochondrial calcium, ATP and ROS love-hate triangle out of balance. *Cell Physiol Biochem* 2008; **22**: 195-204 [PMID: [18769046](#) DOI: [10.1159/000149797](#)]
  - 44 **Valenzuela R**, Illesca P, Echeverría F, Espinosa A, Rincón-Cervera MÁ, Ortiz M, Hernandez-Rodas MC, Valenzuela A, Videla LA. Molecular adaptations underlying the beneficial effects of hydroxytyrosol in the pathogenic alterations induced by a high-fat diet in mouse liver: PPAR- $\alpha$  and Nrf2 activation, and NF- $\kappa$ B down-regulation. *Food Funct* 2017; **8**: 1526-1537 [PMID: [28386616](#) DOI: [10.1039/c7fo00090a](#)]
  - 45 **Ortiz M**, Soto-Alarcón SA, Orellana P, Espinosa A, Campos C, López-Arana S, Rincón MA, Illesca P, Valenzuela R, Videla LA. Suppression of high-fat diet-induced obesity-associated liver mitochondrial dysfunction by docosahexaenoic acid and hydroxytyrosol co-administration. *Dig Liver Dis* 2020; **52**: 895-904 [PMID: [32620521](#) DOI: [10.1016/j.dld.2020.04.019](#)]
  - 46 **Pessayre D**, Fromenty B, Berson A, Robin MA, Lettéron P, Moreau R, Mansouri A. Central role of mitochondria in drug-induced liver injury. *Drug Metab Rev* 2012; **44**: 34-87 [PMID: [21892896](#) DOI: [10.3109/03602532.2011.604086](#)]
  - 47 **McGill MR**, Sharpe MR, Williams CD, Taha M, Curry SC, Jaeschke H. The mechanism underlying acetaminophen-induced hepatotoxicity in humans and mice involves mitochondrial damage and nuclear DNA fragmentation. *J Clin Invest* 2012; **122**: 1574-1583 [PMID: [22378043](#) DOI: [10.1172/JCI59755](#)]
  - 48 **Sayed RH**, Khalil WK, Salem HA, Kenawy SA, El-Sayeh BM. Sulforaphane increases the survival rate in rats with fulminant hepatic failure induced by D-galactosamine and lipopolysaccharide. *Nutr Res* 2014; **34**: 982-989 [PMID: [25439027](#) DOI: [10.1016/j.nutres.2014.10.003](#)]
  - 49 **Lundgren CAK**, Sjöstrand D, Biner O, Bennett M, Rudling A, Johansson AL, Brzezinski P, Carlsson J, von Ballmoos C, Högbom M. Scavenging of superoxide by a membrane-bound superoxide oxidase. *Nat Chem Biol* 2018; **14**: 788-793 [PMID: [29915379](#) DOI: [10.1038/s41589-018-0072-x](#)]
  - 50 **Que X**, Hung MY, Yeang C, Gonen A, Prohaska TA, Sun X, Diehl C, Määttä A, Gaddis DE, Bowden K, Pattison J, MacDonald JG, Ylä-Herttuala S, Mellon PL, Hedrick CC, Ley K, Miller YI, Glass CK, Peterson KL, Binder CJ, Tsimikas S, Witztum JL. Oxidized phospholipids are proinflammatory and proatherogenic in hypercholesterolaemic mice. *Nature* 2018; **558**: 301-306 [PMID: [29875409](#) DOI: [10.1038/s41586-018-0198-8](#)]
  - 51 **Jaeschke H**, Farhood A. Neutrophil and Kupffer cell-induced oxidant stress and ischemia-reperfusion injury in rat liver. *Am J Physiol* 1991; **260**: G355-G362 [PMID: [2003603](#) DOI: [10.1152/ajpgi.1991.260.3.G355](#)]
  - 52 **Xie YL**, Chu JG, Jian XM, Dong JZ, Wang LP, Li GX, Yang NB. Curcumin attenuates lipopolysaccharide/d-galactosamine-induced acute liver injury by activating Nrf2 nuclear translocation and inhibiting NF- $\kappa$ B activation. *Biomed Pharmacother* 2017; **91**: 70-77 [PMID: [28448872](#) DOI: [10.1016/j.biopha.2017.04.070](#)]
  - 53 **Diesen DL**, Kuo PC. Nitric oxide and redox regulation in the liver: Part I. General considerations and redox biology in hepatitis. *J Surg Res* 2010; **162**: 95-109 [PMID: [20444470](#) DOI: [10.1016/j.jss.2009.09.019](#)]
  - 54 **Nakama T**, Hirono S, Moriuchi A, Hasuike S, Nagata K, Hori T, Ido A, Hayashi K, Tsubouchi H. Etoposide prevents apoptosis in mouse liver with D-galactosamine/lipopolysaccharide-induced fulminant hepatic failure resulting in reduction of lethality. *Hepatology* 2001; **33**: 1441-1450 [PMID: [11391533](#) DOI: [10.1053/jhep.2001.24561](#)]
  - 55 **Pathil A**, Warth A, Chamulitrat W, Stremmel W. The synthetic bile acid-phospholipid conjugate ursodeoxycholyl lysophosphatidylethanolamide suppresses TNF $\alpha$ -induced liver injury. *J Hepatol* 2011; **54**: 674-684 [PMID: [21146893](#) DOI: [10.1016/j.jhep.2010.07.028](#)]
  - 56 **Zhou RJ**, Zhao Y, Fan K, Xie ML. Protective effect of apigenin on d-galactosamine/LPS-induced hepatocellular injury by increment of Nrf-2 nucleus translocation. *Naunyn Schmiedeberg's Arch Pharmacol* 2020; **393**: 929-936 [PMID: [31758207](#) DOI: [10.1007/s00210-019-01760-w](#)]
  - 57 **Gilmore TD**. Introduction to NF- $\kappa$ B: players, pathways, perspectives. *Oncogene* 2006; **25**: 6680-6684 [PMID: [17072321](#) DOI: [10.1038/sj.onc.1209954](#)]
  - 58 **Soto-Alarcón SA**, Ortiz M, Orellana P, Echeverría F, Bustamante A, Espinosa A, Illesca P, Gonzalez-Mañán D, Valenzuela R, Videla LA. Docosahexaenoic acid and hydroxytyrosol co-administration fully prevents liver steatosis and related parameters in mice subjected to high-fat diet: A molecular approach. *Biofactors* 2019; **45**: 930-943 [PMID: [31454114](#) DOI: [10.1002/biof.1556](#)]
  - 59 **Wang W**, Zhang Y, Li H, Zhao Y, Cai E, Zhu H, Li P, Liu J. Protective Effects of Sesquiterpenoids from the Root of Panax ginseng on Fulminant Liver Injury Induced by Lipopolysaccharide/d-Galactosamine. *J Agric Food Chem* 2018; **66**: 7758-7763 [PMID: [29974747](#) DOI: [10.1021/acs.jafc.8b00000](#)]



- 10.1021/acs.jafc.8b02627]
- 60 **Wen T**, Wu ZM, Liu Y, Tan YF, Ren F, Wu H. Upregulation of heme oxygenase-1 with hemin prevents D-galactosamine and lipopolysaccharide-induced acute hepatic injury in rats. *Toxicology* 2007; **237**: 184-193 [PMID: [17587481](#) DOI: [10.1016/j.tox.2007.05.014](#)]
- 61 **Wardyn JD**, Ponsford AH, Sanderson CM. Dissecting molecular cross-talk between Nrf2 and NF- $\kappa$ B response pathways. *Biochem Soc Trans* 2015; **43**: 621-626 [PMID: [26551702](#) DOI: [10.1042/BST20150014](#)]
- 62 **Gao K**, Liu F, Chen X, Chen M, Deng Q, Zou X, Guo H. Crocetin protects against fulminant hepatic failure induced by lipopolysaccharide/D-galactosamine by decreasing apoptosis, inflammation and oxidative stress in a rat model. *Exp Ther Med* 2019; **18**: 3775-3782 [PMID: [31616509](#) DOI: [10.3892/etm.2019.8030](#)]
- 63 **Zhang Z**, Tian L, Jiang K. Propofol attenuates inflammatory response and apoptosis to protect d-galactosamine/lipopolysaccharide induced acute liver injury via regulating TLR4/NF- $\kappa$ B/NLRP3 pathway. *Int Immunopharmacol* 2019; **77**: 105974 [PMID: [31735662](#) DOI: [10.1016/j.intimp.2019.105974](#)]
- 64 **Wu YL**, Lian LH, Wan Y, Nan JX. Baicalein inhibits nuclear factor- $\kappa$ B and apoptosis via c-FLIP and MAPK in D-GalN/LPS induced acute liver failure in murine models. *Chem Biol Interact* 2010; **188**: 526-534 [PMID: [20850421](#) DOI: [10.1016/j.cbi.2010.09.008](#)]



## Clinical and Translational Research

# Quantitative multiparametric magnetic resonance imaging can aid non-alcoholic steatohepatitis diagnosis in a Japanese cohort

Kento Imajo, Louise Tetlow, Andrea Dennis, Elizabeth Shumbayawonda, Sofia Mouchti, Timothy J Kendall, Eve Fryer, Shogi Yamanaka, Yasushi Honda, Takaomi Kessoku, Yuji Ogawa, Masato Yoneda, Satoru Saito, Catherine Kelly, Matt D Kelly, Rajarshi Banerjee, Atsushi Nakajima

**ORCID number:** Kento Imajo 0000-0002-1931-6326; Louise Tetlow 0000-0001-6285-4878; Andrea Dennis 0000-0002-0152-6528; Elizabeth Shumbayawonda 0000-0003-0351-2063; Sofia Mouchti 0000-0002-3169-5242; Timothy J Kendall 0000-0002-4174-2786; Eve Fryer 0000-0003-1385-6433; Shogi Yamanaka 0000-0001-8882-3981; Yasushi Honda 0000-0002-1624-5462; Takaomi Kessoku 0000-0002-5587-1386; Yuji Ogawa 0000-0001-7033-088X; Masato Yoneda 0000-0001-7815-549X; Satoru Saito 0000-0002-5666-5218; Catherine Kelly 0000-0002-5834-1234; Matt D Kelly 0000-0002-5834-635X; Rajarshi Banerjee 0000-0003-2022-5218; Atsushi Nakajima 0000-0002-6263-1436.

**Author contributions:** Imajo K and Nakajima A developed the study concept, protocols and initiated the project; Kelly MD and Banerjee R assisted in the further development of the protocol and drafting the clinical study protocol; Imajo K, Nakajima A, Fryer E, Kendall TJ, Yamanaka S, Honda Y, Kessoku T, Ogawa Y, Yoneda M and Saito S contributed to the data collection; Tetlow L, Dennis AM, Shumbayawonda E to the data analysis; Imajo K, Tetlow L, Nakajima A, Dennis AM, Shumbayawonda E, Kelly C, Kelly

**Kento Imajo, Yasushi Honda, Takaomi Kessoku, Yuji Ogawa, Satoru Saito, Atsushi Nakajima,** Department of Gastroenterology and Hepatology, Yokohama City University School of Medicine, Yokohama 236-0004, Japan

**Louise Tetlow, Andrea Dennis, Elizabeth Shumbayawonda, Sofia Mouchti, Catherine Kelly, Matt D Kelly, Rajarshi Banerjee,** Innovation, Perspectum, Oxford OX4 2LL, United Kingdom

**Timothy J Kendall,** Centre for Inflammation Research, University of Edinburgh, Edinburgh, United Kingdom, Edinburgh EH16 4TJ, United Kingdom

**Eve Fryer,** Department of Cellular Pathology, Oxford University Hospitals NHS Foundation Trust, Oxford OX3 9DU, United Kingdom

**Shogi Yamanaka,** Anatomic and Clinical Pathology Department, Yokohama City University Hospital, Yokohama 236-0004, Japan

**Masato Yoneda,** Department of Gastroenterology, Yokohama City University Graduate School of Medicine, Yokohama 236-0004, Japan

**Corresponding author:** Andrea Dennis, PhD, Research Scientist, Innovation, Perspectum, Gemini One, 5520 John Smith Drive, Oxford OX4 2LL, United Kingdom.  
[andrea.dennis@perspectum.com](mailto:andrea.dennis@perspectum.com)

## Abstract

### BACKGROUND

Non-invasive assessment of non-alcoholic steatohepatitis (NASH) is increasing in desirability due to the invasive nature and costs associated with the current form of assessment; liver biopsy. Quantitative multiparametric magnetic resonance imaging (mpMRI) to measure liver fat (proton density fat fraction) and fibroinflammatory disease [iron-corrected T1 (cT1)], as well as elastography techniques [vibration-controlled transient elastography (VCTE) liver stiffness measure], magnetic resonance elastography (MRE) and 2D Shear-Wave elastography (SWE) to measure stiffness and fat (controlled attenuated parameter, CAP) are emerging alternatives which could be utilised as safe surrogates to liver biopsy.

MD and Banerjee R drafted and completed the manuscript. All authors contributed to the final manuscript.

#### Institutional review board

**statement:** The study was conducted in accordance with the ethical principles of the Declaration of Helsinki 2013, was approved by the Ethics Committee of Yokohama City University Hospital and was registered as a clinical trial (UMIN Clinical Trials Registry: UMIN000026145).

#### Conflict-of-interest statement:

Perspectum Ltd is a privately funded commercial enterprise that develops medical devices to address unmet clinical needs, including LiverMultiScan®. LT, ES, AD, MK are all employees of Perspectum. RB is CEO of Perspectum. KI, and AN have no relevant disclosures to this study. TK and EF undertake consultancy work for Perspectum.

**Data sharing statement:** No additional data are available.

**Open-Access:** This article is an open-access article that was selected by an in-house editor and fully peer-reviewed by external reviewers. It is distributed in accordance with the Creative Commons Attribution NonCommercial (CC BY-NC 4.0) license, which permits others to distribute, remix, adapt, build upon this work non-commercially, and license their derivative works on different terms, provided the original work is properly cited and the use is non-commercial. See: <http://creativecommons.org/licenses/by-nc/4.0/>

**Manuscript source:** Unsolicited manuscript

**Specialty type:** Gastroenterology and hepatology

**Country/Territory of origin:** Japan

**Peer-review report's scientific quality classification**

Grade A (Excellent): A  
Grade B (Very good): B  
Grade C (Good): C

## AIM

To evaluate the agreement of non-invasive imaging modalities with liver biopsy, and their subsequent diagnostic accuracy for identifying NASH patients.

## METHODS

From January 2019 to February 2020, Japanese patients suspected of NASH were recruited onto a prospective, observational study and were screened using non-invasive imaging techniques; mpMRI with LiverMultiScan®, VCTE, MRE and 2D-SWE. Patients were subsequently biopsied, and samples were scored by three independent pathologists. The diagnostic performances of the non-invasive imaging modalities were assessed using area under receiver operating characteristic curve (AUC) with the median of the histology scores as the gold standard diagnoses. Concordance between all three independent pathologists was further explored using Krippendorff's alpha ( $\alpha$ ) from weighted kappa statistics.

## RESULTS

$N = 145$  patients with mean age of 60 (SD: 13 years.), 39% females, and 40% with body mass index  $\geq 30$  kg/m<sup>2</sup> were included in the analysis. For identifying patients with NASH, MR liver fat and cT1 were the strongest performing individual measures (AUC: 0.80 and 0.75 respectively), and the mpMRI metrics combined (cT1 and MR liver fat) were the overall best non-invasive test (AUC: 0.83). For identifying fibrosis  $\geq 1$ , MRE performed best (AUC: 0.97), compared to VCTE-liver stiffness measure (AUC: 0.94) and 2D-SWE (AUC: 0.94). For assessment of steatosis  $\geq 1$ , MR liver fat was the best performing non-invasive test (AUC: 0.92), compared to controlled attenuated parameter (AUC: 0.75). Assessment of the agreement between pathologists showed that concordance was best for steatosis ( $\alpha = 0.58$ ), moderate for ballooning ( $\alpha = 0.40$ ) and fibrosis ( $\alpha = 0.40$ ), and worst for lobular inflammation ( $\alpha = 0.11$ ).

## CONCLUSION

Quantitative mpMRI is an effective alternative to liver biopsy for diagnosing NASH and non-alcoholic fatty liver, and thus may offer clinical utility in patient management.

**Key Words:** Corrected T1; Fibro-inflammation; Non-invasive imaging; Non-alcoholic steatohepatitis; Multiparametric magnetic resonance imaging; Non-alcoholic fatty liver disease

©The Author(s) 2021. Published by Baishideng Publishing Group Inc. All rights reserved.

**Core Tip:** There is growing interest in the utility of non-invasive tests in the management of non-alcoholic steatohepatitis (NASH). We explored how magnetic resonance imaging technology can stratify patients with simple fatty liver disease from those with NASH. Our results showed that quantitative magnetic resonance imaging derived metrics showed the strongest correlations to the histological pathological components of NASH with very few technical failures. We also observed very high levels of inter-reader disagreement in histopathological biopsy reads, highlighting the pressing need for alternative diagnostic tests for NASH. Our work therefore supports the use of this non-invasive technology in day-to-day practice.

**Citation:** Imajo K, Tetlow L, Dennis A, Shumbayawonda E, Mouchti S, Kendall TJ, Fryer E, Yamanaka S, Honda Y, Kessoku T, Ogawa Y, Yoneda M, Saito S, Kelly C, Kelly MD, Banerjee R, Nakajima A. Quantitative multiparametric magnetic resonance imaging can aid non-alcoholic steatohepatitis diagnosis in a Japanese cohort. *World J Gastroenterol* 2021; 27(7): 609-623

**URL:** <https://www.wjgnet.com/1007-9327/full/v27/i7/609.htm>

**DOI:** <https://dx.doi.org/10.3748/wjg.v27.i7.609>

Grade D (Fair): 0

Grade E (Poor): 0

**Received:** August 28, 2020**Peer-review started:** August 28, 2020**First decision:** November 3, 2020**Revised:** November 17, 2020**Accepted:** December 28, 2020**Article in press:** December 28, 2020**Published online:** February 21, 2021**P-Reviewer:** Lei YC, Xu CF, Wu B**S-Editor:** Zhang H**L-Editor:** A**P-Editor:** Wang LL

## INTRODUCTION

Non-alcoholic fatty liver disease (NAFLD) is the most common cause of chronic liver disease, affecting approximately 25% of the general population worldwide<sup>[1]</sup> and up to 30% of the general population in Japan<sup>[2]</sup>. Additionally, up to 19% of individuals in south east Asia with body mass index (BMI)  $\leq 25$  kg/m<sup>2</sup> have “lean” or “non-obese” NAFLD<sup>[3,4]</sup>. The scope of disease aetiologies within NAFLD differ in both clinical significance and prognosis<sup>[1,5-7]</sup> on a continuum that encompasses “simple steatosis” or NAFL (hepatic steatosis without inflammation), to non-alcoholic steatohepatitis (NASH) and NASH cirrhosis. NASH results when fat accumulation in the liver triggers inflammatory signals and reactive oxygen species that can amplify liver injury and stimulate fibrosis<sup>[8]</sup>. NASH is predicted to become the leading cause of liver transplant over the coming decade<sup>[1]</sup> as NASH patients have a greater tendency to develop advanced liver fibrosis, cirrhosis, and hepatocellular carcinoma<sup>[9-11]</sup>.

Liver biopsy is the current gold standard for differentiating simple steatosis from NASH as well as staging the severity of fibrosis in patients with NAFLD<sup>[12]</sup>. However, due to the limitations associated with biopsy<sup>[13]</sup>, high procedure costs, high levels of discordance between readers, and poor acceptability by patients, there has been an increase in the use of non-invasive imaging biomarkers to diagnose and monitor the disease.

Vendor-neutral and scalable multiparametric magnetic resonance imaging (mpMRI) measurements of liver fat proton density fat fraction (PDFF) with IDEAL and iron corrected T1-mapping (cT1) are emerging as promising quantitative imaging biomarkers for NASH. MRI liver fat correlates strongly with histologically graded steatosis across the clinical range seen in NASH<sup>[14]</sup> and has high diagnostic accuracy in stratifying all grades of liver steatosis<sup>[15-17]</sup>. cT1 correlates with ballooning<sup>[18]</sup>, and has been shown to predict clinical outcomes in patients with chronic liver disease<sup>[19,20]</sup>. Both metrics have good technical validity with high repeatability and reproducibility across MRI manufacturers and field strengths<sup>[21]</sup>. Additionally, due to their sensitivity to subtle changes in hepatic fat and fibro-inflammation, mpMRI techniques are increasingly used as inclusion criteria endpoints in NASH clinical trials and are included in the FDA Biomarker Qualification Program.

Magnetic resonance elastography (MRE) is an alternative MR based approach that can be used to stage fibrosis. MRE has shown utility in identifying patients with NASH from those with simple steatosis<sup>[22]</sup> whilst also being able to detect the presence of advanced fibrosis in patients with chronic liver disease<sup>[23]</sup>. However, MRE has not demonstrated sufficient utility for the longitudinal monitoring of fibrosis progression or regression<sup>[14,24]</sup>.

Ultrasound based methods such as vibration-controlled transient elastography (VCTE) liver stiffness measure (LSM) have shown good utility in identifying patients with advanced fibrosis<sup>[25,26]</sup>, however they may be less reliable in patients who are morbidly obese; a high-risk group for NASH<sup>[25]</sup>. VCTE controlled-attenuation parameter (CAP) has been shown to be sensitive to early changes in liver fat albeit with a low ability to differentiate steatosis levels.

The aim of this study was to evaluate the diagnostic performance of quantitative mpMRI, MRE, and transient elastography (VCTE and 2D shear-wave elastography) to identify patients with suspected NASH and to report on the correlations between these non-invasive technologies and histology.

## MATERIALS AND METHODS

This was an observational trial conducted and sponsored by the Yokohama City University Hospital between January 2019 and February 2020.  $N = 151$  adult participants who underwent a liver biopsy for suspected NASH were included in this interim analysis. Participants were invited to undergo core liver biopsy if there was evidence of steatosis (Proton density fat fraction  $\geq 5.2\%$  or CAP  $\geq 236$ )<sup>[16]</sup>. Patients were excluded if there was contraindication to MRI, history of alcoholism, or evidence of other chronic liver disease (Figure 1). The study was conducted in accordance with the ethical principles of the Declaration of Helsinki 2013, was approved by the Ethics Committee of Yokohama City University Hospital and was registered as a clinical trial (UMIN Clinical Trials Registry: UMIN000026145).

### Histopathological evaluations

Liver biopsy samples were obtained using a 16-gauge needle biopsy kit with an

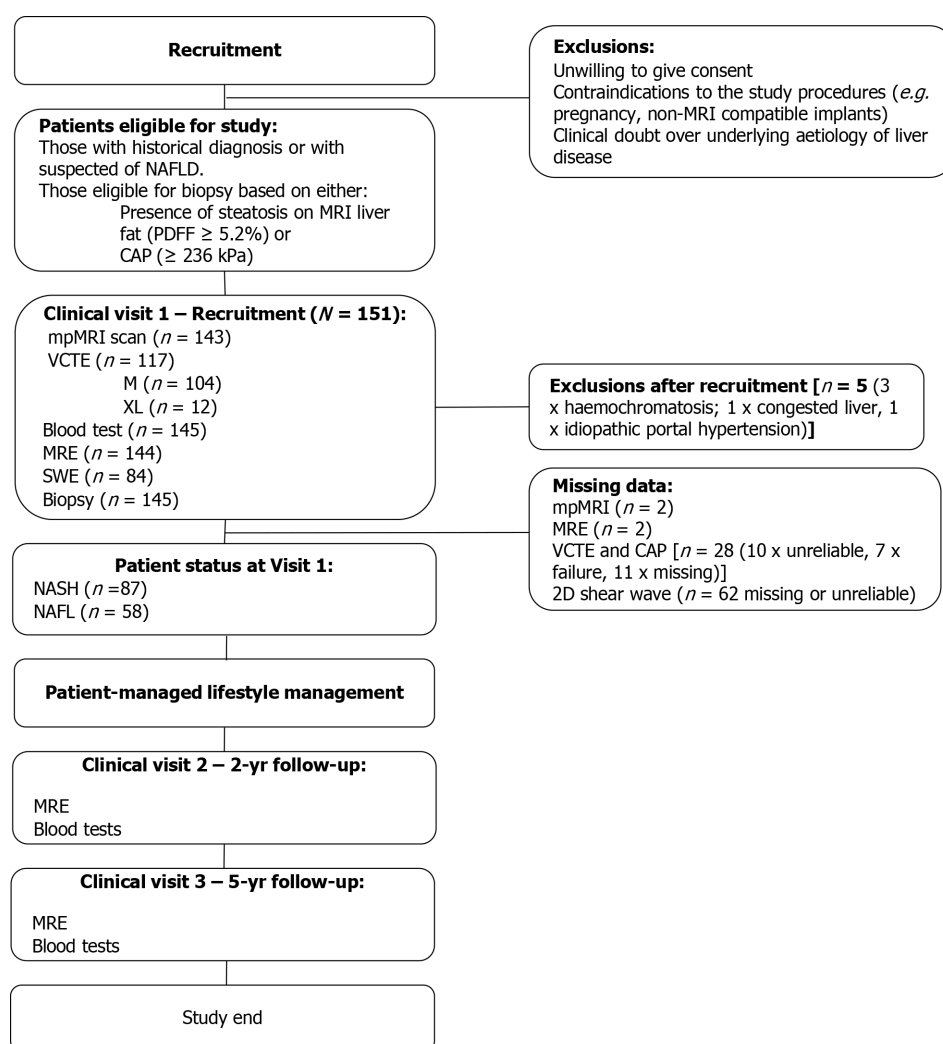


**Figure 1 CONSORT diagram of patient pathway and inclusion into the study.** mpMRI: Quantitative multiparametric magnetic resonance imaging; CAP: Controlled-attenuation parameter; MRE: Magnetic resonance elastography; NASH: Non-alcoholic steatohepatitis; NAFLD: Non-alcoholic fatty liver disease; VCTE: Vibration-controlled transient elastography.

adequate liver biopsy defined as being  $\geq 20$  mm in length and/or with  $\geq 10$  portal tracts. Biopsy samples were assessed independently by three histopathologists, one at YCUH at the time of collection and then later by a further two pathologists using digitalised biopsy slides. Histological scoring of fibrosis, steatosis, lobular inflammation, and hepatocyte ballooning was performed by all pathologists, and overall disease activity was graded according to the NAFLD activity score [NASH Clinical Research Network (NAS)]. NASH was defined as NAS  $\geq 4$ , ballooning  $\geq 1$  and inflammation  $\geq 1$  as described in AASLD guidelines<sup>[12]</sup>. All scores were taken from the median score for each component from the three pathologists.

### Non-invasive biomarkers

MR liver fat and cT1 measurements were made using the non-contrast LiverMultiScan® mpMRI protocol (Perspectum, Oxford, United Kingdom), performed with the patient in the supine position using a 3 Tesla GE Discovery 750W scanner system (GE Healthcare, Milwaukee, WI, United States). The average scan time for this protocol was 10 min. Four single transverse slices were captured through the liver centered on the porta hepatis. Anonymised mpMRI data were analysed off-site by image analysts trained in abdominal anatomy and artefact detection, who were blinded to the clinical data and risk grouping. For MR liver fat, three 15 mm diameter circular regions of interest (ROIs) were selected on the transverse maps to cover a representative sample of the liver parenchyma. For cT1 (ms), three ROIs were placed on the central slice within the typical percutaneous biopsy region. Median values from all pixels within the ROIs were calculated and used as the representative score.

MRE examinations were performed using the same MRI scanner and following a 2-



dimensional MRE protocol<sup>[27]</sup>. Interpretation of MRE images to obtain stiffness values was performed by abdominal radiologists<sup>[22]</sup>. VCTE-LSMs were obtained by one operator using either 3.5 MHz M-probe and/or 2.5 MHz XL-probe dependent upon suitability (waist-hip circumference and BMI) and through use of the automatic probe selection tool embedded within the Fibroscan operating software<sup>[28]</sup>. VCTE-LSM measures with at least 10 valid shots and a success rate of  $\geq 60\%$  were considered reliable and used for statistical analysis. Hepatic steatosis was assessed using the CAP value provided by the device. 2D shear-wave elastography (2D-SWE) measurements were obtained using a Logiq S8 system (GE Healthcare)<sup>[29]</sup>. Example images are shown in [Figure 2](#) for all methods.

### Statistical analysis

Descriptive statistics were used to summarise baseline participant characteristics. Continuous variables were reported as mean and standard deviation, categorical variables were reported as frequency and percentage, and confidence intervals (CI) were reported at the 95% level. Mean difference in biomarker values between those with NAFL and those with NASH were compared using independent t-tests or Wilcoxon signed-rank tests, depending on distribution. Diagnostic performance of non-invasive biomarkers was assessed using area under receiver operator characteristic curve (AUC) with multivariate logistic regressions utilised to assess performance of combined biomarkers. Correlations between median scores from the 3 pathology reads and image-derived markers (MR liver fat, cT1, MRE, VCTE-LSM and CAP) were assessed using Spearman's rank correlation coefficient.

Inter-rater variability analysis between the pathology scores given by the 3 pathologists were performed using tri-variate weighted kappa statistic, with the overall variability seen for each of the histological metrics assessed by Krippendorff's alpha<sup>[30]</sup>.

Statistical analysis was performed using R software version 3.6.1 with  $P < 0.05$  considered to be statistically significant. Case-wise deletion was employed to include only complete cases for MR metrics, VCTE-LSM and CAP for each analysis as appropriate rather than imputing any missing values.

## RESULTS

Of the initial 151 patients who underwent liver biopsy, 145 were eligible for the study. The average age was 60 ( $\pm 13$ ) years, 61% patients were male, 40% BMI  $\geq 30$  kg/m<sup>2</sup> and 60% of patients had NASH (NAS  $\geq 4$  with ballooning  $\geq 1$  and inflammation  $\geq 1$ ; [Table 1](#)). There was a broad range of histology scores across all aspects of the key histopathological hallmarks of NASH ([Table 2](#)). From the entire cohort, one had missing MRE data, two had missing LiverMultiScan<sup>®</sup> data, 28 missing or uninterpretable Fibroscan data, and 61 had missing or uninterpretable 2D-SWE data. Investigation into potential causes of failure for the ultrasound based methods revealed BMI to be significantly higher in the cases in which VCTE-LSM was unreported (31.7 kg/m<sup>2</sup> *vs* 28.1 kg/m<sup>2</sup>,  $P < 0.05$ ), and similarly was elevated in those with missing 2D-SWE (29.5 kg/m<sup>2</sup> *vs* 27.9 kg/m<sup>2</sup>).

### Diagnostic accuracy of non-invasive imaging markers for differentiation of disease activity

**Steatosis (NAFL):** MR Liver fat [AUC: 0.92 (CI: 0.87-0.98)], and CAP [AUC: 0.75 (CI: 0.58-0.92)] both discriminated between steatosis  $\geq 1$ , while the other imaging markers were unable to [cT1 AUC: 0.64 (CI: 0.46-0.82), MRE AUC: 0.53 (CI: 0.33-0.72), VCTE-LSM AUC: 0.60 (CI: 0.37-0.82), 2D-SWE AUC: 0.53 (CI: 0.22-0.84)]. For steatosis  $\geq 2$ , MR liver fat again showed the best performance [MR liver fat: AUC: 0.86 (CI: 0.80-0.93); *vs* CAP AUC: 0.68 (CI: 0.59-0.78)]. 7 patients had CAP technical failure and 10 patients were not able to gain reliable results.

**NASH:** To diagnose steatohepatitis (NAS  $\geq 4$  with at least one in both ballooning and inflammation), MR liver fat [AUC: 0.80 (CI: 0.73-0.87)], cT1 [AUC: 0.75 (CI: 0.67-0.84)], and CAP [AUC: 0.71 (CI: 0.62-0.80)] all had good discriminatory performance, while VCTE-LSM [AUC: 0.56 (CI: 0.45-0.66)], MRE [AUC: 0.57 (CI: 0.47-0.67)] and 2D-SWE [AUC: 0.58 (CI: 0.45-0.71)] were not as effective ([Figure 3](#)). Multivariate analysis to explore the potential for increased diagnostic performance of biomarkers used in combination for identifying those with NASH, revealed the combination of cT1 and MR liver fat [AUC: 0.83 (CI: 0.76-0.90)] was superior to the individual markers and to

**Table 1 Participant demographics**

	Total ( <i>n</i> = 145), mean ± SD (% of cohort)	NASH	NAFL
Total cohort ( <i>n</i> )	145	87	58
Sex (male)	88 (60.7%)	46	42 <sup>a</sup>
Age	60.2 ± 13.1	60.9 ± 13.2	59 ± 12.9
BMI average	28.8 ± 4.7	29.9 ± 4.4	27.1 ± 4.8 <sup>c</sup>
Normal BMI (≥ 18.5 ≤ 22.9)	21.4 ± 1.6 ( <i>n</i> = 17)	<i>n</i> = 6	<i>n</i> = 12
Overweight (≥ 23.0 ≤ 27.9)	25.6 ± 1.1 ( <i>n</i> = 43)	<i>n</i> = 26	<i>n</i> = 26
Obese (≥ 27.5)	32.1 ± 3.2 ( <i>n</i> = 82)	<i>n</i> = 55	<i>n</i> = 20
Blood serum tests			
AST (IU/L)	47.8 ± 27.5	56.4 ± 29.8	34.8 ± 17.1 <sup>c</sup>
ALT (IU/L)	59.8 ± 49.3	71.3 ± 51.5	42.6 ± 41.4 <sup>c</sup>
GGT	85.9 ± 78.4	97.8 ± 85.8	69.3 ± 62.9 <sup>b</sup>
Total bilirubin (mg/dL)	0.86 ± 0.4	0.8 ± 0.3	0.9 ± 0.4
Platelets (× 10 <sup>4</sup> /μL)	19.4 ± 7.3	19.9 ± 7.5	18.8 ± 7
HbA1C (%)	6.5 ± 1.1	6.6 ± 1.0	6.5 ± 1.1
Fasting insulin (mU/mL)	20 ± 14.2	20.6 ± 11.6	19 ± 17.4
Fasting blood glucose (mg/dL)	124 ± 34.7	126.1 ± 32.5	120.8 ± 37.8
Albumin (g/dL)	4.3 ± 0.5	4.3 ± 0.4	4.2 ± 0.5
Non-invasive test			
cT1	871 ± 102 ( <i>n</i> = 143)	907 ± 90 ( <i>n</i> = 87)	817 ± 96 <sup>c</sup> ( <i>n</i> = 56)
MR liver fat	11.4 ± 6.1 ( <i>n</i> = 143)	13.6 ± 5.8 ( <i>n</i> = 87)	8.1 ± 5.1 <sup>c</sup> ( <i>n</i> = 56)
CAP	294.3 ± 47.4 ( <i>n</i> = 117)	309.1 ± 37.1 ( <i>n</i> = 74)	268.9 ± 52.7 <sup>c</sup> ( <i>n</i> = 43)
VCTE-LSM	12.8 ± 9.5 ( <i>n</i> = 117)	13 ± 8.4 ( <i>n</i> = 74)	12.5 ± 11.1 ( <i>n</i> = 43)
MRE	4.2 ± 1.7 ( <i>n</i> = 144)	4.3 ± 1.5 ( <i>n</i> = 88)	4.1 ± 1.9 ( <i>n</i> = 56)
SE	9.3 ± 2.7 ( <i>n</i> = 84)	9.6 ± 2.4 ( <i>n</i> = 50)	8.8 ± 3.1 ( <i>n</i> = 33)
Reported pre-existing conditions			
Hypertensive	<i>n</i> = 71	<i>n</i> = 45	<i>n</i> = 26
Dyslipidaemic	<i>n</i> = 111	<i>n</i> = 72	<i>n</i> = 39
Reported as diabetic	<i>n</i> = 97	<i>n</i> = 59	<i>n</i> = 38

Non-alcoholic steatohepatitis (NASH) were patients with NASH clinical research network ≥ 4 with ballooning ≥ 1. Stars denote significance difference between those with NASH and non-alcoholic fatty liver these levels:

<sup>a</sup>*P* < 0.05.

<sup>b</sup>*P* < 0.01.

<sup>c</sup>*P* < 0.001. MRE: Magnetic resonance elastography; CAP: Controlled-attenuation parameter; VCTE: Vibration-controlled transient elastography; cT1: Corrected T1; BMI: Body mass index; NASH: Non-alcoholic steatohepatitis; NAFL: Non-alcoholic fatty liver.

the combination of VCTE-LSM and CAP in combination [AUC: 0.71 (CI: 0.66-0.8)] (Figure 4).

**Fibrosis:** To measure fibrosis alone, MRE [AUC: 0.97 (CI: 0.94-1.0)], VCTE-LSM [AUC: 0.94 (CI: 0.9-0.99)] and 2D-SWE [AUC: 0.94 (CI: 0.86-1.0)] were all excellent at discriminating for any fibrosis (≥ 1) whilst MR liver fat [AUC: 0.68 (CI: 0.44-0.92)], cT1 [AUC: 0.63 (CI: 0.3-0.97)] and CAP [AUC: 0.6 (CI: 0.39-0.81)] were not as effective. These performances were maintained for discriminating those with more advanced fibrosis (≥ 2): MRE [AUC: 0.92 (CI: 0.87-0.97)]; VCTE-LSM [AUC: 0.88 (CI: 0.81-0.95)]; 2D-SWE [AUC: 0.87 (CI: 0.76-0.99)] compared to cT1 [AUC: 0.62 (CI: 0.49-0.74)] MR liver fat [AUC: 0.60 (CI: 0.48-0.72)] and CAP [AUC: 0.57 (CI: 0.45-0.70)]. VCTE-LSM,

Table 2 Range of histology scores reported across the entire cohort

Histology scores from biopsy (n = 144)				
	Score	Total	NASH	NAFL
Steatosis (Brunt)	0	13	0	13
	1	74	36	37
	2	35	30	5
	3	21	20	1
Lobular inflammation	0	13	0	1
	1	91	48	51
	2	35	35	9
	3	4	3	0
Ballooning	0	39	0	39
	1	72	55	16
	2	32	31	1
	3	0	0	0
Fibrosis (Kleiner)	0	5	1	0
	1	24	10	14
	2	27	16	11
	3	55	39	15
	4	31	19	12
NAS	0	0	0	0
	1	5	0	5
	2	23	0	22
	3	26	0	26
	4	25	25	1
	5	37	35	2
	6	16	16	0
	7	8	8	0
	8	2	2	0

NASH: Non-alcoholic steatohepatitis; NAFL: Non-alcoholic fatty liver.

and to an even greater extent 2D-SWE, however both had high levels of missing data (20% and 42% respectively), likely to be related to elevated obesity.

**Advanced NASH:** To identify those with NASH and fibrosis (NAS  $\geq 4$  with F  $\geq 2$ ), both cT1 [AUC: 0.74 (CI: 0.66-0.82)] and MR liver fat [AUC: 0.71 (CI: 0.63-0.80)] outperformed the other measures; MRE [AUC 0.66 (CI: 0.57-0.75)], VCTE-LSM [AUC: 0.64 (CI: 0.54-0.74)], CAP [AUC: 0.68 (CI: 0.59-0.78)], and 2D-SWE [AUC: 0.62 (CI: 0.49-0.75)]. Combining cT1 and MR liver fat improved the performance [AUC: 0.76 (CI: 0.69-0.84)] and was superior to the combination of VCTE-LSM and CAP [AUC: 0.70 (CI: 0.61-0.79)], (Figure 4).

#### Correlations between image derived biomarkers and histological markers of disease

MRI cT1 correlated significantly with all key aspects of histology [fibrosis, steatosis, ballooning and lobular inflammation ( $r_s = 0.24$ ,  $r_s = 0.29$ ,  $r_s = 0.39$ ,  $r_s = 0.31$ , respectively)] and with overall NAS ( $r_s = 0.58$ ). MR liver fat was positively correlated with steatosis ( $r_s = 0.70$ ), and with inflammation ( $r_s = 0.28$ ), ballooning ( $r_s = 0.29$ ) and overall NAS ( $r_s = 0.64$ ) but was negatively correlated with fibrosis ( $r_s = -0.25$ ). MRE was significantly

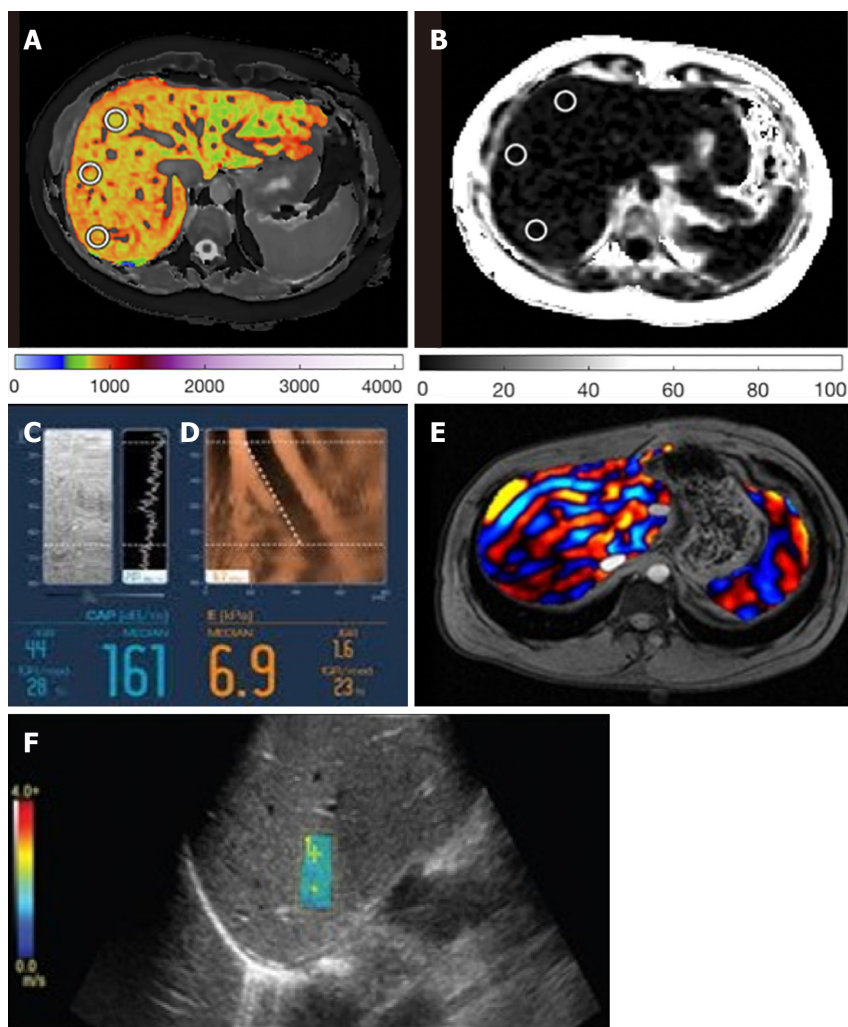


**Figure 2** Example images from each technology. A: Corrected T1 map; B: Magnetic resonance liver fat map; C: Fibroscan controlled-attenuation parameter; D: Fibroscan Liver Stiffness; E: magnetic resonance elastography liver stiffness map; and F: 2D Shear-wave elastography.

correlated with fibrosis ( $r_s = 0.75$ ) as well as ballooning and lobular inflammation ( $r_s = 0.32$ ,  $r_s = 0.16$  respectively) and negatively correlated with steatosis ( $r_s = -0.23$ ). VCTE-LSM correlated significantly with fibrosis ( $r_s = 0.69$ ) and ballooning ( $r_s = 0.29$ ), and CAP with steatosis ( $r_s = 0.39$ ), inflammation ( $r_s = 0.26$ ), ballooning ( $r_s = 0.33$ ) and NAS ( $r_s = 0.49$ ). 2D shear-wave elastography was positively correlated with fibrosis ( $r_s = 0.72$ ) and ballooning ( $r_s = 0.34$ ; Table 3).

### Concordance between pathologists

Assessment of the overall agreement (Krippendorff's alpha) of the pathologists for each histological marker showed that there was moderate agreement for indicators of steatosis ( $\alpha = 0.58$ ) and NAS ( $\alpha = 0.42$ ), fair agreement for ballooning and fibrosis ( $\alpha = 0.40$  for both), and none to slight agreement on lobular inflammation ( $\alpha = 0.11$ ). Assessment of the trivariate weighted kappa scores from individual pathologists for each metric showed no reoccurring pattern of agreement between any two pathologists (Table 4).

## DISCUSSION

The diagnosis of NASH is important as it provides prognostic information indicating an increased risk of fibrosis progression and liver-related mortality but has hitherto been limited because of the need for histological verification. In clinical practice, distinguishing between NAFL, NASH, and NASH with fibrosis is highly desirable for risk stratification. Patients with steatosis can be educated about future cardiovascular risk, and lifestyle measures to prevent them, while those with NASH, or NASH and

Table 3 Spearman's correlation coefficients for all variables

	cT1, (n = 143)	MR liver fat (n = 143)	MRE (n = 144)	VCTE-LSM (n = 117)	CAP (n = 117)	2D SWE (n = 84)
Fibrosis	0.24, $P < 0.01$	-0.25, $P < 0.01$	0.75, $P < 0.001$	0.69, $P < 0.001$	0.05, $P = 0.58$	0.72, $P < 0.001$
Steatosis	0.29, $P < 0.001$	0.70, $P < 0.001$	-0.23, $P < 0.01$	-0.09, $P = 0.23$	0.39, $P < 0.001$	-0.07, $P = 0.53$
Lobular inflammation	0.31, $P < 0.001$	0.28, $P < 0.001$	0.16, $P < 0.01$	0.15, $P = 0.10$	0.26, $P < 0.01$	0.16, $P = 0.15$
Ballooning	0.39, $P < 0.001$	0.29, $P < 0.001$	0.32, $P < 0.01$	0.29, $P < 0.01$	0.33, $P < 0.001$	0.34, $P < 0.001$
NAS	0.58, $P < 0.001$	0.64, $P < 0.001$	0.06, $P = 0.44$	0.13, $P = 0.13$	0.49, $P < 0.001$	0.16, $P = 0.13$

$P < 0.05$ : Correlations with statistical significance. MRE: Magnetic resonance elastography; CAP: Controlled-attenuation parameter; VCTE: Vibration-controlled transient elastography; cT1: Corrected T1; SWE: Shear-Wave elastography; NASH: Non-alcoholic steatohepatitis; LSM: Liver stiffness measure.

Table 4 Inter-rater variability between the three pathologists for each histology metric

Histological metric	Pathologists	Kappa weighted	Lower CI	Upper CI	ASE	P value	Overall inter-rater variability (Krippendorff's alpha)
Steatosis	1 vs 2	0.609	0.517	0.7	0.0467	< 0.0001	0.584
	1 vs 3	0.483	0.388	0.579	0.0489	< 0.0001	
	2 vs 3	0.585	0.485	0.686	0.0513	< 0.0001	
Lobular inflammation	1 vs 2	0.118	0.0631	0.173	0.0281	< 0.0001	0.109
	1 vs 3	0.0376	0.00574	0.0695	0.0163	0.02	
	2 vs 3	0.179	0.0699	0.288	0.0556	0.001	
Ballooning	1 vs 2	0.297	0.205	0.389	0.047	< 0.0001	0.398
	1 vs 3	0.459	0.344	0.573	0.0583	< 0.0001	
	2 vs 3	0.27	0.18	0.36	0.0453	< 0.0001	
Fibrosis	1 vs 2	0.719	0.65	0.788	0.0353	< 0.0001	0.398
	1 vs 3	0.571	0.496	0.647	0.0386	< 0.0001	
	2 vs 3	0.597	0.521	0.672	0.0385	< 0.0001	
NAS	1 vs 2	0.279	0.202	0.357	0.0398	< 0.0001	0.421
	1 vs 3	0.244	0.172	0.316	0.0366	< 0.0001	
	2 vs 3	0.434	0.35	0.518	0.043	< 0.0001	

CI: Confidence intervals.

fibrosis, can be monitored and treated (pioglitazone, clevoglitazar) to reduce the risk of cardiovascular and liver clinical complications. In this study, we were able to identify and differentiate patients with steatosis, NASH, and NASH with fibrosis with good diagnostic performance using non-invasive technologies which characterise liver tissue accurately.

The diagnosis of NASH is based, at present, on the histological presence of steatosis and either lobular inflammation or ballooning, with the presence of fibrosis highlighting disease progression. Currently, the only biomarkers shown to predict outcomes in patients are histological fibrosis and cT1<sup>[19,20,31]</sup>. However, cT1 is sensitive to ballooning, inflammation, steatosis as well as fibrosis, and so cannot be considered a pure fibrosis biomarker. When measuring just fibrosis, MRE had greater correlations to histology and greater sensitivity than other methods but could not by itself distinguish NAFL from NASH or NASH with fibrosis. Whilst ultrasound methods are also effective for staging advanced fibrosis, in line with reported literature<sup>[32-35]</sup>, they can be less reliable in obese patients with higher BMI as observed in the patients in this cohort with missing VCTE and 2D-SWE data. In contrast BMI has not been shown to systematically affect the failure rate for MRE<sup>[23]</sup> or of mpMRI<sup>[36,37]</sup>, except for the very



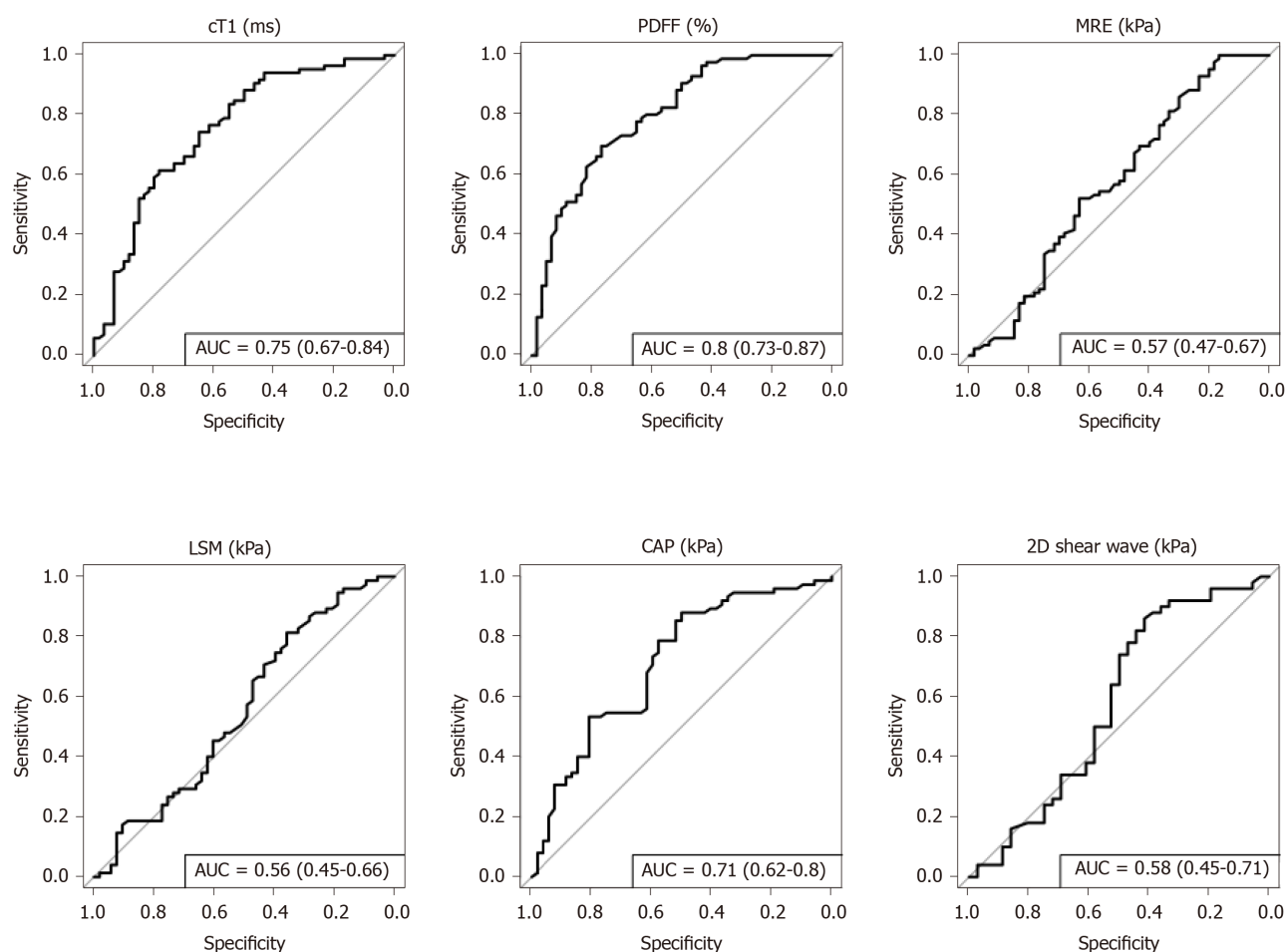


**Figure 3** Receiver operator characteristic curves for discriminating those with non-alcoholic steatohepatitis (NAS  $\geq 4$  and ballooning  $> 1$  or inflammation  $> 1$ ) from those without. Area under the curve and confidence intervals displayed in the legend for each non-invasive measure. MRE: Magnetic resonance elastography; CAP: Controlled-attenuation parameter; cT1: Corrected T1; LSM: Liver stiffness measure; PDFF: Proton density fat fraction.

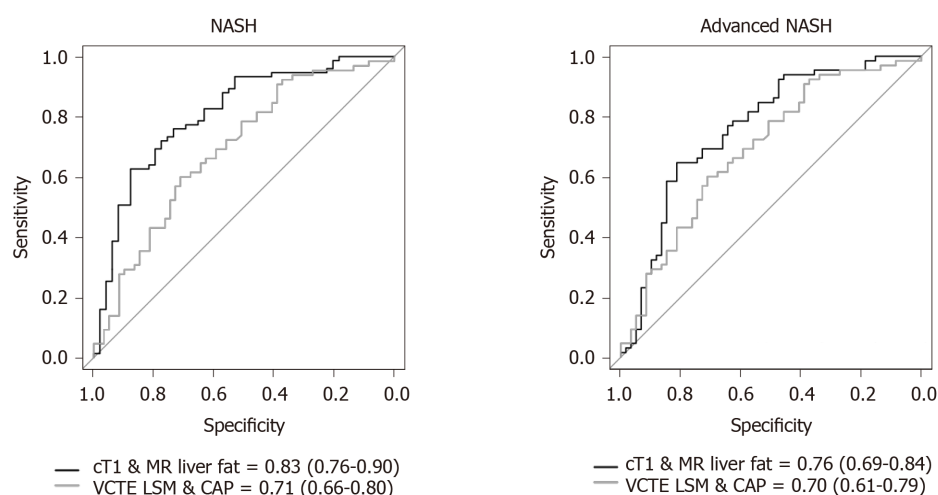


**Figure 4** Receiver operator characteristic curves for discriminating those with non-alcoholic steatohepatitis (left) and those with non-alcoholic steatohepatitis with fibrosis (right). Area under the curve and confidence intervals displayed in the legend for each non-invasive measure. CAP: Controlled-attenuation parameter; VCTE: Vibration-controlled transient elastography; cT1: Corrected T1; NASH: Non-alcoholic steatohepatitis.

unusual circumstances when a participant is simply too large to fit into the scanner. All elastography measures however have been shown to be confounded by iron, steatosis and inflammation<sup>[38]</sup> in the measure of fibrosis.

The assessment of steatosis is important as the accumulation of liver fat is linked with the progression of hepatocyte injury that can ultimately result in fibrosis<sup>[39]</sup>; the downstream consequence of NASH which is linked to poor clinical outcomes<sup>[31]</sup>. In this study, MR liver fat demonstrated better performance than CAP for the detection and differentiation of steatosis grades. As a result, this makes MR liver fat a good marker of NAFL and NASH. However, where cT1 appears to have an advantage over MR liver fat as a non-invasive biomarker for NASH is in the detection and diagnosis of patients with both NASH and fibrosis. Both cT1, and uncorrected T1 have been reported to be elevated in those with advanced liver fibrosis<sup>[40-43]</sup>. A key limitation of MR liver fat as a solo biomarker of NASH is that patients with advanced fibrosis and cirrhosis have lower acclimations of liver fat than those at earlier stages of disease<sup>[44,45]</sup>. Our results, in line with those reported in the literature, demonstrate a negative association between MR liver fat and advanced fibrosis<sup>[44,45]</sup>. This is an important consideration and is reflected in the superior diagnostic accuracy of cT1 when compared to MR liver fat for identifying those with NASH and fibrosis  $\geq 2$ , with the composite marker of cT1 and MR liver fat showing the greatest diagnostic accuracy.

New diagnostic tools are evaluated by comparison to histological measures to evaluate their utility. Nevertheless, recent studies on the reproducibility of histology<sup>[46]</sup> have established that biopsy, as the de facto benchmark, is not perfect. We also observed discordance between different pathologists across the four cardinal pathological features (steatosis, ballooning, lobular inflammation and fibrosis), with no common pattern of concordance seen between any two pathologists. Previous literature discusses the subjective nature of histological grading systems<sup>[47]</sup> which is evident in these findings, demonstrating that subjectivity as well as potential sampling and human error can affect results<sup>[48-50]</sup>. This analysis highlights the need for more robust endpoints with which to evaluate the performance of non-invasive diagnostics. The gold standard would be a tool that predicts clinical outcomes and can thus provide prognosis. Whilst such studies are both time-consuming and costly in order to generate the necessary evidence, encouragingly, initial work in this space has demonstrated potential for cT1 to predict clinical outcomes in patients with chronic liver disease<sup>[19,20]</sup>. It is hoped that further validation of these observations in patients with NASH specifically will aid in the development of a clinical pathway that does not rely on invasive liver biopsy.

This study was not without its limitations, with the pre-screening step prior to liver biopsy likely truncating the correlations that would be observed across the full disease spectrum. While this may also impact the diagnostic accuracy evaluated, this pre-screening approach is representative of clinical practice. Observed failure rates for the ultrasound-based methods also have the potential to skew the results given its dependence on BMI, with patients with high BMI less likely to be included in the study. In practice this has a bearing on the value proposition of such technologies for screening and monitoring as failed measurements will result in necessary further clinical tests for patients.

## CONCLUSION

In summary, this study demonstrates the clinical utility of mpMRI for the stratification of NAFLD, and encourages mpMRI use as a non-invasive alternative to biopsy in the clinical care pathway. Quantitative mpMRI metrics showed the strongest overall correlations to the histological components of NASH with fewer technical failures. mpMRI also out-performed MRE and ultrasound-based elastography methods in the identification of patients with NASH and fibrosis. The ability to risk stratify patients in a single non-invasive test is a particular strength of mpMRI, offering a safe and cost-effective alternative to liver biopsy.

## ARTICLE HIGHLIGHTS

### Research background

Non-alcoholic fatty liver disease affects 25% of the population worldwide and up to 30% in the Japanese population, and in some can progress to non-alcoholic

steatohepatitis (NASH), a leading cause of liver transplant due to its strong propensity to develop into cirrhosis and hepatocellular carcinoma.

### Research motivation

Liver biopsy is the current reference standard for a clinical diagnosis of NASH, a method that is expensive, invasive and suffers from great observer variability. Non-invasive and scalable alternatives are required in order to meet the burgeoning demands of the disease on clinical caseloads across the globe.

### Research objectives

The main objectives of the study were to evaluate the diagnostic performance of non-invasive, image derived metrics to identify patients with suspected NASH. The metrics under investigation included two quantitative multi-parametric magnetic resonance imaging (MRI) measures, iron corrected T1 mapping [(cT1), a marker of fibro-inflammation] and proton density liver fat fraction (a marker of liver fat), magnetic resonance elastography and ultrasound based transient elastography (vibration-controlled transient elastography and 2D shear-wave elastography), both markers of liver stiffness.

### Research methods

In an observational study of patients who were being screened clinically on suspicion of NASH,  $n = 145$  individuals underwent liver biopsy and concomitant imaging measures of liver health. Diagnosis of NASH was based on histology, graded using the NAS- Clinical Research Network scoring system and diagnostic accuracy of the image-derived metrics assessed using area under receiver operator characteristic curve. In addition, the biopsy slides were read by 2 further pathologists and comparisons made to explore the level of agreement on diagnosis between individual doctors.

### Research results

In this study assessing the ability of different non-invasive biomarkers to detect NASH, MR liver fat and cT1 were superior to the other metrics investigated. Crucially however, the composite marker of cT1 and MR liver fat showed the greatest diagnostic accuracy for identifying those with NASH and also those with NASH with fibrosis. These measures also had very few technical failures. This is the first assessment and direct comparison of these technologies in a Japanese cohort. We also observed discordance between different pathologists across the four cardinal pathological features (steatosis, ballooning, lobular inflammation and fibrosis), with no common pattern of agreement seen between any two pathologists.

### Research conclusions

These results demonstrate the clinical utility of quantitative multiparametric magnetic resonance imaging (mpMRI) for the identification and stratification of patients with NASH from those with evidence of NAFLD and encourages mpMRI use as a non-invasive alternative to biopsy in the clinical care pathway. Quantitative mpMRI metrics showed the strongest correlation to the histological components of NASH with fewer technical failures. mpMRI also out-performed magnetic resonance elastography and ultrasound-based elastography methods in the identification of patients with NASH and fibrosis. Liver biopsy suffered from high levels of inter-reading disagreement, highlighting the pressing need for alternative diagnostic tests for NASH.

### Research perspectives

The ability to risk stratify patients in a single non-invasive test is a particular strength of mpMRI, offering a safe and cost-effective alternative to liver biopsy. Future work should be focused on validating these findings further and on longer term outcomes studies to investigate the prognostic natures of these measurements in a Japanese population.

## REFERENCES

- 1 Younossi Z, Anstee QM, Marietti M, Hardy T, Henry L, Eslam M, George J, Bugianesi E. Global burden of NAFLD and NASH: trends, predictions, risk factors and prevention. *Nat Rev Gastroenterol Hepatol* 2018; **15**: 11-20 [PMID: 28930295 DOI: 10.1038/nrgastro.2017.109]

- 2 **Fan JG**, Kim SU, Wong VW. New trends on obesity and NAFLD in Asia. *J Hepatol* 2017; **67**: 862-873 [PMID: 28642059 DOI: 10.1016/j.jhep.2017.06.003]
- 3 **Albhai S**, Chowdhury A, Sanyal AJ. Non-alcoholic fatty liver disease in lean individuals. *JHEP Rep* 2019; **1**: 329-341 [PMID: 32039383 DOI: 10.1016/j.jhepr.2019.08.002]
- 4 **Younes R**, Bugianesi E. NASH in Lean Individuals. *Semin Liver Dis* 2019; **39**: 86-95 [PMID: 30654392 DOI: 10.1055/s-0038-1677517]
- 5 **Angulo P**. Long-term mortality in nonalcoholic fatty liver disease: is liver histology of any prognostic significance? *Hepatology* 2010; **51**: 373-375 [PMID: 20101746 DOI: 10.1002/hep.23521]
- 6 **Singh S**, Allen AM, Wang Z, Prokop LJ, Murad MH, Loomba R. Fibrosis progression in nonalcoholic fatty liver vs nonalcoholic steatohepatitis: a systematic review and meta-analysis of paired-biopsy studies. *Clin Gastroenterol Hepatol* 2015; **13**: 643-54. quiz e39-40 [PMID: 24768810 DOI: 10.1016/j.cgh.2014.04.014]
- 7 **Seki Y**, Kakizaki S, Horiguchi N, Hashizume H, Tojima H, Yamazaki Y, Sato K, Kusano M, Yamada M, Kasama K. Prevalence of nonalcoholic steatohepatitis in Japanese patients with morbid obesity undergoing bariatric surgery. *J Gastroenterol* 2016; **51**: 281-289 [PMID: 26314837 DOI: 10.1007/s00535-015-1114-8]
- 8 **Marra F**, Lotersztajn S. Pathophysiology of NASH: perspectives for a targeted treatment. *Curr Pharm Des* 2013; **19**: 5250-5269 [PMID: 23394092 DOI: 10.2174/13816128113199990344]
- 9 **Wong SW**, Ting YW, Chan WK. Epidemiology of non-alcoholic fatty liver disease-related hepatocellular carcinoma and its implications. *JGH Open* 2018; **2**: 235-241 [PMID: 30483595 DOI: 10.1002/jgh3.12070]
- 10 **Angulo P**, Keach JC, Batts KP, Lindor KD. Independent predictors of liver fibrosis in patients with nonalcoholic steatohepatitis. *Hepatology* 1999; **30**: 1356-1362 [PMID: 10573511 DOI: 10.1002/hep.510300604]
- 11 **Ekstedt M**, Nasr P, Kechagias S. Natural History of NAFLD/NASH. *Curr Hepatol Rep* 2017; **16**: 391-397 [PMID: 29984130 DOI: 10.1007/s11901-017-0378-2]
- 12 **Chalasani N**, Younossi Z, Lavine JE, Charlton M, Cusi K, Rinella M, Harrison SA, Brunt EM, Sanyal AJ. The diagnosis and management of nonalcoholic fatty liver disease: Practice guidance from the American Association for the Study of Liver Diseases. *Hepatology* 2018; **67**: 328-357 [PMID: 28714183 DOI: 10.1002/hep.29367]
- 13 **Piccinino F**, Sagnelli E, Pasquale G, Giusti G. Complications following percutaneous liver biopsy. A multicentre retrospective study on 68,276 biopsies. *J Hepatol* 1986; **2**: 165-173 [PMID: 3958472 DOI: 10.1016/s0168-8278(86)80075-7]
- 14 **Harrison SA**, Dennis A, Fiore MM, Kelly MD, Kelly CJ, Paredes AH, Whitehead JM, Neubauer S, Traber PG, Banerjee R. Utility and variability of three non-invasive liver fibrosis imaging modalities to evaluate efficacy of GR-MD-02 in subjects with NASH and bridging fibrosis during a phase-2 randomized clinical trial. *PLoS One* 2018; **13**: e0203054 [PMID: 30192782 DOI: 10.1371/journal.pone.0203054]
- 15 **Causy C**, Reeder SB, Sirlin CB, Loomba R. Noninvasive, Quantitative Assessment of Liver Fat by MRI-PDFF as an Endpoint in NASH Trials. *Hepatology* 2018; **68**: 763-772 [PMID: 29356032 DOI: 10.1002/hep.29797]
- 16 **Imajo K**, Kessoku T, Honda Y, Tomeno W, Ogawa Y, Mawatari H, Fujita K, Yoneda M, Taguri M, Hyogo H, Sumida Y, Ono M, Eguchi Y, Inoue T, Yamanaka T, Wada K, Saito S, Nakajima A. Magnetic Resonance Imaging More Accurately Classifies Steatosis and Fibrosis in Patients With Nonalcoholic Fatty Liver Disease Than Transient Elastography. *Gastroenterology* 2016; **150**: 626-637. e7 [PMID: 26677985 DOI: 10.1053/j.gastro.2015.11.048]
- 17 **Jayakumar S**, Middleton MS, Lawitz EJ, Mantry PS, Caldwell SH, Arnold H, Mae Diehl A, Ghalib R, Elkhatab M, Abdelmalek MF, Kowdley KV, Stephen Djedjos C, Xu R, Han L, Mani Subramanian G, Myers RP, Goodman ZD, Afdhal NH, Charlton MR, Sirlin CB, Loomba R. Longitudinal correlations between MRE, MRI-PDFF, and liver histology in patients with non-alcoholic steatohepatitis: Analysis of data from a phase II trial of selonsertib. *J Hepatol* 2019; **70**: 133-141 [PMID: 30291868 DOI: 10.1016/j.jhep.2018.09.024]
- 18 **Eddowes PJ**, McDonald N, Davies N, Semple SIK, Kendall TJ, Hodson J, Newsome PN, Flintham RB, Wesolowski R, Blake L, Duarte RV, Kelly CJ, Herlihy AH, Kelly MD, Olliff SP, Hübscher SG, Fallowfield JA, Hirschfield GM. Utility and cost evaluation of multiparametric magnetic resonance imaging for the assessment of non-alcoholic fatty liver disease. *Aliment Pharmacol Ther* 2018; **47**: 631-644 [PMID: 29271504 DOI: 10.1111/apt.14469]
- 19 **Jayaswal ANA**, Levick C, Selvaraj EA, Dennis A, Booth JC, Collier J, Cobbold J, Tunnicliffe EM, Kelly M, Barnes E, Neubauer S, Banerjee R, Pavlides M. Prognostic value of multiparametric magnetic resonance imaging, transient elastography and blood-based fibrosis markers in patients with chronic liver disease. *Liver Int* 2020 [PMID: 32730664 DOI: 10.1111/Liv.14625]
- 20 **Pavlides M**, Banerjee R, Sellwood J, Kelly CJ, Robson MD, Booth JC, Collier J, Neubauer S, Barnes E. Multiparametric magnetic resonance imaging predicts clinical outcomes in patients with chronic liver disease. *J Hepatol* 2016; **64**: 308-315 [PMID: 26471505 DOI: 10.1016/j.jhep.2015.10.009]
- 21 **Bachtiar V**, Kelly MD, Wilman HR, Jacobs J, Newbould R, Kelly CJ, Gyngell ML, Groves KE, McKay A, Herlihy AH, Fernandes CC, Halberstadt M, Maguire M, Jayaratne N, Linden S, Neubauer S, Banerjee R. Repeatability and reproducibility of multiparametric magnetic resonance imaging of the liver. *PLoS One* 2019; **14**: e0214921 [PMID: 30970039 DOI: 10.1371/journal.pone.0214921]
- 22 **Chen J**, Talwalkar JA, Yin M, Glaser KJ, Sanderson SO, Ehman RL. Early detection of nonalcoholic

- steatohepatitis in patients with nonalcoholic fatty liver disease by using MR elastography. *Radiology* 2011; **259**: 749-756 [PMID: [21460032](#) DOI: [10.1148/radiol.11101942](#)]
- 23 **Singh S**, Venkatesh SK, Wang Z, Miller FH, Motosugi U, Low RN, Hassanein T, Asbach P, Godfrey EM, Yin M, Chen J, Keaveny AP, Bridges M, Bohte A, Murad MH, Lomas DJ, Talwalkar JA, Ehman RL. Diagnostic performance of magnetic resonance elastography in staging liver fibrosis: a systematic review and meta-analysis of individual participant data. *Clin Gastroenterol Hepatol* 2015; **13**: 440-451. e6 [PMID: [25305349](#) DOI: [10.1016/j.cgh.2014.09.046](#)]
  - 24 **Castera L**, Friedrich-Rust M, Loomba R. Noninvasive Assessment of Liver Disease in Patients With Nonalcoholic Fatty Liver Disease. *Gastroenterology* 2019; **156**: 1264-1281. e4 [PMID: [30660725](#) DOI: [10.1053/j.gastro.2018.12.036](#)]
  - 25 **Kwok R**, Tse YK, Wong GL, Ha Y, Lee AU, Ngu MC, Chan HL, Wong VW. Systematic review with meta-analysis: non-invasive assessment of non-alcoholic fatty liver disease--the role of transient elastography and plasma cytochrome-18 fragments. *Aliment Pharmacol Ther* 2014; **39**: 254-269 [PMID: [24308774](#) DOI: [10.1111/apt.12569](#)]
  - 26 **Cosyns B**, Lancellotti P. Normal reference values for echocardiography: a call for comparison between ethnicities. *Eur Heart J Cardiovasc Imaging* 2016; **17**: 523-524 [PMID: [26976356](#) DOI: [10.1093/ehjci/jev353](#)]
  - 27 **Yin M**, Talwalkar JA, Glaser KJ, Manduca A, Grimm RC, Rossman PJ, Fidler JL, Ehman RL. Assessment of hepatic fibrosis with magnetic resonance elastography. *Clin Gastroenterol Hepatol* 2007; **5**: 1207-1213. e2 [PMID: [17916548](#) DOI: [10.1016/j.cgh.2007.06.012](#)]
  - 28 **Sandrin L**, Fourquet B, Hasquenoph JM, Yon S, Fournier C, Mal F, Christidis C, Ziol M, Poulet B, Kazemi F, Beaugrand M, Palau R. Transient elastography: a new noninvasive method for assessment of hepatic fibrosis. *Ultrasound Med Biol* 2003; **29**: 1705-1713 [PMID: [14698338](#) DOI: [10.1016/j.ultrasmedbio.2003.07.001](#)]
  - 29 **Ferraioli G**, Tinelli C, Lissandrin R, Zicchetti M, Dal Bello B, Filice G, Filice C. Point shear wave elastography method for assessing liver stiffness. *World J Gastroenterol* 2014; **20**: 4787-4796 [PMID: [24782633](#) DOI: [10.3748/wjg.v20.i16.4787](#)]
  - 30 **Landis JR**, Koch GG. An application of hierarchical kappa-type statistics in the assessment of majority agreement among multiple observers. *Biometrics* 1977; **33**: 363-374 [PMID: [884196](#) DOI: [10.2307/2529786](#)]
  - 31 **Angulo P**, Kleiner DE, Dam-Larsen S, Adams LA, Bjornsson ES, Charatcharoenwithaya P, Mills PR, Keach JC, Lafferty HD, Stahler A, Haflidadottir S, Bendtsen F. Liver Fibrosis, but No Other Histologic Features, Is Associated With Long-term Outcomes of Patients With Nonalcoholic Fatty Liver Disease. *Gastroenterology* 2015; **149**: 389-97. e10 [PMID: [25935633](#) DOI: [10.1053/j.gastro.2015.04.043](#)]
  - 32 **Castéra L**, Foucher J, Bernard PH, Carvalho F, Allaix D, Merrouche W, Couzigou P, de Lédinghen V. Pitfalls of liver stiffness measurement: a 5-year prospective study of 13,369 examinations. *Hepatology* 2010; **51**: 828-835 [PMID: [20063276](#) DOI: [10.1002/hep.23425](#)]
  - 33 **Petta S**, Di Marco V, Cammà C, Butera G, Cabibi D, Craxi A. Reliability of liver stiffness measurement in non-alcoholic fatty liver disease: the effects of body mass index. *Aliment Pharmacol Ther* 2011; **33**: 1350-1360 [PMID: [21517924](#) DOI: [10.1111/j.1365-2036.2011.04668.x](#)]
  - 34 **Tapper EB**, Lok AS. Use of Liver Imaging and Biopsy in Clinical Practice. *N Engl J Med* 2017; **377**: 756-768 [PMID: [28834467](#) DOI: [10.1056/NEJMr1610570](#)]
  - 35 **Cassinotto C**, Boursier J, de Lédinghen V, Lebigot J, Lapuyade B, Cales P, Hiriart JB, Michalak S, Bail BL, Cartier V, Mouries A, Oberti F, Fouchard-Hubert I, Vergnol J, Aubé C. Liver stiffness in nonalcoholic fatty liver disease: A comparison of supersonic shear imaging, FibroScan, and ARFI with liver biopsy. *Hepatology* 2016; **63**: 1817-1827 [PMID: [26659452](#) DOI: [10.1002/hep.28394](#)]
  - 36 **Mojtahed A**, Kelly CJ, Herlihy AH, Kin S, Wilman HR, McKay A, Kelly M, Milanesi M, Neubauer S, Thomas EL, Bell JD, Banerjee R, Harisinghani M. Reference range of liver corrected T1 values in a population at low risk for fatty liver disease-a UK Biobank sub-study, with an appendix of interesting cases. *Abdom Radiol (NY)* 2019; **44**: 72-84 [PMID: [30032383](#) DOI: [10.1007/s00261-018-1701-2](#)]
  - 37 **Wilman HR**, Kelly M, Garratt S, Matthews PM, Milanesi M, Herlihy A, Gyngell M, Neubauer S, Bell JD, Banerjee R, Thomas EL. Characterisation of liver fat in the UK Biobank cohort. *PLoS One* 2017; **12**: e0172921 [PMID: [28241076](#) DOI: [10.1371/journal.pone.0172921](#)]
  - 38 **Thomaides-Brears HB**, Lepe R, Banerjee R, Duncker C. Multiparametric MR mapping in clinical decision-making for diffuse liver disease. *Abdom Radiol (NY)* 2020; **45**: 3507-3522 [PMID: [32761254](#) DOI: [10.1007/s00261-020-02684-3](#)]
  - 39 **Kleiner DE**, Brunt EM. Nonalcoholic fatty liver disease: pathologic patterns and biopsy evaluation in clinical research. *Semin Liver Dis* 2012; **32**: 3-13 [PMID: [22418883](#) DOI: [10.1055/s-0032-1306421](#)]
  - 40 **Heye T**, Yang SR, Bock M, Brost S, Weigand K, Longerich T, Kauczor HU, Hosch W. MR relaxometry of the liver: significant elevation of T1 relaxation time in patients with liver cirrhosis. *Eur Radiol* 2012; **22**: 1224-1232 [PMID: [22302503](#) DOI: [10.1007/s00330-012-2378-5](#)]
  - 41 **Thomsen C**, Christoffersen P, Henriksen O, Juhl E. Prolonged T1 in patients with liver cirrhosis: an in vivo MRI study. *Magn Reson Imaging* 1990; **8**: 599-604 [PMID: [2082130](#) DOI: [10.1016/0730-725x\(90\)90137-q](#)]
  - 42 **Bradley CR**, Cox EF, Scott RA, James MW, Kaye P, Aithal GP, Francis ST, Guha IN. Multi-organ assessment of compensated cirrhosis patients using quantitative magnetic resonance imaging. *J Hepatol* 2018; **69**: 1015-1024 [PMID: [29886155](#) DOI: [10.1016/j.jhep.2018.05.037](#)]



- 43 **Banerjee R**, Pavlides M, Tunnicliffe EM, Piechnik SK, Sarania N, Philips R, Collier JD, Booth JC, Schneider JE, Wang LM, Delaney DW, Fleming KA, Robson MD, Barnes E, Neubauer S. Multiparametric magnetic resonance for the non-invasive diagnosis of liver disease. *J Hepatol* 2014; **60**: 69-77 [PMID: [24036007](#) DOI: [10.1016/j.jhep.2013.09.002](#)]
- 44 **Permutt Z**, Le TA, Peterson MR, Seki E, Brenner DA, Sirlin C, Loomba R. Correlation between liver histology and novel magnetic resonance imaging in adult patients with non-alcoholic fatty liver disease - MRI accurately quantifies hepatic steatosis in NAFLD. *Aliment Pharmacol Ther* 2012; **36**: 22-29 [PMID: [22554256](#) DOI: [10.1111/j.1365-2036.2012.05121.x](#)]
- 45 **Wildman-Tobriner B**, Middleton MM, Moylan CA, Rossi S, Flores O, Chang ZA, Abdelmalek MF, Sirlin CB, Bashir MR. Association Between Magnetic Resonance Imaging-Proton Density Fat Fraction and Liver Histology Features in Patients With Nonalcoholic Fatty Liver Disease or Nonalcoholic Steatohepatitis. *Gastroenterology* 2018; **155**: 1428-1435. e2 [PMID: [30031769](#) DOI: [10.1053/j.gastro.2018.07.018](#)]
- 46 **Davison BA**, Harrison SA, Cotter G, Alkhouri N, Sanyal A, Edwards C, Colca JR, Iwashita J, Koch GG, Dittrich HC. Suboptimal reliability of liver biopsy evaluation has implications for randomized clinical trials. *J Hepatol* 2020; **73**: 1322-1332 [PMID: [32610115](#) DOI: [10.1016/j.jhep.2020.06.025](#)]
- 47 **Sanai FM**, Keeffe EB. Liver biopsy for histological assessment: The case against. *Saudi J Gastroenterol* 2010; **16**: 124-132 [PMID: [20339187](#) DOI: [10.4103/1319-3767.61244](#)]
- 48 **Kleiner DE**, Brunt EM, Van Natta M, Behling C, Contos MJ, Cummings OW, Ferrell LD, Liu YC, Torbenson MS, Unalp-Arida A, Yeh M, McCullough AJ, Sanyal AJ; Nonalcoholic Steatohepatitis Clinical Research Network. Design and validation of a histological scoring system for nonalcoholic fatty liver disease. *Hepatology* 2005; **41**: 1313-1321 [PMID: [15915461](#) DOI: [10.1002/hep.20701](#)]
- 49 **Merriman RB**, Ferrell LD, Patti MG, Weston SR, Pabst MS, Aouizerat BE, Bass NM. Correlation of paired liver biopsies in morbidly obese patients with suspected nonalcoholic fatty liver disease. *Hepatology* 2006; **44**: 874-880 [PMID: [17006934](#) DOI: [10.1002/hep.21346](#)]
- 50 **Pournik O**, Alavian SM, Ghalichi L, Seifizarei B, Mehrmouh L, Aslani A, Anjarani S, Eslami S. Inter-observer and Intra-observer Agreement in Pathological Evaluation of Non-alcoholic Fatty Liver Disease Suspected Liver Biopsies. *Hepat Mon* 2014; **14**: e15167 [PMID: [24497882](#) DOI: [10.5812/hepatmon.15167](#)]



## Retrospective Study

# Clinicopathological features and prognostic factors associated with gastroenteropancreatic mixed neuroendocrine non-neuroendocrine neoplasms in Chinese patients

Yu-Chen Huang, Ning-Ning Yang, Hong-Chun Chen, Yuan-Li Huang, Wen-Tian Yan, Ru-Xue Yang, Nan Li, Shan Zhang, Pan-Pan Yang, Zhen-Zhong Feng

**ORCID number:** Yu-Chen Huang 0000-0002-7740-5634; Ning-Ning Yang 0000-0003-0691-7293; Hong-Chun Chen 0000-0002-7751-5390; Yuan-Li Huang 0000-0001-9899-811X; Wen-Tian Yan 0000-0001-5260-4701; Ru-Xue Yang 0000-0001-8818-2272; Nan Li 0000-0002-5522-4252; Shan Zhang 0000-0001-7891-6906; Pan-Pan Yang 0000-0003-3633-6844; Zhen-Zhong Feng 0000-0001-9385-3157.

**Author contributions:** Huang YC collected the clinical data and prepared the manuscript; Huang YC and Yang NN designed the study and supervised the statistical data; Huang YC and Chen HC designed the research and contributed to the analyses; Huang YL, Yan WT, Yang RX, Li N, Zhang S, and Yang PP provided clinical advice; Feng ZZ made the pathologic diagnosis and supervised the report.

**Supported by** The Natural Science Foundation of Anhui Province, No. 1908085MH275; the Key Project of Science and Technology Development Foundation of Bengbu Medical College, No. BYKF201710; and the Graduate Innovation Program of Bengbu Medical College, No. Byycx20064.

Yu-Chen Huang, Ning-Ning Yang, Hong-Chun Chen, Yuan-Li Huang, Wen-Tian Yan, Nan Li, Zhen-Zhong Feng, Department of Pathology, The First Affiliated Hospital of Bengbu Medical College, Bengbu 233000, Anhui Province, China

Yu-Chen Huang, Ning-Ning Yang, Hong-Chun Chen, Yuan-Li Huang, Wen-Tian Yan, Nan Li, Zhen-Zhong Feng, Department of Pathology, Bengbu Medical College, Bengbu 233000, Anhui Province, China

Ru-Xue Yang, Department of Pathology, The First Affiliated Hospital of Anhui Medical University, Hefei 230000, Anhui Province, China

Shan Zhang, Department of Pathology, The Second People's Hospital of Hefei, Hefei 230000, Anhui Province, China

Pan-Pan Yang, Department of Pathology, The Second Affiliated Hospital of Anhui Medical University, Hefei 230000, Anhui Province, China

**Corresponding author:** Zhen-Zhong Feng, PhD, Professor, Department of Pathology, First Affiliated Hospital of Bengbu Medical College, No. 287 Changhuai Road, Longzihu District, Bengbu 233000, Anhui Province, China. [fzz18297301626@163.com](mailto:fzz18297301626@163.com)

## Abstract

### BACKGROUND

The incidence of mixed neuroendocrine-non-neuroendocrine neoplasms (MiNEN) is low. To improve our understanding of this rare tumor type and optimally guide clinical treatment, associated risk factors, clinical manifestations, and prognosis must be explored.

### AIM

To identify risk factors that influence the prognosis of patients with gastroenteropancreatic MiNEN (GEP-MiNEN).

### METHODS

We retrospectively analyzed the clinical data of 46 patients who were diagnosed with GEP-MiNEN at the First Affiliated Hospital of Bengbu Medical College

**Institutional review board**

**statement:** This study was reviewed and approved by the Ethics Committee of the First Affiliated Hospital of Bengbu Medical College.

**Informed consent statement:** All patients provided written informed consent.

**Conflict-of-interest statement:** We have no financial relationships to disclose.

**Data sharing statement:** No additional data are available.

**Open-Access:** This article is an open-access article that was selected by an in-house editor and fully peer-reviewed by external reviewers. It is distributed in accordance with the Creative Commons Attribution NonCommercial (CC BY-NC 4.0) license, which permits others to distribute, remix, adapt, build upon this work non-commercially, and license their derivative works on different terms, provided the original work is properly cited and the use is non-commercial. See: <http://creativecommons.org/licenses/by-nc/4.0/>

**Manuscript source:** Unsolicited manuscript

**Specialty type:** Gastroenterology and hepatology

**Country/Territory of origin:** China

**Peer-review report's scientific quality classification**

Grade A (Excellent): A  
Grade B (Very good): 0  
Grade C (Good): 0  
Grade D (Fair): 0  
Grade E (Poor): 0

**Received:** November 15, 2020

**Peer-review started:** November 15, 2020

**First decision:** December 17, 2020

**Revised:** December 24, 2020

**Accepted:** January 13, 2021

**Article in press:** January 13, 2021

**Published online:** February 21, 2021

**P-Reviewer:** Tonelli F

**S-Editor:** Zhang L

(Anhui, China) between January 2013 and December 2017. Risk factors influencing the prognosis of the patients were assessed using Kaplan-Meier curves and cox regression models. We compared the results with 55 randomly selected patients with gastroenteropancreatic GEP neuroendocrine tumors, 47 with neuroendocrine carcinomas (NEC), and 58 with poorly differentiated adenocarcinoma.

**RESULTS**

Among the 46 patients with GEP-MiNEN, thirty-five had gastric tumors, nine had intestinal tumors (four in the small intestine and five in the colon and rectum), and two had pancreatic tumors. The median age of the patients was 66 (41-84) years, and the male-to-female ratio was 2.83. Thirty-three (71.7%) patients had clinical stage III and IV cancers. Distant metastasis occurred in 14 patients, of which 13 had metastasis to the liver. The follow-up period was 11-72 mo, and the median overall survival was 30 mo. Ki-67 index  $\geq 50\%$ , high proportion of NEC, lymph node involvement, distant metastasis, and higher clinical stage were independent risk factors affecting the prognosis of patients with GEP-MiNEN. The median overall survival was shorter for patients with NEC than for those with MiNEN (14 mo *vs* 30 mo,  $P = 0.001$ ), but did not significantly differ from those with poorly differentiated adenocarcinoma and MiNEN (30 mo *vs* 18 mo,  $P = 0.453$ ).

**CONCLUSION**

A poor prognosis is associated with rare, aggressive GEP-MiNEN. Ki-67 index, tumor composition, lymph node involvement, distant metastasis, and clinical stage are important factors for patient prognosis.

**Key Words:** Mixed neuroendocrine non-neuroendocrine neoplasm; Mixed adenoneuroendocrine carcinoma; Prognosis; Gastro-entero-pancreatic tract

©The Author(s) 2021. Published by Baishideng Publishing Group Inc. All rights reserved.

**Core Tip:** A poor prognosis is associated with gastroenteropancreatic mixed neuroendocrine-non-neuroendocrine neoplasms, a rare, aggressive type of tumor. Ki-67 index, tumor composition, lymph node involvement, distant metastasis, and clinical stage are important factors for patient prognosis.

**Citation:** Huang YC, Yang NN, Chen HC, Huang YL, Yan WT, Yang RX, Li N, Zhang S, Yang PP, Feng ZZ. Clinicopathological features and prognostic factors associated with gastroenteropancreatic mixed neuroendocrine non-neuroendocrine neoplasms in Chinese patients. *World J Gastroenterol* 2021; 27(7): 624-640

**URL:** <https://www.wjgnet.com/1007-9327/full/v27/i7/624.htm>

**DOI:** <https://dx.doi.org/10.3748/wjg.v27.i7.624>

**INTRODUCTION**

Mixed neuroendocrine-non-neuroendocrine neoplasms (MiNEN) comprise a group of extremely rare heterogeneous tumors, accounting for  $> 5\%$  of all gastrointestinal neuroendocrine tumors<sup>[1]</sup>. However, their prevalence might be largely underestimated due to diagnostic limitations and insufficient scientific understanding<sup>[2]</sup>. This type of tumor is characterized by a mixture of neuroendocrine and non-neuroendocrine components, each accounting for  $> 30\%$  of the tumor. The most common combination is a mixture of adenocarcinomas and neuroendocrine carcinomas, defined as mixed adeno-neuroendocrine carcinoma (MANEC) in the 2010 version of the World Health Organization (WHO) digestive system tumor classification. Although non-neuroendocrine components are usually adenocarcinomas, they can also be squamous cell carcinomas, sarcomas, or other types of tumors<sup>[3-5]</sup>. The 2019 edition of the WHO digestive system classification categorizes MANEC as MiNEN, which comprises a mixture of other types of tumors and neuroendocrine neoplasms, and thus

L-Editor: Wang TQ

P-Editor: Ma YJ



comprehensively describes the potential biological entities that constitute this tumor<sup>[4]</sup>.

MiNEN have been identified in the stomach, intestines, pancreas, biliary tract, appendix, and cervix. The clinical manifestations, treatment, and prognosis of this type of tumor are not clear due to a dearth of reports<sup>[4,6-8]</sup>. We retrospectively analyzed the clinicopathological data of 46 patients with gastroenteropancreatic MiNEN (GEP-MiNEN) and identified risk factors that influence prognosis. We also compared prognostic differences between GEP-MiNEN and gastroenteropancreatic neuroendocrine tumors (NET), neuroendocrine carcinomas (NEC), and poorly differentiated adenocarcinoma to improve the understanding of GEP-MiNEN and to guide future clinical treatment.

## MATERIALS AND METHODS

### Patient selection

We searched the pathological databases of the First Affiliated Hospital of Bengbu Medical College (Bengbu, China) using the following keywords: Mixed adenoneuroendocrine carcinoma, MANEC, mixed neuroendocrine non-neuroendocrine tumor, and MiNEN between January 2013 and December 2017, and limited the tumor site to the gastrointestinal tract and the pancreas. We retrieved data on 46 patients who matched the diagnostic criteria. Two senior pathologists reviewed and categorized these patients according to the current diagnostic criteria for MiNEN as defined by the WHO (2019). This study was approved by the Ethics Committee of The First Affiliated Hospital of Bengbu Medical College (No. 2020057). All patients provided written informed consent to use their clinical data.

### Inclusion criteria

The WHO (2019) classifies MiNEN as tumors of the digestive system characterized by presence of neuroendocrine and non-neuroendocrine components, each accounting for > 30% of the tumor<sup>[4]</sup>. The inclusion criteria were as follows: All patients were treated surgically, including by endoscopy and laparotomy; the postoperative pathology was diagnosed as MiNEN by two senior doctors; the tumor was in the stomach, intestine, or pancreas, and the patient had no history of other malignant tumors; and preoperative radiotherapy or chemotherapy had not been administered.

### Methods

Tumor tissues were fixed with 10% neutral formaldehyde, embedded in paraffin, sliced into 4 µm-thick sections, and then stained with hematoxylin and eosin. The sections were histologically analyzed using a light microscope. Tumors were clinically staged according to the American Joint Committee on Cancer (8<sup>th</sup> edition).

Sections were immunohistochemically analyzed using the EnVision method with the following primary monoclonal antibodies for Ki-67 (mouse anti-human antibody, clone MIB-1), cluster of differentiation (CD) 56 (mouse anti-human antibody, clone 56C04), synaptophysin (rabbit anti-human antibody, clone SP11), and chromogranin A (CgA; rabbit anti-human antibody, clone SP12) (all from Maixin Biotechnology Co., Ltd., Fuzhou, China). Ki-67 staining revealed brownish-yellow granules in the nuclei of tumor cells, and ≥ 20%, 21%-50%, and ≥ 51% stained nuclei were regarded as immunohistochemically positive, low expression, and high expression, respectively. The CD56 signal was observed on cell membranes, whereas Syn and CgA signals were located in the cytoplasm. Overall survival (OS) was defined as the time elapsed from the date of surgery to the date of death or the end of follow-up.

### Follow-up

Follow-up was conducted for 46 patients by either reviewing their information files, making phone calls, or sending out e-mails from the date of diagnosis until December 31, 2019. The OS of the patients who survived or were lost to follow-up was excluded at the date of their last follow-up.

### Statistical analysis

Data were statistically analyzed using statistic package for social science 25.0 (IBM Corp., Armonk, NY, United States). Categorical and continuous variables were analyzed using chi-square tests and independent-sample *t*-test, respectively. Survival was assessed using univariate Kaplan-Meier analysis and survival curves. Survival rates between groups were compared using log-rank tests, and OS rates were analyzed

using multivariate Cox regression models. Values with  $P < 0.05$  were considered statistically significant. The statistical methods were reviewed by Lian-Guo Fu from Bengbu Medical College.

## RESULTS

### *Clinicopathological information of patients*

The clinicopathological data of 46 patients (males,  $n = 34$ ; male-to-female ratio, 2.83: 1; average age, 65 (41-84) years; median age, 66 years) with GEP-MiNEN were analyzed. Among the forty-six patients, thirty-five patients had gastric tumors, nine had intestinal tumors, and two had pancreatic tumors. The tumor diameter was  $\geq 5$  and  $< 5$  cm in 29 and 17 patients, respectively. Microscopy revealed a significant proportion of tumors categorized as NEC and as adenocarcinoma in 28 (60.9%) and 18 (39.1%) patients, respectively. Nerve invasion and vascular tumor thrombus were evident in 27 (58.7%) and 26 (56.5%) of the 46 patients, respectively. Furthermore, 34 (74.0%) of the 46 patients had lymph node involvement, and 14 (30.4%) had distant metastasis. Tumors metastasized to the liver in thirteen of these fourteen patients (three tumors were discovered during surgery), and to the ovary in one patient (Table 1).

### *Microscopic and immunohistochemical features*

The 46 patients exhibited GEP-MiNEN comprising medium or poorly differentiated adenocarcinoma combined with neuroendocrine carcinoma (Figure 1A). Among them, thirty-three had poorly differentiated adenocarcinoma and four had mucinous adenocarcinomas. In 13 patients with moderately differentiated adenocarcinoma, the neuroendocrine component was NEC G3. The adenocarcinoma in these patients had an irregular papillary, adenoid, sieve, or nested distribution, and cells had round or oval nuclei, and coarse and granular chromatin (Figure 1B). The neuroendocrine carcinomas were nested, with an organoid-like distribution, and comprised small cubic or cylindrical tumor cells with round nuclei, reduced cytoplasm, an increased nucleoplasm ratio, and fine nuclear chromatin (Figure 1C).

The adenocarcinoma components expressed cytokeratin (Figure 1D), and most did not express neuroendocrine cancer markers. The neuroendocrine cancer components expressed CgA, Syn, and CD56. All patients were positive for CgA (Figure 1E), 35 were positive for Syn (76.1%) (Figure 1F), and 32 were positive for CD56 (69.6%). The Ki-67 proliferation index was  $> 50\%$  (high expression) and  $< 50\%$  (low expression) in 29 and 17 patients, respectively.

### *Follow-up and survival analysis*

Follow-up was conducted for the patients for a median of 39 (11-72) mo. As of December 31, 2019, a total of forty-two cases were subjected to follow-up and four cases were lost to the follow-up process (8.7%). By the end of the follow-up process, 27 patients had succumbed to tumor-related death. The average and median survivals were  $28.60 \pm 15.14$  and 30 mo, respectively (range, 12-43 mo). Univariate analysis using log-rank tests indicated that the age of the patients, tumor size, Ki-67 index, tumor composition (proportion of neuroendocrine and non-neuroendocrine tumor), degree of adenocarcinoma differentiation, lymph node involvement, vascular tumor thrombus, neurological recidivism, distant metastasis, and clinical stage were associated with OS ( $P < 0.05$ ). Table 2 and Figure 2A-J respectively show the results of univariate analysis of survival and survival curves. Patients aged  $\geq 65$  years with a tumor diameter  $\geq 5$  cm, a Ki-67 index  $\geq 50$ , high NEC, poorly differentiated adenocarcinoma, lymph node involvement, vascular tumor thrombus, nerve invasion, distant metastasis, and high clinical stage had a reduced OS. Sex ( $P = 0.464$ ) and tumor location ( $P = 0.056$ ) were not significantly associated with OS.

Meaningful indicators in the univariate analysis were included in the Cox regression analysis, and the results showed that Ki-67 index  $\geq 50\%$  ( $P = 0.008$ ), lymph node involvement (95%CI: 1.667-25.197,  $P = 0.007$ ), distant metastasis (95%CI: 0.037-0.540,  $P = 0.004$ ), increased proportion of NEC ( $P = 0.039$ ), and clinical stage ( $P = 0.024$ ) were independent risk factors that affected the OS of patients with GEP-MiNEN (Figure 2K and Table 3).

### *Comparative analysis of GEP-MiNEN, NET, and NEC*

We selected 55 patients [males,  $n = 24$ ; average age at diagnosis, 49 (11-85) years] with gastrointestinal pancreatic neuroendocrine tumors (GEP-NET) in the intestine ( $n = 39$ ),



Table 1 Patients' characteristics

Variable	Frequency (n)	Ratio (%)
Gender		
Male	34	73.9
Female	12	26.1
Age (yr)	66 (41-84)	
< 65	20	43.5
≥ 65	26	56.5
Location		
Stomach	35	76.1
Intestine	9	19.6
Pancreas	2	4.3
Size (cm)	5.4 (0.5-18)	
< 5 cm	25	54.3
≥ 5 cm	21	45.7
Ki- 67 index		
< 50%	17	37.0
≥ 50%	29	63.0
Proportions of two components		
NEC higher	28	60.9
AC higher	18	39.1
Histological grade of adenocarcinoma		
Moderately differentiated	13	28.3
Poorly differentiated	33	71.7
Neuroendocrine component		
NET	0	0
NEC	46	100
Lymph node metastasis		
Presence	34	73.9
Absence	12	26.1
Vascular tumor thrombus		
Presence	26	56.5
Absence	20	43.5
Neurological recidivism		
Presence	27	58.7
Absence	19	41.3
Distant metastasis		
Presence	14	30.4
Absence	32	69.6
Clinical TNM stage		
I + II	13	28.3
III	23	50.0
IV	10	21.7

NET: Neuroendocrine tumors; NEC: Neuroendocrine carcinomas.

pancreas ( $n = 9$ ), and stomach ( $n = 7$ ). The average tumor size was 1.7 cm. Lymph nodes were involved in 13 patients, and two had distant metastasis (the small intestine was the primary site of all tumors; one case metastasized to the liver and the other to the pancreas). Eight of the fifty-five patients were lost to follow-up. Tumor location, lymph node involvement, and distant metastasis significantly differed between patients with GEP-NET and MiNEN. By the end of the follow-up period, the median OS was significantly longer in the patients with NET than in the patients with MiNEN (50 mo *vs* 30 mo,  $P < 0.001$ ).

We selected 47 patients [males,  $n = 34$ ; average age at diagnosis, 64 (range, 40-83 years)] with gastrointestinal pancreatic neuroendocrine carcinoma (GEP-NEC) tumors located in the stomach ( $n = 26$ ), intestine ( $n = 15$ ), and pancreas ( $n = 6$ ). The average tumor size was 5.2 cm. Lymph nodes were involved in 33 cases, and 21 patients had distant metastasis. Tumors metastasized to the pancreas ( $n = 1$ ), to both the liver and rectum ( $n = 1$ ), abdominal cavity ( $n = 4$ ), and liver ( $n = 15$ ). Six patients were lost to follow-up. The effects of sex, age, tumor size, tumor location, lymph node involvement, and distant metastasis on OS did not significantly differ between GEP-NEC and MiNEN ( $P > 0.05$  for all). The median OS was significantly shorter in the patients with GEP-NEC than in those with MiNEN (14 *vs* 30 mo,  $P = 0.001$ ; Table 4).

### Comparative analysis of GEP-MiNEN and poorly differentiated adenocarcinoma

We selected 58 patients [average age, 61 (31-81) years; male,  $n = 37$ ] with poorly differentiated gastrointestinal pancreatic adenocarcinoma located in the stomach ( $n = 42$ ), intestines ( $n = 12$ ), and pancreas ( $n = 4$ ). The tumors were  $< 5$  and  $\geq 5$  cm in 25 and 33 patients, respectively. Lymph node involvement and distant metastasis were found in 47 and 16 patients, respectively. Sex, age, tumor size, tumor location, lymph node involvement, and distant metastasis did not significantly differ between the two groups ( $P > 0.05$  for all); median OS did not differ either (30 mo *vs* 18 mo,  $P = 0.453$ ; Table 5).

## DISCUSSION

In the 2010 WHO classification of digestive diseases, MANEC is defined as “a tumor with the morphologically recognizable glandular epithelial and neuroendocrine phenotype and is defined as cancer because both components are malignant.” A mixture of squamous cell carcinoma and neuroendocrine components has also been identified in some esophageal and anal tumors<sup>[4]</sup>. At least 30% of malignancies are deemed eligible for classification as MANEC<sup>[9]</sup>. For instance, a typical adenocarcinoma without the morphological characteristics of a neuroendocrine tumor, in which immunohistochemical staining reveals scattered neuroendocrine markers, should not be diagnosed as “adenocarcinoma with neuroendocrine differentiation”. In 2017, the classification of pancreatic neuroendocrine tumors was modified by the WHO and classified together with digestive tumors. The previous term, MANEC, was replaced by MiNEN<sup>[10]</sup>. The WHO stipulated in 2019 that the term MiNEN is applicable to all digestive tract and neuroendocrine tumors of the digestive system and that these tumors are classified as NET, NEC, and MiNEN. The MiNEN comprise non-neuroendocrine (mostly adenomas or adenocarcinomas, and rarely squamous cell carcinomas) and neuroendocrine components (NETG1, NETG2, NEC), either of which must account for at least 30% of the tumor<sup>[11,12]</sup>. While MiNEN have been found in most organs, they are usually found in the gastrointestinal tract and pancreas<sup>[5,13,14]</sup>.

The diagnosis of MiNEN is primarily based on tumor cytology and structure, and neuroendocrine components can be confirmed by immunolabeling with synaptophysin, chromogranin A, and CD56<sup>[7]</sup>. The recent widespread application of immunohistochemistry has shown that MiNEN tumors are not as rare as previously hypothesized, and the morbidity and mortality rates of gastrointestinal MiNEN are constantly increasing at an alarming pace<sup>[15]</sup>. However, knowledge of MiNEN remains limited. The two cellular components of MiNEN are difficult to distinguish, especially when both are poorly differentiated, and they are often misdiagnosed as adenocarcinomas or grade 3 neuroendocrine tumors<sup>[16]</sup>. We identified MiNEN as a combination of moderately or poorly differentiated adenocarcinoma and NEC. Therefore, in addition to NET, our control group comprised patients with NEC and

Table 2 Univariate analysis of overall survival

Variable	n	Log-rank	P value
Gender		0.537	0.464
Male	31		
Female	11		
Age (yr)		4.815	0.028
< 65	17		
≥ 65	25		
Location		5.747	0.056
Stomach; Intestine	32; 8		
Pancreas	2		
Size (cm)		5.106	0.024
< 5 cm	22		
≥ 5 cm	20		
Ki-67 index		9.349	0.002
< 50%	17		
≥ 50%	25		
Proportion of the two components		9.421	0.002
NEC higher	26		
AC higher	16		
Histological grade of adenocarcinoma		11.303	0.001
Moderately differentiated	13		
Poorly differentiated	29		
Lymph node metastasis		8.800	0.003
Presence	32		
Absence	10		
Vascular tumor thrombus		12.250	< 0.001
Presence	25		
Absence	17		
Neurological recidivism		11.056	0.001
Presence	26		
Absence	16		
Distant metastasis		44.917	< 0.001
Presence	10		
Absence	32		
Clinical TNM stage		48.942	< 0.001
I + II	13		
III	19		
IV	10		

NEC: Neuroendocrine carcinomas; TNM: Tumor node metastasis.

poorly differentiated adenocarcinoma.

Most MiNEN cases develop slowly and manifest as nonspecific clinical symptoms like those of traditional adenocarcinoma. The disease, for many patients, is usually in its advanced stages by the time when a physician is consulted, and most demonstrate lymph node and distant metastasis, indicating that most conventional adenocarcinoma cases with MiNEN are characterized by aggressive behavior and a poor prognosis<sup>[7,16]</sup>. The GEP-MiNEN tumors analyzed herein were most prevalent in the stomach of the 46 patients, followed by the intestine and pancreas. We found that 58.7%, 56.5%, 74.0%, and 30.4% of the patients had nerve invasion, vascular tumor thrombus, lymph node involvement, and distant metastasis, respectively. The most common site of distant metastasis was the liver [13 (28.3%) of 46]. Lymph node involvement ( $P = 0.007$ ) and distant metastasis ( $P = 0.004$ ) were independent risk factors for the OS of patients. These results suggest that MiNEN cases have significant invasive potential.

Nie *et al*<sup>[17]</sup> suggested that the degree of differentiation of the adenocarcinoma and the neuroendocrine cancer cells of gastric MANEC affect prognosis. A lower degree of cancer cell differentiation was associated with a worse prognosis. The prognosis of patients with gastrointestinal MANEC largely depends on the stage and type of neuroendocrine components of the tumor, suggesting that NEC components comprise a key prognostic indicator<sup>[7,14,18-20]</sup>. Park *et al*<sup>[21]</sup> have suggested that gastric cancer with neuroendocrine differentiation indicates a poor prognosis, and the degree of such differentiation can serve as an independent prognostic indicator.

The neuroendocrine components of the 46 analyzed GEP-MiNEN were NEC G3, and the adenocarcinomas were either moderately differentiated or poorly differentiated. The median OS was significantly shorter for patients with poorly differentiated adenocarcinoma, compared to that observed in those with moderately differentiated adenocarcinoma (20 mo *vs* 40 mo,  $P = 0.001$ ). Furthermore, the median OS was significantly shorter in patients with major NEC compared to that in patients with major adenocarcinoma (20 mo *vs* 43 mo,  $P = 0.002$ ). Multivariate analysis selected major NEC as an independent risk factor for OS (95% CI: 1.065-11.286,  $P = 0.039$ ). This further shows that the degree of adenocarcinoma differentiation and the proportion of NEC severely impact the survival and prognosis of patients, which is consistent with the findings of previous studies<sup>[2,17,18,22,23]</sup>.

Xie *et al*<sup>[19]</sup> examined 80 patients with gastric MANEC and associated a Ki-67 index  $\geq 60\%$  with poor survival and higher recurrence rates. Milione *et al*<sup>[23]</sup> have reported that the Ki-67 index of the NEC component is the most powerful prognostic indicator, and that the risk of death is 8-fold higher in patients with Ki-67  $\geq 55\%$  than in those with Ki-67  $< 55\%$ . The median OS of our patients was significantly shorter for patients with a Ki-67 index  $\geq 50\%$  than for those with a Ki-67 index  $< 50\%$  (25 mo *vs* 43 mo,  $P = 0.002$ ). In line with previous studies, we also identified the Ki-67 index as an independent prognostic indicator of OS (95% CI: 1.466-12.459,  $P = 0.008$ ).

Among the 46 patients examined herein, 33 (71.7%) had clinical stages III and IV GEP-MiNEN at the time of diagnosis. By the end of the follow-up, 22 of these 33 patients succumbed (within an average of 20.13 mo). The median OS was significantly shorter for patients with stages III and IV, compared to that in patients with stage I + II tumors (20 mo *vs* 40 mo,  $P < 0.001$ ). Multivariate analysis showed that clinical stage was an independent risk factor for the OS of the patients (95% CI: 0.077-0.837,  $P = 0.024$ ), which was consistent with the findings of the study by Song *et al*<sup>[24]</sup>. Our findings were in line with those of a previous study in which a prognostic model based on tumor node metastasis staging combined with tumor composition ratio and Ki-67 index achieved a similar discriminative ability<sup>[19]</sup>.

Brathwaite *et al*<sup>[16]</sup> found that the prognosis was worse for MANEC than conventional adenocarcinoma and low-grade neuroendocrine tumors. Others<sup>[22]</sup> have suggested that the prognosis of gastric MANEC is worse than that of gastric adenocarcinoma. However, whether the prognosis is better for patients with gastric MANEC than NEC patients is not clear. One study found no significant differences in survival between patients with gastric and colorectal MANEC and NEC<sup>[25]</sup>. Watanabe *et al*<sup>[26]</sup> found that disease-free survival and OS rates were significantly lower among patients with MANEC than patients with adenocarcinoma. The prognosis of patients, especially those with stage III MANEC, is as poor as that of NEC patients compared with colorectal adenocarcinoma. La Rosa *et al*<sup>[27]</sup> suggested that MANEC tumors containing well-differentiated NET and adenocarcinoma components should be regarded as adenocarcinomas, while MANEC tumors containing poorly differentiated NEC components should be regarded as NEC.

We found that 34 (74.0%) of the 46 patients with MiNEN had lymph node involvement, which was slightly more than the 33 (70.2%) of the 47 patients with NEC. However, distant metastasis was more prevalent in patients with NEC than in those

**Table 3 Multivariate Cox regression analysis results of overall survival**

Variable	B	SE	Wald $\chi^2$	P value	HR	95%CI
Ki-67 index	1.452	0.546	7.078	0.008	4.273	1.466-12.459
Lymph node metastasis	1.869	0.693	7.277	0.007	6.481	1.667-25.197
Distant metastasis	-1.962	0.686	8.171	0.004	0.141	0.037-0.540
NEC/AC proportion	1.243	0.602	4.262	0.039	3.467	1.065-11.286
Clinical stage	-1.374	0.610	5.070	0.024	0.253	0.077-0.837

NEC: Neuroendocrine carcinomas; CI: Confidence interval; HR: Hazard ratio.

with MiNEN [21 (44.7%) of 47 *vs* 14 (30.4%) of 46], which was consistent with previous findings<sup>[6,28]</sup>. Furthermore, the metastatic behavior of the two types of tumors might differ; MiNEN usually involve regional lymph nodes, while NEC frequently exhibit distant metastasis, suggesting that NEC are more aggressive. We found that the median OS was significantly longer for patients with MiNEN than those with NEC (30 mo *vs* 14 mo,  $P = 0.001$ ).

Few reports have described the prognosis of patients with MiNEN and poorly differentiated adenocarcinoma. Among forty-two of the forty-six patients with GEP-MiNEN who had complete follow-up data, fourteen had distant, thirteen had liver, and one had ovarian metastases. Among the 50 out of the 58 patients with poorly differentiated adenocarcinoma who had complete follow-up data, 16 developed distant metastases to the liver ( $n = 10$ ), abdominal cavity ( $n = 4$ ), and ovaries ( $n = 2$ ), where a Klugeberg tumor formed. Sex, age, tumor size, tumor location, Ki-67 index, lymph node involvement, distant metastasis, and clinical stage did not significantly differ between patients with MiNEN and those with poorly differentiated adenocarcinoma ( $P > 0.05$  for all). Furthermore, median OS did not significantly differ between these patients (30 mo *vs* 18 mo,  $P = 0.453$ ).

Although the histological origin and molecular mechanism of MiNEN remain controversial, the findings of the existing molecular and genetic studies on MiNEN of the digestive system have shown that neuroendocrine and non-neuroendocrine components share a common monoclonal origin<sup>[29-32]</sup>. The origin of MiNEN is associated with mutations in MiNEN-related genes, including *TP53*, *BRAF*, and *KRAS*<sup>[2,16,25]</sup>, of which the *TP53* mutation is the most common<sup>[29]</sup>. Milione *et al*<sup>[23]</sup> showed a higher frequency of chromosomal and genetic abnormalities in neuroendocrine, compared to that in non-neuroendocrine components, indicating that non-neuroendocrine progression to a neuroendocrine cellular phenotype was more frequent than previously thought. Microsatellite instability might be a driving factor for the development of gastrointestinal neuroendocrine tumors<sup>[16]</sup>. Conventional colorectal adenocarcinomas and MANEC might have a common genetic profile<sup>[25]</sup>, and might respond to chemotherapy for colorectal adenocarcinoma, revealing a genetic connection between most colorectal MANEC and NET and the adenocarcinoma family.

In the absence of contraindications, the main treatment following a diagnosis of GEP-MiNEN is radical surgery. Chemotherapy is the treatment of choice for poorly differentiated, or rapidly progressing advanced tumors. Cisplatin/5-FU combined with etoposide is the most common chemotherapeutic regimen applied to treat MiNEN and is similar to those used to treat adenocarcinomas<sup>[12,31,33]</sup>. Neoadjuvant chemotherapy significantly improves the OS of patients with locally advanced NEC and MANEC in the stomach with an acceptable level of toxicity<sup>[34]</sup>. Surgical removal of each metastasis combined with systemic chemotherapy can significantly improve the prognosis of patients with colorectal MiNEN tumors that have already metastasized to distant locations<sup>[35]</sup>. An optimal combination of systemic chemotherapy and somatostatin analogs such as octreotide and lanreotide can prolong the progression-free survival of patients with metastatic neuroendocrine tumors<sup>[12]</sup>.

## CONCLUSION

Overall, GEP-MiNEN are rare and heterogeneous tumors with a highly variable prognosis for which there are no clear treatment guidelines. Although we found a



**Table 4** Comparative of mixed neuroendocrine-non-neuroendocrine neoplasms, neuroendocrine tumors, and neuroendocrine carcinomas

Variable	NET (n = 55)	NEC (n = 47)	MiNEN (n = 46)	P value	
				NET vs MiNEN	NEC vs MiNEN
Male/female	24/31	34/13	34/12	0.004	0.864
Age [yr, mean (range)]	49 (11-85)	64 (40-83)	65 (41-84)	< 0.001	0.857
Location				< 0.001	0.162
Stomach	7	26	35		
Intestine	39	15	9		
Pancreas	9	6	2		
Size [cm, mean (range)]	1.7 (0.2-11)	5.2 (1.5-16.0)	5.4 (0.5-18)	< 0.001	0.742
Ki-67 index				< 0.001	0.051
< 2%	15	2	0		
2%-20%	39	5	1		
> 20%	1	40	45		
Lymph node metastasis				< 0.001	0.691
Presence	13	33	34		
Absence	42	14	12		
Distant metastasis				< 0.001	0.156
Presence	2	21	14		
Absence	53	26	32		
Survival time (mo)				< 0.001	0.001
Median	50	14	30		
Mean	49.3	34	28.6		
Follow-up				< 0.001	0.054
Dead	3	34	27		
Alive	44	7	15		

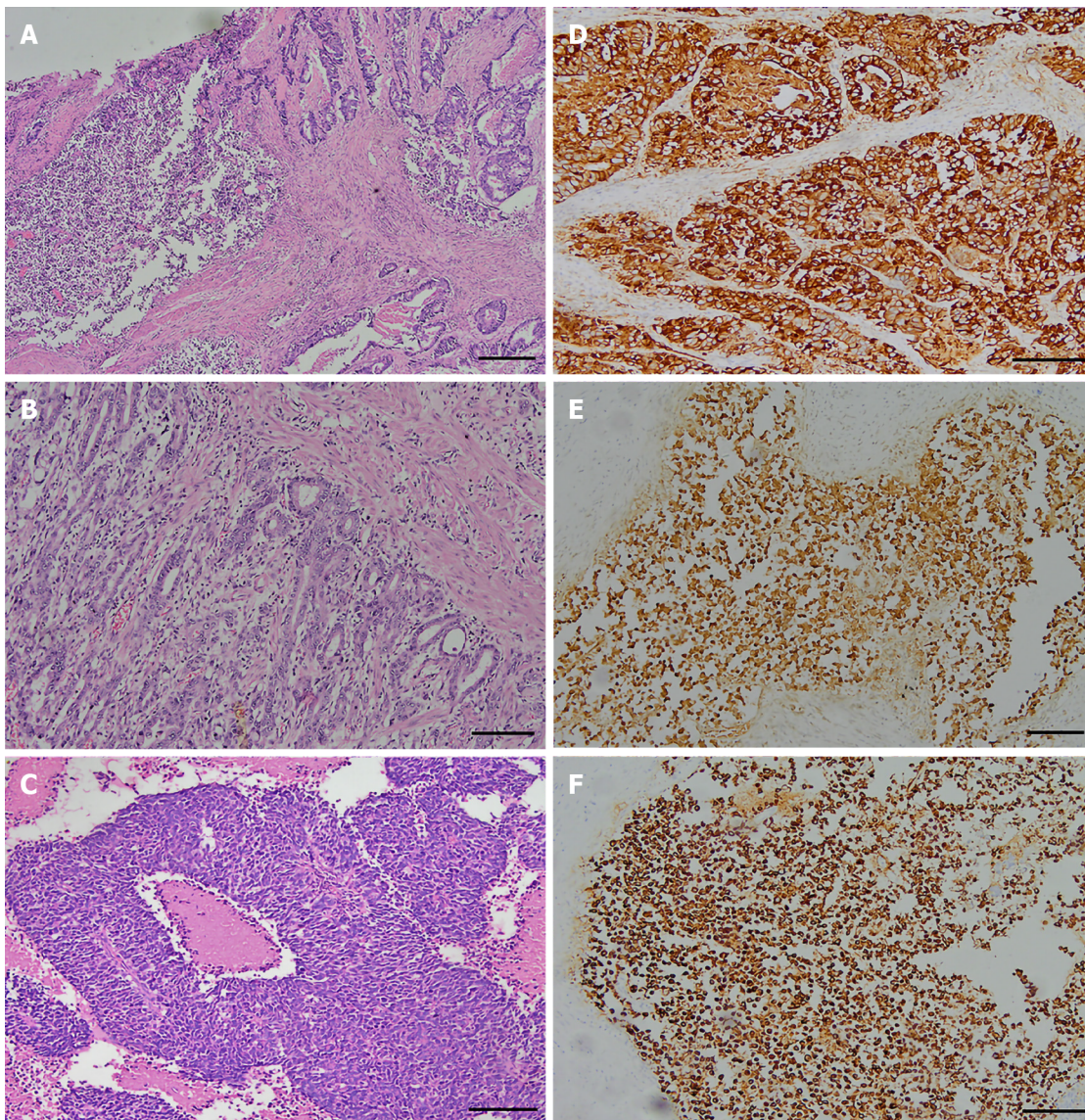
MiNEN: Mixed neuroendocrine-non-neuroendocrine neoplasms; NET: Neuroendocrine tumors; NEC: Neuroendocrine carcinomas.

worse prognosis for patients with MiNEN than for those with NEC, it did not significantly differ from that of patients with poorly differentiated adenocarcinoma. Thus, patients with GEP-MiNEN and those with adenocarcinoma should be similarly treated. Furthermore, the treatment of any suspected or diagnosed GEP-MiNEN patient should be discussed at a multidisciplinary expert meeting to determine optimal personalized treatment for individual patients. The number of patients in the present retrospective study was limited by the rarity of GEP-MiNEN, and they were sourced from a single institution. Therefore, further multicenter, larger-cohort studies are warranted to clarify the clinicopathological features and biological behavior of GEP-MiNEN.

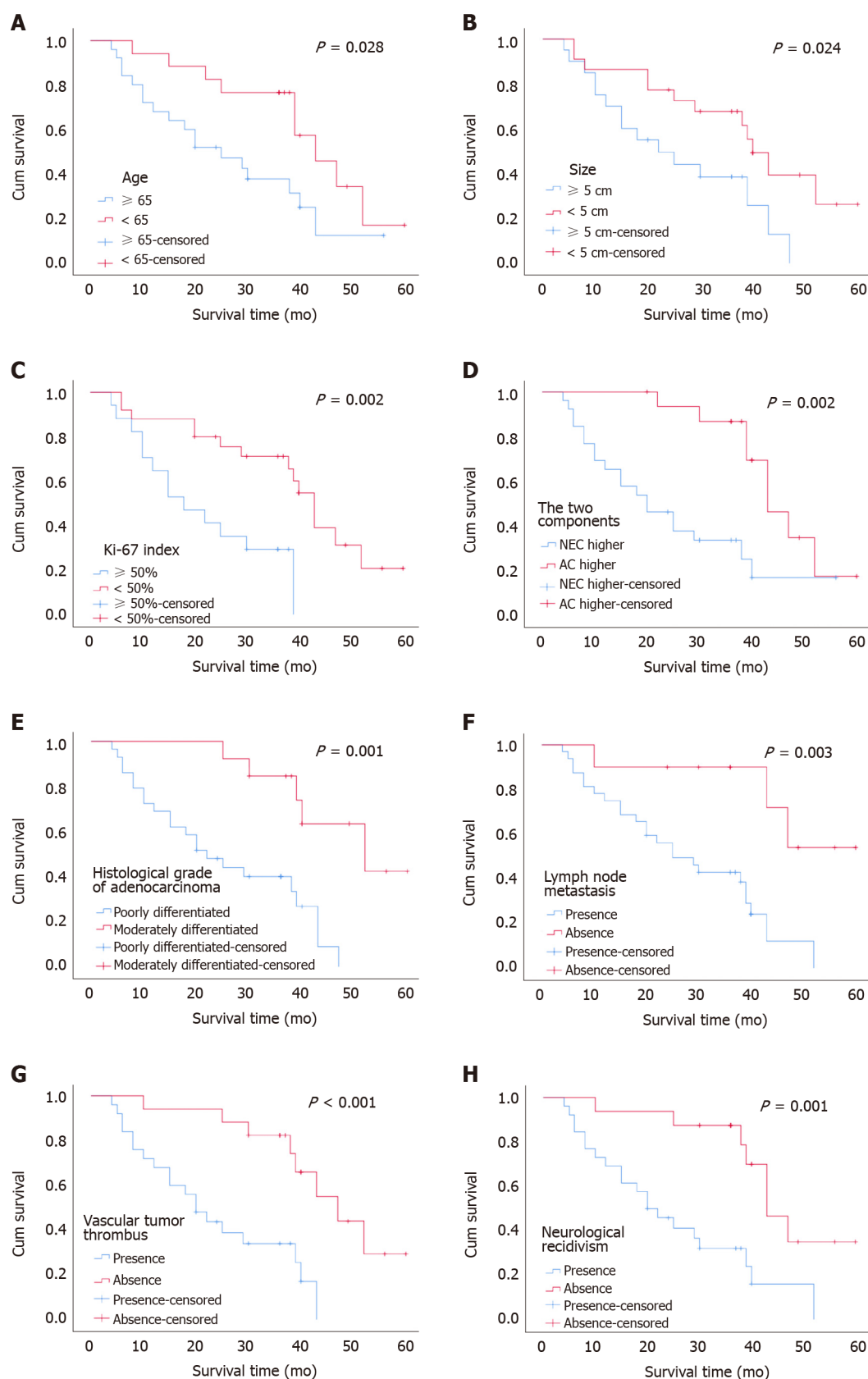
**Table 5 Comparison between patients with mixed neuroendocrine-non-neuroendocrine neoplasms and those with poorly differentiated adenocarcinoma**

Variable	Poorly differentiated adenocarcinoma (n = 58)	MiNEN (n = 46)	P value
Male/female	37/21	34/12	0.271
Mean age, years, (range)	61 (31-81)	65 (41-84)	0.055
Location			0.836
Stomach	42	35	
Intestine	12	9	
Pancreas	4	2	
Size (cm)			0.254
< 5	25	25	
≥ 5	33	21	
Ki- 67 index			0.104
< 50%	13	17	
≥ 50%	45	29	
Lymph node metastasis			0.385
Presence	47	34	
Absence	11	12	
Distant metastasis			0.750
Presence	16	14	
Absence	42	32	
Clinical TNM stage			0.402
I + II	10	13	
III	34	23	
IV	14	10	
Survival time (mo)			0.453
Median	18	30	
Mean	24.3	28.6	
Follow-up			0.863
Dead	33	27	
Alive	17	15	

MiNEN: Mixed neuroendocrine-non-neuroendocrine neoplasms; TNM: Tumor node metastasis.



**Figure 1** Histopathological and immunohistochemical findings of gastroenteropancreatic mixed neuroendocrine-non-neuroendocrine neoplasms. A: Neuroendocrine carcinoma (left) and adenocarcinoma (right) (Hematoxylin-eosin staining, scale bar 200  $\mu$ m); B: Adenocarcinoma component (Hematoxylin-eosin staining, scale bar 200  $\mu$ m); C: Neuroendocrine component (Hematoxylin-eosin staining, scale bar 100  $\mu$ m); D: Cytokeratin-positive adenocarcinoma (EnVision, scale bar 100  $\mu$ m); E: CgA-positive neuroendocrine (EnVision, scale bar 100  $\mu$ m); F: Syn-positive neuroendocrine (EnVision, scale bar 100  $\mu$ m).





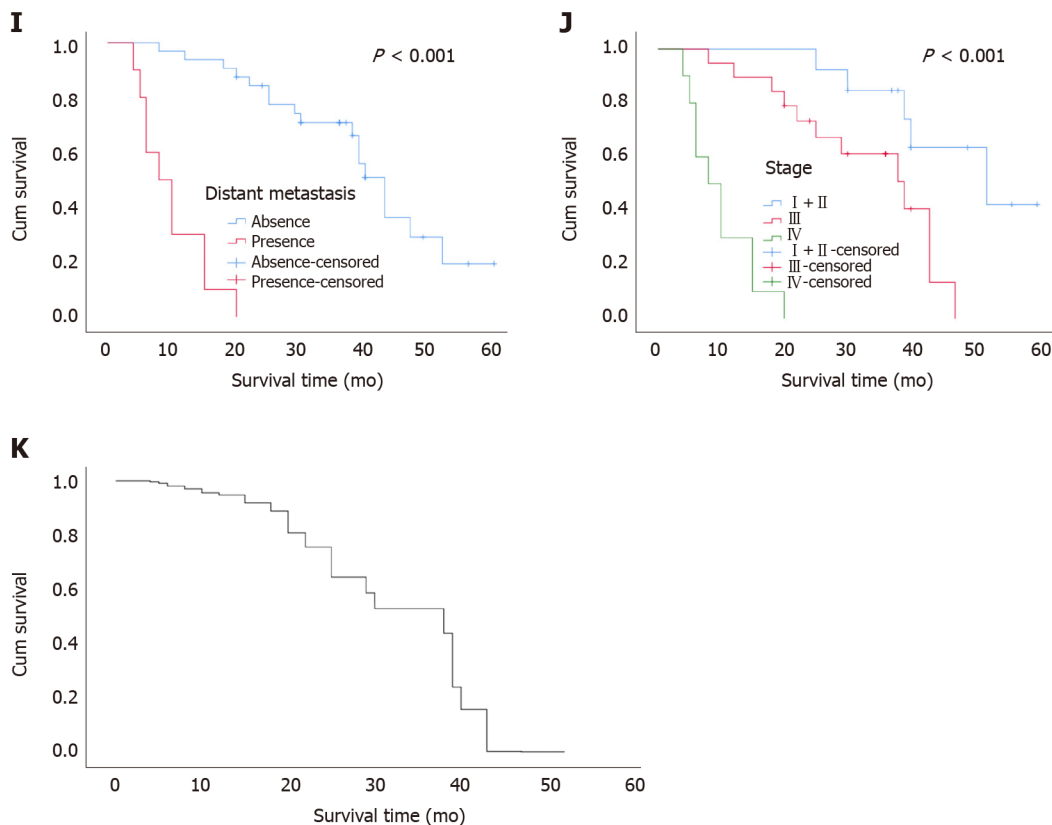


**Figure 2** Kaplan-Meier curves of overall survival among 46 patients with gastroenteropancreatic mixed neuroendocrine-non-neuroendocrine neoplasms. Overall survival grouped by A: Age ( $P = 0.028$ ); B: Tumor size ( $P = 0.024$ ); C: Ki-67 index ( $P = 0.002$ ); D: Proportions of NEC and adenocarcinoma ( $P = 0.002$ ); E: Adenocarcinoma differentiation ( $P = 0.001$ ); F: Lymph node metastasis ( $P = 0.003$ ); G: Vascular tumor thrombus ( $P < 0.001$ ); H: Nerve invasion ( $P = 0.001$ ); I: Distant metastasis ( $P < 0.001$ ); and J: Clinical stage ( $P < 0.001$ ); K: Overall survival of 46 patients with gastroenteropancreatic mixed neuroendocrine-non-neuroendocrine neoplasms.

## ARTICLE HIGHLIGHTS

### Research background

Mixed neuroendocrine-non-neuroendocrine neoplasms (MiNEN) are a rare tumor type. However, their prevalence might be largely underestimated due to diagnostic limitations and insufficient scientific understanding. The clinical manifestations, treatment, and prognosis of this type of tumor are still poorly understood. Our research on the risk factors, clinical manifestations, and prognosis related to this rare tumor type is of great significance for optimizing clinical treatment.

### Research motivation

MiNEN associated risk factors, clinical manifestations, and prognosis must be explored to improve our understanding of this rare tumor type and optimize clinical treatment.

### Research objectives

We have identified the risk factors that influence the prognosis of patients with gastroenteropancreatic MiNEN (GEP-MiNEN). We also compared prognostic differences between GEP-MiNEN and gastroenteropancreatic neuroendocrine tumors, neuroendocrine carcinomas (NEC), and poorly differentiated adenocarcinoma to improve the understanding of GEP-MiNEN and to guide future clinical treatment.

### Research methods

This is a single-center, retrospective study. We retrospectively analyzed the clinical data of patients who were diagnosed with GEP-MiNEN. Risk factors influencing patient prognosis were assessed using Kaplan-Meier curves and Cox regression models. We compared the results with randomly selected patients with gastroenteropancreatic neuroendocrine tumors, NEC, and poorly differentiated adeno-



carcinomas.

### Research results

Most GEP-MiNEN in our study were gastric tumors, a few were intestinal tumors, and a minority, pancreatic tumors. The median overall survival was 30 mo. Ki-67 index  $\geq 50\%$ , high proportion of NEC, lymph node involvement, distant metastasis, and higher clinical stage were independent risk factors affecting the prognosis of patients with GEP-MiNEN. The median overall survival was shorter for patients with NEC than for those with MiNEN but did not significantly differ from those with poorly differentiated adenocarcinoma and MiNEN. Thus, patients with GEP-MiNEN and those with adenocarcinoma should be similarly treated. Furthermore, the treatment of any suspected or diagnosed GEP-MiNEN patient should be discussed at a multidisciplinary expert meeting to determine optimal personalized treatment. However, the number of patients in the present retrospective study was limited by the rarity of GEP-MiNEN, and they were sourced from a single institution. Therefore, further multicenter, larger-cohort studies are warranted to clarify the clinicopathological features and biological behavior of GEP-MiNEN.

### Research conclusions

A poor prognosis is associated with GEP-MiNEN. Ki-67 index, tumor composition, lymph node involvement, distant metastasis, and clinical stage are important factors for patient prognosis.

### Research perspectives

In view of the limited number of patients and the short-term follow-up of our study, a larger prospective study with long-term follow-up is needed to confirm our results.

## ACKNOWLEDGEMENTS

We would like to thank Dr. Lian-Guo Fu for significant contributions to data analysis.

## REFERENCES

- 1 **de Mestier L**, Cros J, Neuzillet C, Hentic O, Egal A, Muller N, Bouché O, Cadiot G, Ruszniewski P, Couvelard A, Hammel P. Digestive System Mixed Neuroendocrine-Non-Neuroendocrine Neoplasms. *Neuroendocrinology* 2017; **105**: 412-425 [PMID: 28803232 DOI: 10.1159/000475527]
- 2 **Frizziero M**, Chakrabarty B, Nagy B, Lamarca A, Hubner RA, Valle JW, McNamara MG. Mixed Neuroendocrine Non-Neuroendocrine Neoplasms: A Systematic Review of a Controversial and Underestimated Diagnosis. *J Clin Med* 2020; **9** [PMID: 31963850 DOI: 10.3390/jcm9010273]
- 3 **Merola E**, Zandee WT, de Mestier L, Klumpen HJ, Makulik K, Geboes K, van Velthuisen ML, Couvelard A, Cros J, van Eeden S, Hoorens A, Stephenson T, Zajęcki W, de Herder W, Munir A. Histopathological Revision for Gastro-Entero-Pancreatic Neuroendocrine Neoplasms in Expert Centers: Does it Make the Difference? *Neuroendocrinology* 2020 [DOI: 10.1159/000507082]
- 4 **Assarzadegan N**, Montgomery E. What is New in 2019 World Health Organization (WHO) Classification of Tumors of the Digestive System: Review of Selected Updates on Neuroendocrine Neoplasms, Appendiceal Tumors, and Molecular Testing. *Arch Pathol Lab Med* 2020 [PMID: 32233993 DOI: 10.5858/arpa.2019-0665-RA]
- 5 **La Rosa S**, Sessa F, Uccella S. Mixed Neuroendocrine-Nonneuroendocrine Neoplasms (MiNENs): Unifying the Concept of a Heterogeneous Group of Neoplasms. *Endocr Pathol* 2016; **27**: 284-311 [PMID: 27169712 DOI: 10.1007/s12022-016-9432-9]
- 6 **Oneda E**, Liserre B, Bianchi D, Rota L, Savelli G, Zorzi F, Zaniboni A. Diagnosis of Mixed Adenoneuroendocrine Carcinoma (MANEC) after Neoadjuvant Chemotherapy for Pancreatic and Gastric Adenocarcinoma: Two Case Reports and a Review of the Literature. *Case Rep Oncol* 2019; **12**: 434-442 [PMID: 31275134 DOI: 10.1159/000501200]
- 7 **Pham QD**, Mori I, Osamura RY. A Case Report: Gastric Mixed Neuroendocrine-Nonneuroendocrine Neoplasm with Aggressive Neuroendocrine Component. *Case Rep Pathol* 2017; **2017**: 9871687 [PMID: 28626594 DOI: 10.1155/2017/9871687]
- 8 **Qiu S**, Pellino G, Warren OJ, Mills S, Goldin R, Kontovounisios C, Tekkis PP. Mixed adenoneuroendocrine carcinoma of the colon and rectum. *Acta Chir Belg* 2018; **118**: 273-277 [PMID: 29911510 DOI: 10.1080/00015458.2018.1482697]
- 9 **Bosman FT**. International Agency for Research on Cancer: WHO Classification of Tumours of the Digestive System, 4th ed. Lyon. IARC, 2010
- 10 **Inzani F**, Petrone G, Rindi G. The New World Health Organization Classification for Pancreatic

- Neuroendocrine Neoplasia. *Endocrinol Metab Clin North Am* 2018; **47**: 463-470 [PMID: 30098710 DOI: 10.1016/j.ecl.2018.04.008]
- 11 Nagtegaal ID, Odze RD, Klimstra D, Paradis V, Rugge M, Schirmacher P, Washington KM, Carneiro F, Cree IA; WHO Classification of Tumours Editorial Board. The 2019 WHO classification of tumours of the digestive system. *Histopathology* 2020; **76**: 182-188 [PMID: 31433515 DOI: 10.1111/his.13975]
  - 12 Skalický A, Višejnová L, Dubová M, Malkus T, Skalický T, Troup O. Mixed neuroendocrine-non-neuroendocrine carcinoma of gallbladder: case report. *World J Surg Oncol* 2019; **17**: 55 [PMID: 30902091 DOI: 10.1186/s12957-019-1598-4]
  - 13 Di Palma S, Mufaddal M, Iyer V, Sciarra A, La Rosa S. Does Mixed Neuroendocrine-Nonneuroendocrine Neoplasm (MiNEN) of the Parathyroid Gland Exist? *Head Neck Pathol* 2020 [PMID: 32506375 DOI: 10.1007/s12105-020-01178-4]
  - 14 Frizziero M, Wang X, Chakrabarty B, Childs A, Luong TV, Walter T, Khan MS, Morgan M, Christian A, Elshafie M, Shah T, Minicozzi A, Mansoor W, Meyer T, Lamarca A, Hubner RA, Valle JW, McNamara MG. Retrospective study on mixed neuroendocrine non-neuroendocrine neoplasms from five European centres. *World J Gastroenterol* 2019; **25**: 5991-6005 [PMID: 31660035 DOI: 10.3748/wjg.v25.i39.5991]
  - 15 Wang J, He A, Feng Q, Hou P, Wu J, Huang Z, Xiao Z, Sun C, Liao W, Wu L. Gastrointestinal mixed adenoneuroendocrine carcinoma: a population level analysis of epidemiological trends. *J Transl Med* 2020; **18**: 128 [PMID: 32169074 DOI: 10.1186/s12967-020-02293-0]
  - 16 Brathwaite SA, Smith SM, Wai L, Frankel W, Hays J, Yearsley MM, Abdel-Misih S. Mixed adenoneuroendocrine carcinoma: A review of pathologic characteristics. *Hum Pathol* 2018; **73**: 184-191 [PMID: 29288693 DOI: 10.1016/j.humpath.2017.12.009]
  - 17 Nie L, Li M, He X, Feng A, Wu H, Fan X. Gastric mixed adenoneuroendocrine carcinoma: correlation of histologic characteristics with prognosis. *Ann Diagn Pathol* 2016; **25**: 48-53 [PMID: 27806846 DOI: 10.1016/j.anndiagpath.2016.09.004]
  - 18 Harada K, Sato Y, Ikeda H, Maylee H, Igarashi S, Okamura A, Masuda S, Nakanuma Y. Clinicopathologic study of mixed adenoneuroendocrine carcinomas of hepatobiliary organs. *Virchows Arch* 2012; **460**: 281-289 [PMID: 22358181 DOI: 10.1007/s00428-012-1212-4]
  - 19 Xie JW, Lu J, Wang JB, Lin JX, Chen QY, Cao LL, Lin M, Tu RH, Huang ZN, Lin JL, Zheng CH, Li P, Huang CM. Prognostic factors for survival after curative resection of gastric mixed adenoneuroendocrine carcinoma: a series of 80 patients. *BMC Cancer* 2018; **18**: 1021 [PMID: 30348122 DOI: 10.1186/s12885-018-4943-z]
  - 20 Zheng SL, Yip VS, Pedica F, Prachalias A, Quaglia A. Intrahepatic bile duct mixed adenoneuroendocrine carcinoma: a case report and review of the literature. *Diagn Pathol* 2015; **10**: 204 [PMID: 26589730 DOI: 10.1186/s13000-015-0439-1]
  - 21 Park JY, Ryu MH, Park YS, Park HJ, Ryoo BY, Kim MG, Yook JH, Kim BS, Kang YK. Prognostic significance of neuroendocrine components in gastric carcinomas. *Eur J Cancer* 2014; **50**: 2802-2809 [PMID: 25201164 DOI: 10.1016/j.ejca.2014.08.004]
  - 22 Sun L, Zhang J, Wang C, Zhao S, Shao B, Guo Y, Liu Y, Sun Y. Chromosomal and molecular pathway alterations in the neuroendocrine carcinoma and adenocarcinoma components of gastric mixed neuroendocrine-nonneuroendocrine neoplasm. *Mod Pathol* 2020; **33**: 2602-2613 [PMID: 32461621 DOI: 10.1038/s41379-020-0579-z]
  - 23 Milione M, Maisonneuve P, Pellegrinelli A, Grillo F, Albarello L, Spaggiari P, Vanoli A, Tagliabue G, Pisa E, Messerini L, Centonze G, Inzani F, Scarpa A, Papotti M, Volante M, Sessa F, Fazio N, Pruneri G, Rindi G, Solcia E, La Rosa S, Capella C. Ki67 proliferative index of the neuroendocrine component drives MANEC prognosis. *Endocr Relat Cancer* 2018; **25**: 583-593 [PMID: 29592868 DOI: 10.1530/ERC-17-0557]
  - 24 Song LJ, Yuan L. Comparative analysis of colorectal mixed adenoneuroendocrine carcinoma and adenocarcinoma with neuroendocrine differentiation: a population-based study. *Int J Clin Exp Pathol* 2019; **12**: 922-932 [PMID: 31933902]
  - 25 Jesinghaus M, Konukiewicz B, Keller G, Kloor M, Steiger K, Reiche M, Penzel R, Endris V, Arsenic R, Hermann G, Stenzinger A, Weichert W, Pfarr N, Klöppel G. Colorectal mixed adenoneuroendocrine carcinomas and neuroendocrine carcinomas are genetically closely related to colorectal adenocarcinomas. *Mod Pathol* 2017; **30**: 610-619 [PMID: 28059096 DOI: 10.1038/modpathol.2016.220]
  - 26 Watanabe J, Suwa Y, Ota M, Ishibe A, Masui H, Nagahori K, Tsuura Y, Endo I. Clinicopathological and Prognostic Evaluations of Mixed Adenoneuroendocrine Carcinoma of the Colon and Rectum: A Case-Matched Study. *Dis Colon Rectum* 2016; **59**: 1160-1167 [PMID: 27824701 DOI: 10.1097/DCR.0000000000000702]
  - 27 La Rosa S, Marando A, Sessa F, Capella C. Mixed Adenoneuroendocrine Carcinomas (MANECs) of the Gastrointestinal Tract: An Update. *Cancers (Basel)* 2012; **4**: 11-30 [PMID: 24213223 DOI: 10.3390/cancers4010011]
  - 28 Zhang P, Wang W, Lu M, Zeng C, Chen J, Li E, Tan H, Wang W, Yu X, Tang Q, Zhao J, Shen L, Li J. Clinicopathological features and outcome for neuroendocrine neoplasms of gastroesophageal junction: A population-based study. *Cancer Med* 2018; **7**: 4361-4370 [PMID: 30062861 DOI: 10.1002/cam4.1702]
  - 29 Scardoni M, Vittoria E, Volante M, Rusev B, Bersani S, Mafficini A, Gottardi M, Giandomenico V, Malleo G, Butturini G, Cingarlini S, Fassan M, Scarpa A. Mixed adenoneuroendocrine carcinomas of

- the gastrointestinal tract: targeted next-generation sequencing suggests a monoclonal origin of the two components. *Neuroendocrinology* 2014; **100**: 310-316 [PMID: [25342539](#) DOI: [10.1159/000369071](#)]
- 30 **Paniz Mondolfi AE**, Slova D, Fan W, Attiyeh FF, Afthinos J, Reidy J, Pang Y, Theise ND. Mixed adenoneuroendocrine carcinoma (MANEC) of the gallbladder: a possible stem cell tumor? *Pathol Int* 2011; **61**: 608-614 [PMID: [21951672](#) DOI: [10.1111/j.1440-1827.2011.02709.x](#)]
  - 31 **Gurzu S**, Fetyko A, Bara T, Banias L, Butiurca VO, Bara T Jr, Tudorache V, Jung I. Gastrointestinal mixed adenoneuroendocrine carcinoma (MANEC): An immunohistochemistry study of 13 microsatellite stable cases. *Pathol Res Pract* 2019; **215**: 152697 [PMID: [31704155](#) DOI: [10.1016/j.prp.2019.152697](#)]
  - 32 **Nassereddine H**, Poté N, Théou-Anton N, Lamoureux G, Fléjou JF, Couvelard A. A gastric MANEC with an adenocarcinoma of fundic-gland type as exocrine component. *Virchows Arch* 2017; **471**: 673-678 [PMID: [28653202](#) DOI: [10.1007/s00428-017-2178-z](#)]
  - 33 **Zhang M**, Zhao P, Shi X, Zhao A, Zhang L, Zhou L. Clinicopathological features and prognosis of gastroenteropancreatic neuroendocrine neoplasms in a Chinese population: a large, retrospective single-centre study. *BMC Endocr Disord* 2017; **17**: 39 [PMID: [28705205](#) DOI: [10.1186/s12902-017-0190-6](#)]
  - 34 **Ma F**, Wang B, Xue L, Kang W, Li Y, Li W, Liu H, Ma S, Tian Y. Neoadjuvant chemotherapy improves the survival of patients with neuroendocrine carcinoma and mixed adenoneuroendocrine carcinoma of the stomach. *J Cancer Res Clin Oncol* 2020; **146**: 2135-2142 [PMID: [32306127](#) DOI: [10.1007/s00432-020-03214-w](#)]
  - 35 **Kanazawa Y**, Kikuchi M, Imai Y, Katakami N, Kaihara S, Shinohara S. Successful Treatment of a Mixed Neuroendocrine-Nonneuroendocrine Neoplasm of the Colon with Metastases to the Thyroid Gland and Liver. *Case Rep Otolaryngol* 2020; **2020**: 5927610 [PMID: [32099708](#) DOI: [10.1155/2020/5927610](#)]



Retrospective Study

## Effect of liver inflammation on accuracy of FibroScan device in assessing liver fibrosis stage in patients with chronic hepatitis B virus infection

Ling-Ling Huang, Xue-Ping Yu, Ju-Lan Li, Hui-Ming Lin, Na-Ling Kang, Jia-Ji Jiang, Yue-Yong Zhu, Yu-Rui Liu, Da-Wu Zeng

**ORCID number:** Ling-Ling Huang 0000-0001-9307-9181; Xue-Ping Yu 0000-0002-1157-2501; Ju-Lan Li 0000-0003-4222-2966; Hui-Ming Lin 0000-0002-1312-8703; Na-Ling Kang 0000-0001-6923-5754; Jia-Ji Jiang 0000-0003-0637-7653; Yue-Yong Zhu 0000-0002-0746-4911; Yu-Rui Liu 0000-0003-0553-846X; Da-Wu Zeng 0000-0003-3818-0062.

**Author contributions:** Huang LL, Liu YR, Yu XP, Li JL contributed equally to this work; Huang LL, Zeng DW and Liu YR conceived and designed the experiments; Huang LL, Jiang JJ and Zeng DW performed the experiments; Huang LL, Yu XP, Zeng DW and Zhu YY analyzed the data; Li JL, Lin HM and Kang NL contributed the reagents/materials/analysis tools; Huang LL and Zeng DW wrote the manuscript; all authors approved the final version of the manuscript.

**Supported by** Science and Technology Department of Fujian Province, China, No. 2019Y0015 and No. 2019J01432; Chinese National 13<sup>th</sup> Five-Year Plan's Science and Technology Projects, No. 2017ZX10202201; Quanzhou Science and Technology Project of Fujian Province, China, No.

Ling-Ling Huang, Hui-Ming Lin, Na-Ling Kang, Jia-Ji Jiang, Yue-Yong Zhu, Yu-Rui Liu, Da-Wu Zeng, Department of Hepatology, Hepatology Research Institute, The First Affiliated Hospital, Fujian Medical University, Fuzhou 350005, Fujian Province, China

Xue-Ping Yu, Ju-Lan Li, Department of Infectious Diseases, The First Hospital of Quanzhou Affiliated to Fujian Medical University, Quanzhou 362000, Fujian Province, China

Yue-Yong Zhu, Fujian Key Laboratory of Precision Medicine for Cancer, Fujian Key Laboratory of Laboratory Medicine, The First Affiliated Hospital, Fujian Medical University, Fuzhou 350005, Fujian Province, China

**Corresponding author:** Da-Wu Zeng, MD, PhD, Associate Chief Physician, Doctor, Department of Hepatology, Hepatology Research Institute, The First Affiliated Hospital, Fujian Medical University, No. 20 Chazhong Road, Taijiang District, Fuzhou 350005, Fujian Province, China. [zengdw1980@fjmu.edu.cn](mailto:zengdw1980@fjmu.edu.cn)

### Abstract

#### BACKGROUND

Transient elastography (FibroScan) is a new and non-invasive test, which has been widely recommended by the guidelines of chronic hepatitis B virus (HBV) management for assessing hepatic fibrosis staging. However, some confounders may affect the diagnostic accuracy of the FibroScan device in fibrosis staging.

#### AIM

To evaluate the diagnostic value of the FibroScan device and the effect of hepatic inflammation on the accuracy of FibroScan in assessing the stage of liver fibrosis in patients with HBV infection.

#### METHODS

The data of 416 patients with chronic HBV infection who accepted FibroScan, liver biopsy, clinical, and biological examination were collected from two hospitals retrospectively. Receiver operating characteristic (ROC) curves were used to analyze the diagnostic performance of FibroScan for assessing the stage of liver fibrosis. Any discordance in fibrosis staging by FibroScan and pathological scores was statistically analyzed. Logistic regression and ROC analyses were used to

2018Z074.

**Institutional review board**

**statement:** This study was approved by the Institutional Review Board of Fujian Medical University.

**Informed consent statement:** The need for informed consent was waived due to the retrospective nature of the study.

**Conflict-of-interest statement:** We have no financial relationships to disclose.

**Open-Access:** This article is an open-access article which was selected by an in-house editor and fully peer-reviewed by external reviewers. It is distributed in accordance with the Creative Commons Attribution Non Commercial (CC BY-NC 4.0) license, which permits others to distribute, remix, adapt, build upon this work non-commercially, and license their derivative works on different terms, provided the original work is properly cited and the use is non-commercial. See: <http://creativecommons.org/licenses/by-nc/4.0/>

**Manuscript source:** Unsolicited manuscript

**Specialty type:** Gastroenterology and hepatology

**Country/Territory of origin:** China

**Peer-review report's scientific quality classification**

Grade A (Excellent): 0  
Grade B (Very good): 0  
Grade C (Good): C  
Grade D (Fair): 0  
Grade E (Poor): 0

**Received:** November 26, 2020

**Peer-review started:** November 26, 2020

**First decision:** December 21, 2020

**Revised:** December 30, 2020

**Accepted:** January 13, 2021

**Article in press:** January 13, 2021

**Published online:** February 21, 2021

**P-Reviewer:** Izumi N

**S-Editor:** Fan JR

**L-Editor:** Webster JR

analyze the accuracy of FibroScan in assessing the stage of fibrosis in patients with different degrees of liver inflammation. A non-invasive model was constructed to predict the risk of misdiagnosis of fibrosis stage using FibroScan.

**RESULTS**

In the overall cohort, the optimal diagnostic values of liver stiffness measurement (LSM) using FibroScan for significant fibrosis ( $\geq F2$ ), severe fibrosis ( $\geq F3$ ), and cirrhosis (F4) were 7.3 kPa [area under the curve (AUC) = 0.863], 9.7 kPa (AUC = 0.911), and 11.3 kPa (AUC = 0.918), respectively. The rate of misdiagnosis of fibrosis stage using FibroScan was 34.1% (142/416 patients). The group of patients who showed discordance between fibrosis staging using FibroScan and pathological scores had significantly higher alanine aminotransferase and aspartate aminotransferase levels, and a higher proportion of moderate to severe hepatic inflammation, compared with the group of patients who showed concordance in fibrosis staging between the two methods. Liver inflammation activity over 2 (OR = 3.53) was an independent risk factor for misdiagnosis of fibrosis stage using FibroScan. Patients with liver inflammation activity  $\geq 2$  showed higher LSM values using FibroScan and higher rates of misdiagnosis of fibrosis stage, whereas the diagnostic performance of FibroScan for different fibrosis stages was significantly lower than that in patients with inflammation activity  $< 2$  (all  $P < 0.05$ ). A non-invasive prediction model was established to assess the risk of misdiagnosis of fibrosis stage using FibroScan, and the AUC was 0.701.

**CONCLUSION**

Liver inflammation was an independent risk factor affecting the diagnostic accuracy of FibroScan for fibrosis stage. A combination of other related non-invasive factors can predict the risk of misdiagnosis of fibrosis staging using FibroScan.

**Key Words:** Liver stiffness measurement; Fibrosis stage; Liver inflammation; Hepatitis B virus; FibroScan; Predictive model

©The Author(s) 2021. Published by Baishideng Publishing Group Inc. All rights reserved.

**Core Tip:** Transient elastography (FibroScan) is a recommended non-invasive test for evaluation of liver fibrosis in patients with chronic hepatitis B virus (HBV) infection. In this study, we demonstrated the good performance of FibroScan in predicting liver fibrosis staging. However, we found discordance between Fibroscan fibrosis staging and pathological score. Liver inflammation was an independent risk factor affecting the accuracy of FibroScan assessing HBV-related liver fibrosis staging. The combination of other related non-invasive factors can predict the risk of FibroScan staging misdiagnosis, and may be helpful for guiding the diagnosis and therapy of chronic HBV infection.

**Citation:** Huang LL, Yu XP, Li JL, Lin HM, Kang NL, Jiang JJ, Zhu YY, Liu YR, Zeng DW. Effect of liver inflammation on accuracy of FibroScan device in assessing liver fibrosis stage in patients with chronic hepatitis B virus infection. *World J Gastroenterol* 2021; 27(7): 641-653

**URL:** <https://www.wjgnet.com/1007-9327/full/v27/i7/641.htm>

**DOI:** <https://dx.doi.org/10.3748/wjg.v27.i7.641>

**INTRODUCTION**

Approximately 248 million individuals worldwide have been infected with chronic hepatitis B virus (HBV)<sup>[1]</sup>, which can develop into hepatic failure, cirrhosis, and tumorigenesis, causing nearly 650000 deaths every year<sup>[2]</sup>. Hepatic fibrosis is an intermediate stage in the progression of chronic hepatic disease from mild hepatitis to decompensated cirrhosis<sup>[2,3]</sup>. Therefore, timely and accurate assessment of hepatic



P-Editor: Ma YJ



fibrosis stage is helpful to determine the optimal treatment plan, so as to minimize and delay the progression of liver injury<sup>[3,4]</sup>. Although liver biopsy is the gold standard for evaluating the stage of liver fibrosis, it is invasive, expensive, and accompanied by potential complications and sampling errors<sup>[5]</sup>. Transient elastography (FibroScan) is a new non-invasive test<sup>[3,6]</sup> that can replace biopsy, and it has been widely recommended by the guidelines on HBV management for assessing the stage of hepatic fibrosis<sup>[4]</sup>. Therefore, considering liver biopsy only in patients at a high fibrosis stage could minimize unnecessary biopsies.

The Society of Radiologists in Ultrasound consensus statement on liver elastography indicated that liver stiffness measurement (LSM) obtained using ultrasound elastography is associated with the degree of hepatic fibrosis<sup>[7]</sup>. However, increased LSM values as per transient elastography in acute hepatitis do not actually reflect the grade of liver fibrosis. During an acute attack of chronic liver disease, LSM values are affected by liver inflammatory activity indices such as serum total bilirubin (TBIL) and alanine aminotransferase (ALT), which may overestimate the liver fibrosis stage. The 2019 Chinese guidelines for chronic hepatitis B and the non-invasive liver fibrosis guidelines of the European Society and Latin American Society of Hepatology indicated that the diagnostic cutoffs of LSM should be adapted to ALT levels that assess the stage of HBV-related fibrosis<sup>[8,9]</sup>. In clinical practice, elevated ALT levels in many patients with chronic hepatic disease reflect hepatic inflammatory injury. Many studies have suggested that the cutoff value of LSM tends to increase and its diagnostic accuracy tends to decrease with elevated ALT level<sup>[10,11]</sup>; however, whether pathological hepatic inflammation would similarly affect cutoff values and the diagnostic accuracy of LSM in assessing the stage of hepatic fibrosis remains unclear.

In this study, we aimed to investigate in detail the impact of liver inflammation on LSM values and the diagnostic performance of FibroScan in assessing the stage of fibrosis in patients with chronic HBV infection.

## MATERIALS AND METHODS

### Research population

The study protocol was approved by the Institutional Review Board of Fujian Medical University, Fuzhou, China, and the need for written informed consent from patients was waived owing to the retrospective nature of the study. As shown in **Figure 1**, a total of 416 patients aged 18 years and above with chronic HBV infection who consented to undergo FibroScan and liver biopsy were enrolled in The First Affiliated Hospital of Fujian Medical University, and The First Hospital of Quanzhou Affiliated to Fujian Medical University between January 2014 and December 2019. Chronic HBV infection was defined as the persistent presence of hepatitis B surface antigen (HBsAg) and HBV-DNA in the serum for more than 6 mo. Patients with other types of hepatitis virus infections; those with body mass index (BMI) > 28 kg/m<sup>2</sup>; those with fatty liver disease, alcoholic liver disease, drug-induced liver disease, autoimmune liver disease, genetic, or metabolic disease; those with decompensated cirrhosis, malignant tumors, or severe extrahepatic disease or pregnancy; and those with unreliable LSM values by FibroScan were excluded. Patients with hepatic steatosis by histology of liver biopsy were also excluded. All patients were examined using FibroScan, and fasting venous blood samples were collected for routine clinical examination within 1 wk of liver biopsy.

### Clinical and laboratory parameters

Information regarding the following clinical parameters was collected: Patient age, sex, weight, height, status of alcohol consumption, and history of HBV infection. The BMI was calculated as weight (kg)/height<sup>2</sup> (m<sup>2</sup>). Serum samples were collected after the patients fasted for 8 h at night, for the following measurements: HBsAg, hepatitis B envelope antigen (HBeAg), HBV-DNA, TBIL, ALT, aspartate aminotransferase (AST), albumin (ALB), prothrombin time (PT), platelet (PLT), and alpha-fetoprotein.

### Liver stiffness measurement by FibroScan

LSM was performed using FibroScan 502 (Echosens, Paris, France). The detection method was followed as per the user manual, and the monitoring points were selected from the right anterior axillary line to the axillary midline 7, 8 or 8, 9 intercostals of the patient. The LSM values could be considered reliable when at least 10 valid measurements yielded a success rate of more than 60% and the interquartile range/median was less than 30%. The median value was determined as the final result

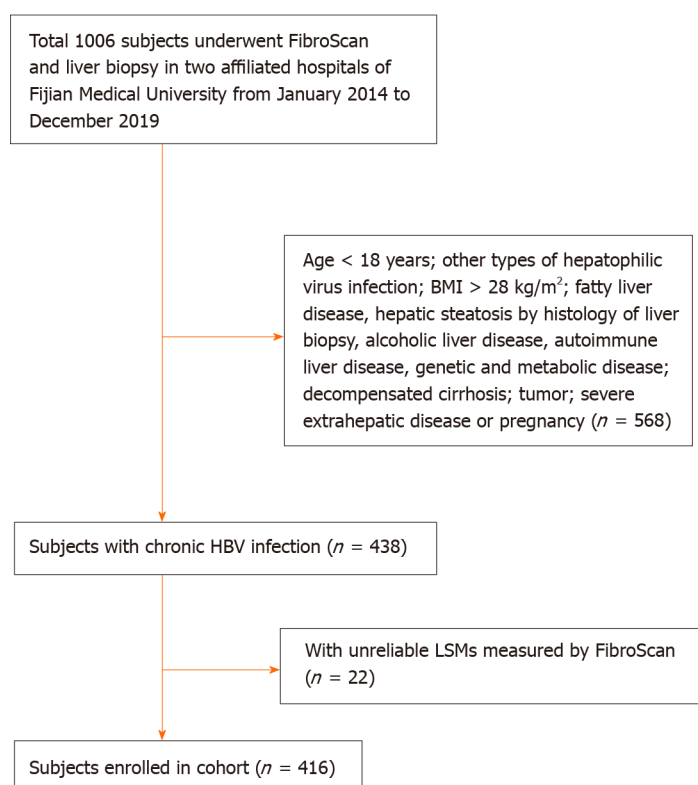


**Figure 1 Flowchart of patient enrolment.** BMI: Body mass index; HBV: Hepatitis B virus; LSM: Liver stiffness measurements; FibroScan: Transient elastography.

of liver stiffness, and its unit was kPa. FibroScan was performed by an expert certified technician.

### Liver histology assessment

Percutaneous liver biopsy was performed using 16-gauge modified aspiration needles (ACUSON; Siemens, United States) under ultrasound guidance. Qualified liver specimens with a minimum length of 1.5 cm and having more than six portal veins were fixed in 4% neutral formalin, embedded in paraffin, and stained with hematoxylin and eosin (H&E) and Masson's trichrome by two experienced pathologists who were blinded to the LSM values of FibroScan and clinical data. The pathological diagnosis was graded according to the METAVIR score standard<sup>[12]</sup>, as follows: F0, no fibrosis; F1, fibrous enlargement in the manifold area without septa; F2, fibrous enlargement in the manifold area and few septa; F3, plentiful septa without cirrhosis; and F4, early cirrhosis. Significant fibrosis was defined as  $\geq$  F2; advanced fibrosis, as  $\geq$  F3; and cirrhosis, as F4. Hepatic inflammation activity according to the degree of piecemeal necrosis (PN) was graded as A0, none; A1, mild PN; A2, moderate PN; and A3, severe PN<sup>[12]</sup>.

### Statistical analysis

Measurement and enumeration data were expressed as the means with standard deviation or median and ratio or composition ratio, respectively. Student's *t*-test, Chi-squared test, and Mann-Whitney *U* test were performed for comparative analysis, and the Spearman test was performed for correlation analyses. Receiver operating characteristic (ROC) curves were used to analyze the diagnostic performance and obtain the optimal cut-off value of FibroScan for assessing the stage of liver fibrosis. Multivariate regression analyses were employed to select the independent risk factors related to the misdiagnosis of the stage of fibrosis using FibroScan, and a non-invasive risk prediction model was constructed. To compare the area under the curves (AUCs) of the prediction model with that of other single related factors, the DeLong test was applied. Statistical analyses were performed using SPSS v23.0 (SPSS Inc. Chicago, IL, United States) and MedCalc v19.1 (MedCalc Software Bvba, Ostend, Belgium). A two-sided  $P < 0.05$  was considered statistically significant.

## RESULTS

### Demographic and clinical characteristics

In total, 416 patients were enrolled in this study (Table 1). All patients were HBsAg positive, and most of them were male (73.3%) and HBeAg positive (57.0%). The mean age, BMI, TBIL, ALB, ALT, AST, PLT, HBV DNA, PT, and LSM values were 38.67 years, 22.90 kg/m<sup>2</sup>, 17.11 µmol/L, 42.50 g/L, 95.25 IU/L, 58.46 IU/L, 187.46 × 10<sup>9</sup>/L, 4.98 log IU/mL, 12.20 s, and 9.83 kPa, respectively. According to the METAVIR score, the distribution of the stage of liver fibrosis was as follows: F0-F1 = 175 (42.1%), F2 = 106 (25.5%), F3 = 67 (16.1%), and F4 = 68 (16.3%). The distribution of liver inflammation activity was as follows: A0 = 17 (4.1%), A1 = 236 (56.7%), A2 = 119 (28.6%), and A3 = 44 (10.6%).

### Diagnostic value of FibroScan for staging of liver fibrosis

Using hepatic pathology and METAVIR fibrosis stages as a reference, the LSM values of FibroScan were positively associated with hepatic fibrosis ( $r = 0.732$ ). In the overall cohort, the optimal diagnostic LSM values of FibroScan for significant fibrosis ( $\geq F2$ ), severe fibrosis ( $\geq F3$ ), and cirrhosis (F4) were 7.3 kPa (AUC = 0.863), 9.7 kPa (AUC = 0.911), and 11.3 kPa (AUC = 0.918), respectively (Table 2).

### Discordance in stage of liver fibrosis between FibroScan and pathological scores

Misdiagnosis of the stage of fibrosis using FibroScan was defined when at least one stage of liver fibrosis was discordant with that observed using pathological staging in the METAVIR scoring system. The 416 patients were accordingly divided into the concordance group ( $n = 274$ ) and discordance group ( $n = 142$ ). Figure 2 shows the distribution of predicted fibrosis stage by FibroScan in different pathological stages of liver fibrosis. The rate of misdiagnosis using FibroScan was 34.1% (142/416 patients), and 8.2% (34/416) of the patients showed a discordance between the values obtained using the two methods for two stages. In total, 81 patients showed discordance (19.5%) attributed to overstaging by FibroScan, and the remaining 61 patients showed discordance (14.7%) attributed to understaging. There were no significant differences in the demography, HBV virology, and LSM values obtained using FibroScan between the two groups. However, in the discordance group, ALT and AST levels, the proportion of liver inflammation activity over 2, and significant fibrosis were significantly higher than the levels in the concordance group ( $P < 0.001$ ) (Table 1).

### Factors related to misdiagnosis of liver fibrosis stage by FibroScan

Univariate analysis revealed that ALT levels  $\geq 5$  times the upper limit of normal (5 ULN), AST levels  $\geq 2$  ULN, and liver inflammation activity over 2 ( $A \geq 2$ ) were significantly related to misdiagnosis of the stage of liver fibrosis by FibroScan ( $P < 0.001$ ). Subsequently, these variables were subjected to multiple regression analyses. Finally, liver inflammation activity  $\geq 2$  (OR = 3.53, 95%CI: 2.11-5.92,  $P < 0.001$ ) was considered an independent risk factor for mis-staging of liver fibrosis using FibroScan (Table 3).

### Effect of liver inflammation on diagnostic accuracy of FibroScan staging

Figure 3 shows the effect of liver inflammation on LSM values obtained using FibroScan for different stages of fibrosis. Within each fibrosis stage, namely F0-1, F2, F3, and F4, the LSM values of patients with inflammation activity  $\geq 2$  ( $A \geq 2$ ) were significantly higher than those of patients with inflammation activity  $< 2$  ( $A < 2$ ) (all  $P < 0.05$ ).

Figure 4 shows the prevalence of misdiagnosis of the stage of liver fibrosis using FibroScan staging in patients with different liver inflammation activities. Patients with inflammation activity  $\geq 2$  had higher rates of FibroScan mis-staging (55.8% vs 20.2%,  $P < 0.001$ ), over-staging (36.8% vs 8.3%,  $P < 0.001$ ), and under-staging (19.0% vs 11.9%,  $P = 0.044$ ), compared with patients with inflammation activity  $< 2$ .

Figure 5 shows the effect of liver inflammation activity on the diagnostic performance of FibroScan for different fibrosis stages. In patients with inflammation activity  $< 2$ , the diagnostic performance of FibroScan for significant fibrosis ( $\geq F2$ ), advanced fibrosis ( $\geq F3$ ), and cirrhosis (F4) were significantly better than that in patients with inflammation activity  $\geq 2$  (0.831 vs 0.702, 0.903 vs 0.815, and 0.941 vs 0.836, all  $P < 0.05$ ), as observed by comparing the AUCs.

**Table 1 Demographic characteristics and clinical features of our patient cohort**

	All (n = 416)	Concordance group (n = 274)	Discordance group (n = 142)	P value
Age (yr)	38.67 ± 10.47	38.41 ± 10.63	39.18 ± 10.18	0.467
Male, n	305 (73.3)	209 (76.3)	96 (67.6)	0.058
BMI (kg/m <sup>2</sup> )	22.90 ± 2.64	22.88 ± 2.49	22.94 ± 2.92	0.833
TBIL (μmol/L)	17.11 ± 21.56	17.70 ± 23.30	15.98 ± 17.73	0.402
Albumin (g/L)	42.50 ± 5.02	42.57 ± 5.05	42.37 ± 5.00	0.706
ALT (IU/L)	95.25 ± 52.0	78.90 ± 99.89	126.10 ± 118.46	< 0.001
AST (IU/L)	58.46 ± 108.85	49.05 ± 55.44	76.61 ± 62.80	< 0.001
PLT (10 <sup>9</sup> /L)	187.46 ± 56.53	186.36 ± 56.86	189.59 ± 56.04	0.916
HBsAg (Log IU/mL)	3.42 ± 0.97	3.38 ± 1.04	3.50 ± 0.80	0.258
HBeAg positive (%)	237 (57.0)	155 (56.6)	82 (57.7)	0.818
HBV-DNA (Log IU/mL)	4.98 ± 2.18	4.95 ± 2.16	5.05 ± 2.23	0.641
PT (s)	12.20 ± 0.98	12.17 ± 1.03	12.25 ± 0.88	0.387
AFP (ng/mL)	11.37 ± 34.59	11.98 ± 36.80	10.20 ± 29.95	0.597
LSM (kPa)	9.83 ± 7.70	9.75 ± 7.21	9.97 ± 5.14	0.751
Fibrosis stage <sup>1</sup> , n				< 0.001
F0-1	175 (42.1)	143 (52.2)	32 (22.5)	
F2	106 (25.5)	49 (17.9)	57 (40.1)	
F3	67 (16.1)	23 (8.4)	44 (31.0)	
F4	68 (16.3)	59 (21.5)	9 (6.3)	
Inflammation grade <sup>1</sup> , n				< 0.001
A0	17 (4.1)	15 (5.5)	2 (1.4)	
A1	236 (56.7)	187 (68.2)	49 (34.5)	
A2	119 (28.6)	49 (17.9)	70 (49.3)	
A3	44 (10.6)	23 (8.4)	21 (14.8)	

<sup>1</sup>According to METAVIR system, the liver fibrosis stage ranged from 0 to 4, and liver inflammation grade ranged from 0 to 3. BMI: Body mass index; TBIL: Total bilirubin; ALT: Alanine aminotransferase; AST: Aspartate aminotransferase; PLT: Platelet count; HBV: Hepatitis B virus; PT: Prothrombin time; AFP: Alpha fetoprotein; LSM: Liver stiffness measurements; HBsAg: Hepatitis B surface antigen; HBeAg: Hepatitis B envelope antigen.

**Table 2 Accuracy of liver stiffness measurement values by transient elastography in diagnosing ≥ F2, ≥ F3, and F4, as measured by area under the receiver operating characteristic curve (n = 416)**

Fibrosis stage	AUC (95%CI)	Sensitivity (%)	Specificity (%)	PPV (%)	NPV (%)	Cut-off point
≥ F2	0.863 (0.826-0.895)	83.40	81.71	86.01	78.49	≥ 7.3
≥ F3	0.911 (0.880-0.937)	80.74	87.19	76.59	89.72	≥ 9.7
F4	0.918 (0.887-0.942)	86.76	89.08	61.47	97.10	≥ 11.3

AUC: Area under the receiver operating characteristic curve; NPV: Negative predictive value; PPV: Positive predictive value; ≥ F2: Significant fibrosis; ≥ F3: Advanced fibrosis; F4: Cirrhosis.

### **Development of a non-invasive prediction model for misdiagnosis of liver fibrosis stage using FibroScan**

The ALT and AST levels were positively correlated with hepatic inflammation ( $r = 0.534$  and  $0.527$ ,  $P < 0.001$ ) by the Spearman's test, and these were significantly related with misdiagnosis of fibrosis stage using FibroScan (all  $P < 0.001$ ) (Table 3). Using

**Table 3 Univariate and multivariate regression analyses of risk of misdiagnosis of fibrosis stage by transient elastography in all patients**

Variables	Univariate analyses		Multivariate analyses	
	OR (95%CI)	P value	OR (95%CI)	P value
Age (yr)	1.00 (0.99-1.03)	0.472		
Male, <i>n</i>	0.65 (0.42-1.02)	0.059		
BMI (kg/m <sup>2</sup> )	1.01 (0.93-1.09)	0.832		
TBIL > 2 ULN (μmol/L)	0.68 (0.24-1.92)	0.464		
Albumin (g/L)	0.99 (0.95-1.03)	0.707		
ALT <sup>1</sup> (IU/L)				
< 2 ULN	Reference	Reference	Reference	Reference
2-5 ULN	2.16 (1.31-3.56)	0.003	1.00 (0.52-1.93)	0.996
≥ 5 ULN	4.93 (2.66-9.12)	< 0.001	1.11 (0.44-2.76)	0.996
AST <sup>1</sup> ≥ 2 ULN (IU/L)	4.42 (2.73-7.16)	< 0.001	2.05 (0.97-4.34)	0.059
PLT (10 <sup>9</sup> /L)	1.00 (0.99-1.01)	0.580		
HBsAg (Log IU/mL)	1.13 (0.91-1.40)	0.258		
HBeAg positive	1.05 (0.70-1.58)	0.818		
HBV-DNA (Log IU/mL)	1.02 (0.93-1.12)	0.636		
PT (s)	1.09 (0.89-1.34)	0.408		
AFP (ng/mL)	1.00 (0.99-1.01)	0.622		
Inflammation activity <sup>2</sup>				
A < 2	Reference	Reference	Reference	Reference
A ≥ 2	5.01 (3.24-7.74)	< 0.001	3.53 (2.11-5.92)	< 0.001

<sup>1</sup>Normal alanine aminotransferase and aspartate aminotransferase levels are 40 U/L for women and men.

<sup>2</sup>Inflammation activity was calculated as a range of 0-3 according to the METAVIR system. BMI: Body mass index; TBIL: Total bilirubin; ALT: Alanine aminotransferase; AST: Aspartate aminotransferase; PLT: Platelet count; HBV: Hepatitis B virus; PT: Prothrombin time; AFP: Alpha fetoprotein; ULN: Upper limit of normal; HBsAg: Hepatitis B surface antigen; HBeAg: Hepatitis B envelope antigen.

these related factors, a non-invasive prediction model was developed to identify the risk of misdiagnosis using FibroScan, as follows:  $\text{logit}(P) = -1.477 + (0.139, 0.732) \times \text{ALT levels (2-5, } \geq 5 \text{ ULN)} + 1.310 \times \text{AST levels (} > 2 \text{ ULN)} + (1.056, 0.815, -0.154) \times \text{FibroScan-predicted fibrosis staging (F2, F3, and F4)}$ .

We compared the prediction performance of the model with that of other single related factors to evaluate the misdiagnosis of the stage of liver fibrosis using FibroScan (Figure 6). The AUC value of the prediction model was 0.701 (95%CI: 0.655-0.745), which was significantly higher than that of ALT levels (0.636, 95%CI: 0.588-0.683), AST levels (0.639, 95%CI: 0.590-0.685) and FibroScan-predicted fibrosis stages (0.611, 95%CI: 0.562-0.658) (all  $P < 0.001$ ). The cut-off point, sensitivity, and specificity of the model were 0.340, 63.38%, and 67.52%, respectively.

## DISCUSSION

Accurate evaluation of the stage of hepatic fibrosis is important in patients with chronic HBV infection for determining the initiation of antiviral therapy and is an important index for evaluating the efficacy of antiviral therapy. FibroScan is a recommended non-invasive test for evaluation of liver fibrosis in patients with chronic HBV infection<sup>[4,13]</sup>. In the present study, we confirmed that LSM values obtained using FibroScan were positively correlated with hepatic fibrosis and demonstrated the good performance of FibroScan in predicting the stage of liver fibrosis. We found that the optimal diagnostic LSM values of FibroScan for significant fibrosis ( $\geq$  F2), severe fibrosis ( $\geq$  F3), and cirrhosis (F4) were 7.3 kPa (AUC = 0.863), 9.7 kPa (AUC = 0.911),



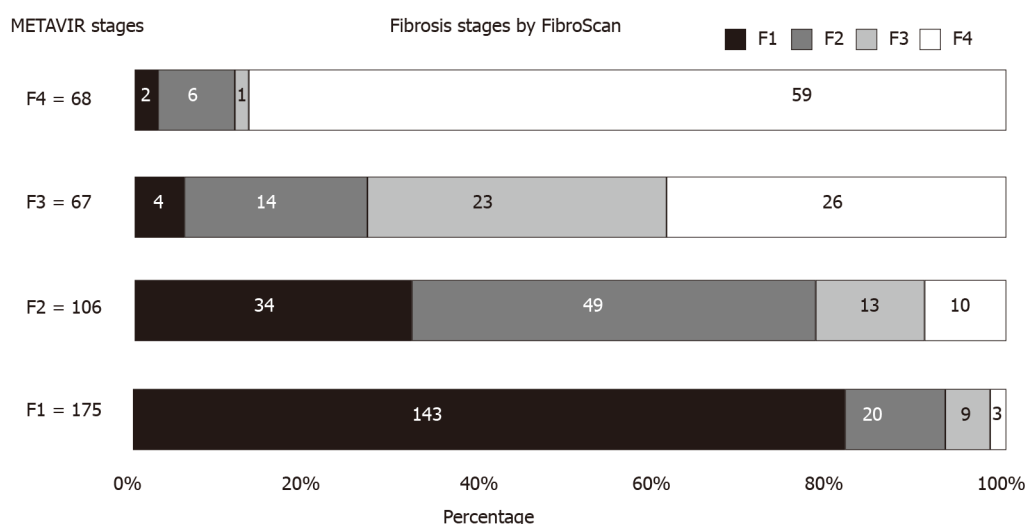


**Figure 2** Distribution of predicted fibrosis stages by transient elastography according to different METAVIR liver fibrosis stages. FibroScan: Transient elastography.

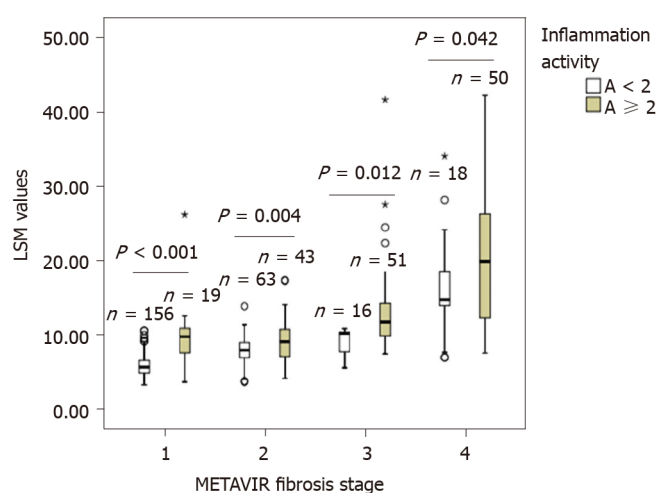


**Figure 3** Comparison of liver stiffness measurement values by transient elastography in patients with different liver inflammation activities in different METAVIR fibrosis stages. LSM: Liver stiffness measurements.

and 11.3 kPa (AUC = 0.918), respectively. Our results are consistent with those of previous studies<sup>[6,14,15]</sup>.

Although LSM values measured by ultrasound elastography are related to the stage of fibrosis, they could be affected by acute hepatitis, high ALT and/or AST levels, obstructive cholestasis, and infiltrative hepatic disease<sup>[7,16,17]</sup>. We explored the relationship between various anthropometric, biochemical, and pathological parameters and the diagnostic accuracy of FibroScan for determining the stage of liver fibrosis. A discordance between the fibrosis stage determined using FibroScan and that determined by pathological examination was observed in 34.1% of the patients (142/416), with 19.5% of patients (81/416) over-staged and 14.7% of patients (61/416) under-staged in our study. Compared with patients who showed concordance between values obtained using the two methods, those who showed discordance had significantly higher ALT and AST levels, and a higher proportion of moderate to severe liver inflammatory activity. Furthermore, multivariate analysis showed that liver inflammatory activity over 2 was an independent risk factor for misdiagnosis of fibrosis stage using FibroScan.

However, the bias caused by liver inflammation in the assessment of liver fibrosis stage using FibroScan is still unclear. The changes occurring in liver enzymes during inflammatory degeneration, necrosis, and fibrosis of hepatic cells are strong indicators of inflammation, in which ALT and AST are the most valuable serum biochemical indices for the detection of liver injury. Many studies have shown that elevated LSM

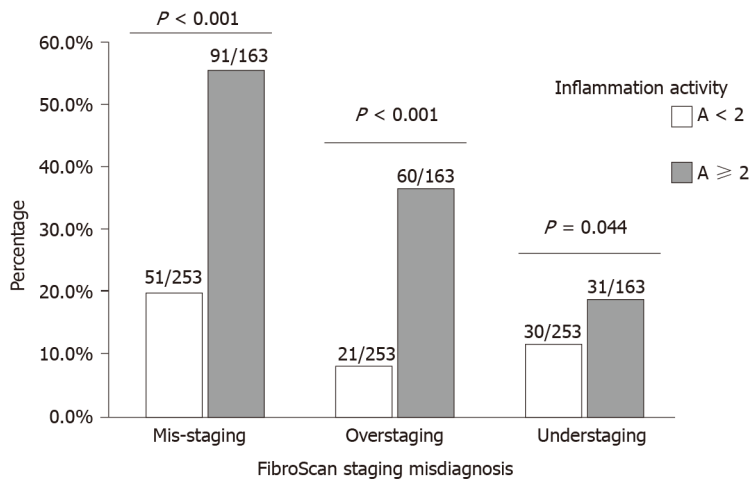


**Figure 4** Prevalence of misdiagnosis of stage of liver fibrosis by transient elastography in patients with different inflammatory activities.

values were related to increased ALT levels, and have proposed a variety of dual cut-offs of LSM values adapted to ALT levels, which may improve the diagnostic performance of FibroScan in evaluating the stage of hepatic fibrosis in patients with chronic HBV infection<sup>[10,11,18]</sup>. The elevated baseline LSM values due to liver inflammation in patients with elevated ALT levels could lead to inappropriate overestimation of the stage of liver fibrosis. We found that patients with inflammation activity  $\geq 2$  had higher LSM values in each fibrosis stage among F0-1, F2, F3, and F4 (all  $P < 0.05$ ), and a higher percentage of mis-staging (55.8% *vs* 20.2%,  $P < 0.001$ ), over-staging (36.8% *vs* 8.3%,  $P < 0.001$ ), and under-staging (19.0% *vs* 11.9%,  $P = 0.044$ ) using FibroScan, compared with patients with inflammation activity  $< 2$ . Other studies reported a lack of these correlations and indicated that mildly increased ALT levels did not affect the performance of LSM in assessing hepatic fibrosis in patients with chronic HBV infection<sup>[19,20]</sup>. A recent study reported that the sensitivity and specificity of LSM values for assessing the stage of liver fibrosis were significantly lower in patients with ALT levels  $\geq 2$  times the ULN<sup>[11]</sup>. Our study findings are consistent with this result. We found that FibroScan was significantly better in predicting significant fibrosis ( $\geq F2$ ), advanced fibrosis ( $\geq F3$ ), and cirrhosis (F4) in patients with inflammation activity  $< 2$  than in patients with inflammation activity  $\geq 2$ , by comparing the AUCs (0.831 *vs* 0.702, 0.903 *vs* 0.815, and 0.941 *vs* 0.836, all  $P < 0.05$ ). Therefore, we concluded that the diagnostic accuracy of LSM was mainly influenced by significantly elevated ALT levels (ALT  $> 2$  ULN), acute viral hepatitis, HBV flares, and the severity of liver fibrosis.

At present, many non-invasive models have been developed to diagnose liver fibrosis. The WHO guidelines on chronic HBV infection recommended that LSM and APRI are the most helpful detection methods to evaluate hepatic fibrosis with limited resources<sup>[21]</sup>. The accuracy of LSM values could be affected by inflammation and other influencing factors. FibroScan may yield low LSM values and underestimate or misdiagnose the stage of liver fibrosis in patients with mild hepatic inflammation, and it may show elevated LSM values and overestimate or misdiagnose cirrhosis in patients with severe inflammation. In our study, the severity of liver inflammation was an independent risk factor for misdiagnosis of the stage of liver fibrosis using FibroScan; however, the measurement of severity entailed an invasive procedure. Therefore, we used other relevant non-invasive factors to predict the risk of misdiagnosis using FibroScan, which may be of great significance in determining the fibrosis stage or performing liver biopsy, and may guide the diagnosis of and therapy of chronic HBV infection. Our model consisted of three routinely assessed parameters (ALT levels, AST levels, and FibroScan-predicted fibrosis staging), which showed better performance than those of other single related factors in predicting the risk of misdiagnosis of the stage of hepatic fibrosis using FibroScan staging by ROC analysis. According to this model, more attention should be paid to patients at a high risk of being misdiagnosed using FibroScan, a comprehensive evaluation of the degree of hepatic fibrosis should be conducted, and further liver biopsy should be performed, if necessary, to determine whether antiviral therapy needs to be initiated immediately.

This study has several limitations. First, the effects of controlled attenuation parameters and histological steatosis on the diagnostic performance of FibroScan were

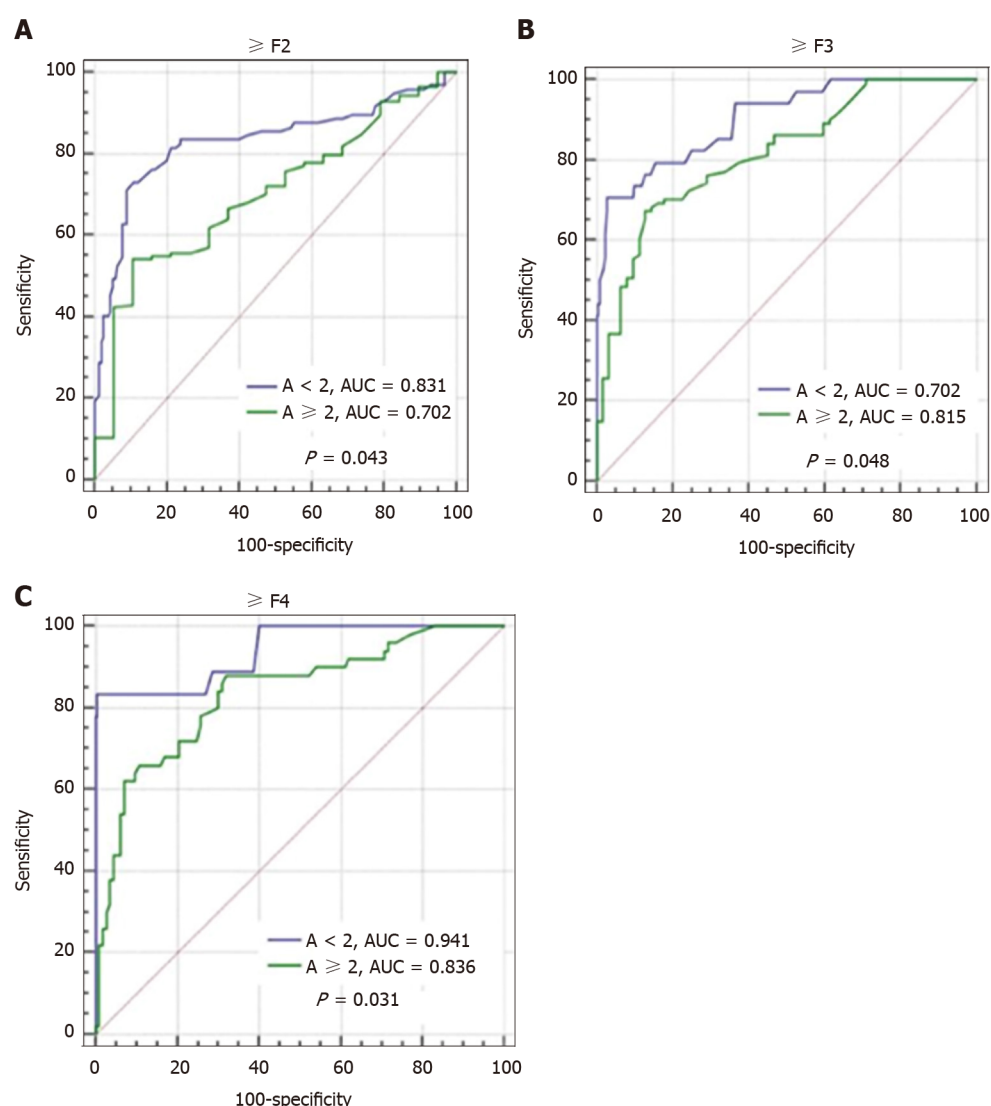


**Figure 5** Comparison of effects of different liver inflammatory activities on diagnostic performance of transient elastography in assessing different fibrosis stages. A:  $\geq F2$ ; B:  $\geq F3$ ; C: F4. AUC: Area under the curve;  $\geq F2$ : Significant fibrosis;  $\geq F3$ : Advanced fibrosis; F4: Cirrhosis.

not discussed. Second, the sample size of the study was very small. An extensive liver biopsy database should be established to comprehensively evaluate the reliable cut-off value of FibroScan for assessing the stage of liver fibrosis. Third, the results of our study warrant further verification in large-scale, multicenter cohort studies.

## CONCLUSION

In conclusion, liver inflammation is an independent risk factor that affects the accuracy of FibroScan in assessing the stage of HBV-related liver fibrosis. A combination of other related non-invasive factors can help predict the risk of misdiagnosis of the stage of liver fibrosis using FibroScan, which may help to decide whether liver biopsy is required and guide the diagnosis of and therapy of chronic HBV infection.

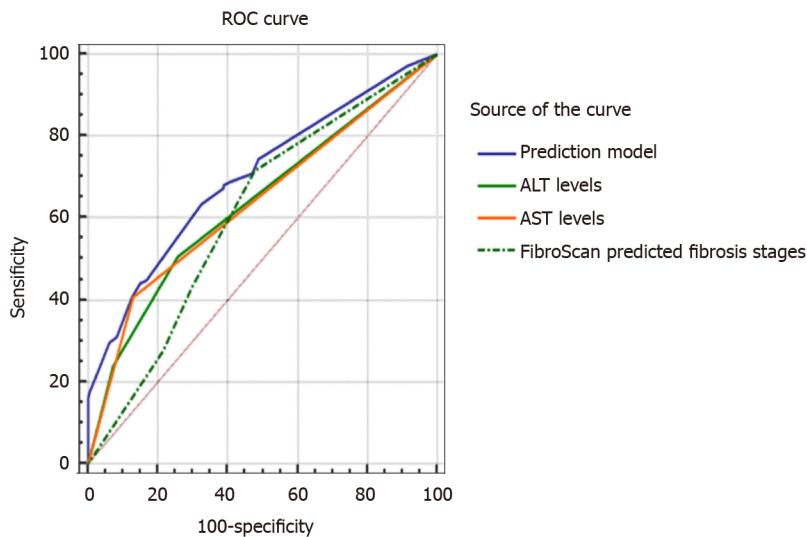


**Figure 6** Comparison of receiver operating characteristic curves in prediction model and single related factors with regard to misdiagnosis of the stage of liver fibrosis using transient elastography. ALT: Alanine aminotransferase; AST: Aspartate aminotransferase; ROC: Receiver operating characteristic; FibroScan: Transient elastography.

## ARTICLE HIGHLIGHTS

### Research background

Transient elastography (FibroScan) is a new and non-invasive test, which can replace biopsy and has been widely recommended by the guidelines of chronic hepatitis B virus (HBV) management for assessing hepatic fibrosis staging. Liver stiffness measurement (LSM) by FibroScan is associated with the degree of hepatic fibrosis, but can also be confounded by liver necroinflammation, alanine aminotransferase (ALT), cholestasis, portal hypertension, hepatic congestion, and body mass index (BMI) and other factors, which may affect the diagnostic accuracy of the FibroScan device in fibrosis staging.

### Research motivation

Many studies suggested that the cutoff value of LSM tends to increase with elevated ALT level, and its diagnostic accuracy tends to decrease with elevated ALT level, but it is not clear whether pathological hepatic inflammation would similarly affect LSM values and diagnostic accuracy of FibroScan assessing hepatic fibrosis.

### Research objectives

We aimed to evaluate the diagnostic value of FibroScan and the effect of hepatic inflammation on the accuracy of FibroScan assessing liver fibrosis staging in patients with chronic HBV infection, and to develop a predictive model combining other related non-invasive confounders to predict the risk of FibroScan staging misdiagnosis.

### Research methods

The data of 416 patients with chronic HBV infection who accepted FibroScan, liver biopsy, clinical, and biological examination were retrospectively collected between January 2014 and December 2019 from two affiliated hospitals of Fujian Medical University. Receiver operating characteristic (ROC) curves were used to analyze the data. The diagnostic performance of FibroScan for the stage of liver fibrosis was analyzed using ROC curves. Any discordance in fibrosis staging by FibroScan and pathological scores was statistically analyzed. The accuracy of FibroScan in assessing the stage of fibrosis in patients with different degrees of liver inflammation was analyzed using Logistic regression and ROC curves. A non-invasive model was constructed to predict the risk of misdiagnosis of fibrosis stage using FibroScan.

### Research results

We confirmed that LSM values obtained using FibroScan were positively correlated with hepatic fibrosis and demonstrated the good performance of FibroScan in

predicting the stage of liver fibrosis. However, discordance between the fibrosis stage determined using FibroScan and that determined by pathological examination was observed in some patients. Furthermore, we found that liver inflammatory activity over 2 was an independent risk factor for misdiagnosis of fibrosis stage using FibroScan. Patients with liver inflammation activity  $\geq 2$  showed higher LSM values using FibroScan and higher rates of misdiagnosis of fibrosis stage, whereas the diagnostic performance of FibroScan for different fibrosis stages was significantly lower than that in patients with inflammation activity  $< 2$ . A non-invasive prediction model was established to assess the risk of misdiagnosis of fibrosis stage using FibroScan, and the area under the curve was 0.701, which was superior to that observed using other single related factors.

### Research conclusions

Liver inflammation was an independent risk factor affecting the diagnostic accuracy of FibroScan for HBV-related fibrosis staging. The combination of other related non-invasive factors can predict the risk of misdiagnosis of fibrosis staging using FibroScan, and may be helpful for making decisions on liver biopsy and guiding the diagnosis and therapy of chronic HBV infection.

### Research perspectives

This multi-center cross-sectional study developed and evaluated a noninvasive model to predict the risk of misdiagnosis of fibrosis staging using FibroScan, thus an extensive liver biopsy database should be established to comprehensively evaluate the reliable cut-off value of FibroScan for assessing the stage of liver fibrosis and further verify the diagnostic performance of this model in future prospective studies.

## REFERENCES

- Schweitzer A, Horn J, Mikolajczyk RT, Krause G, Ott JJ. Estimations of worldwide prevalence of chronic hepatitis B virus infection: a systematic review of data published between 1965 and 2013. *Lancet* 2015; **386**: 1546-1555 [PMID: 26231459 DOI: 10.1016/S0140-6736(15)61412-X]
- Wu JF, Chang MH. Natural history of chronic hepatitis B virus infection from infancy to adult life - the mechanism of inflammation triggering and long-term impacts. *J Biomed Sci* 2015; **22**: 92 [PMID: 26487087 DOI: 10.1186/s12929-015-0199-y]
- Shiha G, Ibrahim A, Helmy A, Sarin SK, Omata M, Kumar A, Bernstien D, Maruyama H, Saraswat V, Chawla Y, Hamid S, Abbas Z, Bedossa P, Sakhuja P, Elmahatab M, Lim SG, Lesmana L, Sollano J, Jia JD, Abbas B, Omar A, Sharma B, Payawal D, Abdallah A, Serwah A, Hamed A, Elsayed A, AbdelMaqsood A, Hassanein T, Ihab A, GHaziuan H, Zein N, Kumar M. Asian-Pacific Association for the Study of the Liver (APASL) consensus guidelines on invasive and non-invasive assessment of hepatic fibrosis: a 2016 update. *Hepatol Int* 2017; **11**: 1-30 [PMID: 27714681 DOI: 10.1007/s12072-016-9760-3]
- European Association for the Study of the Liver. EASL 2017 Clinical Practice Guidelines on the management of hepatitis B virus infection. *J Hepatol* 2017; **67**: 370-398 [PMID: 28427875 DOI: 10.1016/j.jhep.2017.03.021]
- Ilic I, Milovanovic T. The risk-benefit assessment of liver biopsy in times of non-invasive screening for liver fibrosis. *J Hepatol* 2020; **73**: 701-702 [PMID: 32546400 DOI: 10.1016/j.jhep.2020.05.017]
- Jia J, Hou J, Ding H, Chen G, Xie Q, Wang Y, Zeng M, Zhao J, Wang T, Hu X, Schuppan D. Transient elastography compared to serum markers to predict liver fibrosis in a cohort of Chinese patients with chronic hepatitis B. *J Gastroenterol Hepatol* 2015; **30**: 756-762 [PMID: 25353058 DOI: 10.1111/jgh.12840]
- Dietrich CF, Bamber J, Berzigotti A, Bota S, Cantisani V, Castera L, Cosgrove D, Ferraioli G, Friedrich-Rust M, Gilja OH, Goertz RS, Karlas T, de Knecht R, de Ledinghen V, Piscaglia F, Procopet B, Saftoiu A, Sidhu PS, Sporea I, Thiele M. EFSUMB Guidelines and Recommendations on the Clinical Use of Liver Ultrasound Elastography, Update 2017 (Long Version). *Ultraschall Med* 2017; **38**: e48 [PMID: 30176678 DOI: 10.1055/a-0641-0076]
- Chinese Society of Infectious Diseases, Chinese Medical Association, Chinese Society of Hepatology Chinese Medical Association. [The guidelines of prevention and treatment for chronic hepatitis B (2019 version)]. *Zhonghua Gan Zang Bing Za Zhi* 2019; **27**: 938-961 [PMID: 31941257 DOI: 10.3760/cma.j.issn.1007-3418.2019.12.007]
- European Association for Study of Liver, Asociacion Latinoamericana para el Estudio del Higado. EASL-ALEH Clinical Practice Guidelines: Non-invasive tests for evaluation of liver disease severity and prognosis. *J Hepatol* 2015; **63**: 237-264 [PMID: 25911335 DOI: 10.1016/j.jhep.2015.04.006]
- Song ZZ. Acute viral hepatitis increases liver stiffness values measured by transient elastography. *Hepatology* 2008; **48**: 349-50; author reply 350 [PMID: 18571790 DOI: 10.1002/hep.22385]
- Zeng J, Zheng J, Jin JY, Mao YJ, Guo HY, Lu MD, Zheng HR, Zheng RQ. Shear wave elastography for liver fibrosis in chronic hepatitis B: Adapting the cut-offs to alanine aminotransferase levels



- improves accuracy. *Eur Radiol* 2019; **29**: 857-865 [PMID: [30039224](#) DOI: [10.1007/s00330-018-5621-x](#)]
- 12 **Bedossa P**, Poynard T. An algorithm for the grading of activity in chronic hepatitis C. The METAVIR Cooperative Study Group. *Hepatology* 1996; **24**: 289-293 [PMID: [8690394](#) DOI: [10.1002/hep.510240201](#)]
  - 13 **Sarin SK**, Kumar M, Lau GK, Abbas Z, Chan HL, Chen CJ, Chen DS, Chen HL, Chen PJ, Chien RN, Dokmeci AK, Gane E, Hou JL, Jafri W, Jia J, Kim JH, Lai CL, Lee HC, Lim SG, Liu CJ, Locarnini S, Al Mahtab M, Mohamed R, Omata M, Park J, Piratvisuth T, Sharma BC, Sollano J, Wang FS, Wei L, Yuen MF, Zheng SS, Kao JH. Asian-Pacific clinical practice guidelines on the management of hepatitis B: a 2015 update. *Hepatol Int* 2016; **10**: 1-98 [PMID: [26563120](#) DOI: [10.1007/s12072-015-9675-4](#)]
  - 14 **Chon YE**, Choi EH, Song KJ, Park JY, Kim DY, Han KH, Chon CY, Ahn SH, Kim SU. Performance of transient elastography for the staging of liver fibrosis in patients with chronic hepatitis B: a meta-analysis. *PLoS One* 2012; **7**: e44930 [PMID: [23049764](#) DOI: [10.1371/journal.pone.0044930](#)]
  - 15 **Verveer C**, Zondervan PE, ten Kate FJ, Hansen BE, Janssen HL, de Knecht RJ. Evaluation of transient elastography for fibrosis assessment compared with large biopsies in chronic hepatitis B and C. *Liver Int* 2012; **32**: 622-628 [PMID: [22098684](#) DOI: [10.1111/j.1478-3231.2011.02663.x](#)]
  - 16 **Ferraioli G**, Filice C, Castera L, Choi BI, Sporea I, Wilson SR, Cosgrove D, Dietrich CF, Amy D, Bamber JC, Barr R, Chou YH, Ding H, Farrokhi A, Friedrich-Rust M, Hall TJ, Nakashima K, Nightingale KR, Palmeri ML, Schafer F, Shiina T, Suzuki S, Kudo M. WFUMB guidelines and recommendations for clinical use of ultrasound elastography: Part 3: liver. *Ultrasound Med Biol* 2015; **41**: 1161-1179 [PMID: [25800942](#) DOI: [10.1016/j.ultrasmedbio.2015.03.007](#)]
  - 17 **Barr RG**, Wilson SR, Rubens D, Garcia-Tsao G, Ferraioli G. Update to the Society of Radiologists in Ultrasound Liver Elastography Consensus Statement. *Radiology* 2020; **296**: 263-274 [PMID: [32515681](#) DOI: [10.1148/radiol.2020192437](#)]
  - 18 **Chan HL**, Wong GL, Choi PC, Chan AW, Chim AM, Yiu KK, Chan FK, Sung JJ, Wong VW. Alanine aminotransferase-based algorithms of liver stiffness measurement by transient elastography (Fibroscan) for liver fibrosis in chronic hepatitis B. *J Viral Hepat* 2009; **16**: 36-44 [PMID: [18673426](#) DOI: [10.1111/j.1365-2893.2008.01037.x](#)]
  - 19 **Li Q**, Chen L, Zhou Y. Diagnostic accuracy of liver stiffness measurement in chronic hepatitis B patients with normal or mildly elevated alanine transaminase levels. *Sci Rep* 2018; **8**: 5224 [PMID: [29588489](#) DOI: [10.1038/s41598-018-23646-2](#)]
  - 20 **Seo YS**, Kim MY, Kim SU, Hyun BS, Jang JY, Lee JW, Lee JI, Suh SJ, Park SY, Park H, Jung EU, Kim BS, Kim IH, Lee TH, Um SH, Han KH, Kim SG, Paik SK, Choi JY, Jeong SW, Jin YJ, Lee KS, Yim HJ, Tak WY, Hwang SG, Lee YJ, Lee CH, Kim DG, Kang YW, Kim YS; Korean Transient Elastography Study Group. Accuracy of transient elastography in assessing liver fibrosis in chronic viral hepatitis: A multicentre, retrospective study. *Liver Int* 2015; **35**: 2246-2255 [PMID: [25682719](#) DOI: [10.1111/liv.12808](#)]
  - 21 Guidelines for the Prevention, Care and Treatment of Persons with Chronic Hepatitis B Infection. Geneva: World Health Organization; 2015 [PMID: [26225396](#)]



## Clinical Trials Study

# Simultaneous partial splenectomy during liver transplantation for advanced cirrhosis patients combined with severe splenomegaly and hypersplenism

Wen-Tao Jiang, Jian Yang, Yan Xie, Qing-Jun Guo, Da-Zhi Tian, Jun-Jie Li, Zhong-Yang Shen

**ORCID number:** Wen-Tao Jiang 0000-0002-6592-4322; Jian Yang 0000-0001-9481-0407; Yan Xie 0000-0002-7812-8632; Qing-Jun Guo 0000-0002-9108-489X; Da-Zhi Tian 0000-0002-6664-041X; Jun-Jie Li 0000-0001-8318-3372; Zhong-Yang Shen 0000-0001-8536-3780.

**Author contributions:** Jiang WT is the first author; Yang J and Xie Y are the co-first authors; Jiang WT contributed to study conception; Yang J and Xie Y contributed to data collection; Yang J contributed to manuscript drafting; Jiang WT, Yang J, Xie Y, Guo QJ, Tian DZ, Li JJ and Shen ZY contributed critical revision of the manuscript for important intellectual content.

**Supported by** National Natural Science Foundation of China, No. 81870444; Tianjin Natural Science Foundation, No. 19JCQNJC10300; and Spring Bud Plan of Tianjin First Central Hospital, No. TFCCHCL201801.

### Institutional review board

**statement:** This study was approved by the Ethics Committee of Tianjin First Central Hospital (Approval No. 2019N168KY).

### Clinical trial registration statement:

This study is registered at Chinese

Wen-Tao Jiang, Jian Yang, Yan Xie, Qing-Jun Guo, Da-Zhi Tian, Jun-Jie Li, Zhong-Yang Shen, Department of Liver Transplantation, Tianjin First Center Hospital, First Clinical Institute of Tianjin Medical University, Tianjin 300192, China

Wen-Tao Jiang, Yan Xie, Qing-Jun Guo, Da-Zhi Tian, Jun-Jie Li, Zhong-Yang Shen, Organ Transplantation Center, Tianjin First Center Hospital, Tianjin 300192, China

Jian Yang, Department of Hepatological Surgery, Zibo Central Hospital, Zibo 255000, Shandong Province, China

**Corresponding author:** Zhong-Yang Shen, MD, Dean, Doctor, Department of Liver Transplantation, Tianjin First Center Hospital, First Clinical Institute of Tianjin Medical University, No. 24 Fukang Road, Nankai District, Tianjin 300192, China.  
[yangjian06281@126.com](mailto:yangjian06281@126.com)

## Abstract

### BACKGROUND

The most effective treatment for advanced cirrhosis and portal hypertension is liver transplantation (LT). However, splenomegaly and hypersplenism can persist even after LT in patients with massive splenomegaly.

### AIM

To examine the feasibility of performing partial splenectomy during LT in patients with advanced cirrhosis combined with severe splenomegaly and hypersplenism.

### METHODS

Between October 2015 and February 2019, 762 orthotopic LTs were performed for patients with end-stage liver diseases in Tianjin First Center Hospital. Eighty-four cases had advanced cirrhosis combined with severe splenomegaly and hypersplenism. Among these patients, 41 received partial splenectomy during LT (PSLT group), and 43 received only LT (LT group). Patient characteristics, intraoperative parameters, and postoperative outcomes were retrospectively analyzed and compared between the two groups.

### RESULTS

Clinical Trial Registry. The registration identification number is ChiCTR-TRC-10001070.

**Informed consent statement:** All study participants, or their legal guardian, provided informed written consent prior to study enrollment.

**Conflict-of-interest statement:** The authors declare no conflicts of interest.

**Data sharing statement:** Participants gave informed consent for data sharing.

**CONSORT 2010 statement:** The authors have read the CONSORT 2010 statement, and the manuscript was prepared and revised according to the CONSORT 2010 statement.

**Open-Access:** This article is an open-access article that was selected by an in-house editor and fully peer-reviewed by external reviewers. It is distributed in accordance with the Creative Commons Attribution NonCommercial (CC BY-NC 4.0) license, which permits others to distribute, remix, adapt, build upon this work non-commercially, and license their derivative works on different terms, provided the original work is properly cited and the use is non-commercial. See: <http://creativecommons.org/licenses/by-nc/4.0/>

**Manuscript source:** Unsolicited manuscript

**Specialty type:** Gastroenterology and hepatology

**Country/Territory of origin:** China

**Peer-review report's scientific quality classification**

Grade A (Excellent): 0  
Grade B (Very good): 0  
Grade C (Good): C  
Grade D (Fair): 0  
Grade E (Poor): 0

**Received:** November 25, 2020

**Peer-review started:** November 25, 2020

**First decision:** December 8, 2020

The incidence of postoperative hypersplenism (2/41, 4.8%) and recurrent ascites (1/41, 2.4%) in the PSLT group was significantly lower than that in the LT group (22/43, 51.2%; 8/43, 18.6%, respectively). Seventeen patients (17/43, 39.5%) in the LT group required two-stage splenic embolization, and further splenectomy was required in 6 of them. The operation time and intraoperative blood loss in the PSLT group ( $8.6 \pm 1.3$  h;  $640.8 \pm 347.3$  mL) were relatively increased compared with the LT group ( $6.8 \pm 0.9$  h;  $349.4 \pm 116.1$  mL). The incidence of postoperative bleeding, pulmonary infection, thrombosis and splenic arterial steal syndrome in the PSLT group was not different to that in the LT group, respectively.

## CONCLUSION

Simultaneous PSLT is an effective treatment and should be performed in patients with advanced cirrhosis combined with severe splenomegaly and hypersplenism to prevent postoperative persistent hypersplenism.

**Key Words:** Liver transplantation; Partial splenectomy; Hypersplenism; Splenomegaly; Liver cirrhotic; Megalosplenism

©The Author(s) 2021. Published by Baishideng Publishing Group Inc. All rights reserved.

**Core Tip:** In this article, for the first time, we describe partial splenectomy during liver transplantation (PSLT) in patients with advanced cirrhosis combined with severe splenomegaly and hypersplenism. PSLT can effectively alleviate the severity of postoperative hypersplenism and ascites in megalosplenism patients.

**Citation:** Jiang WT, Yang J, Xie Y, Guo QJ, Tian DZ, Li JJ, Shen ZY. Simultaneous partial splenectomy during liver transplantation for advanced cirrhosis patients combined with severe splenomegaly and hypersplenism. *World J Gastroenterol* 2021; 27(7): 654-665

**URL:** <https://www.wjgnet.com/1007-9327/full/v27/i7/654.htm>

**DOI:** <https://dx.doi.org/10.3748/wjg.v27.i7.654>

## INTRODUCTION

Liver cirrhosis is the leading cause of liver disease related morbidity and mortality worldwide and is often accompanied by portal hypertension and splenomegaly<sup>[1]</sup>. The most effective treatment for advanced cirrhosis and portal hypertension is liver transplantation (LT)<sup>[2]</sup>. Splanchnic hemodynamics change dramatically after LT, including improved portal outflow resistance, decreased portal vein pressure, and movement of accumulated blood from viscera to the systemic circulation. These changes significantly increase portal vein flow, gradually improve spleen congestion, and further ameliorate splenomegaly and hypersplenism<sup>[3]</sup>.

However, splenomegaly and hypersplenism can persist even after LT in patients with massive splenomegaly<sup>[4]</sup>. Persistent hypersplenism-related pancytopenia may interfere with the management of immunosuppressive therapy<sup>[5]</sup>. Splenomegaly may further result in excessive portal pressure or splenic artery steal syndrome. The resulting decrease in hepatic arterial inflow can then affect liver graft function<sup>[6]</sup>. The most common therapies for splenomegaly and hypersplenism are total splenectomy during LT (TSLT) and selective splenic artery embolization (SAE) after LT<sup>[7]</sup>, but they have considerable limitations.

TSLT is associated with increased operative time and additional blood loss<sup>[6]</sup>. Furthermore, TSLT increases the risk of postoperative complications, such as overwhelming post-splenectomy infection syndrome (OPIS), reactive thrombocytosis, and portal venous system thrombosis<sup>[8,9]</sup>. It remains controversial whether simultaneous splenectomy during LT is beneficial in these patients.

SAE after LT is a secondary treatment used in addition to surgery to manage hypersplenism in patients with cirrhosis and portal hypertension<sup>[7]</sup>. However, SAE after LT results in a high risk of infection<sup>[10]</sup>. Patients with cirrhosis are often debilitated and may have compromised immunity. The immune-compromised nature of a transplant recipient magnifies the risk of major infectious complications. Serious

**Revised:** December 20, 2020**Accepted:** January 13, 2021**Article in press:** January 13, 2021**Published online:** February 21, 2021**P-Reviewer:** Gelmini R**S-Editor:** Gao CC**L-Editor:** Webster JR**P-Editor:** Ma YJ

complications may occur after SAE, such as abdominal infection, pancreatitis, splenic abscess, and splenic rupture. Post-embolization syndrome, characterized by fever and/or abdominal pain, occurs in up to 78% of patients following SAE<sup>[11]</sup>. Other disadvantages of SAE include high recurrence rates, and difficulty accessing the embolic area<sup>[12]</sup>.

Cirrhosis with severe splenomegaly and hypersplenism is common, yet satisfactory treatment is lacking<sup>[13]</sup>. In our center, splenectomy during LT has been used for more than ten years, but was abandoned due to uncontrollable postoperative complications, such as portal vein thrombosis, insufficient portal vein flow, and OPIS<sup>[6,8,9]</sup>. Later, we performed LT without intraoperative intervention<sup>[8]</sup>. If hypersplenism or portal hypertension persisted after surgery, then we performed SAE<sup>[7]</sup>. However, we found that this process increased the risk of infection due to extensive splenic infarction and prolonged the patient's discharge time. A method that limits the extent of splenectomy and spares splenic function is necessary.

To realize this need, we first proposed and designed the procedure of partial splenectomy during LT (PSLT), which is an all-in-one treatment for post-LT complications. In this article, we demonstrate the role of PSLT in the treatment of advanced cirrhosis with severe splenomegaly and hypersplenism.

## MATERIALS AND METHODS

### Patient selection

Between October 2015 and February 2019, 762 cases of classic orthotopic LT were performed at our institution. Among these, there were 84 cases of advanced cirrhosis combined with severe splenomegaly (Figure 1) and hypersplenism. Forty-one cases received PSLT (PSLT group), and 43 cases received only LT with no intervention (LT group). Patient characteristics, intraoperative parameters, and postoperative outcomes were compared between the LT and PSLT groups and retrospectively analyzed. All patients were followed-up regularly by the same surgical team. No patients were lost during follow-up. The last census date for the study was October 31, 2020. All grafts used for LT were obtained from deceased donors, and no organs from executed prisoners were used. All deceased donations complied with the China Organ Donation Program. This study was approved by the ethics committee of Tianjin First Central Hospital.

The inclusion criteria for the 2 groups were the same and are as follows: (1) Indication for LT; (2) The primary disease was benign liver disease or liver cancer meeting the Milan criteria; (3) Model for End-Stage Liver Disease (MELD) score < 25 and the patient was in a stable condition; and (4) Severe splenomegaly (spleen volume > 1000 mL) and hypersplenism (platelet count < 50 × 10<sup>9</sup>/L). In our previous studies, hypersplenism persisted after LT in most patients with a spleen volume >1000 mL and platelet count < 50 × 10<sup>9</sup>/L<sup>[14]</sup>. The exclusion criteria included: (1) MELD score > 25; (2) Severe perisplenic adhesions; (3) Accompanying splenic tumor; and (4) Spleen volume < 1000 mL or platelet count > 50 × 10<sup>9</sup>/L.

### Surgical procedure of PSLT

Partial splenectomy was performed after classic orthotopic LT (caval replacement) as follows: The primary splenic artery was isolated, exposed, and prepared for clamping to prevent uncontrolled bleeding (Figure 2A and B). According to the anatomic classification of the spleen vessels evaluated by preoperative spiral computed tomography (CT) three-dimensional reconstruction, hilar vessels from the lower pole of the spleen were selectively closed with a vascular clamp (usually, half or one third of the spleen was removed as shown in Figure 3; and the cutting planes defined for spleen resection should be maintained above the costal margin; meanwhile, adjusted as per the intraoperative flow by Doppler ultrasound: portal vein flow should be more than 100 mL/100 g/min and hepatic artery blood flow should be more than 35 mL/100 g/min). The relevant ischemic demarcation line was then observable (Figure 2E), and the resection was performed along the demarcation line (Figure 2F). A Cavitron ultrasonic surgical aspirator and bipolar coagulation forceps were used to split the spleen. Hemostasis was performed along the resection line using surgical, bipolar coagulation, and argon beam (Figure 2G). Segmental hilar vessels were allowed to remain with the splenic remnant. Bleeding should be carefully avoided ensuring safety. The splenic artery was clamped with conventional forceps during the splenic incision, and the tube structure was clipped with titanium clamps. After repeated hemostasis, the splenic artery was opened again to assess the presence of





Figure 1 Preoperative computed tomography scan of patients with advanced cirrhosis combined with severe splenomegaly.

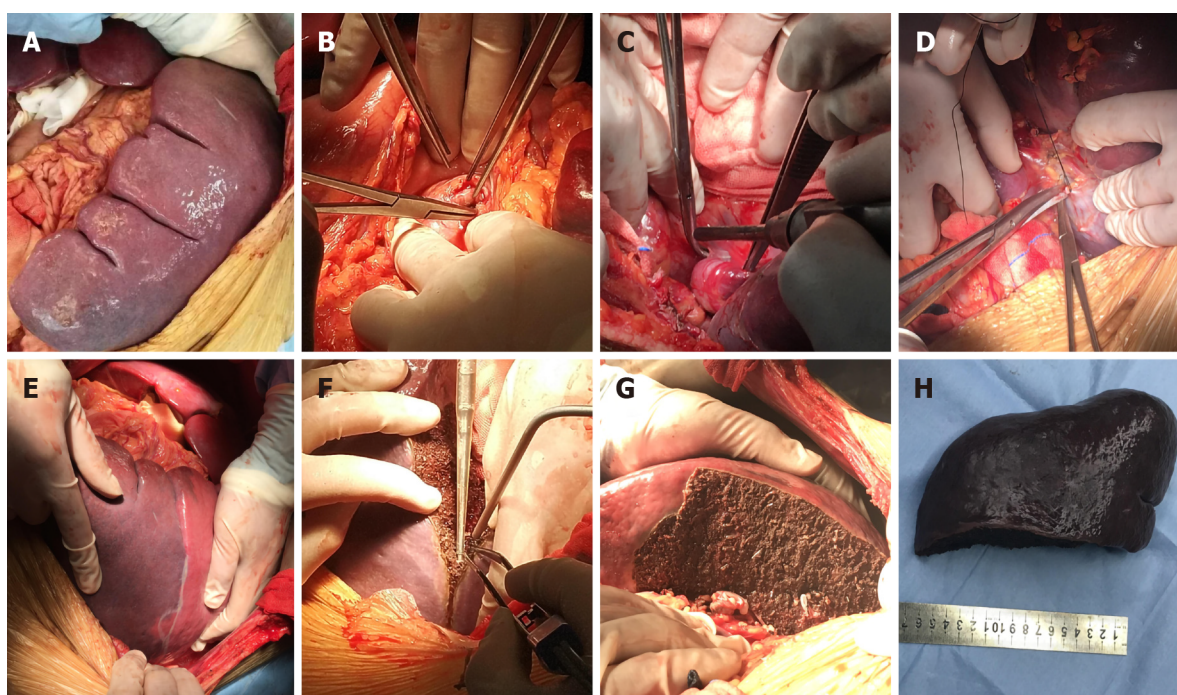


Figure 2 Surgical procedure of partial splenectomy during liver transplantation. A: Partial splenectomy for severe hypersplenism was performed after classic orthotopic liver transplantation; B: The main splenic artery was isolated and exposed; C: The hilar vessels from the lower pole of the spleen were selectively ligated; D: The main collateral circulation of the spleen was isolated and ligated; E: Ischemic demarcation line became observable; F: The spleen was resected along the ischemic line using a Cavitron ultrasonic surgical aspirator and bipolar coagulation forceps; G: The segmental hilar vessels were allowed to remain with the splenic remnant; H: The spleen specimen.

hemostasis, and the drainage tube and hemostatic gauze were placed last.

### **Perioperative management and assessment**

After LT, blood biochemistry was performed regularly to monitor liver function. Color Doppler ultrasound was reviewed every day for one week and every three days for one month to monitor the dynamic flow of the hepatic artery, portal vein, and vena cava. All patients were analyzed by the same senior color Doppler ultrasound operator. Enhanced CT was reexamined preoperatively and postoperatively at 1, 6,



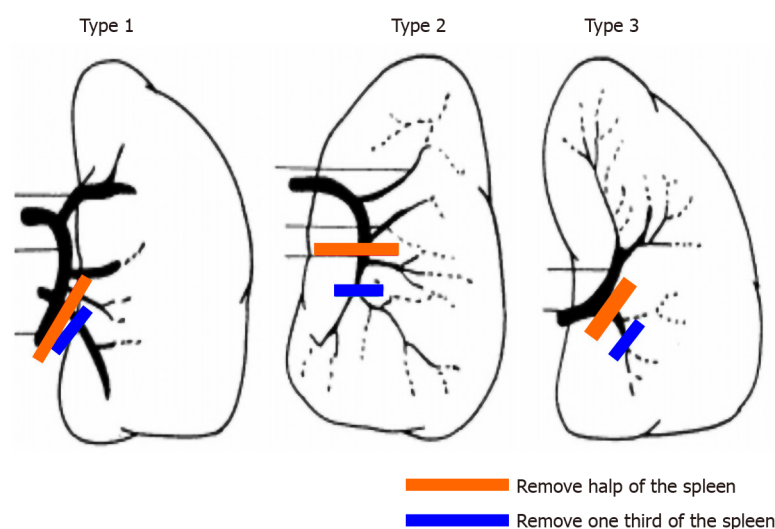


**Figure 3** Removal of half or one third of the spleen according to the splenic hilum vessel anatomy. The red line represents half splenectomy, and the green line represents one-third splenectomy.

and 12 mo to measure spleen volume.

The Chi-square test, Fisher exact test, and paired t-test were used to compare patient characteristics, intraoperative parameters, and postoperative results in the LT group and PSLT group. All quantitative data were expressed as mean  $\pm$  SD. SPSS 21.0 was used for statistical analysis, and  $P < 0.05$  was considered statistically significant.

## RESULTS

### Preoperative characteristics

As shown in Tables 1 and 2, there was no difference in preoperative characteristics between the two groups. The MELD scores in the LT group and PSLT group were  $19.4 \pm 4.9$  and  $20.7 \pm 4.6$  points, respectively, and the Graft /Recipient Weight Ratios (%) were  $1.4 \pm 0.5$  and  $1.4 \pm 0.6$ , respectively. Preoperative spleen volumes in the LT group and PSLT group were  $1665 \pm 611$  cm<sup>3</sup> and  $1711 \pm 682$  cm<sup>3</sup>, respectively, and platelet counts were  $38.6 \pm 14.7 \times 10^3/\text{mm}^3$  and  $36.9 \pm 14.1 \times 10^3/\text{mm}^3$ , respectively. Preoperative portal vein blood flow in the LT and PSLT groups was  $12.4 \pm 3.9$  and  $11.8 \pm 3.7$  cm/s, respectively, and preoperative hepatic arterial blood flow in the two groups was  $40.3 \pm 22.1$  and  $40.9 \pm 21.7$  cm/s, respectively.

### Operative characteristics

As summarized in Table 3, the total operation time in the PSLT group ( $8.6 \pm 1.3$  h) was longer than that in the LT group ( $6.8 \pm 0.9$  h), and the time required for partial splenectomy was  $1.8 \pm 0.3$  h (range 1.6 to 2.1 h). Intraoperative blood loss in the PSLT group ( $640.8 \pm 347.3$  mL) was more than that in the LT group ( $349.4 \pm 116.1$  mL), and blood loss during partial splenectomy was  $85.6 \pm 79.2$  mL (range 50 to 350 mL). The weight of excised spleen in the PSLT group was  $787 \pm 371.4$  g (range 342 to 1806 g). The mean portal flow in the LT group and PSLT group increased from  $12.4 \pm 3.9$  cm/s and  $11.8 \pm 3.7$  cm/s preoperative to  $47.6 \pm 14.1$  cm/s and  $42.7 \pm 13.8$  cm/s postoperative, respectively. The mean hepatic artery blood flow in the PSLT group ( $49.3 \pm 13.6$  cm/s) was higher than that in the LT group ( $42.6 \pm 11.4$  cm/s).

### Postoperative outcome

As shown in Figure 4A, spleen volume in the LT group and PSLT group decreased from  $1665 \pm 611$  cm<sup>3</sup> and  $1711 \pm 682$  cm<sup>3</sup> preoperative to  $1316 \pm 397$  cm<sup>3</sup> and  $745 \pm 189$  cm<sup>3</sup> at postoperative 1 mo,  $1157 \pm 361$  cm<sup>3</sup> and  $668 \pm 174$  cm<sup>3</sup> at postoperative 6 mo, and  $1041 \pm 364$  cm<sup>3</sup> and  $581 \pm 179$  cm<sup>3</sup> at postoperative 12 mo, respectively. Postoperative blood flow in the hepatic artery and portal vein were monitored by color Doppler ultrasound. Compared with the LT group, hepatic artery flow increased in the PSLT group and portal vein flow decreased (Figure 4B and C).

In the PSLT group, platelet counts increased to the peak level at postoperative day 14, and leukocyte counts increased to the peak value at postoperative day 7. Both

**Table 1 Preoperative characteristics**

	LT group (n = 43)	PSLT group (n = 41)	P value
Gender (male/female)	27/16	28/13	0.651
Age, yr	49.2 ± 12.8	52.7 ± 13.1	0.219
Indication for transplantation			
Hepatitis B cirrhosis	19	21	0.662
Hepatic malignancy	10	8	0.792
Alcoholic cirrhosis	8	6	0.772
Autoimmune liver disease	2	3	0.672
<i>etc.</i>	4	3	> 0.99
MELD score at transplantation	19.4 ± 4.9	20.7 ± 4.6	0.214
PreOP biology			
Total bilirubin (μmol/L)	133.0 ± 106.9	128.5 ± 97.2	0.841
Serum creatinine (μmol/L)	96.1 ± 72.6	82.6 ± 66.3	0.377
INR	1.6 ± 0.6	1.7 ± 0.6	0.447
Plasma ammonia (μmol/L)	59.7 ± 21.5	57.6 ± 23.4	0.669
PreOP platelet count, 10 <sup>3</sup> /mm <sup>3</sup>	38.6 ± 14.7	36.9 ± 14.1	0.590
PreOP spleen volume, cm <sup>3</sup>	1665 ± 611	1711 ± 682	0.745
PreOP PV flow, cm/s	12.4 ± 3.9	11.8 ± 3.7	0.472
PreOP HA flow, cm/s	40.3 ± 22.1	40.9 ± 21.7	0.453

LT: Liver transplantation; PSLT: Partial splenectomy during liver transplantation; HA: Hepatic artery; PV: Portal vein; MELD: Model for End-Stage Liver Disease; INR: International normalized ratio; PreOP: Preoperative.

**Table 2 Donors' characteristics**

	LT group (n = 43)	PSLT group (n = 41)	P value
Gender (male/female)	31/12	28/13	> 0.99
Age, yr	42.6 ± 16.3	44.5 ± 15.9	0.665
Cause of death			
Cerebral trauma	24	22	> 0.99
Cerebrovascular accident	10	8	0.792
Brain tumor (glioma)	4	5	0.735
Hypoxic brain injury	2	3	0.672
<i>etc.</i>	3	3	> 0.99
ICU stay, d	2.71 ± 2.05	2.83 ± 2.24	0.798

LT: Liver transplantation; PSLT: Partial splenectomy during liver transplantation; ICU: Intensive care unit.

platelet counts and leukocyte counts in the PSLT group increased faster than those in the LT group, resulting in a significant difference between the groups. Platelet count was  $139.4 \pm 72.4 \times 10^3/\text{mm}^3$  in the PSLT group and  $84.1 \pm 51.5 \times 10^3/\text{mm}^3$  in the LT group at postoperative 12 mo ( $P < 0.001$ ). Leukocyte count was  $3.6 \pm 1.4 \times 10^3/\text{mm}^3$  in the PSLT group and  $1.9 \pm 0.8 \times 10^3/\text{mm}^3$  in the LT group at postoperative 12 mo ( $P < 0.001$ ).

Postoperative complications in the two groups are summarized in Table 4. The incidence of postoperative hypersplenism (2/41, 4.8%) and recurrent ascites (1/41, 2.4%) in the PSLT group were significantly lower than that in the LT group

**Table 3** Operative characteristics

	LT group (n = 43)	PSLT group (n = 41)	P value
Operating time, h	6.8 ± 0.9	8.6 ± 1.3	< 0.001
Time for PS		1.8 ± 0.3	
Blood loss, mL	349.4 ± 116.9	440.8 ± 141.3	0.002
During PS		85.6 ± 79.2	
PostOP HA flow, cm/s	42.6 ± 11.4	49.3 ± 13.6	0.016
PostOP PV flow, cm/s	47.6 ± 14.1	42.7 ± 13.8	0.022
Weight of PS, g		787 ± 371.4	
Percentage of PS, (n)			
Half of spleen		23	
Third of spleen		18	

LT: Liver transplantation; PSLT: Partial splenectomy during liver transplantation; HA: Hepatic artery; PV: Portal vein; PreOP: Preoperative.

**Table 4** Postoperative complications, n (%)

	LT group (n = 43)	PSLT group (n = 41)	P value
Postoperative hypersplenism	22 (51.1)	2 (4.8)	< 0.001
Recurrent ascites	8 (18.6)	1 (2.4)	0.029
Reoperation due to post-op bleeding	2 (4.6)	3 (7.3)	0.672
Postoperative pulmonary infection	5 (11.6)	4 (9.7)	> 0.99
Post-op thrombosis	1 (2.3)	1 (2.4)	> 0.99
Splenic arterial steal syndrome	4 (9.3)	0	0.116
Two-stage splenic embolization	17 (39.5)	0	< 0.001
Further splenectomy	6 (13.9)	0	0.026

LT: Liver transplantation; PSLT: Partial splenectomy during liver transplantation.

(22/43, 51.2%; 8/43, 18.6%, respectively). Seventeen patients (17/43, 39.5%) in the LT group required multiple partial splenic embolization (PSE) to relieve postoperative persistent hypersplenism in 15 and refractory ascites in 2. Six of them required further splenectomy after PSE, 2 patients due to persistent severe splenic infarction syndrome, 2 patients due to persistent hypersplenism despite embolization, 1 patient due to splenic abscess with repeated infection after PSE, and 1 patient due to hypersplenism and persistent abdominal pain after PSE. In the PSLT group, no patient underwent two-stage splenic embolization or surgery for postoperative persistent hypersplenism.

Other postoperative complications requiring reoperation were postoperative bleeding ( $n = 3$ ), pulmonary infection ( $n = 4$ ), thrombosis ( $n = 1$ ) and splenic arterial steal syndrome ( $n = 0$ ) in the PSLT group, which were similar to those ( $n = 2$ ,  $n = 5$ ,  $n = 1$ ,  $n = 4$ , respectively) in the LT group. In-hospital mortality did not occur in either group.

## DISCUSSION

Partial splenectomy can be used to treat severe splenomegaly and hypersplenism, and its safety and efficacy have been confirmed<sup>[15,16]</sup>. Partial splenectomy reduces spleen volume and alleviates the symptoms of hypersplenism while maintaining the immunological functions of the spleen. These beneficial effects have also been confirmed in animal models. However, so far there are no reports on the application of partial splenectomy in LT.

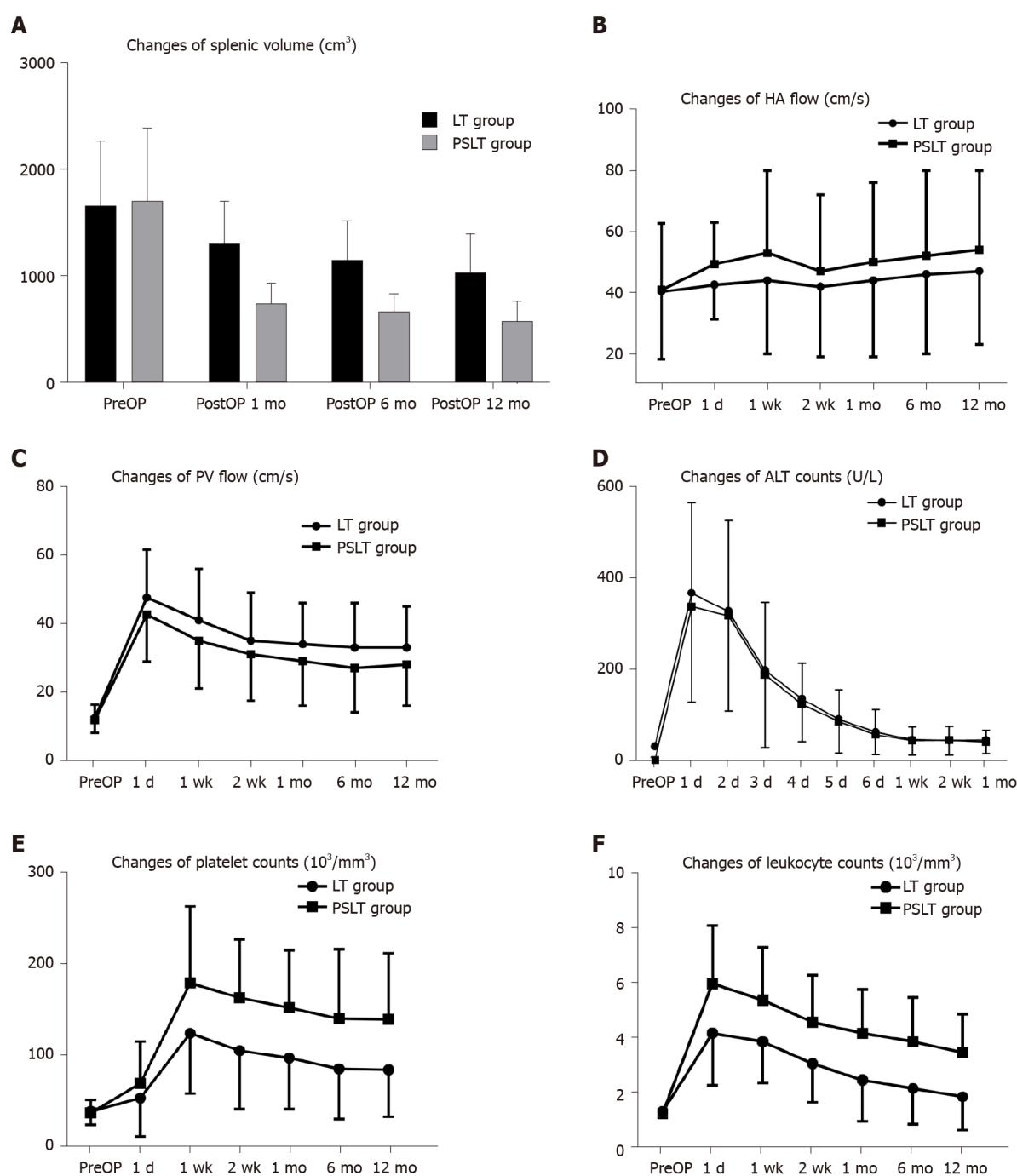


**Figure 4** Postoperative changes in the two groups. A: Spleen volume; B: Hepatic artery flow; C: Portal vein flow; D: Alanine transaminase; E: Platelet count; F: Leukocyte count. HA: Hepatic artery; PV: Portal vein; ALT: Alanine transaminase; PreOP: Preoperative.

In this article, we described the PSLT procedure for advanced cirrhosis with severe splenomegaly and hypersplenism. Hypersplenism/splenomegaly can lead to post-LT complications and PSLT could offer an all-in-one intervention to mitigate these clinically-relevant issues. As our data showed, although partial splenectomy took 1.5-2 h and resulted in blood loss of 50-350 mL, the PSLT group showed significant improvement in ascites and hypersplenism after transplantation, and no recurrence of splenomegaly or hypersplenism was observed during follow-up. In the LT group, the average spleen volume after 12 mo is still greater than 1000 cm<sup>3</sup>, and 51% of the patients will continue to have hypersplenism. Most of them must undergo the second stage of splenic embolization or splenectomy to improve hematological parameters to allow the use of other myelosuppressive drugs.

Most previous studies on partial splenectomy in patients with cirrhosis advocated subtotal splenectomy and reported that approximately 90% of the spleen can be removed to ensure a curative effect<sup>[16,17]</sup>. However, the magnitude of PSLT was far less,

and the therapeutic effect was also significant. In our study, we usually remove half or one third of the spleen according to the splenic hilum vessel anatomy, as shown in [Figure 3](#). We also try to maintain the cutting planes of spleen resection above the costal margin to protect the spleen section. In addition, we found that intraoperative resection ratio and splenic volume reduction ratio reassessed by CT scan after surgery were significantly different ([Figure 5](#)). The reduction degree of spleen volume varies by patient, and may be related to the history of liver disease and the severity of splenic hyperplasia. Patients with a long history of cirrhosis and severe splenic hyperplasia are more likely to have poor relief of hypersplenism after LT.

However, the present study is retrospective and only included relatively few patients from a single center. Large multicenter studies with long-term follow-up are necessary. In addition, we have not applied this procedure in living donor LT patients. Further studies are needed to investigate whether partial splenectomy during living donor LT can reduce portal vein perfusion and prevent small spleen syndrome, as well as treat hypersplenism.

---

## CONCLUSION

---

In conclusion, PSLT solves a series of problems such as end-stage liver disease, hypersplenism, splenomegaly and hemodynamic disorder all at once, so patients do not need to receive two-stage splenic embolization or splenectomy. However, PSLT requires up to 25% longer operation time and the need for blood products, which would raise concerns in transplant surgeons. Appropriate patient selection is necessary to ensure that the benefits outweigh the risks. According to our experience, patients with preoperative severe splenomegaly (spleen volume > 1000 mL) and hypersplenism (platelet count <  $50 \times 10^9/L$ ) are more likely to have intractable hypersplenism after LT, and PSLT is recommended. PSLT is not recommended when the patient has a MELD score > 25, severe perisplenic adhesions, accompanied by splenic tumor, splenic volume < 1000 mL or platelet count >  $50 \times 10^9/L$ .



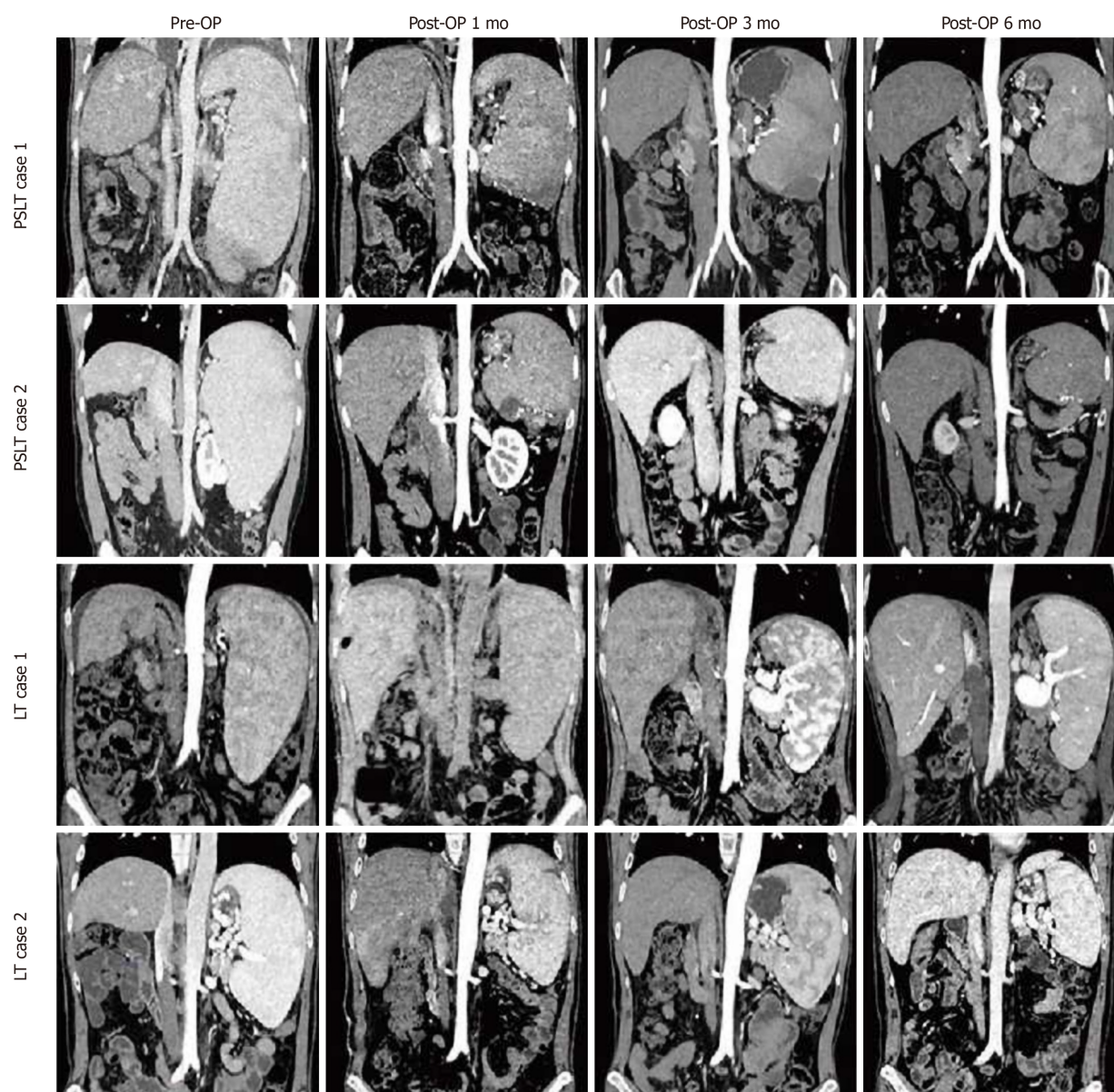


**Figure 5** Chronologic changes in the splenic volume after liver transplantation or partial splenectomy during liver transplantation. PreOP: Preoperative; LT: Liver transplantation; PSLT: Partial splenectomy during liver transplantation.

## ARTICLE HIGHLIGHTS

### Research background

The most effective treatment for advanced cirrhosis and portal hypertension is liver transplantation (LT). However, splenomegaly and hypersplenism can persist even after LT in patients with massive splenomegaly. Persistent hypersplenism-related pancytopenia may interfere with the management of immunosuppressive therapy. Splenomegaly may further result in excessive portal pressure or splenic artery steal syndrome. The resulting decrease in hepatic arterial inflow can then affect liver graft function.

### Research motivation

The most common therapies for splenomegaly and hypersplenism are total splenectomy during LT and selective splenic artery embolization after LT, but they have considerable limitations. Cirrhosis with severe splenomegaly and hypersplenism is common, yet satisfactory treatment is lacking. To realize this need, we first proposed and designed the procedure of partial splenectomy during LT (PSLT), which is an all-in-one treatment for post-LT complications.

### Research objectives

To examine the feasibility of performing partial splenectomy during LT in patients with advanced cirrhosis combined with severe splenomegaly and hypersplenism.

### Research methods

Between October 2015 and February 2019, 762 cases of classic orthotopic LT were performed at our institution. Among these, there were 84 cases of advanced cirrhosis combined with severe splenomegaly and hypersplenism. Forty-one cases received PSLT (PSLT group), and 43 cases received only LT with no intervention (LT group). Patient characteristics, intraoperative parameters, and postoperative outcomes were compared between the LT and PSLT groups and retrospectively analyzed.

### Research results

The incidence of postoperative hypersplenism and recurrent ascites in the PSLT group was significantly lower than that in the LT group. Seventeen patients in the LT group required two-stage splenic embolization, and further splenectomy was required in 6 of them. The operation time and intraoperative blood loss in the PSLT group were relatively increased compared with the LT group. The incidence of postoperative bleeding, pulmonary infection, thrombosis and splenic arterial steal syndrome in the PSLT group was similar to that in the LT group, respectively.

### Research conclusions

PSLT can reduce the incidence of postoperative hypersplenism and recurrent ascites, and reduce the risk of secondary splenic embolization and splenectomy, but the operation time and intraoperative blood loss were increased.

### Research perspectives

According to our experience, patients with preoperative severe splenomegaly and hypersplenism are more likely to have intractable hypersplenism after LT, and PSLT is recommended.

## REFERENCES

- 1 **Khanna R**, Sarin SK. Noncirrhotic Portal Hypertension: Current and Emerging Perspectives. *Clin Liver Dis* 2019; **23**: 781-807 [PMID: 31563222 DOI: 10.1016/j.cld.2019.07.006]
- 2 **Kockerling D**, Nathwani R, Forlano R, Manousou P, Mullish BH, Dhar A. Current and future pharmacological therapies for managing cirrhosis and its complications. *World J Gastroenterol* 2019; **25**: 888-908 [PMID: 30833797 DOI: 10.3748/wjg.v25.i8.888]
- 3 **Mukhtar A**, Dabbous H. Modulation of splanchnic circulation: Role in perioperative management of liver transplant patients. *World J Gastroenterol* 2016; **22**: 1582-1592 [PMID: 26819524 DOI: 10.3748/wjg.v22.i4.1582]
- 4 **Kawano F**, Ishizaki Y, Yoshimoto J, Fujiwara N, Kawasaki S. Factors Affecting Persistent Splenomegaly After Adult-to-Adult Living Donor Liver Transplantation Using a Left Lobe. *Transplant Proc* 2019; **51**: 1946-1949 [PMID: 31279408 DOI: 10.1016/j.transproceed.2019.02.033]
- 5 **Molina Perez E**, Fernández Castroagudín J, Seijo Ríos S, Mera Calviño J, Tomé Martínez de Rituerto S, Otero Antón E, Bustamante Montalvo M, Varo Perez E. Valganciclovir-induced leukopenia in liver transplant recipients: influence of concomitant use of mycophenolate mofetil. *Transplant Proc* 2009; **41**: 1047-1049 [PMID: 19376423 DOI: 10.1016/j.transproceed.2009.02.033]
- 6 **Chezmar JL**, Redvanly RD, Nelson RC, Henderson JM. Persistence of portosystemic collaterals and splenomegaly on CT after orthotopic liver transplantation. *AJR Am J Roentgenol* 1992; **159**: 317-320 [PMID: 1632346 DOI: 10.2214/ajr.159.2.1632346]
- 7 **DuBois B**, Mobley D, Chick JFB, Srinivasa RN, Wilcox C, Weintraub J. Efficacy and safety of partial splenic embolization for hypersplenism in pre- and post-liver transplant patients: A 16-year comparative analysis. *Clin Imaging* 2019; **54**: 71-77 [PMID: 30553121 DOI: 10.1016/j.clinimag.2018.11.012]
- 8 **Golse N**, Mohkam K, Rode A, Pradat P, Ducerf C, Mabrut JY. Splenectomy during whole liver transplantation: a morbid procedure which does not adversely impact long-term survival. *HPB (Oxford)* 2017; **19**: 498-507 [PMID: 28233673 DOI: 10.1016/j.hpb.2017.01.020]
- 9 **Badawy A**, Hamaguchi Y, Satoru S, Kaido T, Okajima H, Uemoto S. Evaluation of safety of concomitant splenectomy in living donor liver transplantation: a retrospective study. *Transpl Int* 2017; **30**: 914-923 [PMID: 28512755 DOI: 10.1111/tri.12985]
- 10 **Ricci K**, Asharf EH. The use of splenic artery embolization to maintain adequate hepatic arterial inflow after hepatic artery thrombosis in a split liver transplant recipient. *Int J Surg Case Rep* 2018; **51**: 241-243 [PMID: 30218820 DOI: 10.1016/j.ijscr.2018.09.003]
- 11 report on dracunculiasis cases, January–October 2014. *Wkly Epidemiol Rec* 2014; **89**: 587-588

- [PMID: 25538996]
- 12 **Koconis KG**, Singh H, Soares G. Partial splenic embolization in the treatment of patients with portal hypertension: a review of the english language literature. *J Vasc Interv Radiol* 2007; **18**: 463-481 [PMID: 17446537 DOI: 10.1016/j.jvir.2006.12.734]
  - 13 **Gangireddy VG**, Kanneganti PC, Sridhar S, Talla S, Coleman T. Management of thrombocytopenia in advanced liver disease. *Can J Gastroenterol Hepatol* 2014; **28**: 558-564 [PMID: 25222481 DOI: 10.1155/2014/532191]
  - 14 **He J**, Guo QJ, Xie Y, Zhang L, Tian DZ, Wang HH, Chen CY, Jiang WT. Application of image post-processing technique to measure spleen volume and evaluate the effect of orthotopic liver transplantation on relieving hypersplenism. *Zhonghua Qiguan Yizhi Zazhi* 2019; **40**: 107-11 [DOI: 10.3760/cma.j.issn.0254-1785.2019.02.010]
  - 15 **Guan YS**, Hu Y. Clinical application of partial splenic embolization. *ScientificWorldJournal* 2014; **2014**: 961345 [PMID: 25538966 DOI: 10.1155/2014/961345]
  - 16 **Chu H**, Han W, Wang L, Xu Y, Jian F, Zhang W, Wang T, Zhao J. Long-term efficacy of subtotal splenectomy due to portal hypertension in cirrhotic patients. *BMC Surg* 2015; **15**: 89 [PMID: 26205377 DOI: 10.1186/s12893-015-0077-2]
  - 17 **Radević B**, Jesić R, Sagić D, Perisić V, Nenezić D, Popov P, Ilijevski N, Dugalić V, Gajin P, Vucurević G, Radak Dj, Trebjesanin Z, Babić D, Kastratović D, Matic P. [Partial resection of the spleen and spleno-renal shunt in the treatment of portal hypertension with splenomegaly and hypersplenism]. *Acta Chir Jugosl* 2002; **49**: 93-98 [PMID: 12587456 DOI: 10.2298/aci0203093r]



Published by **Baishideng Publishing Group Inc**  
7041 Koll Center Parkway, Suite 160, Pleasanton, CA 94566, USA

**Telephone:** +1-925-3991568

**E-mail:** [bpgoffice@wjgnet.com](mailto:bpgoffice@wjgnet.com)

**Help Desk:** <https://www.f6publishing.com/helpdesk>

<https://www.wjgnet.com>

